Charles University

Faculty of Science

Department of Experimental Plant Biology

Ing Jozef Lacek

Charakterizace faktorů podílejících se na regulaci intracelulární dynamiky vybraných auxinových přenašečů

Characterization of factors participating in regulation of intracellular dynamics of auxin carriers

PhD. Thesis

Supervisor: prof. RNDr. Eva Zažímalová, CSc.

Advisor: Dr.nat.techn. Katarzyna Retzer

Praha, 2023

Declarations

I declare that I wrote this thesis autonomously, using data from my own research and those I have actively participated in. This work is not submitted as candidature for any other degree. All sources of information were properly cited. Jozef Lacek

24.1.2023 Prague

Acknowledgement

I deeply acknowledge my parents and my family for immeasurable support they gave me and keep giving me. Next, I want to thank and acknowledge my supervisor Eva Zažímalová who gave me chance to enter the world of science and changed my life forever, and her ever-present support which was there whenever it was needed, and even when I wasn't expecting it. I gladly acknowledge every single member of Laboratory of hormonal regulations in plants who helped me to become who I am today. I acknowledge my consultant Milada Čovanová who had the patience to be with me in the very beginning of my study and scientific carrier.

And – last but not least - my biggest acknowledgement and thanks belongs to my consultant Katarzyna Retzer. She showed me how to love science in ways I didn't think about. She supported me and inspired me every single day we have worked together; her skills of understanding science amaze me and I hope that by learning from her I can one day become as good scientist as she is today.

Abstract

Plants are known to adjust the orientation of their organs, shoot and root, to ensure maximal energy generation and nutrient uptake, but also to avoid toxic growth conditions. Directional growth regulation depends on asymmetric plant organ growth and it is crucial to ensure plant survival. It is orchestrated on cellular level in concert with exogenous and intrinsic signals. Even though tropistic growth responses of plants were described by Darwin on macroscopic level already in 1880, now it is necessary to understand molecular mechanisms that underpin efficient modulation of directional plant growth.

During my studies I focused on factors that modulate directional root growth regulation. The root is a complex, three-dimensional object, which continuously modifies its shape and growth path. Since the root needs to expand its surface to supply the plant with nutrients and water, it is important to understand how roots cope with changing growth conditions while exploring the soil. If the root cannot manage to grow through soil efficiently, mechanical impedance and lack of resources will also restrict shoot growth as well. Manifold signaling pathways coordinate the complex processes that underpin efficient root growth, including those modulated by phytohormones, sugars, flavonoids and other metabolites. Detailed mechanistic studies of how those signaling cascades are interconnected on subcellular level are still partly missing. Previously published studies showed that the key molecular players, which are responsible for the asymmetric distribution of auxin, often called a morphogen, delimit directional root growth and speed depending on growth conditions, including changing energy supply. On molecular level, auxin distribution is controlled through precise regulation of localization, abundance and activity of auxin carriers.

My thesis consists of published articles that demonstrate on one side the importance of molecular regulation of a proteins involved in auxin distribution and thereby modulation of root growth. Furthermore, I showed how the inability to steer directional root growth in mutants with delimited auxin distribution in roots impairs the roots' ability to react to exogenous growth conditions. My research allowed to describe the importance of two highly conserved cysteines in the protein sequence of the auxin transporter PIN-FORMED 2, which determine the protein abundance and subcellular distribution. This results in different root waving pattern, which reflects the difficulty of the root to compensate deviation of root growth that occurs when a root is grown on the surface of agar supplemented growth medium. The intensive study of root growth dynamics further resulted in a better understanding of how cultivation conditions affect orchestration of directional root growth. Therefore, in my follow-up publications I described the relationship between exogenous signals and auxin dependent modulation of directional root growth by observing root growth responses of mutants lacking either a well-studied plasma membrane located auxin importers or exporters.

Finally, I contributed to two studies that dissect the interplay of efficient actin cytoskeleton assembly and auxin homeostasis for proper root growth. I am highly interested in establishing novel methods to enhance the sensitivity of mass-spectrometric analysis of phytohormonal metabolism. I measured and evaluated the differences of hormone metabolism in mutants (i), lacking a central modulator of actin branching, ARP2/3 complex, and (ii), a mutant with altered phospholipid content that lacks two phosphatidylinositol 4-kinases.

In summary, my efforts allowed to further dissect levels of directional root growth regulation, which is highly dependent on fine-tuned auxin distribution and signaling in the root tip.

Souhrn

U rostlin je známo že mají schopnost nasměrovat svoje části, jak prýt, tak kořeny, pro zabezpečení maximálního zisku energie a příjmu živin, ale taky pro možnost vyhnout se toxickým podmínkám pro svůj růst. Regulace směru růstu, který zabezpečuje přežití rostliny, závisí na schopnosti rostlinných orgánů růst asymetricky. Asymetrický růst je regulován na buněčné úrovni na základě exogenních i interních signálů. Již v roce 1880 Darwin popsal tropismy a směrový růst na makroskopické úrovni; v současnosti je nevyhnutelné pochopit molekulární mechanismy, které zajišťují efektivní regulaci směrového růstu rostlin.

V rámci svého studia jsem se zaměřil na mechanismy regulace směru růstu u rostlin. Kořen je komplexní trojrozměrný objekt, který stále upravuje svůj tvar a směr růstu. Vzhledem k tomu, že kořen potřebuje zvětšovat svůj povrch, aby byl schopen zajistit přísun živin a vody, je důležité pochopit, jak je kořen schopen adaptaci na konstantně se měnící růstové podmínky způsobené prorůstáním dál do půdy zvládnout. Pokud kořen není schopen prorůstat půdou efektivně kvůli silnému mechanickému odporu nebo nedostatku živin, pak je ovlivněn i růst prýtu. Optimální růst kořene je komplexní proces, na kterém se podílí rozmanitá spleť signálních drah, které jsou ovlivněny rostlinnými hormony, cukry, flavonoidy a jinými metabolity. Detailní studie propojení těchto drah na buněčné úrovni zatím chybí. Publikované studie potvrdily vliv faktorů ovlivňujících asymetrickou distribuci auxinu (někdy též označovaného jako morfogen) na rychlost a směr růstu kořene v závislosti na okolních podmínkách, včetně dostatku energie. Distribuce auxinu je na molekulární úrovni kontrolovaná pomocí regulace lokalizace, množství a aktivity auxinových přenašečů.

Moje práce sestává z publikací, poukazujících na význam regulace proteinů důležitých pro distribuci auxinu na molekulární úrovni, a zároveň ovlivňující růst kořenů. Dále poukazují na ztrátu schopnosti kořenů reagovat na vnější podmínky u mutantů s poruchou směrového růstu, kde je schopnost správné distribuce auxinu v kořeni narušena. Můj výzkum umožnil popsat význam dvou vysoce konzervovaných cysteinů v proteinové sekvenci auxinového přenašeče PIN-FORMED2, kde tyto cysteiny určují abundanci a subcelulární lokalizaci tohoto proteinu. Výsledkem záměny těchto cysteinů za alanin je změna ve schopnosti korigovat směr růstu kořene, což vede k odlišnému vzorci růstu na kultivačním médiu. Intenzivním studiem dynamiky kořenového růstu jsem přispěl k lepšímu pochopení, jak kultivační podmínky ovlivňují směrový růst kořene. Proto jsem se v dalších publikacích soustředil na popis vztahů mezi vnějšími signály a směrovým růstem kořene v závislosti na auxinu, a to pomocí sledování růstových odpovědí mutantů, kterým chybí funkce některých proteinů podílejících se na auxinovém transportu na plasmatické membráně.

Nakonec jsem přispěl svou prací ke dvěma publikacím, které zkoumají interakci mezi správně sestaveným aktinovým cytoskeletem a homeostází auxinu pro zabezpečení optimálního růstu kořene. Dalším z mých experimentálních zájmů a zaměření je zlepšování citlivosti metod hmotnostní spektrometrie pro měření metabolitů rostlinných hormonů. Změřil jsem a zhodnotil změny hormonálního metabolismu v mutantech, které postrádají funkční centrální modulátor aktinového větvení – komplex ARP2/3, a mutantů dvou fosfatidylinositol-4-kinas, které mají změny ve svém fosfolipidovém složení.

V souhrnu, má práce přispěla k rozklíčování různých úrovní regulace směrového růstu kořene, který je závislý na přesně nastavené regulaci distribuce auxinu a příjmu auxinových signálů v kořenové špičce.

Abbreviations

Arp2/3 Actin related protein 2/3 complex

ArpC3 Actin related protein 2/3 complex subunit3

ArpC4 Actin related protein 2/3 complex subunit4

AUX1 AUXIN RESISTANT 1

D-root dark grown root system

DZ differentiation zone

EZ elongation zone

IAA INDOLE-3-ACETIC ACID

LatB Latrunculin B

LR lateral root

M meristem

PAT polar auxin transport

PI4Kß1ß2 PHOSPHATIDYLINOSITOL-4-PHOSPHATE KINASES ß1 and ß2

PIN2 PIN-FORMED 2

PM plasma membrane

TZ transition zone

Content

1. Aims

This cumulative thesis consists of published studies that dissect the importance of fine-tuned auxin distribution and homeostasis for efficient modulation of directional root growth. Additionally, the studies demonstrate the immense impact of exogenous growth conditions on the modulation of root growth direction.

Therefore, the aims of the thesis cover:

a) Post-translational regulations of the plasma-membrane-located auxin efflux transporter PIN2 and how they impact directional root growth modulation.

b) Effect of growth conditions on directional root growth and the importance of the auxin influx carrier AUXI and efflux transporter PIN2 to counterbalance deviation of root growth depending on exogenous stimuli.

c) Analyzing auxin metabolism in mutants mimicking the auxin-related phenotypes.

2. Introduction.

2.1 Phytohormone auxin and its role in root growth modulation

Already in the 19th century, Charles and Francis Darwin described a compound (at that time still chemically unidentified) that was regulating phototropic response. In 1928 Frits Went was able to isolate the major, still unknown compound, that was later identified as indole-3-acetic acid, IAA, and named after the Greek word auxein for 'to grow'; (*1*). Later on, more native compounds related to IAA were discovered, such as indole-3-butyric acid (IBA) (*2*), 4-chloroindole-3-acetic acid (4-Cl-IAA) (*3*) and phenyl acetic acid (PAA) (*4*).

The phytohormone auxin is well-known for its fundamental role in orchestrating plant growth (*5*, *6*, *15*, *7–14*) . Auxin transport, biosynthesis and metabolism are constantly modulated to build up the necessary auxin gradients in the plant, which finally orchestrate developmental processes and shape the plant architecture depending on environmental conditions (*11*, *16*, *17*). Auxin signaling modulates transcription, translation and post-translational regulation of proteins, which result in altered cell proliferation, elongation and subcellular reorganization (*10*, *11*, *18*, *19*) Auxin is not produced all over the plant, but it is required in all plant cells to orchestrate their development and adaptation (*12*, *13*, *20–24*) . Auxin is primarily synthesized in young leaves, from where it is transported actively, with the assistance of plasma membrane (PM)-integrated system of influx and efflux carriers, from cell to cell, building up gradients, which underpin almost all growth processes. This process is known as polar auxin transport (PAT) (*13*, *25*).

IAA as a weak organic acid; its non-dissociated form allows for diffusion across the PM into the cell, and its active influx, mostly via AUX1/LAX protein family, increases uptake speed by 10 to 20 fold (*26–28*). Since the cytoplasm has a neutral pH, in which IAA dissociates into IAA-anion and proton, the IAA-anion is trapped in the cell and it can be transported out of cells only via active export (*29*) through PIN and/or ABCB proteins.

The modulation and regulation of PM localization of the auxin carriers were studied thoroughly for PIN proteins. In contrast, less is known for AUX1/LAXes, maybe because of the importance of PINs for mediating auxin flow directionality, while AUX1 is needed “only” to maintain the appropriate transport speed (*9*, *30*, *39–42*, *31–38*) . In roots, the root-specific PIN2 spatial and temporal distribution along the PM needs to be rapidly adapted to continuously changing environmental conditions, to allow the efficient developmental and growth adaptation (*11*, *18*, *40*, *41*, *43–47*). In general, subcellular distribution and intracellular trafficking of PIN proteins is maintained by reorganization of the endomembrane system in concert with other organelles, including proper assembly of the cytoskeleton, which all depend on the

growth conditions of the plant (*15*, *40*, *56–58*, *48–55*). The impact of the so-called short looped PINs (PIN5, PIN6, PIN8) and members of other auxin transporting proteins upstream of directional root growth control are less understood but also considered (*13*, *59–64*). Together with regulation of auxin biosynthesis and its metabolic control, PAT defines local variations in the hormone levels, which are perceived and transmitted to induce hormonally controlled adjustments in gene expression and activity (*60*, *65–68*). Different components of auxin signaling are known to orchestrate plant plasticity in shoot and root. Among many responses in the root, root architecture, including root length, number of lateral roots, and root hair development are affected. However, a detailed mapping of events required for directional root growth adaptation is still under investigation (*10*, *15*, *16*, *67*, *69–72*).

2.2. Polar Auxin Transport

2.2.1 Auxin influx

Active auxin uptake into cells is mediated by influx carriers, represented predominantly by the AUXIN1/LIKE-AUX1 (AUX1/LAX) protein family (*73*). The AUX1/LAX family in *Arabidopsis thaliana* consists of four highly conserved genes called *AUX1*, *LAX1*, *LAX2*, and *LAX3* (*39*, *74*). The most studied family member is AUX1, followed by LAX3 (*39*). Whereas *aux1* mutants are agravitropic and have a decreased number of lateral roots, *lax3* mutation results in delayed lateral root (LR) emergence, and together, LAX3 and AUX1 act concomitantly to regulate lateral root development by regulating the LR priming and emergence (*75*, *76*) . Auxin uptake experiments in heterologous expression systems have confirmed that AUX1 and LAXes are high-affinity auxin transporters (*28*, *77–80*). AUX1 activity was proven to be especially important for root development and growth adaptation, and in the root, it is expressed in the columella, lateral root cap, epidermis, and stele tissues to mediate auxin transport from shoot and root (*27*, *81*, *82*).

On the cellular level, AUX1 acts as an auxin and proton symporter to enhance auxin uptake by 10-20 fold, with maximum functionality at pH 5.7, which was supported by *loph1*, a loss-of-function mutant of AUX1 that exhibits diminished root growth at low pH (*27*, *83*, *84*). Furthermore, ATP hydrolysis and H+ extrusion activities of the PM H+-ATPase were reduced in *loph1* roots, which together with lower auxin redistribution along the root suggest that AUX1 activity is required to also modulate the PM-H+-ATPase function (*84*). AUX1 activity was also connected to cytoskeleton rearrangements, and AUX1-mediated influx inhibits cell elongation immediately in the root (*85–87*). Detailed studies of the spatial distribution of AUX1 using reduction of its expression in individual root tissues showed that AUX1 is required in the lateral root cap cells and epidermis cells to modulate directional root growth (*27*).

The epidermal auxin response is essential for establishing the gravitropic curvature, whereby a lateral auxin gradient is supposed to influence the expansion ability of all cells in all elongation zone tissues (*88*). Therefore, it was not surprising that our most recent publication described that AUX1 is involved in directional root growth modulation and elongation rate orchestration in so-called root growth penetration assays (*82*) See chapter 3.2.3.

Although no changes in AUX1 subcellular distribution upon induced tropistic stimuli were observed, evidence for the AUX1 intracellular trafficking was delivered from studies dealing with mutants of proteins involved in various intracellular sorting events (*89–91*). AUX1 abundance at the PM is diminished under growth conditions requiring primary root growth stop, including exposure to toxic compounds (*92*).

2.2.2 Auxin efflux

A well-studied protein family of auxin efflux transporters, the PIN-FORMED (PIN) proteins, shows a rate-limiting and directional function in cellular auxin efflux (*5*, *93–95*). The family of Arabidopsis *PIN* genes consists of eight members (*PIN1-PIN8*), and five out of corresponding proteins, i.e. PIN1-4 and PIN7 proteins are located at the PM with partially polar distribution to define the auxin gradient establishment (*29*, *52*, *95–100*) . *PIN1* is expressed in the stele, which is involved in the rootward auxin transport (*101*, *102*). Redistribution of auxin from the very root tip is associated with PIN3 and PIN7 that localize to the PM of root cap columella cells and were shown to gain polar distribution upon gravitropic stimulus, which could then initiate asymmetric auxin distribution upstream of root growth direction adaptation (*57*, *103*). *pin3* or *pin7* single mutants and their combination exhibit only subtle defects in root gravitropism, suggesting redundant activities of other auxin transport proteins (*57*). In contrast, knock-out mutants of AUX1 and PIN2 show pronounced loss of directional root growth control, and their ability to facilitate shootward auxin transport along the lateral root cap cells and epidermis towards the root elongation zone underpins the regulation of root growth adaptation (*27*, *104–106*). Opposite to the known details about the AUX1 action and the corresponding cell biology knowledge, the present information about the biochemistry behind PIN-facilitated auxin transport is still limited; however, the detailed mechanism of namely PIN2 intracellular transport is intensively studied now (*14*, *34*, *38*, *39*, *107*) .

2.2.2.1. The fundamental role of PIN2 for directional root growth control

Loss of or mis-regulation of PIN2 activity results in altered root development and growth adaptation (*13*, *15*, *50*, *108*, *109*). PIN2 activity, abundance and distribution are rapidly adjusted according to perceived signals of exogenous and internal events (*14*, *15*, *112–116*, *25*, *37*, *40*, *41*, *49*, *50*, *110*, *111*). PIN2 abundance is modulated from transcriptional to post-translational level through different cellular mechanisms, including orchestration of tRNA modifications to balance the translation rate, till rearranging its intracellular trafficking routes to regulate its degradation (*44*, *45*). In their long loop, which is integrated between two PM-integrated transmembrane domains, PIN proteins possess, several well-documented phosphorylation sites, which upon phosphorylation either contribute to the proteins polarity regulation or even activity status (*11*, *14*, *25*, *117–119*). Although several post-translational modifications of PIN2 are known, they still cannot be assigned to particular developmental or growth adaptation processes.

2.2.2.2Post-translational modifications of PIN2 determine its function

The complex relationships between PIN2 protein modifications and their impact on root physiology have been particularly dissected (*47*). Reporter proteins with constitutive modifications of the PIN2 protein sequence partially helped to understand the intracellular redistribution of PIN2 along the PM or the endomembrane system. Those modifications resulted either in the changed distribution along or lower abundance at the PM, with visible alterations of root growth pattern (*43*, *45*, *47*). Fusion between the PIN2 protein sequence and one ubiquitin moiety stimulated its continuous internalization from the PM followed by intracellular transport towards the lytic vacuole, which lowers its abundance dramatically at the PM and results in agravitropic root growth (*45*, *46*, *120*). Replacing with alanines the only two conserved cysteines in the PIN2 protein sequence, which are flanking the loop and according to computational modelling they face towards the PM, changed the ability of the protein to anchor in the PM partially, thereby changing its distribution pattern along the PM. When grown on inclined surfaces, the roots exhibit less pronounced root waviness (*47*). Putative requirement of those cysteines as targets of modifications upon changes in the redox status of the root during the root growth adaptation cannot be excluded, and further investigations are needed to decipher in more detail the tight connection that is suggested between regulation of PIN protein function and reactive oxygen species/flavonol-orchestrated cellular processes (*47*, *50*, *121–127*).

Intracellular distribution of proteins relies on flawless establishment of the endomembrane system, which is tightly connected to properly and flexible arrangements of the cytoskeleton (*40*, *51*, *54*,

55, *57*, *58*, *128–130*). Recent studies have shown that proper actin filament assembly is tightly interconnected with proper endomembrane trafficking (*131*) and plays a role in various cellular responses such as adaptation to environmental changes, immunity and differentiation (*7*, *51*, *56*, *87*, *132*). However, in plants, we have still minimal knowledge on the molecular basis of the role of actin filament structure and its distinct influence on proper auxin carrier targeting to the lytic vacuole (*51*, *87*). Interestingly, the induction of actin depolymerization by applying Latrunculin B (Lat B), accompanied by reduced PAT, did not inhibit but even promoted root gravitropism, even though other studies showed Lat B action is highly concentration-dependent (*133–135*). Actin filament depolymerization with Lat B promotes PIN2 accumulation in the root elongation zone by inhibiting F-actin assembly, linking proper actin filament assembly to auxin carrier regulation (*55*). This corresponds to the requirement of proper actin filament assembly for PIN2 transport towards the lytic vacuole, as depolymerization of the actin cytoskeleton inhibits this pathway (*130*). So, in the case of understanding the interplay between subcellular reorganization and rearrangement of trafficking routes of PIN2 upon individual stimuli and the resulting adaptation processes, much effort was made. Nevertheless, more detailed studies are necessary to decipher the orchestration of individual processes upstream of directional root growth control and root growth pattern formation, as the root simultaneously perceives and responds to manifold stimuli. Adaptations of experimental setups, which reduce the number of perceived stimuli, are getting more and more popular and include careful control of media supplementation, shading roots from direct root illumination or experiments under microgravity, and growing roots inside instead of along growth medium, as well as improved microscopy techniques to avoid undesirable gravitropic stimulus.

2.3 Interplay of environmental signals and auxin dependent root growth responses

Root growth adaptation to changing environmental conditions requires efficient growth rearrangements, which in the case of tropistic stimuli require the immediate establishment of asymmetric auxin gradients (*107*, *136*). Symmetric and asymmetric auxin distribution is actively regulated along the plant body and depends not only on exogenous stimuli but also on plant internal signals, including information about the plant's health, resources, and energy status (*15*, *16*, *39*, *49*, *95*, *98*, *108*, *137–139*)

During the efforts to dissect the interplay of environmental stimuli on auxin transport, and thereby on root growth, it became evident that direct illumination and exogenous sugar supplementation has a profound impact on auxin dependent root growth responses (*50*, *82*, *140*, *141*) Roots of higher plants evolved to grow in darkness and surrounded by soil, along the gravity vector, towards beneficial and away from toxic areas (*50*, *123*, *132*, *142*, *143*). They adjust growth direction and speed according to their ever-changing environment, which includes e.g. changes in soil density or depletion of nutrients, such as e.g.

sugars. It also results in reduced root growth and directional root growth control, which - in the combination of different genetic backgrounds - can result in a wide range of alterations of root growth pattern formation (*41*, *49*, *147*, *148*, *50*, *111*, *115*, *140*, *142*, *144–146*) . A comprehensive review about all known tropistic root responses was recently published by (*149*).

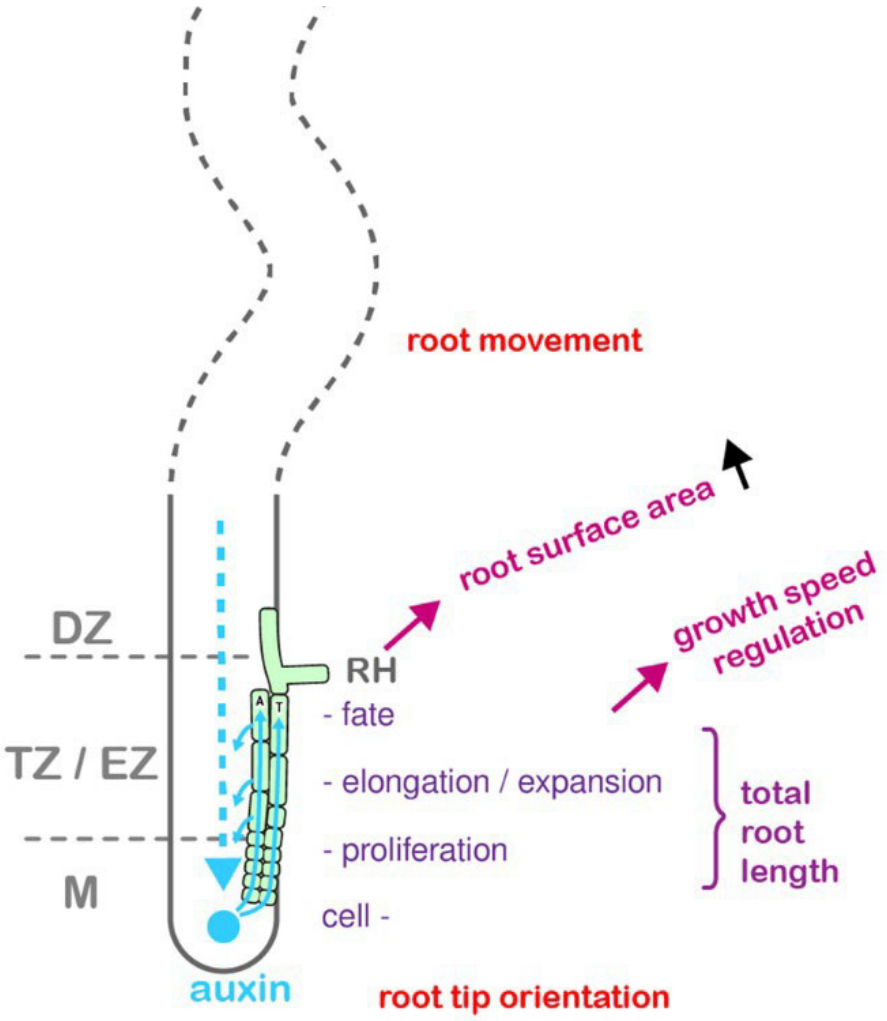

Figure 1. Overview of processes described in the introduction that require fine-regulated auxin flow in the root tip. Root shape and function is highly dependent on proper spatial and temporal modulation of shootward auxin transport. Establishment of auxin maxima and minima are crucial to regulate almost every aspect of plant development and growth adaptation, including meristematic activity, cell elongation till cell fate determination. Diminished or wrongly regulated auxin distribution through the root tip results in impaired root development and reduced ability to respond to environmental stimuli, including the orchestration of directional root growth. Finally, proper root function requires adjustment of the root system architecture, by outgrowing lateral roots and root hairs, to enlarge root surface, which is also delimited when shootward auxin transport is mis-regulated.

As summarized in Figure 1, PIN-FORMED 2 (auxin efflux) and AUXIN-RESISTANT 1 (auxin influx) are necessary for regulation of meristem (M) activity including transition of cells to elongation, transition and differentiation zone (TZ, EZ, DZ). Local modification of cell expansion in elongation zone is crucial to changes of root growth direction based on tropistic responses which establish root movement patterns

Root epidermis consists of trichoblast/root hair and atrichoblast cells. Auxin is priming the identity of root hair cells and promotes their elongation rate which increase the active surface of roots for acquiring water and nutrients. Directional root growth regulation depends on modulation of cell elongation, which among others, is regulated by the AUX1 and PIN2 actions. Perhaps, depending on available energy resources, modulation of the elongation rate in the root elongation zone (EZ) depends on the speed of the cytoplasmic streaming, which represents an intracellular force that defines autonomous movement of lateral root cap responding to internal cues (*150*, *151*). Overall, energy availability in the form of carbohydrates, which are generated as a product of photosynthetic activity, profoundly affects cell morphology and flexibility. The impact of individual sugars on root development regulation is currently in the focus of research (*48*, *49*, *156*, *111*, *140*, *141*, *144*, *152–155*) . Sugars act as both energy resource and signaling molecules, and they also serve as building bricks of cell components, including the cell wall, which all together underpin the speed of cellular processes and define mechanical properties of a cell (*48*, *65*, *157–164*).

2.3.1 Modulation of directional root growth depending on growth conditions

The force of gravity is defined as weak but continuous, and it acts during a plant life from the same position with the same strength (*113*, *165*). Higher plants evolved to grow their above-ground organs opposite to the gravity vector (negative gravitropism), and below-ground organ – primary root - along the gravity vector (positive gravitropism) (*113*, *166–168*) . It is the root tip that is sensing the direction of the gravity vector, and it is assumed that it goes through the movement of the statoliths in the columella cells, although it is not definitely proven yet (*107*, *113*, *169*, *170*). Further, it is unknown how the perceived signal is transmitted to execute directional root growth correction. However, besides *aux1* and *pin2,* there are several mutants, corresponding proteins of which are ranging in their function from cell fate modulators to regulators of subcellular organization, which exhibit root growth deviation from vertical axis or show diminished response to gravitropic stimulus (*107*). Anyway, a detailed map of cellular and subcellular events showing how perception, transmission and adaptation of gravitropism are aligned to ensure efficient directional root growth is still missing and will probably require more stringent experimental setups that eliminate unnecessary additive exogenous stimuli. Over time, it became more and more evident that other stimuli can override gravitropic response and that individual mutants and growth

conditions can modify root to such an extent that form and dynamics of the root tip are strongly altered (*171–173*). Up-to-date, a positive gravitropic response seems to be divided into four steps:, sensing the gravity vector in the columella, biochemical signal production and its transduction, differential cell adaptation to induce bending, and finally, a period of gravitropic signal attenuation to prevent over bending (*45*, *88*, *107*, *113*, *170*, *174*). Gravitropic index, which defines root growth deviation from vertical axis, is often evaluated to compare the ability of a mutant to maintain directional root growth or to investigate the impact of growth conditions (*171*). Deviation from vertical axis, of course, can be mediated by diverse exogenous and intrinsic events and must be taken with precaution when gravitropism is studied (*111*, *140*, *144*, *155*, *175*). For example, not only is PIN2 abundance and trafficking differently regulated upon unilateral and direct root illumination, but direct root illumination, additively with sucrose supplementation, result in more deviation (*50*, *110*, *115*, *140*). A detailed summary, to which extent of the direct root illumination interferes with directional root growth modulation, and which experimental setups were developed to reduce the impact of light on root growth was recently published by Lacek et al., 2021(*50*).

3. Published content

3.1. Review articles

3.1.1. Polar Auxin Transport

Authors: Jozef Lacek, Katarzyna Retzer, Christian Luschnig, Eva Zažímalová

Summary:

This review is focused on group of plant signaling compounds (auxins) and their proper distribution highlighting polar auxin transport in plants. Proper plant growth, development and adaptation to external and internal stimuli is regulated by auxins. Temporal and spatial control of auxin levels, which cause asymmetric auxin distribution and establishes auxin minima and maxima, is a key to activate mechanisms of plant growth development and adaptation processes. The appropriate local auxin level is achieved by regulation of its biosynthesis as well as metabolic control, and through the active, cell-to-cell transport relying on auxin carriers that are embedded in the plasma membrane. Polar auxin transport is mediated from shoot apical meristem to root tip (basipetal) and from root tip upwards to root elongation zone (acropetal). Owing to the physical–chemical properties of the auxin molecule, the asymmetric (polar) localization of auxin efflux carriers, analogous in neighboring cells, determines the direction of intercellular auxin flow.

PIN protein family is plant specific group of eight auxin carriers. Based on the size of their central loop, two types of PINs can be distinguished: Type-I, which represents group of plasma membrane-localized proteins with ability to maintain auxin efflux, and Type-II, which are at least partly present on the membrane of endoplasmic reticulum and are likely to regulate localization/compartmentation of auxin within the plant cell. Influx of auxin into cells is mediated via the AUX1/LAX protein family, which at optimal pH can increase auxin influx from 10 to 20-fold compared to passive diffusion. ABC proteins are known for transport of various cargo through the plasma membrane. Several ABC B-type proteins are proven to specifically transport auxin, and in some cases, the direction of it can be regulated based on the actual auxin content within the cell they are localized in. Regulation of polar auxin transport is mediated through several mechanisms on different levels. Transcriptional level of auxin carriers' control is facilitated by specific auxin response factors while posttranslational regulation includes phosphorylation, ubiquitination, as well as endocytosis and protein sorting. Lipid membrane composition and other phytohormones also play important role in regulation of abundance and polarity of auxin carriers which in turn regulates polar auxin transport.

My contribution: As the first author, I summarized results of the original research papers, and contributed to writing and editing the text.

Polar Auxin Transport

Advanced article

Lacek Jozef, *Institute of Experimental Botany CAS, Prague, The Czech Republic*

Retzer Katarzyna, *Institute of Experimental Botany CAS, Prague, The Czech Republic*

Luschnig Christian, *University of Natural Resources and Life Sciences (BOKU), Vienna, Austria*

Zažímalová Eva, *Institute of Experimental Botany CAS, Prague, The Czech Republic*

Based in part on the previous version of this eLS article 'Polar Auxin Transport' (2007) by Isabelle Bohn Courseau and Jan Traas.

Article Contents

Online posting date: 17th April 2017

Auxins, a group of plant signalling compounds, ensure proper growth and development of the plant in relation to both external and internal stimuli. Within a plant, auxin is distributed asymmetrically, thus creating local auxin maxima and minima. Such asymmetric auxin distribution underlies many developmental and stress adaptation processes and facilitates their spatial and temporal coordination. The appropriate local auxin level is achieved by regulation of biosynthesis, metabolism and through active, cell-to-cell transport relying on auxin carriers that are embedded in the plasma membrane. Owing to the physical–chemical properties of the auxin molecule, the asymmetric (polar) localisation of auxin efflux carriers, analogous in neighbouring cells, determines the direction of intercellular auxin flow (polar auxin transport). With respect to the important function of polar auxin transport for plant development, the polar auxin transport machinery is subject to a tight control at multiple regulatory levels.

Introduction

Auxins, which represent a group of rather simple organic compounds, are nowadays known as key regulators of plant growth (Bennett and Leyser, 2014; Habets and Offringa, 2014). However, auxin research has a long and colourful history. Already in the nineteenth century, Julius von Sachs and Charles and Francis Darwin postulated the existence of then unknown plant growth regulators influencing diverse aspects of plant development and adaptation to environmental changes. In 1926, Went was able to isolate a major endogenous auxin, indole-3-acetic acid (IAA) (**Figure 1a**), which was given its trivial name after the Greek word 'auxein' – to grow, elongate – [reviewed by Retzer *et al*., (2014)]. Related auxinic compounds have been identified later on, for example indole-3-butyric acid (IBA), 4-chloroindole-3-acetic acid (4-Cl-IAA) and phenylacetic acid (PAA), exhibiting activities distinct from but overlapping with those of IAA (Simon and Petrášek, 2011). The biological role of IAA has been studied extensively during the past decades, and its activities throughout the life cycle of plants are meanwhile well understood (Bennett and Leyser, 2014; Habets and Offringa, 2014). Auxin activities in shaping plant architecture and morphogenesis can principally be attributed to its impact on cell division, cell expansion and cell differentiation. Variations in the intensity of auxin-induced effects on these principal cellular processes define plant growth and development in response to intrinsic and environmental determinants and are influenced by various parameters: This involves responsiveness to auxin, which depends on the effectiveness of auxin perception and signalling, and the ways how auxin pool becomes available (establishing auxin homeostasis) for signalling pathways, thereby together modulating spatiotemporal variations in auxin sensitivity. **See also**: **Shoot Branching and Plant Architecture**; **Transcriptional Regulation in Plants**

Variations in auxin homeostasis are under tight metabolic control, with several auxin biosynthesis pathways being characterised in higher plants. In *Arabidopsis*, tryptophan-dependent auxin biosynthesis has been characterised to some extent, with juvenile organs representing a major site for auxin synthesis (reviewed by Gao and Zhao, 2014). IBA represents another auxin source; as in some species and/or tissues, it is converted to IAA via β-oxidation in peroxisomes and suggested to backup tryptophan-dependent auxin metabolism (Strader and Bartel, 2011). Intracellular compartmentalisation represents an additional means to control activity of auxin, as suggested for auxin shuttling between cytoplasm and endoplasmic reticulum (ER) or, alternatively, the vacuolar compartment (reviewed by

eLS subject area: Plant Science

How to cite:
Jozef, Lacek; Katarzyna, Retzer; Christian, Luschnig; and Eva, Zažímalová (April 2017) Polar Auxin Transport. In: eLS. John Wiley & Sons, Ltd: Chichester.
DOI: 10.1002/9780470015902.a0020116.pub2

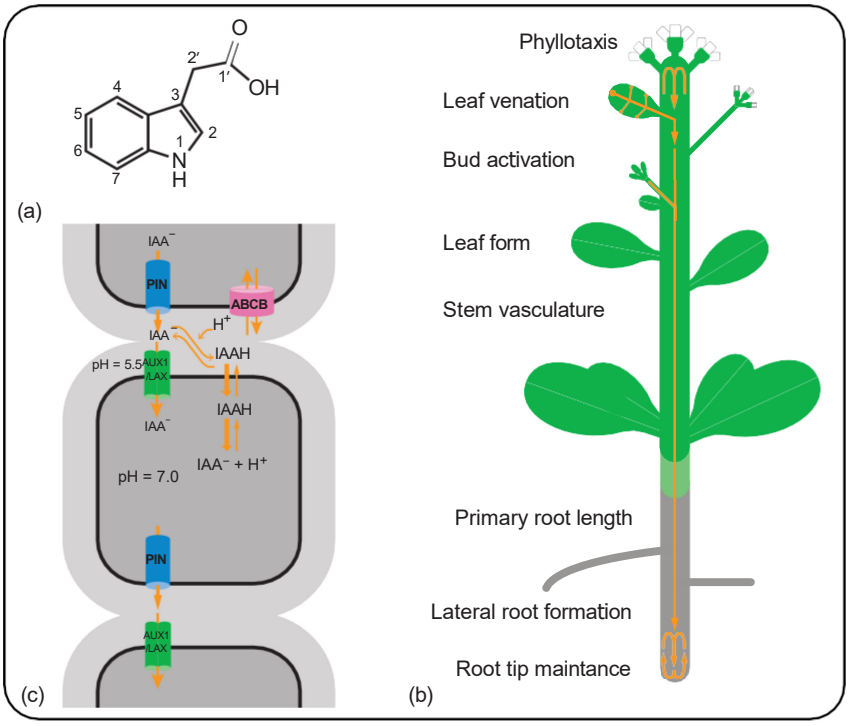

Figure 1 Auxin and its transport. (a) Chemical structure of the most abundant native auxin indole-3-acetic acid (IAA). (b) Auxin flow through plant. Postembryonic plant growth and development is regulated by auxin distribution (symbolised by arrows) to create auxin minima and maxima. In the shoot, reverse, and in the root, inverse fountain-like auxin flow (Benková *et al.*, 2003) maintains proper plant growth and allows adaptation to environmental changes. Main processes regulated by auxin are emphasised. Adapted from Prusinkiewicz and Runions (2012) © John Wiley and Sons Ltd. (c) Cell-to-cell auxin transport. The short-distance, cell-to-cell auxin transport is achieved by the defined, often polar, localisation of individual transporters and underlies the formation of auxin minima and maxima, which are important for proper plant growth and adaptation to environmental stimuli. IAA (auxin) can enter the cell either in a protonated form (IAAH) via passive transport or as an anion through the influx carriers from the family AUX1/LAX and some members of the ABCB family. Inside the cell, IAAH dissociates because of the higher pH within the cytoplasm. IAA anion (IAA^-) cannot pass the membrane by passive diffusion; therefore, it must be exported by active transport through plasma membrane-localised efflux carriers belonging to either PIN of ABCB families. Thus, the auxin efflux carriers represent bottlenecks in auxin movement through cells and it is their polar localisation (if analogous in neighbouring cells) that determines the direction of the auxin flow.

Scheuring and Kleine-Vehn, 2014); movement of auxin across the ER membrane seems to be mediated by transport proteins belonging to PIN-FORMED (PIN5, PIN6 and PIN8; Mravec *et al.*, 2009) and PIN-LIKES (PILS) families (reviewed by Barbez and Kleine-Vehn, 2013), whereas vacuolar transport requires activity of WALLS ARE THIN 1 (WAT1; Ranocha *et al.,* 2013). Conjugation to various simple organic compounds has been described for ER-resident IAA, resulting either in reversible inactivation of the growth regulator or representing an intermediate of irreversible, oxidative auxin degradation (Gao and Zhao, 2014).

Finally, and main subject of this overview, carrier protein-mediated cell-to-cell transport of auxin has been found to be crucial for a tight control of auxin-regulated developmental processes (examples are given in **Figure 2**). Specifically, variations in abundance, activity and subcellular localisation of such plasma membrane-(PM)-localised transport have been associated with establishment and maintenance of auxin concentration and hence activity gradients (Petrášek and Friml, 2009; Grones and Friml, 2015). Owing to the central role in plant morphogenesis that has been attributed to controlled auxin distribution within the plant body, it is no big surprise that elements of the auxin transport machinery have been subject to intense investigation. Here, we try to summarise recent progress in this quickly proliferating field of plant research, with particular emphasis on regulatory and physiological implications of directional (polar) auxin transport in the plant's interaction with its environment.

Polar Auxin Transport and Its Mediators

From the first zygotic cell division on, active auxin transport shapes differentiation of the entire plant body (Smit and Weijers, 2015). This depends on the establishment of auxin transport routes from source to sink sites, ensuring timely delivery of the growth regulator to its target sites. This process is known as polar auxin transport (PAT), which was initially characterised by applying labelled IAA to plant tissue and was demonstrated to be an active, protein-mediated process although one part of auxin pool is transported by passive auxin-flux in the phloem over long distances [reviewed by Petrášek and Friml, (2009)].

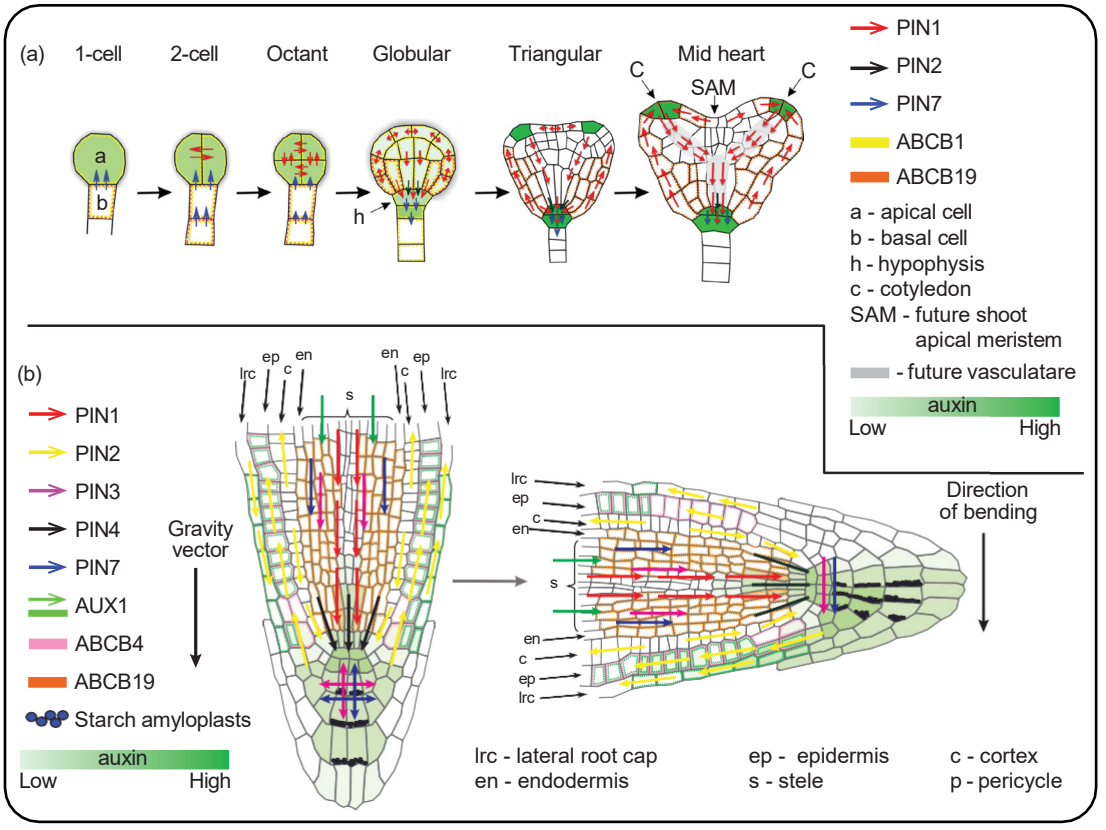

Figure 2 Auxin transporters and auxin flow during embryogenesis and root gravitropic response. Auxin regulates many aspects of plant development and adaptation to environmental stimuli. In this figure, we describe the involvement of polar auxin transport at early steps of plant development (embryogenesis) and during the response of the root to gravitropic stimulus. Adapted from Petrášek and Friml (2009). (a) Auxin distribution during embryogenesis. Arrows indicate auxin flow mediated by a particular transporter; dotted lines indicate the cell-type-specific localisation of particular auxin transporters with no obvious polarity. PIN7, localised at the apical sides of the suspensor cells (s), transports auxin towards the apical cell (a) that forms the proembryo; therefore, PIN1, which is localised at all inner cell sides, distributes auxin homogenously. ABCB1 and ABCB19 cooperate during this initial stage and are localised apolarly in all cells or only in the uppermost suspensor cell, respectively. The crucial moment in the setting of the basal end of the apical–basal embryonic axis occurs during the early globular stage, when PIN1 starts to be localised basally in the proembryonal cells, and PIN7 is simultaneously shifted from the apical to the basal plasma membrane of suspensor cells. These PIN polarity rearrangements reverse the auxin flow downwards and, with the aid of PIN4, lead to auxin accumulation in the forming hypophysis (h). At this stage, ABCB19 helps to maintain the auxin distribution in the outer layers of the embryo. In triangular- and heart-stage embryos, bilateral symmetry is established through auxin maxima at the incipient cotyledon (c) primordia. These auxin maxima are generated by PIN1 activity in the epidermis; in the inner cells of cotyledon primordia, however, PIN1 mediates basipetal auxin transport towards the root pole. SAM, future shoot apical meristem. (b) Positive root gravitropism. In starch-containing, gravity-sensing columella cells, PIN3 is relocalised from a symmetric distribution (left) towards the newly established bottom side after gravistimulation (right). The auxin that is redirected to the lower side of the root tip is further transported to the elongation zone by epidermal PIN2/AUX1mediated flow, where it inhibits the cell growth and causes the downward bending of the root. ABCB4 and ABCB19 are considered to regulate gravitropic response, as their mutants show enhanced root gravitropic bending. Coloured arrows indicate auxin flow mediated by a particular transporter; dotted lines indicate the cell-type-specific localisation of particular auxin transporters with no obvious polarity and black arrows indicate the gravity vector (left) and the direction of bending (right). Adapted from Petrášek and Friml (2009) © Company of Biologists Ltd.

Major PAT routes (**Figure 1b**) involve transport from the shoot apex towards the root tip (basipetal in shoot and acropetal in root or 'rootward' transport) and furthermore from the very root tip into the root elongation zone [basipetal, or 'shootward' transport; review by Petrášek and Friml (2009)]. Additional transport routes have been associated with defined processes, such as lateral auxin transport in the regulation of directional, tropic organ growth and auxin cycling in the outer cell files of root meristem, crucial for stabilising established auxin maxima (Petrášek and Friml, 2009; Habets and Offringa, 2014).

PAT occurs via coaction of the active cell-to-cell transport and passive diffusion (**Figure 1c**), in a polar manner to create hormone maxima and minima [reviewed by Reemmer and Murphy (2014)]. IAA is a weak acid (pK_a 4.75) and in the apoplast at a pH of 5.5, around 15% of IAA is protonated (IAAH). According to the chemiosmotic hypothesis for PAT, protonated and thus less polar IAAH would enter the cell via diffusion across the PM, followed by its deprotonation in the almost pH-neutral cytoplasmic compartment (reviewed by Habets and Offringa, 2014). As a result, any further translocation of the resulting IAA^-

anion across the PM thus would rely predominantly on specific protein-dependent transport activities. Consequently, variations in the distribution of relevant carrier proteins in distinct PM domains would define the overall directionality of auxin flow throughout cell files or entire organs. Several auxin transport activities have been identified in recent years [reviewed by Zažímalová *et al.*, (2010)], which were initiated with characterisation of AUXIN1/LIKE-AUX1 (AUX1/LAX), facilitating cellular auxin uptake and paralleling passive diffusion processes (Bennett *et al.*, 1996). In contrast, some members of the PIN protein family act in cellular auxin efflux (Luschnig *et al*., 1998; Gälweiler *et al*., 1998; review by Kˇrecˇek *et al.,* 2009), which has also been demonstrated for some MULTIDRUG RESISTANCE/PHOSPHOGLYCOPROTEIN/ATP-BINDING CASSETTE OF B-TYPE (MDR/PGP/ABCB) proteins, with one of them reported to act both in auxin uptake and efflux (Kubeš *et al*., 2012). Apart from these canonical auxin transport activities, additional PM-located transporters have been associated with PAT. Nitrate transceptor NRT1.1, for example, links variations in nitrate availability to cellular auxin influx (Krouk *et al*. 2010).

AUX1/LAX Proteins

Auxin import into cells is facilitated by AUX1/LAX proteins, structurally resembling amino acid permeases, and reinforcing passive hormone diffusion specifically under physiological conditions with a high demand for auxin (reviewed by Swarup and Péret, 2012). Homologues of AUX1/LAX are present throughout the plant kingdom and their sequence is highly conserved (Hoyerová *et al*., 2008; Habets and Offringa, 2014). An ancient function for members of this family is indicated by the identification of AUX1/LAX orthologs in several single-celled and colony-forming chlorophyta species (De Smet and Beeckman, 2011). *Arabidopsis* AUX1 (AtAUX1) has been studied since the early 1980s, when it was described as root gravitropism mutant, resistant to the auxin analogue 2,4-D (Bennett *et al*., 1996). Later, it turned out that AUX1 expression and polar PM localisation, specifically in root epidermis and lateral root (LR) cap cells, are essential for gravitropic root bending (**Figure 2b**), presumably via mediating auxin flow from the very root tip into the root elongation zone (Sato *et al.,* 2015). Heterologous *AUX1* expression in *Xenopus* oocytes and further analysis *in planta* demonstrated high-affinity IAA transport activity with a pH optimum between 5 and 6 and approximately 15-times greater than passive membrane diffusion [review by Swarup and Péret (2012)]. This appears also the case for additional members of the *Arabidopsis* AUX1/LAX family, jointly involved in various developmental events. Redundant, overlapping activities for AUX1/LAX proteins are, for example, essential for the control of phyllotactic leaf patterning, reflected by severe aberrations in leaf positioning of *aux1 lax* loss-of-function mutant combinations (cf. **Figure 3d**, **f** and **g**) (Robert *et al*., 2015). AUX1 and LAX3 in particular have been implicated in LR development, jointly acting in LR initiation and emergence, highlighting key functions for members of this protein family in plant organogenesis (Swarup and Péret, 2012).

PIN-FORMED Proteins

Perhaps the most prominent case of so far identified auxin transport proteins is represented by the PIN-FORMED (PIN) family. Originally, identified as mutants with severe defects in plant development, subsequent cloning and functional characterisation of several different PIN proteins then revealed their central function in the regulation of polarity establishment in course of plant development (Petrášek and Friml, 2009; Zažímalová *et al*., 2010; Grones and Friml, 2015). The so-called type-I PIN proteins show PM localisation and are characterised by two hydrophobic domains, each with five predicted transmembrane helices, that are separated by a hydrophilic domain which apparently faces the cytoplasm (Kˇrecˇek *et al*., 2009; Nodzyn´ski *et al*., 2016). Type-II PINs (almost) lack the central loop and show preferential localisation to the ER, where they might control intracellular auxin transport (Mravec *et al*., 2009; Kˇrecˇek *et al*., 2009). However, and as is the case for AUX1/LAX proteins, the topology of PIN proteins remains poorly understood, with exception of a singly study, utilising pH-dependent quenching of different fluorescent reporter proteins and resulting in a first glimpse on the possible topology of PM-localised PINs (Nodzyn´ski *et al*., 2016).

Eight *PIN* genes have been identified in the *Arabidopsis* genome, with PIN-FORMED 1 (PIN1), PIN2, PIN3, PIN4 and PIN7 localising to the PM and acting in cellular auxin efflux (Vieten *et al.,* 2007; Kˇrecˇek *et al.,* 2009; Petrášek and Friml, 2009; Grones and Friml, 2015). PIN1 and PIN2 exhibit polar PM localisation, whereas PIN3, 4 and 7 exhibit both polar and nonpolar PM-localisation, depending on the cell type and growth conditions [reviewed by Habets and Offringa (2014)]. Such protein distribution, and dynamic variations therein, is believed to be essential for establishment and maintenance of auxin concentration gradients driving manifold processes during embryo patterning, organogenesis and tropisms (Petrášek and Friml, 2009; Zažímalová *et al*. 2010; Smit and Weijers, 2015). PM-localised PIN1, PIN2, PIN3, PIN4 and PIN7 all contain a large central hydrophilic loop characteristic for type-I PINs, while ER-resident PIN5 and PIN8 lack this domain. PIN6 is predicted to form an intermediate sized central loop and it was shown to be localised on both the PM and the ER (Simon *et al*., 2016). Interestingly, PIN proteins are found exclusively in plants and they seem to originate in streptophyte algae at the ER. However, the capacity to change PIN localisation at the PM from polar to nonpolar is crucial for developmental events in seed plants, and it was first established during polarised growth of tip-growing plant cells (Viaene *et al*., 2013, 2014).

Among the *Arabidopsis* type-I PINs, PIN1 acts in control of auxin distribution essentially throughout the entire lifecycle of plants (Okada *et al*., 1991; Gälweiler *et al*., 1998; recent review by Grones and Friml, 2015). Loss of *PIN1* results in pin-shaped inflorescence axes that fail to produce fertile flowers (cf. **Figure 3a** and **b**), a phenotype that can be phenocopied by application of high concentrations of inhibitors of PAT, such as 1-naphthylphthalamic acid (NPA) or 2,3,5-triiodobenzoic acid (TIBA) (Okada *et al*., 1991; Gälweiler *et al*., 1998), while

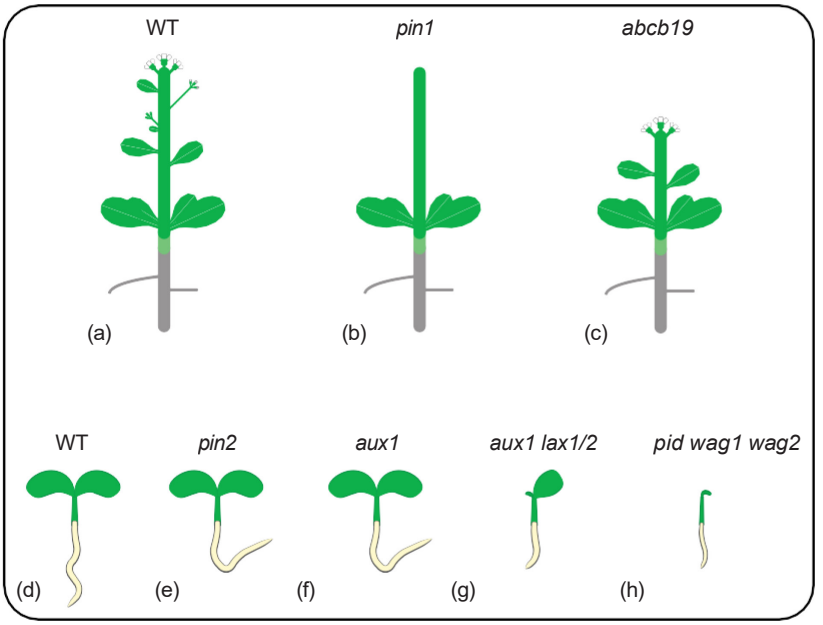

Figure 3 Mutant versions of crucial auxin transporters. Often, single mutants of auxin transporters do not show a dramatic phenotype, owing to the high redundancy within the protein families [described in Vieten *et al.*, (2005)]. The figure shows the most obvious phenotypes of selected auxin transporter mutants. (a) Phenotype of full-grown wild type plant. (b) The auxin efflux carrier PIN-FORMED 1 (PIN1) is expressed almost everywhere in the plant, but *pin1* mutants are characterised typically by an inflorescence meristem that does not initiate any flowers, resulting in the formation of a naked inflorescence stem (Gälweiler *et al.*, 1998). (c) The *abcb19* (ARABIDOPSIS THALIANA ATPBINDING CASSETTE B19) mutant shows phenotype consisting of several features connected to auxin action but the most obvious one is reduced stem height (partial dwarfism; Noh *et al.*, 2001). (d) Phenotype of wild-type *Arabidopsis* seedling. (e) Loss of function of an auxin influx transporter, *aux1* (AUXIN RESISTANT 1 (AUX1); Bennett *et al.*, 1996), as well as of the efflux transporter *pin2* (f) (EIR1/PIN-FORMED 2 (PIN2)/AGR1; Luschnig *et al.*, 1998; Müller *et al.*, 1998), results in agravitropic roots, as auxin is not only regulating proper plant growth but also adaptation to environmental changes, such as gravity stimulus. (g) Proper auxin distribution is crucial for organ development; therefore, the triple mutant of the auxin influx carrier aux1 lax1/2 results in misshaped seedlings (Robert *et al.*, 2015). (h) Loss of the closely related AGCVIII protein kinases *pid wag1 wag2*, which orchestrate the proper localisation of distinct auxin carriers, results in arrested development (Dhonukshe *et al.*, 2010).

localised application of auxin to *pin1* inflorescences induces floral organ formation underlining a key role for position-dependent auxin gradient formation during organogenesis. Together with additional PINs, PIN1 mediates rootward PAT from the shoot apex into the very root tip of *Arabidopsis* seedlings, controlling a range of patterning processes (Petrášek and Friml, 2009; Habets and Offringa, 2014). These events are well understood in root meristems, in which the entire set of *Arabidopsis* type-I PIN proteins orchestrates auxin distribution via redundant and nonredundant activities (Petrášek and Friml, 2009; Habets and Offringa, 2014). This requires activities of PIN1 together with PIN4 and PIN7 to accumulate auxin in columella root cap cells via the stele (Petrášek and Friml, 2009). Further shootward transport into the root elongation zone is mediated by PIN3 and PIN7 activities in the root cap cells, followed by PIN2-controlled auxin transport via LR cap and epidermis cells into root elongation zone. Notably, PIN2 has also been suggested to function in rootward transport via the root cortex, which together with its shootward transport activity establishes an auxin reflux loop, crucial for stabilising auxin flow in the process of root proliferation and differentiation (**Figure 2b**) (Petrášek and Friml, 2009). **See also**: **Gravitropic Signaling in Plants**

ABCB Proteins

ABCB proteins belong to a large membrane transporter family; few of them were shown to act as auxin transporters (Noh *et al.*, 2001), which are localised mostly in a nonpolar manner to the PM and show less dynamic trafficking compared to PIN proteins (Cho and Cho, 2013). ABCB1, ABCB4 and ABCB19 (*abcb19* mutant is shown in **Figure 3c**) require immunophillin-like protein TWD1 for their targeting to the PM (Geisler *et al.,* 2003). ABCB1 and ABCB19 were associated with long-distance auxin transport, as rootward auxin transport is even stronger reduced in *abcb19* and *abcb1abcb19* than in *pin1* mutants (Cho and Cho, 2013). ABCB19 was further described as a negative regulator of auxin-dependent tropic bending responses, owing to the increased rates of phototropic bending of the mutant (Peer *et al.,* 2011). ABCB19 stabilises PIN1 at the PM, as it localises to parts of the PM called detergent-resistant membrane (DRM), enriched in sitosterol and glucosylceramide. ABCB4 acts as influx carrier under low IAA concentration, whereas it changes to an efflux pump at high IAA amount (Kubeš *et al.,* 2012). ABCB4 is involved in root growth processes, shootward auxin transport and the mutant displays slightly enhanced root gravitropic bending.

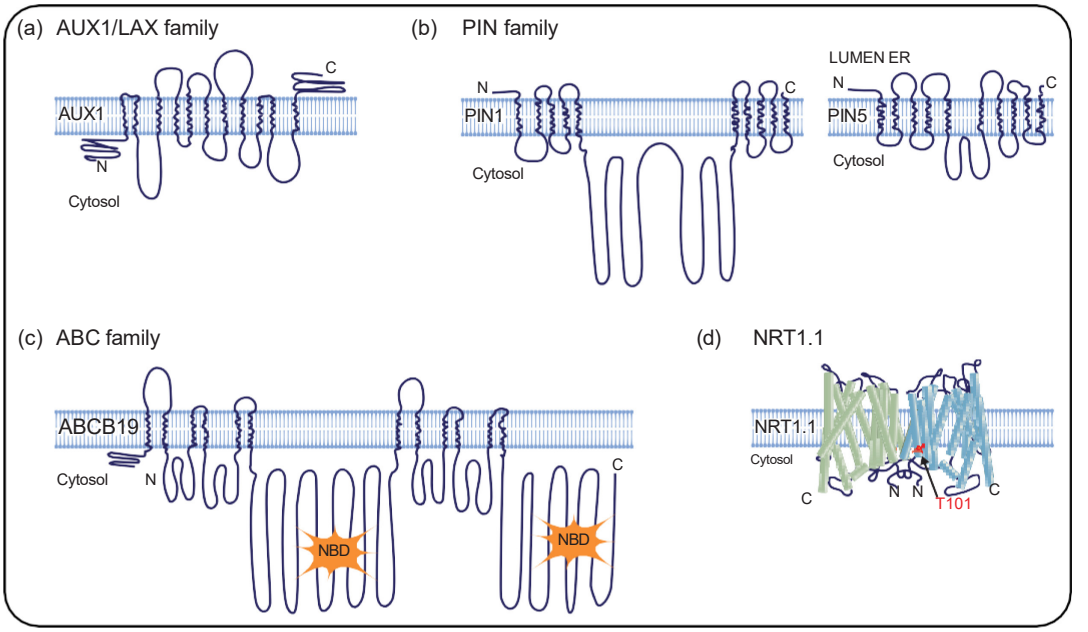

Figure 4 Predicted auxin transporters topology. (a) Auxin transporters of the AUX1/LAX family represented by the auxin influx carrier *At*AUX1, auxin transporters of the PIN family represented by the auxin efflux carrier *At*PIN1 with long cytosolic loop, (b) the endoplasmic reticulum (ER)-localised auxin carrier *At*PIN5 with short cytosolic loop (b) and (c) auxin transporters of the ABCB family represented by the auxin efflux carrier *At*ABCB19. Adapted from Petrášek *et al*. (2011) © Springer. (d) *At*NRT1.1 primarily functions as a dual-affinity transporter, which can change its affinity for nitrate in response to substrate availability. The figure shows a cylinder representation of the *At*NRT1.1 dimer with highlighted Thr101. The two monomers are coloured in pale green and light blue, according to Sun and Zheng (2015).

ABCB proteins support the other auxin carriers in the auxin distribution through the plant, as auxin is transported from the shoot to the root tip by PIN1 and ABCB19, while in the root, ABCB1 and ABCB19 exclude auxin from root cap cells and PIN2 and ABCB4 redirect auxin shootward in cortical and epidermal cells [reviewed by Cho and Cho (2013)].

Predicted topology of various auxin carriers is shown in **Figure 4**.

Regulation of the Polar Auxin Transport Machinery

Perhaps due to their important function in plant development, auxin transport proteins were found to be subject to stringent control mechanisms at multiple regulatory levels. This involves adjustments of carrier activities via transcriptional as well as posttranscriptional control. Variations in auxin transport activities arising from such regulation, cause variations in auxin flow, ultimately resulting in a delicate fine-tuning of plant patterning and adaptation (monograph by Zažímalová *et al.,* 2014 and references therein).

Regulation of auxin carriers transcription

Transcription of auxin transport proteins has been shown to respond to various stimuli, and recently, a few reports demonstrated how such regulation might participate in the regulation of plant morphogenesis. Auxin controls transcript levels of its transporters, which requires the activity of AUXIN-RESPONSE FACTOR (ARF) transcriptional regulators (Grones and Friml, 2015; Enders and Strader, 2015). For example, Arabidopsis ARF5/MONOPTEROS (MP) was shown to bind to *PIN1, 3* and *7* promoter elements, a response that appears essential for pattern formation and organogenesis throughout the plant's life cycle (Krogan *et al*., 2016). In related approaches, AUXIN RESPONSE FACTOR7 (ARF7) and the ARF7-regulated FOUR LIPS/MYB124 (FLP) were found to control *PIN3* as well as LATERAL ORGAN BOUNDARIES-DOMAIN 29 (*LBD29*) transcript levels, via binding to their respective promoters (Chen *et al*., 2015; Porco *et al*., 2016). LBD29 in turn regulates transcription of auxin influx transporter LAX3, which, together with auxin-mediated variations in *PIN3* transcription, has pronounced effects on LR formation (Chen *et al*., 2015; Porco *et al.*, 2016). These findings beautifully highlight the importance to coordinate activities of distinct auxin transport mechanisms via transcriptional circuits. Numerous additional stimuli were found to impact on transcript levels of auxin transport proteins, and it will be exciting to learn about the biological roles of resulting adjustments in auxin transport and distribution.

Posttranslational regulatory mechanisms orchestrating intracellular trafficking

Deciphering mechanisms of posttranscriptional control of auxin transport proteins has led to amazing insights into protein sorting

in general and its implications for plant development in particular (Luschnig and Vert, 2014; Armengot *et al*., 2016). As is the case for any PM protein, sorting of auxin transport proteins involves a defined order of events, guiding their subcellular distribution and abundance in a spatiotemporal context, which in turn defines auxin transport rates with all its consequences for morphogenesis. PM proteins are subject to vesicular transport from the ER via the Golgi and trans-Golgi network/early endosomes (TGN/EE) to the PM (Luschnig and Vert, 2014). Components of the secretory sorting pathway appear well conserved in eukaryotes. The multisubunit exocyst protein complex, for example, is also present in plants and seemingly required for PIN delivery to the PM (Drdová *et al*., 2013), indicated by alterations in PAT and pronounced defects in PIN sorting upon loss of Arabidopsis exocyst subunit SEC6 (Tan *et al.,* 2016).

Protein targeting to the PM is followed by their (re)-internalisation via an endocytic sorting pathway. In case of PIN proteins, initial steps depend on recognition by the clathrin sorting machinery, guiding cargo back to the TGN/EE. From there, cargo protein is either recycled to the PM or internalised into multivesicular bodies (MVBs) for its ultimate degradation in the lytic vacuole. Protein recycling has been linked to the function of ARF-GEF GNOM as well as the activity of the retromer protein complex, implicated in cargo recognition. This is indicated by mutant phenotypes, which in case of a loss of GNOM, results in cargo accumulation in the so-called recycling endosomes (RE), while deficiencies in retromer activity have been associated with increased vacuolar targeting of PM cargo. Sorting into MVBs, and subsequent cargo release into the vacuole on the other hand, requires elements of the so-called ESCRT-machinery, mediating cargo recognition and further guidance to the lytic compartment [reviewed by Luschnig and Vert (2014)].

It is the interplay between these distinct protein trafficking routes, taking places at various intersections, which ultimately decides about cargo retention time and abundance at the PM. Mechanisms and processes controlling this interplay are various, some of which demonstrated to affect auxin transport proteins as well.

Posttranslational modification by ubiquitination regulating auxin carrier abundance

A key determinant, triggering vacuolar sorting of membrane proteins is their reversible modification by the small protein modifier ubiquitin (Luschnig and Vert, 2014). Ubiquitination has so far been demonstrated for root-specific PIN2, which is seemingly modified by ubiquitin chains linked via lysine 63, a type of modification, signalling vacuolar targeting in eukaryotes. Upon interference with PIN2 ubiquitination by mutagenesis of a substantial number of lysines found in its central hydrophilic loop and representing potential ubiquitination sites, PIN2 was no longer efficiently targeted to the vacuole and such mutant pin2 alleles were no longer capable of rescuing a pin2 loss-of-function allele, indicating that this type of modification is indeed essential for protein function (Leitner *et al.*, 2012). Thus, reversible protein ubiquitination seemingly affects PIN protein levels at the PM, which in turn could influence auxin flow rates and interdependent developmental processes.

Posttranslational modification by phosphorylation controlling auxin carrier polarity and abundance

Control of phosphorylation represents another type of protein modification, which was found to affect the function of auxin transport components at different regulatory levels [reviewed by Armengot *et al.* (2016)]. Specifically, members of the AGC protein kinase family were shown to modulate polar targeting as well as the activity of PIN and ABCB proteins, respectively. PINOID (PID) represents the founding member of the AGCVIII subfamily in Arabidopsis, mutants of which develop growth defects strikingly resembling those of *pin1* loss-of-function alleles. Further analysis demonstrated an apical-to-basal shift of polarly localised PIN proteins in *pid* mutant background (Friml *et al.*, 2004). Related findings were made in a *pid wag1 wag2* triple mutant defective in three closely related AGCVIII protein kinases (**Figure 3h**), in which apically located PIN2 in root epidermis cells got relocated to the basal PM domain (Dhonukshe *et al.,* 2010). Opposite observations have been made in a *PID* overexpression line, in which basally localised PIN proteins underwent a basal-to-apical switch in their subcellular localisation. Evidently, such relocation of PINs should result in major adjustments in the directionality of auxin transport, which is indicated by pronounced variations in the expression pattern of auxin-responsive reporter proteins. Severe mutant phenotypes that can be observed in *pid/wag* loss- or gain-of-function lines therefore are likely the result of redistribution of PIN proteins. This led to the question whether or not PIN proteins represent actual substrates for PID/WAG-encoded kinase activity. Several experiments suggest that this could indeed be the case: Both *in vitro* and *in vivo* experiments indicated that PID recognises three highly conserved potential phosphorylation sites found in the hydrophilic PIN loop region. Mutagenesis of these sites creates *pin* alleles either mimicking constitutive phosphorylation or no longer phosphorylated; here, altered PIN localisation observed in *pid/wag* gain- and loss-of-function lines could be recapitulated. This indicates that PID/WAG-mediated phosphorylation of PINs functions indeed as a PIN polarity determinant. Furthermore, PROTEIN PHOSPHATASE 6 (PP6) holoenzyme has been identified as antagonist of PID/WAGs, catalysing dephosphorylation of PIN proteins (Ballesteros *et al*., 2013). Consistently, a loss of PP6 subunits results in PIN localisation opposite to that observed in *pid/wag* loss-of-function lines, supporting models in which dephosphorylated PINs have a tendency to accumulate at the basal domain, whereas phosphorylation triggers their sorting to the apical pole.

Apart from antagonistic activities of PID/WAG and PP6, additional kinases belonging to the AGC1 subfamily were found to modify PIN proteins at a distinct but overlapping set of phosphorylation sites (Zourelidou *et al*., 2014). D6 PROTEIN

KINASE (D6PK) and closely related D6PK-LIKE (D6PKL) were found to localise predominantly to the basal pole of cells, colocalising with basally accumulating PIN proteins (Barbosa *et al*., 2014; Willige *et al*., 2013). However, unlike PID/WAG-mediated phosphorylation, D6PKs do not strikingly affect localisation of PIN proteins, but rather affect activity of PIN proteins in cellular auxin efflux, as has been convincingly demonstrated by transport assays in *Xenopus* oocytes (Zourelidou *et al*., 2014). Differing effects of PIN phosphorylation at overlapping, and differing phosphorylation sites, argue for distinct roles of protein kinase activity in the regulation of PINs. This might also be the case for ABCB-type proteins, as PID was demonstrated to phosphorylate ABCB1 and to modulate its activity upon heterologous expression in tobacco cells (Henrichs *et al*., 2012). Furthermore, ABCB19-driven auxin efflux activity is negatively regulated by the action of the blue-light photoreceptor kinase PHOTROPIN1 (PHOT1; Christie *et al*., 2011). It is still unclear though, if and how aforementioned kinase activities could affect interlinked functions of PINs and ABCBs in directional distribution of auxin. It is also not known by which mechanisms phosphorylation of auxin transport proteins could affect protein localisation and activities. Recently, Arabidopsis peptidyl-prolyl *cis/trans* isomerase Pin1At has been demonstrated to modulate distribution of PIN1 via pathways, overlapping with activities of PID and PP6 (Xi *et al*., 2016). The authors of this study furthermore provided experimental evidence for a scenario, in which PIN phosphorylation promotes Pin1At-catalysed *cis/trans* conformational changes in the central loop domain (Xi *et al*., 2016). It will be very interesting to learn whether or not such conformational changes could impact on function and subcellular localisation of PINs.

Cellular processes that are involved in regulation of auxin carrier proteins are depicted in **Figure 5**.

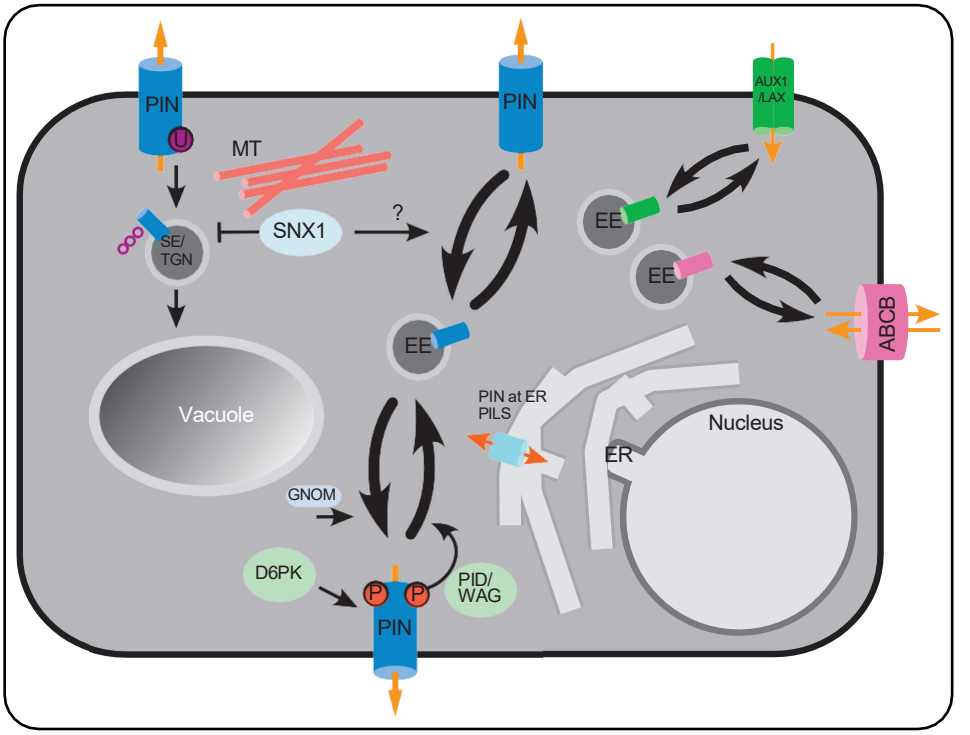

Figure 5 Cellular processes involved in auxin transport regulation. This figure shows a schematic overview of cellular distribution of main auxin carriers and processes that are involved in control of their abundance, localisation and activity. Cellular uptake of auxin is mediated by proteins from the auxin influx carrier family AUX1/LAX and by selected ABCB transporters. Cellular auxin efflux requires the action of certain ABCB transporters, and PINs (PIN1, 2, 3, 4, 7) at the plasma membrane (PM). Localisation of PINs (PIN5, 6, 8) at the endoplasmic reticulum (ER) membrane, together with some proteins from the PILS family, leads to compartmentalisation of auxin between cytoplasm and lumen of the ER, thus modifying overall auxin metabolic conversion. Auxin homeostasis is sensed by nuclear TIR1/AFB-Aux/IAA coreceptor complexes. Intracellular trafficking of the auxin transporters regulates their abundance at the PM, comprising both recycling back to the PM (GNOM-dependent, over early endosomes, EE) and the targeting to the lytic vacuole for degradation (over sorting endosomes (SE) and the trans-Golgi network (TGN)). Although all auxin transporters undergo intracellular trafficking, PIN2 was most studied so far. Endocytic sorting and further targeting of PIN proteins into the lytic vacuole depends on putative retromer subunit SNX1, which functions as a gating factor, promoting protein recycling to the PM and thereby antagonising vacuolar sorting. CLASP-mediated tethering of SNX1 to microtubules links PIN sorting to cytoskeleton components. Posttranslational modifications regulate the abundance, polarity and activity of auxin transporters: ubiquitylation targets PINs towards the lytic vacuole, phosphorylation regulates either their polarity (by PID/WAG) towards apical PM or their activity (by D6PK). U, ubiquitin; P, phosphate and MT, microtubules. Adapted from Retzer *et al*. (2014) © Springer.

Membrane Lipid Composition Mediating Auxin Carrier Sorting

Lipid composition of cellular compartments represents another major determinant in the regulation of protein sorting and some studies revealed its role in the regulation of PAT. Sterols, together with saturated phospholipids and sphingolipids, cluster together with diverse membrane proteins at the TGN, influencing sorting to the PM and thereby contribute to trafficking of PINs, ABCBs and AUX1 to their respective membrane domains (Yang *et al.*, 2013). Upon loss of Arabidopsis *CYCLOPROPYL ISOMERASE1* (*CPD1*), in particular, PIN2 was found to accumulate at apical and basal domains of root meristem epidermis cells, highlighting a role for sterol composition in sorting decisions and cellular polarity establishment. Deficiencies in sphingolipid biosynthesis interfere with the sorting of PINs and AUX1 during early steps of the secretory pathway [reviewed by Luschnig and Vert (2014)]. This also appears to be the case for sphingolipids characterised by α-hydroxylated acyl-chains that become enriched in secretory vesicle subdomains of trans-Golgi network, modulating PIN2 polar sorting to apical PM domains in root meristem cells (Wattelet-Boyer *et al*., 2016).

Phosphatidylinositol phosphates (PIPs) represent a class of lipid molecules characterised by different phosphorylation patterns at their inositol group. While representing only a minor fraction among membrane lipids, PIPs control various aspects of membrane protein sorting. A characteristic feature of distinct PIPs is their quite heterogeneous distribution in different cellular compartments, a feature underlying their function as docking platforms mediating intracellular vesicle translocation along defined sorting routes. PI4P and PI(4,5)P2, for example, were found to exhibit a slightly polar PM localisation, enriched at basal and apical domains. Consistently, phosphatidylinositol 4-phosphate 5-kinases PIP5K1 and PIP5K2, which mediate phosphorylation of PI4P on position 5 to give PI(4,5)P2, exhibit a similar polar localisation and were also found to affect PAT. *Pip5k1 pip5k2* double mutants, in particular, exhibit prominent deficiencies in auxin-controlled aspects of plant morphogenesis and adaptive growth responses, which has been associated with altered PIN sorting dynamics and polar PM distribution observed in these mutants [currently reviewed by Armengot *et al*. (2016)]. It is not yet clear how variations in PIP composition might affect sorting and polarity of PIN proteins, but some kind of interplay with additional PIN polarity determinants appears possible. PI4P and PI(4,5)P2 were shown to interact with AGC-type kinases PID and D6PK *in vitro*, and PID targeting to the PM appears to depend on electrophysiological properties of PI4P (Armengot *et al.,* 2016). Whether or not such sorting control impacts on phosphorylation and hence subcellular targeting of PIN proteins remains to be determined though.

Additional Regulatory Mechanisms

Apart from the aforementioned controlling machineries that are currently explored in more detail, numerous additional effectors of PAT have been identified. This involves small compounds, acting as inhibitors of PAT, affecting protein sorting or activity of auxin transport proteins [reviewed recently by Klíma *et al*., (2016)]. Several of these are synthetic compounds and they serve to elucidate various aspects of PAT and its physiological significance (above all NPA, and TIBA). However, there is an increasing body of evidence indicating the existence of naturally occurring compounds interfering with auxin transport and/or establishment and maintenance of auxin homeostasis (e.g. products of phenylpropanoid pathway, Steenackers *et al.,* 2016).

There are also established links between various hormone-signalling events and their effects on PAT. Strigolactone, for example, affects shoot branching by modulating PIN1 sorting in a clathrin-dependent manner, influencing auxin distribution in the stem and regulating lateral bud outgrowth (Shinohara *et al*., 2013*).* Further interactions were reviewed by Luschnig and Vert (2014): Cytokinin specifically regulates PIN1 trafficking and polar deposition at the PM at early stages of LR primordium formation; gibberellic acid controls PIN2 sorting and auxin distribution in gravistimulated roots, presumably by differential stabilisation of PIN2 at the PM; related effects on endocytic PIN sorting have been observed in response to treatment with methyl jasmonate.

These examples highlight excessive crosstalk between PAT and a highly diverse array of signalling events taking place throughout the life cycle of a higher plant. It remains essentially unresolved though, how all these pathways might combine in order to coordinate various signals and PAT in the developing plant body. Integration of these events into a single coherent model remains a challenge for future research.

Acknowledgements

Research work of the authors is currently supported by grants from the Czech Science Foundation (16-10948S) and the Czech Ministry of Education, Youth and Sports (project LD15088) to E.Z., and by the FWF (Austrian Science Fund P25931) to C.L. We thank Juergen Retzer for his work as an illustrator and Jan Petrášek for valuable discussions.

References

Armengot L, Caldarella E, Marquès-Bueno MM and Martínez MC (2016) The protein kinase CK2 mediates cross-talk between auxin- and salicylic acid-signaling pathways in the regulation of PINOID transcription. *PLoS ONE* **11**: 1–15.

Ballesteros I, Domínguez T, Sauer M, *et al.* (2013) Specialized functions of the PP2A subfamily II catalytic subunits PP2A-C3 and PP2AC4 in the distribution of auxin fluxes and development in Arabidopsis. *Plant Journal* **73**: 862–872.

Barbez E and Kleine-Vehn J (2013) Divide Et Impera-cellular auxin compartmentalization. *Current Opinion in Plant Biology* **16**: 78–84.

Barbosa ICR, Zourelidou M, Willige BC, Weller B and Schwechheimer C (2014) D6 PROTEIN KINASE activates auxin transport-dependent growth and PIN-FORMED phosphorylation at the plasma membrane. *Developmental Cell* **29**: 674–685.

Benková E, Michniewicz M, Sauer M, *et al.* (2003) Local, efflux-dependent auxin gradients as a common module for plant organ formation. *Cell* **115**: 591–602.

Bennett MJ, Marchant A, Green HG, *et al.* (1996) Arabidopsis AUX1 gene: a permease-like regulator of root gravitropism. *Science (New York, N.Y.)*, **273**: 948–950.

Bennett T and Leyser O (2014) In: Zažímalová E, Petrášek J and Benková E (eds) *Auxin and Its Role in Plant Development*. Vienna: Springer Vienna.

Chen Q, Liu Y, Maere S, *et al.* (2015) A coherent transcriptional feed-forward motif model for mediating auxin-sensitive PIN3 expression during lateral root development. *Nature Communications* **6**: 8821.

Cho M and Cho H-T (2013) The function of ABCB transporters in auxin transport. *Plant Signaling & Behavior* **8**: e22990.

Christie JM, Yang H, Richter GL, *et al.* (2011) Phot1 inhibition of ABCB19 primes lateral auxin fluxes in the shoot apex required for phototropism. *PLoS Biology* **9**: e1001076.

De Smet I and Beeckman T (2011) Asymmetric cell division in land plants and algae: the driving force for differentiation. *Nature Reviews. Molecular Cell Biology* **12**: 177–188.

Dhonukshe P, Huang F, Galvan-Ampudia CS, *et al.* (2010) Plasma membrane-bound AGC3 kinases phosphorylate PIN auxin carriers at TPRXS(N/S) motifs to direct apical PIN recycling. *Development* **137**: 3245–3255.

Drdová EJ, Synek L, Pecˇenková T, *et al.* (2013) The exocyst complex contributes to PIN auxin efflux carrier recycling and polar auxin transport in Arabidopsis. *Plant Journal* **73**: 709–719.

Enders TA and Strader LC (2015) Auxin activity: past, present, and future. *American Journal of Botany* **102**: 180–196.

Friml J, Yang X, Michniewicz M, *et al.* (2004) A PINOID-dependent binary switch in apical-basal PIN polar targeting directs auxin efflux. *Science* **306**: 862–865.

Galweiler L, Guan C, Muller A, *et al.* (1998) Regulation of polar auxin transport by AtPIN1 in Arabidopsis vascular tissue. *Science* **282**: 2226–2230.

Gao Y and Zhao Y (2014) *Auxin and Its Role in Plant Development*, vol. **33**, pp. 21–33. Vienna: *Springer*.

Geisler M, Kolukisaoglu HU, Bouchard R, *et al.* (2003) TWISTED DWARF1, a unique plasma membrane-anchored immunophilin-like protein, interacts with Arabidopsis multidrug resistance-like transporters AtPGP1 and AtPGP19. *Molecular Biology of the Cell* **14**: 4238–4249.

Grones P and Friml J (2015) Auxin transporters and binding proteins at a glance. *Journal of Cell Science* **128**: 1–7.

Habets MEJ and Offringa R (2014) PIN-driven polar auxin transport in plant developmental plasticity: a key target for environmental and endogenous signals. *New Phytologist* **203**: 362–377.

Henrichs S, Wang B, Fukao Y, *et al.* (2012) Regulation of ABCB1/PGP1-catalysed auxin transport by linker phosphorylation. *The EMBO Journal* **31**: 2965–2980.

Hoyerová K, Perry L, Hand P, *et al.* (2008) Functional characterization of PaLAX1, a putative auxin permease, in heterologous plant systems. *Plant Physiology* **146**: 1128–1141.

Klíma P, Lanˇková M and Zažímalová E (2016) Inhibitors of plant hormone transport. *Protoplasma* **253**: 1391–1404.

Kˇrecˇek P, Skůpa P, Libus J, *et al.* (2009) The PINFORMED (PIN) protein family of auxin transporters. *Genome Biology* **10**: 249.

Krogan NT, Marcos D, Weiner AI and Berleth T (2016) The auxin response factor MONOPTEROS controls meristem function and organogenesis in both the shoot and root through the direct regulation of PIN genes. *New Phytologist* **212**: 42–50.

Krouk G, Lacombe B, Bielach A, *et al.* (2010) Nitrate-regulated auxin transport by NRT1.1 defines a mechanism for nutrient sensing in plants. *Developmental Cell* **18**: 927–937.

Kubeš M, Yang H, Richter GL, *et al.* (2012) The Arabidopsis concentration-dependent influx/efflux transporter ABCB4 regulates cellular auxin levels in the root epidermis. *Plant Journal* **69**: 640–654.

Leitner J, Retzer K, Korbei B and Luschnig C (2012) Dynamics in PIN2 auxin carrier ubiquitylation in gravity-responding Arabidopsis roots. *Plant Signaling & Behavior* **7**: 1271–1273.

Luschnig C, Gaxiola RA, Grisafi P and Fink GR (1998) EIR1, a root-specific protein involved in auxin transport, is required for gravitropism in Arabidopsis thaliana. *Genes and Development* **12**: 2175–2187.

Luschnig C and Vert G (2014) The dynamics of plant plasma membrane proteins: PINs and beyond. *Development* **141**: 2924–2938.

Mravec J, Skůpa P, Bailly A, *et al.* (2009) Subcellular homeostasis of phytohormone auxin is mediated by the ER-localized PIN5 transporter. *Nature* **459**: 1136–1140.

Müller A, Guan C, Gälweiler L, *et al.* (1998) *AtPIN2* defines a locus of *Arabidopsis* for root gravitropism control. *The EMBO Journal* **17**: 6903–6911.

Nodzyn´ski T, Vanneste S, Zwiewka M, *et al.* (2016) Enquiry into the topology of plasma membrane localized PIN auxin transport components. *Molecular Plant* **9**: 1504–1519.

Noh B, Murphy AS and Spalding EP (2001) Multidrug resistance-like genes of Arabidopsis required for auxin transport and auxin-mediated development. *The Plant Cell* **13**: 2441–2454.

Okada K, Ueda J, Komaki MK, Bell CJ and Shimura Y (1991) Requirement of the auxin polar transport system in early stages of Arabidopsis floral bud formation. *The Plant Cell* **3**: 677–684.

Peer WA, Blakeslee JJ, Yang H and Murphy AS (2011) Seven things we think we know about auxin transport. *Molecular Plant* **4**: 487–504.

Petrášek J, Malínská K and Zažímalová E (2011) Auxin transporters controlling plant development. In: Geisler M and Venema K (eds) *Transporters and Pumps in Plant Signaling*, pp. 255–290, Series "Signaling and Communication in Plants" 7,. Berlin Heidelberg: Springer-Verlag.

Petrášek J and Friml J (2009) Auxin transport routes in plant development. *Development* **136**: 2675–2688.

Porco S, Larrieu A, Du Y, *et al.* (2016) Lateral root emergence in *Arabidopsis* is dependent on transcription factor LBD29 regulating auxin influx carrier *LAX3*. *Development* **143**: 3340–3349.

Prusinkiewicz P and Runions A (2012) Computational models of plant development and form. *New Phytologist* **193**: 549–569.

Ranocha P, Dima O, Nagy R, *et al.* (2013) Arabidopsis WAT1 is a vacuolar auxin transport facilitator required for auxin homeostasis. *Nature Communications* **4**: 2625.

Reemmer J and Murphy AS (2014) In: Zažímalová E, Petrášek J and Benková E (eds) *Auxin and Its Role in Plant Development*. Vienna: Springer Vienna.

Retzer K, Butt H, Korbei B and Luschnig C (2014) The far side of auxin signaling: fundamental cellular activities and their contribution to a defined growth response in plants. *Protoplasma* **251**: 731–746.

Robert HS, Grunewald W, Sauer M, *et al.* (2015) Plant embryogenesis requires AUX/LAX-mediated auxin influx. *Development* **142**: 702–711.

Sato EM, Hijazi H, Bennett MJ, Vissenberg K and Swarup R (2015) New insights into root gravitropic signalling. *Journal of Experimental Botany* **66**: 2155–2165.

Scheuring D and Kleine-Vehn J (2014) In: Zažímalová E, Petrášek J and Benková E (eds) *Auxin and Its Role in Plant Development*. Vienna: Springer Vienna.

Shinohara N, Taylor C and Leyser O (2013) Strigolactone can promote or inhibit shoot branching by triggering rapid depletion of the auxin efflux protein PIN1 from the plasma membrane. *PLoS Biology* **11**: e1001474.

Simon S and Petrášek J (2011) Why plants need more than one type of auxin. *Plant Science* **180**: 454–460.

Simon S, Skůpa P, Viaene T, *et al.* (2016) PIN6 auxin transporter at endoplasmic reticulum and plasma membrane mediates auxin homeostasis and organogenesis in Arabidopsis. *New Phytologist* **211**: 65–74.

Smit ME and Weijers D (2015) The role of auxin signaling in early embryo pattern formation. *Current Opinion in Plant Biology* **28**: 99–105.

Steenackers WJ, Klíma P, Quareshy M, *et al.* (2016) Cis-cinnamic acid is a novel, natural auxin efflux inhibitor that promotes lateral root formation. *Plant Physiology* **173**: 552–565.

Strader LC and Bartel B (2011) Transport and metabolism of the endogenous auxin precursor indole-3-butyric acid. *Molecular Plant* **4**: 477–486.

Sun J, Zheng N (2015) Molecular Mechanism Underlying the Plant NRT1.1 Dual-Affinity Nitrate Transporter. *Frontiers in Physiology* **6**: 386. DOI: 10.3389/fphys.2015.00386.

Swarup R and Péret B (2012) AUX/LAX family of auxin influx carriers-an overview. *Frontiers in Plant Science* **3**: 225.

Tan X, Cao K, Liu F, *et al.* (2016) Arabidopsis COG complex subunits COG3 and COG8 modulate golgi morphology, vesicle trafficking homeostasis and are essential for pollen tube growth. *PLoS Genetics* **12**: 1–24.

Viaene T, Delwiche CF, Rensing SA and Friml J (2013) Origin and evolution of PIN auxin transporters in the green lineage. *Trends in Plant Science* **18**: 5–10.

Viaene T, Landberg K, Thelander M, *et al.* (2014) Directional auxin transport mechanisms in early diverging land plants. *Current Biology* **24**: 2786–2791.

Vieten A, Sauer M, Brewer PB and Friml J (2007) Molecular and cellular aspects of auxintransport-mediated development. *Trends in Plant Science* **12**: 160–168.

Vieten A, Vanneste S, Wisniewska J, *et al.* (2005) Functional redundancy of PIN proteins is accompanied by auxin-dependent cross-regulation of PIN expression. *Development (Cambridge, England)*, **132**: 4521–4531.

Wattelet-Boyer V, Brocard L, Jonsson K, *et al.* (2016) Enrichment of hydroxylated C24- and C26-acyl-chain sphingolipids mediates PIN2 apical sorting at *trans*-Golgi network subdomains. *Nature Communications* **7**: 12788. DOI: 10.1038/ncomms12788 doi:.

Willige BC, Ahlers S, Zourelidou M, *et al.* (2013) D6PK AGCVIII kinases are required for auxin transport and phototropic hypocotyl bending in Arabidopsis. *The Plant Cell* **25**: 1674–1688.

Xi W, Gong X, Yang Q, Yu H and Liou Y-C (2016) Pin1At regulates PIN1 polar localization and root gravitropism. *Nature Communications* **7**: 10430.

Yang H, Richter GL, Wang X, *et al.* (2013) Sterols and sphingolipids differentially function in trafficking of the Arabidopsis ABCB19 auxin transporter. *Plant Journal* **74**: 37–47.

Zažímalová E, Petrášek J and Benková E (eds) (2014) *Auxin and Its Role in Plant Development*. Vienna: Springer-Verlag Wien.

Zazímalová E, Murphy AS, Yang H, Hoyerova K and Hosek P (2010) Auxin transporters — why so many? *Cold Spring Harbor Perspectives in Biology* **2**: a001552.

Zourelidou M, Absmanner B, Weller B, *et al.* (2014) Auxin efflux by PIN-FORMED proteins is activated by two different protein kinases, D6 PROTEIN KINASE and PINOID. *eLife* **3**: e02860.

Further Reading

Bennett T, Hines G and Leyser O (2014) Canalization: what the flux? *Trends in Genetics* **30**: 41–48.

Bishopp A and Bennett MJ (2014) Hormone crosstalk: directing the flow. *Current Biology* **24**: R366R368.

Taiz L, Zeiger E, Moller IM and Murphy A (eds) (2015) *Plant Physiology and Development*. Sunderland, MA: Sinauer Associates.

3.1.2. Lessons Learned from the Studies of Roots Shaded from Direct Root Illumination

Authors: Jozef Lacek†, Judith Garcia-Gonzales†, Wolfram Weckwerth, Katarzyna Retzer

† contributed equally

Summary:

In this review we highlight that direct root illumination, which is still a very frequent part of standard cultivation methods, can mask or even modify native responses and affect regulatory mechanisms of root growth, architecture and adaptation. Direct root illumination triggers light escape mechanism, reduce nutrient uptake, affects root morphology and its effects interfere with several other regulatory pathways, which is limiting the range of our ability to study real native processes, and distinguish regulatory mechanisms from one to another. We summarize some of available methods that limit direct root illumination and allows us to study regulatory mechanisms without additive stress.

My contribution: As a joint first author, I contributed with summarizing sources for the review, and also in writing and editing of this manuscript.

International Journal of
Molecular Sciences

MDPI

Review

Lessons Learned from the Studies of Roots Shaded from Direct Root Illumination

Jozef Lacek [1,2], Judith García-González [1,2], Wolfram Weckwerth [3,4] and Katarzyna Retzer [1,*]

[1] Laboratory of Hormonal Regulations in Plants, Institute of Experimental Botany, Czech Academy of Sciences, 165 02 Prague, Czech Republic; lacek@ueb.cas.cz (J.L.); garciago.judith@gmail.com (J.G.-G.)
[2] Department of Experimental Plant Biology, Faculty of Science, Charles University, 128 00 Prague, Czech Republic
[3] Department of Functional and Evolutionary Ecology, Molecular Systems Biology (MoSys), Faculty of Life Sciences, University of Vienna, Djerassiplatz 1, 1030 Wien, Austria; wolfram.weckwerth@univie.ac.at
[4] Vienna Metabolomics Center (VIME), University of Vienna, Djerassiplatz 1, 1030 Wien, Austria
* Correspondence: retzer@ueb.cas.cz

Abstract: The root is the below-ground organ of a plant, and it has evolved multiple signaling pathways that allow adaptation of architecture, growth rate, and direction to an ever-changing environment. Roots grow along the gravitropic vector towards beneficial areas in the soil to provide the plant with proper nutrients to ensure its survival and productivity. In addition, roots have developed escape mechanisms to avoid adverse environments, which include direct illumination. Standard laboratory growth conditions for basic research of plant development and stress adaptation include growing seedlings in Petri dishes on medium with roots exposed to light. Several studies have shown that direct illumination of roots alters their morphology, cellular and biochemical responses, which results in reduced nutrient uptake and adaptability upon additive stress stimuli. In this review, we summarize recent methods that allow the study of shaded roots under controlled laboratory conditions and discuss the observed changes in the results depending on the root illumination status.

Keywords: D-rootsystem; direct root illumination; root growth; reactive oxygen species; flavonols; abiotic stress; light escape mechanism; auxin; cytokinin; dark-grown roots

Citation: Lacek, J.; García-González, J.; Weckwerth, W.; Retzer, K. Lessons Learned from the Studies of Roots Shaded from Direct Root Illumination. *Int. J. Mol. Sci.* **2021**, *22*, 12784. https://doi.org/10.3390/ijms222312784

Academic Editor: Bin Liu

Received: 22 October 2021
Accepted: 24 November 2021
Published: 26 November 2021

1. Introduction

Plants have evolved a finely tuned network of signaling pathways to simultaneously adapt to multiple, continuously occurring changes in environmental conditions [1–4]. Environmental changes can either affect shoot or root development locally or influence the development and growth behavior of the entire plant [1,2]. External stimuli range from changing light conditions that affect the photosynthetic activity and serve as a signal to control organ growth, to energy-consuming responses to abiotic and biotic stresses that challenge plant productivity [1,5,6]. Plants are very flexible and have an amazing ability to change cell shape and tissue organization to respond to exogenous stimuli [7–11]. To ensure efficient plant growth and productivity we need to understand how plants adapt under less beneficial environmental conditions. Plants are divided into the aboveground located shoot and the underground located root [2,4]. The shoot produces energy in the form of carbohydrates via photosynthesis, wherefore its productivity primarily depends on light quality and intensity [4,6,12–14]. Plant productivity also depends on the delivery of water and nutrients from the soil, which are taken up over the root [4,15]. The root needs to navigate through the soil towards beneficial areas rich in water and nutrients, but to avoid obstacles, also in the form of toxic compounds [16–18]. To orchestrate root development and the modulation of directional root growth, plants have evolved cellular mechanisms that rely on the spatially and temporally regulated distribution of signaling molecules, including sugars, phytohormones, and Reactive Oxygen Species (ROS) [4,9,18–24]. Direct

root illumination not only affects root growth alone but leads to altered communication between shoot and root, which also modulates the distribution of signaling molecules and eventually reduces efficient nutrient uptake, and negatively affects the ability of plants to adapt to additive stress stimuli [6,9,25,26]. In this review, we summarize recent findings showing how established laboratory growth conditions, which include plant cultivation on growth medium with roots exposed to light, affect plant development and root responses to abiotic stresses.

2. Standard Laboratory Conditions and Their Effects on Root Growth

Environmental conditions, on the one hand, shape the overall architecture of the plant, but also determine its ability to cope with additive stress stimuli at the level of individual organs down to the cells [3,9,23,26–30]. Roots have evolved to anchor the plant in the soil and also to absorb water and minerals from it [3,4] Furthermore, roots developed to direct the growth direction along the gravity vector and to avoid direct illumination [9,26,30]. As early as 1880, Darwin and Darwin suggested in their study 'The Power of Movement in Plants' directional root growth depending on growth conditions [31]. Like all land species, terrestrial plants developed mechanisms to orient themselves along the gravity vector [18]. However, negative phototropism of the root, the active root growth away from light, is also mediated in the very root tip [32]. Therefore, the conditions under which the plants are grown must be taken into account, as they can lead to additive responses or even mask phenotypes [9,26,29,30,33]. To make roots accessible for microscopy, phenotypic analysis, cell biological, and biochemical approaches, seedlings are grown in laboratories on plates with roots exposed to light (Figure 1), often in combination with sugar supplementation to enhance seedling growth [24,26,29,30]. While these standardized laboratory growth conditions may seem convenient and practical at first glance, they have recently been shown to have profound effects on root growth, architecture, root hair emergence and elongation, nutrient uptake, and ultimately whole plant growth [26,28–30]. In particular, the combination of light exposure of roots and exogenous sugar supplementation, usually sucrose or glucose, resulted in the biggest changes in root growth and responses to other exogenous stimuli compared to non-illuminated roots [24,29,30]. Sugars, as products of photosynthesis in the leaves, are actively distributed to the roots, where they not only function as building blocks for new molecule biosynthesis and energy source to enhance cellular activity, but also as signaling molecules [4]. By combining exogenous carbon sources and phytohormones with different illumination conditions for shoot and root, it became clearer to what extent the signaling cascades are interdependent and even overlap each other [26,29,30,34].

The regulation of root growth (e.g., the timing of lateral root and root hair emergence, directional root growth) is highly dependent on the finely tuned distribution of numerous signaling molecules, including sugars, ROS, phytohormones, and other small molecules whose availability per cell is strongly modulated by internal and external conditions [4,16,19,29,33,35–37]. Therefore, the direct interplay of phytohormones, light, and sugar signaling pathways in roots exposed to direct illumination compared to shaded roots has been the target of several recent studies [4,21,23,24,26–28,32,37–40]. Overlapping results show particularly striking differences in ROS production and distribution along the root, but also changes in phytohormone regulated responses have been reported [9,27,38,41].

The number of studies addressing the effects of direct root illumination on the outcome of stress response experiments, nutrient uptake, shoot–root communication, and the ability to modulate root architecture and directional root growth, is steadily increasing. In addition to efforts to track root growth directly in soil [42], several experimental setups have been described, which allow cultivation of seedlings in plates on sterile medium, but shade the roots from direct light exposure [43]. The reasons behind the efforts to keep roots growing under more natural light conditions, but still on a sterile medium, result from the wish to prepare plant material for microscopy studies, phenotypic analysis, and further molecular biological studies. These approaches range from optimized medium preparation

with charcoal [41] to the use of the so-called D-root system, which has recently become very popular [26]. Laboratories either use the D-root box available for purchase, as first described by Silva-Navas et al., 2015 [26–30,33], adaptations to study root illumination responses [6,44] or versions made of black cardboard [36,45]. However, regardless of the method used to shade the roots from direct root illumination, the results obtained are reproducible. Among the most obvious differences in root trait establishment depending on the illumination status include reduced root growth by direct root illumination due to lower meristematic activity, but increased root elongation rate, also known as root escape mechanism. In addition, seedlings with roots exposed to direct root illumination show an overall lower nutrient uptake capacity and a more sensitive response to abiotic stresses [9,26–30]. Finally, differential root development under direct illumination results in altered shoot growth, as shoots with shaded roots accumulate less mass and anthocyanins, demonstrating differential distribution of resources throughout the plant and fitness depending on the experimental growth conditions chosen [26].

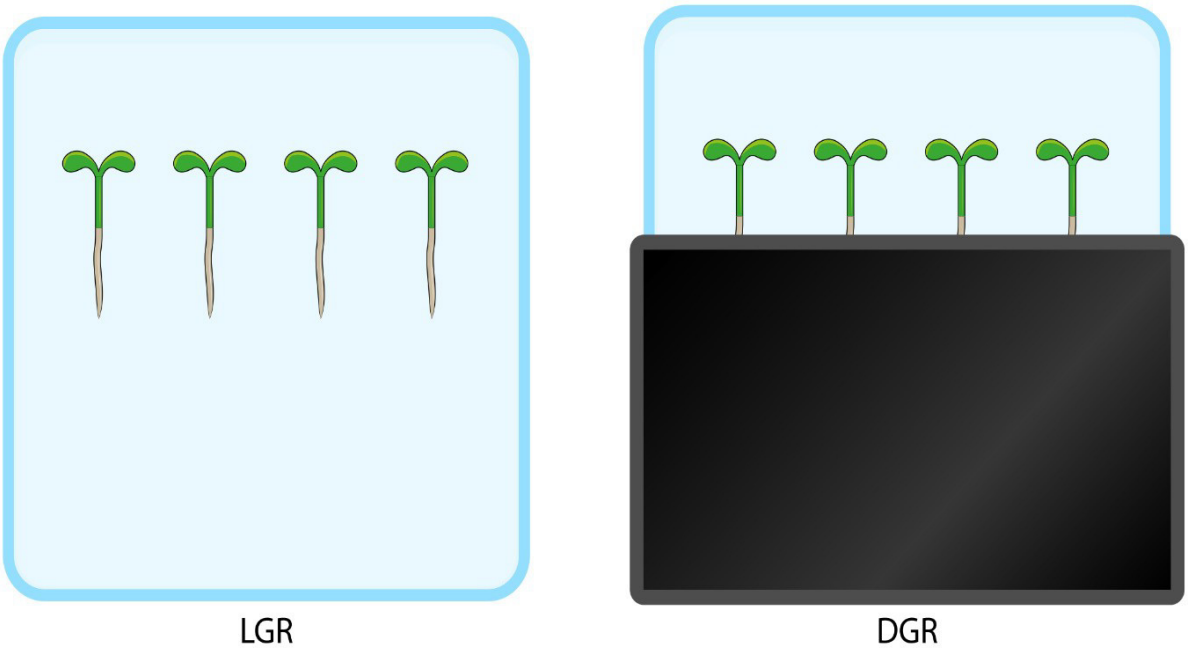

Figure 1. Schematic representation of the principle of light versus dark-grown roots. To shade roots from direct illumination, a cover is used, often made of methacrylate or black cardboard. A video showing how to assemble the so-called D-root system, which is widely used in the D-root community studying *Arabidopsis thaliana* and was designed by the del Pozo laboratory, is available online https://www.researchgate.net/publication/281436423_Assembling_the_D-root_system (accessed on 23 November 2021) [26].

3. Differences in Root Growth Adaptation Depending on Root Illumination Status

3.1. Root Traits Altered by Direct Illumination

Roots are positive gravitropic and negative phototropic, and they evolved to grow into soil shaded from light [4,7,44]. Roots also express photoreceptors, which allows them to adapt directional root growth to avoid direct illumination [3,21]. Furthermore, light perception also results in altered root growth rate, sensitivity to additive stress stimuli, and changes in root system architecture establishment depending on the activated photoreceptor and the illuminated area of the root [1,32,40]. Therefore, roots respond differently to direct root illumination depending on the wavelength or direction of illumination. Comprehensive reviews of the photoreceptors expressed in roots and involved in the modulation of root growth can be found in Zdarska et al., 2015, Silva-Navas et al., 2015 and van Gelderen et al., 2018, among others [3,21,26]. Root meristem activity is modulated upon exogenous and endogenous stimuli [2,4,46–50]. Cell proliferation comes to a halt when environmental conditions are not favorable for the plant, such as when red, energy-

intensive light is perceived [9,23,26,32]. After leaving the meristem, cells pass through the transition and elongation zone towards the differentiation zone, where cell fate depends on maturation and growth as well as environmental stimuli. It has been reported that blue light receptors appear to modulate the elongation rate above the meristem [9,26,51].

The application of the D-root system confirmed that the quality of light has an impact on root growth, by studying the effect of individual wavelengths on plants lacking single photoreceptors [26]. Silva-Navas et al., 2015, in their comprehensive study of differences in plant growth between seedlings with light- and dark-grown roots (LGR, DGR), showed that LGR are up to 25% shorter compared to DGR [26]. García-González et al., 2021a, and b, showed that the difference in total root length is more pronounced when sucrose is added to the growth medium [29,30]. When comparing publications that evaluated total root length as a function of root illumination status, it became clear that the difference in root length was less pronounced in seedlings younger than seven days after germination, but was striking from twelve days after germination [26,30] (Figure 2). Direct root illumination also causes root growth to deviate from vertical (Figure 2), which in turn is enhanced by the addition of sugar to the growth medium [24,29]. In addition, the length of root hairs closer to the meristem is increased, which is likely due to the increased concentrations of ROS in LGR [28,29]. Recently, ROS were shown to be critical modulators of root hair elongation and lateral root outgrowth and root growth in general [26,27,40,52–56]. It has also been shown that ROS modulate negative phototropism even upon brief irradiation with blue light of 82 µmol m^{-2} s^{-1} for 10 s, and roots immediately responded by producing ROS in the root tip, which was accompanied by a rapid increase in root growth rate, a phenomenon they termed Root Escape Tropism [9,23,32,40,41].

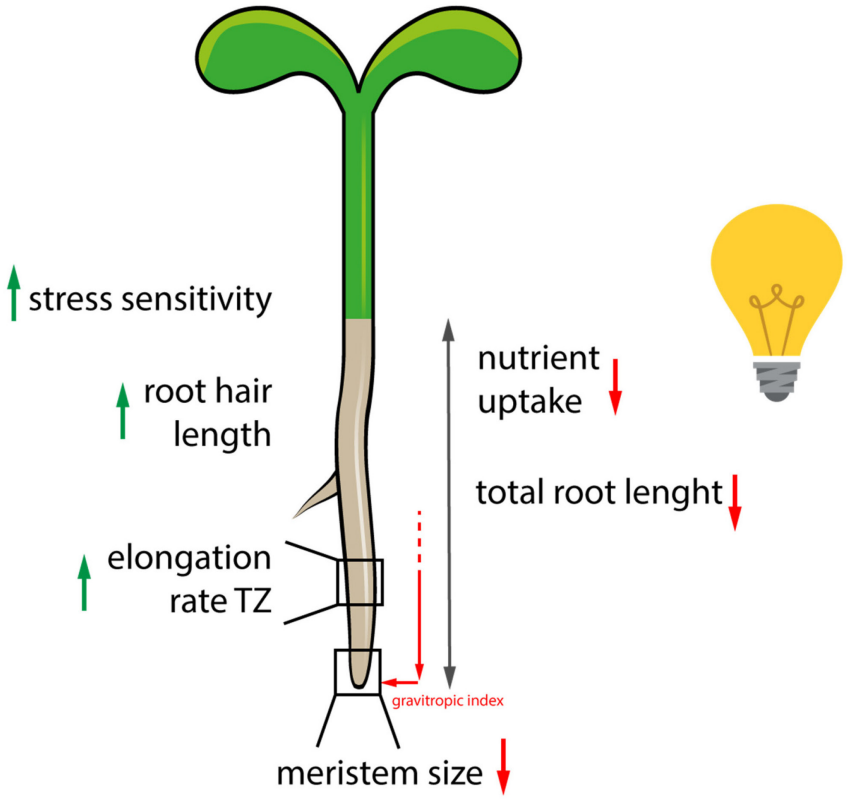

Figure 2. Summary of repeatedly observed root traits, which differ depending on the root illumination status. When roots are shaded from direct root illumination, independent studies from different laboratories confirmed a higher activity of the meristem, better efficiency in nutrient uptake, and better coordinated directional root growth. Furthermore, cell elongation rate in the transition zone (TZ) is reduced, as the light-induced Root Escape Mechanism is missing. Moreover, light-grown roots show enhanced sensibility towards additive stress treatment and cope less efficiently or slower upon stress application, probably due to elevated reactive oxygen species production (ROS), which activates stress response signaling pathways. Elevated ROS levels are suspected further to induce root hair outgrowth and elongation closer to the meristem in light-grown roots.

3.2. The Modulation of Root Growth at the Cellular Level Depends Strongly on the Interplay between Reactive Oxygen Species and Flavonols

The root absorbs water and nutrients from the soil, which determines the productivity of the plant [2,4]. Direct illumination of the root results in decreased accumulation of nutrients, including potassium, sodium, and molybdate [26]. Only iron was accumulated in the root and shoot of plants whose roots were exposed to light, and since iron dissolution is modulated by redox reactions [57], photocatalysis of various ROS in LGR could stimulate iron accumulation [26]. In addition, accumulation of ROS also plays an important role in modulating additive stress responses of roots, such as nitrogen deficiency [26]. Total root length and ion accumulation are reduced in LGRs under N deficiency, while DGRs show limited reduction in total root length under N deficiency [26,58,59]. LGRs have an overall increased content of individual ROS [55], but the content of ROS scavengers is also increased, which eventually leads to a decrease of specific ROS compared to DGR, which needs further investigation [26]. ROS scavengers in the form of secondary metabolites, especially flavonols, accumulate in LGR, which are crucial for the proper regulation of root light avoidance [27]. Silva-Navas et al, 2016 described how phototropic reactions in LGR are orchestrated by hydrogen peroxide and cytokinin, which stimulate the accumulation of flavonols along the transition zone to promote cell elongation, even in an asymmetric manner under unilateral root illumination [27]. Under unilateral illumination, roots accumulate flavonols closer to the light source, resulting in asymmetric cell elongation that forces the root to bend away from the light [27]. Blue light is known to activate the PHOTOTROPIN1 (PHOT1) receptor in the root transition zone, where it is associated with modulation of the subcellular distribution of the auxin efflux carrier PIN-FORMED 2 (PIN2) [51,60].

The length of the root is determined by the proliferation rate of the meristem, which is reduced when the root is directly illuminated, and by the elongation rate of the cells, which is stimulated to enable the light escape mechanism in the root [9,27]. It is worth noting that the proliferation rate is suppressed in LGR due to phototoxicity, which has been associated with increased flavonol levels [27]. Meristematic activity is also reduced when the whole plant is shifted into darkness, but the gradual shutdown of root growth results from the reduction of photosynthetic activity of the shoot and changes in shoot–root communication [3] Therefore, data obtained from whole plants shifted to darkness or even etiolated plants should be taken with caution and cannot be compared with results from D-root experiments [30]. Previous studies have already shown that the suppression of meristematic activity in illuminated roots is primarily due to UV-B triggered ROS accumulation [9,55]. Overall, meristematic activity is balanced by ROS accumulation depending on environmental conditions and the ability to produce ROS scavengers to maintain efficient root growth [27,40,49,56,61,62]. The rate of cell elongation in the transition zone of DGR is slower than in LGR or DGR treated with flavonols, while the final cell size in differentiated cells is similar in DGR and LGR [27]. This is also consistent with a study showing that illuminated roots respond more slowly when exposed to a NaCl gradient [9]. Cell expansion depends on the finely tuned establishment of the cytoskeleton, and several studies have shown that direct illumination of roots alters its appearance, including increased actin polymerization and bundling, which could be the reason for altered dynamics of root growth responses of LGR [9,43]. Modulation of the cytoskeleton is responsible for various morphological changes at the cellular and subcellular levels, including the properties of lytic vacuoles, intracellular trafficking, and plasma membrane (PM) responses [33,37,39,63–65]. Several changes have been linked to the regulation of auxin distribution in the root, so it is not surprising that responses to hormones are also affected by direct root illumination [21,23,33].

3.3. Phytohormones

Phytohormone biosynthesis, distribution, and metabolism, either to store or to degrade them, highly depends on the developmental stage of the plant, but also the availability of resources and growth conditions [2,22]. Shoot and root influence each other in the

production of individual hormones and exchange them to promote or inhibit the growth of individual organs or tissues [2]. Since recent studies have shown that the illumination status of individual plant organs has a profound effect on overall plant growth, it is not surprising that LGR and DGR responded differently to exogenous hormone application [26]. Exogenous hormone treatment showed greater inhibition of total root length of DGR compared to LGR when treated with epi-brassinolide (eBl), abscisic acid, the cytokinin 6-benzylaminopurine, the synthetic auxin 2,4-dichlorophenoxy-acetic acid (2,4-D), and the auxin transport inhibitor 1-N-naphthylphthalamic acid [26].

The close interplay of auxin transport, biosynthesis, conjugation, perception, and signaling [66–68] enables constant plant growth through a balance between cell division and elongation. While total root length was more inhibited by 2,4-D in LGR compared to DGR, the natural auxin indole-3-acetic acid had the opposite effect, suggesting that light attenuates the inhibition of root growth by 2,4-D [26]. Mutants of genes involved in auxin signaling, *auxin resistance protein 1-12* and *transporter inhibitor response 1-1*, developed a higher number of lateral roots in DGR compared with wild type, but total root length was not affected [26]. Root illumination might affect auxin homeostasis, which would explain the differential response to different auxins as well as root growth and morphogenesis, but detailed studies have not yet been completed. So far, preliminary insights have been gained into the modulation of auxin carrier distribution and subcellular localization in response to root illumination status [33,38,51]. Fine-tuned polar auxin transport ensures over long distances an active and regulated transport and gradient establishment on tissue and cellular level, followed by subcellular rearrangements to modulate plant growth [65,68,69]. Auxin efflux carriers have been extensively studied in terms of their intracellular distribution, transport, and posttranslational modifications that modulate their activity and abundance at the PM [16,33,35,70,71], but all of these studies were either done in LGR or in plants that were grown etiolated or dark-shifted. Only recently, a few studies have been published focusing on the distribution of PIN1 and PIN2 in DGR. Direct root illumination results in lower levels of PIN1 in the stele of the root, which have been shown to be modulated post-translationally, as the transcript levels did not change depending on the illumination status of the root [27]. Furthermore, internalization of PIN2:mcherry occurs from the PM towards the lytic vacuole, which is not visible when PIN2 is tagged to a pH sensitive fluorescent protein [27,33,38,39,51]. The intracellular targeting of PIN2 to the lytic vacuole is mediated by ubiquitination, and fusion between PIN2 and a single ubiquitin unit increases the turnover of PIN2 from the PM directly into the lytic vacuole, which can be inhibited by exogenous eBL treatment [33,72]. While PIN2:ubq turnover in LGR can be inhibited by eBL, leading to increased PIN2:ubq levels at the PM, wild-type PIN2 abundance at the PM increases significantly after eBL treatment only in DGR, but no longer in LGR, which is consistent with previous studies suggesting that root illumination leads to stabilization of PIN2 at the PM [33]. In addition, a recent study showed that direct root illumination, which leads to increased root hair outgrowth closer to the meristem in wild-type roots, is reduced in the PIN2 knockout mutant *eir1-4*, consistent with the importance of shoot-directed auxin transport for PIN2-mediated root hair outgrowth [4,29,73]. Regulated shootward auxin distribution has been well described to ensure proper root growth and thus plant nutrition [19,74,75]. This includes processes such as cell division, regulation of cell expansion, directional root growth, root hair outgrowth, and development of lateral roots, which are modulated by finely tuned auxin gradients, thus most studies have targeted auxin-related mechanisms [1,4,76,77]. The regulatory role of auxin distribution and signaling in the root were intensively studied, but the understanding of how exactly auxin distribution and homeostasis are modulated upon distinct environmental conditions is still incomplete [29,37,73,78,79]. Therefore, reducing external stimuli by using the D-root system allows us to dissect better which signaling pathways are in which way interconnected [15,48,80]. It has been shown that direct illumination of roots increases the amount of flavonols, and exogenous application of flavonols results in lower PIN1 levels in the root, which could limit the delivery of auxin from the shoot to the root tip [27]. Flavonols

are known to control auxin distribution in the root at multiple levels, including inhibition of auxin transport and modulation of indole-3-acetic acid (IAA) catabolism [81–84]. The reduction of LGR meristem size could on one hand directly result from lower auxin levels, as auxin drives meristematic activity to a certain extent [85,86], but data showing auxin distribution along the root depending on the illumination status are still outstanding. Alternatively, an altered cytokinin:auxin ratio might modulate the cell fate switch between meristem and transition zone [27,87,88]. Cytokinin itself seems in LGR to induce flavonol biosynthesis via SHORT HYPOCOTYL 2 (SHY2) to reduce auxin transporter abundance and thereby, delivery of auxin to the root tip [27]. This corresponds to previously obtained data that describe how cytokinin and auxin signaling pathways interact to modulate root meristem [27,87,89]. Moreover, the application of the D-rootsystem allowed defining a new role of the cytokinin cis-zeatin in orchestrating root growth adaptation, including regulation of root hair outgrowth, upon phosphate deficiency [28].

Possible, cross-talks in-between individual phytohormonal signaling pathways and responses to root illumination status are outstanding, and could probably reveal regulatory mechanisms that were masked so far. Light perception and root growth modulation are connected over signaling pathways of other hormones too [32], but how far they differ in DGR must be still investigated. For example, BR signaling is induced in roots upon blue light illumination and is known to modulate ROS and ethylene synthesis to restrict root growth [90,91]. Plant roots are very plastic and can adjust their tissue organization and cell appearance during abiotic stress responses, whereby direct root illumination results in changes the sensitivity of plants towards individual external stimuli [26,92].

3.4. Additive Stress Responses under Direct Root Illumination

Environmental conditions are constantly changing and plants, as sessile organisms, must often adapt rapidly to stimuli that occur simultaneously [1]. The composition of the soil is also not uniform and can change during root growth. Not only are nutrients unevenly distributed or dissolved, but there may be a sudden accumulation of toxic compounds or a decrease in the availability of water [1,28,49,93]. Environmental pollution and extreme weather conditions affect plant growth by activating multiple response pathways simultaneously, usually leading to reversible growth arrest or even plant death [94]. Direct root illumination triggers additional stress responses that do not occur in DGR; therefore, to understand how roots respond in nature the D-root system or similar advice will provide more accurate results [26]. The establishment of ROS gradients in the root tip is known to be crucial to rapidly modulate root architecture and growth upon stress exposure [26,27,53,55,56]. As elevated ROS levels impair N uptake in roots, which massively affects resource accumulation required for mass production of plants [58], it is not surprising that LGR are shorter than DGR under N deprivation [26]. Phosphate deficiency (Pi) combined with direct root illumination significantly inhibited root meristem activity by up to 50% and stimulated root hair outgrowth closer to the root meristem, whereas root hair elongation was impaired [28]. Total root length was even more impaired of LGR under osmotic or salt stress [26]. Application of osmotic stress in the form of 250mM mannitol inhibited root growth of LGR by 55% but only 44% of DGR and treatment of LGR with 100mM NaCl resulted in 40% shorter roots while DGR where inhibited only by 27% [26]. In addition to a more drastic reduction in root growth of LGR when grown directly on NaCl, LGR also show slower salt avoidance, halotropism, when grown on split plates where NaCl is added only to the lower part of the plate and seedlings are placed on medium without salt [9]. Furthermore, it has been shown that particular irradiation of the root tip with UV-B lowers root response to salinity [9]. Moreover, the UV-B receptor UV RESISTANCE LOCUS 8 (UVR8) is involved in growth reduction under drought, which again shows that multiple stress responses are regulated by overlapping signaling pathways, and additional stress in form of direct root illumination may mask or alter research outcomes [9]. AtUVR8 further complements an osmosensitive *Saccharomyces cerevisiae* mutant and its overexpression in *Arabidopsis thaliana* leads to reduced primary root growth, especially under osmotic and

salt stress, which is again associated with flavonoid accumulation [9,95]. On the one hand, lateral root growth seems to be rather promoted under salt stress growth conditions to increase root surface area and search for water and nutrients [1], but it is impaired when the root is exposed to excessive illumination, especially UV-B [9]. Studying the adaptation of root system architecture under toxic growth conditions, including salt stress and drought, is crucial as the availability of unpolluted soil and water for crop production continuously decreases, leading to devastating crop losses [93,96–98]. To study plant stress responses in soil, Rhizotrons, also known as Rhizoboxes, are used, which still allow monitoring of root growth under controlled conditions [42,96,99,100]. Results obtained from DGR are more comparable to studies done on soil compared to LGR. Recent studies on the adaptation of pearl millet root growth to drought in so-called high-temperature tubes with sensors at the top and bottom of the tube to monitor water content made it possible to observe changes in the proteome and metabolome during drought stress [96]. Combined evaluation of changes at the proteomic level and metabolomic analysis of root exudates confirmed modulation of auxin homeostasis and linked increased flavonoid production to the observed reduction in root growth [101]. This demonstrates the importance of performing basic research under more natural conditions to allow a smoother transition of findings into applied science. Furthermore, Rhizotrons are commonly used to examine the interaction of roots with the rhizosphere, which is very sensitive to light, and most studies have been conducted on roots grown in soil [100,102]. Therefore, recent attempts to study biotic interactions with the root, which can be beneficial or threatening, include the use of transparent artificial soil for DGR, which in turn will allow a more detailed study of root growth adaptation at the cellular level under more natural conditions [103,104].

4. Conclusions

Roots have evolved as below-ground organs of the plant, and direct light illumination triggers stress responses that result in escape growth away from the light source and morphological and cellular changes, including responses to phytohormones and other small molecules that act as signaling molecules, such as ROS and flavonols. Two growth conditions of *Arabidopsis thaliana* seedlings are manifested in the majority of laboratories studying plant development and growth adaptation. One is to grow seedlings on agar plates with roots continuously exposed to light to the same extent as the shoot. Direct root illumination results in altered root architecture, which origins in changes at the subcellular level, including altered auxin carrier abundance and subcellular distribution. The other habit is to add sugar to the growth medium to enhance the growth rate of the seedlings, which has a massive impact on the genetics, molecular biology, metabolomics, etc., of the roots. The triggered responses negatively affect nutrient uptake and lead to molecular changes, including altered gene expression, proteome and metabolome, not only in the root itself but also in the shoot. In addition, fine-tuning of directional root growth is affected, reducing the efficiency of root maneuvers. Finally, recent studies have shown that direct illumination masks phenotypes or alter the responses of the experiments performed. The application of tools that protect roots from direct light illumination will lead to results that are closer to natural plant responses and will allow a more reliable transfer of knowledge from basic to applied plant science. Since most of the research data obtained so far come from studies with roots exposed to light and fed exogenous sugars, we will make surprising revelations and discover new connections between signaling pathways in the future, but overall, these findings will help us to better understand how roots and plants adapt to ever-changing environmental conditions.

Author Contributions: J.L., J.G.-G., W.W. and K.R. wrote and edited the article. All authors have read and agreed to the published version of the manuscript.

Funding: This work was supported by the Ministry of Education, Youth and Sports of Czech Republic from European Regional Development Fund 'Centre for Experimental Plant Biology': Project no. CZ.02.1.01/0.0/0.0/16_019/0000738.

Institutional Review Board Statement: Not applicable.

Informed Consent Statement: Not applicable.

Data Availability Statement: No new data were created or analyzed in this study. Data sharing is not applicable to this article.

Conflicts of Interest: The authors declare no conflict of interest.

References

1. Pierik, R.; Testerink, C. The Art of Being Flexible: How to Escape from Shade, Salt, and Drought1. *Plant Physiol.* **2014**, *166*, 5–22. [CrossRef]
2. Bailey-Serres, J.; Pierik, R.; Ruban, A.; Wingler, A. The Dynamic Plant: Capture, Transformation, and Management of Energy. *Plant Physiol.* **2018**, *176*, 961–966. [CrossRef]
3. Van Gelderen, K.; Kang, C.; Pierik, R. Light Signaling, Root Development, and Plasticity. *Plant Physiol.* **2018**, *176*, 1049–1060. [CrossRef] [PubMed]
4. Retzer, K.; Weckwerth, W. The Tor–Auxin Connection Upstream of Root Hair Growth. *Plants* **2021**, *10*, 150. [CrossRef]
5. Calleja-Cabrera, J.; Boter, M.; Oñate-Sánchez, L.; Pernas, M. Root Growth Adaptation to Climate Change in Crops. *Front. Plant Sci.* **2020**, *11*, 544. [CrossRef] [PubMed]
6. Miotto, Y.; Da Costa, C.T.; Offringa, R.; Kleine-Vehn, J.; Maraschin, F.D. Effects of Light Intensity on Root Development in a D-Root Growth System. *Front. Plant Sci.* **2021**, *92*, 122–125.
7. Vandenbrink, J.P.; Kiss, J.Z. Plant Responses to Gravity. *Semin. Cell Dev. Biol.* **2019**, *92*, 122–125. [CrossRef] [PubMed]
8. Szepesi, Á. Halotropism: Phytohormonal Aspects and Potential Applications. *Front. Plant Sci.* **2020**, *11*, 571025. [CrossRef]
9. Yokawa, K.; Fasano, R.; Kagenishi, T.; Baluška, F. Light as Stress Factor to Plant Roots—Case of Root Halotropism. *Front. Plant Sci.* **2014**, *5*, 718. [CrossRef]
10. Li, H.; Testerink, C.; Zhang, Y. How Roots and Shoots Communicate through Stressful Times. *Trends Plant Sci.* **2021**, *26*, 940–952. [CrossRef]
11. Geisler, M.; Wang, B.; Zhu, J. Auxin Transport during Root Gravitropism: Transporters and Techniques. *Plant Biol.* **2014**, *16*, 50–57. [CrossRef]
12. Fürtauer, L.; Weiszmann, J.; Weckwerth, W.; Nägele, T. Dynamics of Plant Metabolism during Cold Acclimation. *Int. J. Mol. Sci.* **2019**, *20*, 5411. [CrossRef] [PubMed]
13. Walter, A.; Nagel, K.A. Root Growth Reacts Rapidly and More Pronounced than Shoot Growth towards Increasing Light Intensity in Tobacco Seedlings. *Plant Signal. Behav.* **2006**, *1*, 225–226. [CrossRef]
14. Nagel, K.A.; Schurr, U.; Walter, A. Dynamics of Root Growth Stimulation in Nicotiana Tabacum in Increasing Light Intensity. *Plant Cell Environ.* **2006**, *29*, 1936–1945. [CrossRef]
15. Grierson, C.; Nielsen, E.; Ketelaarc, T.; Schiefelbein, J. Root Hairs. *Arab. B.* **2014**, *12*, e0172. [CrossRef]
16. Ötvös, K.; Marconi, M.; Vega, A.; O'Brien, J.; Johnson, A.; Abualia, R.; Antonielli, L.; Montesinos, J.C.; Zhang, Y.; Tan, S.; et al. Modulation of Plant Root Growth by Nitrogen Source-defined Regulation of Polar Auxin Transport. *EMBO J.* **2021**, *40*, e106862. [CrossRef]
17. Zhang, Y.; Friml, J. Auxin Guides Roots to Avoid Obstacles during Gravitropic Growth. *New Phytol.* **2020**, *225*, 1049–1052. [CrossRef] [PubMed]
18. Konstantinova, N.; Korbei, B.; Luschnig, C. Auxin and Root Gravitropism: Addressing Basic Cellular Processes by Exploiting a Defined Growth Response. *Int. J. Mol. Sci.* **2021**, *22*, 2749. [CrossRef] [PubMed]
19. Jozef, L.; Katarzyna, R.; Christian, L.; Eva, Z. Polar Auxin Transport. *eLS* **2017**, 1–11. [CrossRef]
20. Retzer, K.; Korbei, B.; Luschnig, C. Auxin and Tropisms. In *Auxin and Its Role in Plant Development*; Springer: Vienna, Austria, 2014. [CrossRef]
21. Zdarska, M.; Dobisová, T.; Gelová, Z.; Pernisová, M.; Dabravolski, S.; Hejátko, J. Illuminating Light, Cytokinin, and Ethylene Signalling Crosstalk in Plant Development. *J. Exp. Bot.* **2015**, *66*, 4913–4931. [CrossRef] [PubMed]
22. Yamoune, A.; Cuyacot, A.R.; Zdarska, M.; Hejatko, J. Hormonal Orchestration of Root Apical Meristem Formation and Maintenance in *Arabidopsis*. *J. Exp. Bot.* **2021**, *72*, 6768–6788. [CrossRef]
23. Wan, Y.; Yokawa, K.; Baluška, F. *Arabidopsis* Roots and Light: Complex Interactions. *Mol. Plant* **2019**, *12*, 1428–1430. [CrossRef] [PubMed]
24. Mishra, B.S.; Singh, M.; Aggrawal, P.; Laxmi, A. Glucose and Auxin Signaling Interaction in Controlling *Arabidopsis* Thaliana Seedlings Root Growth and Development. *PLoS ONE* **2009**, *4*, e4502. [CrossRef] [PubMed]
25. Jiang, K.; Moe-Lange, J.; Hennet, L.; Feldman, L.J. Salt Stress Affects the Redox Status of *Arabidopsis* Root Meristems. *Front. Plant Sci.* **2016**, *7*, 81. [CrossRef]
26. Silva-Navas, J.; Moreno-Risueno, M.A.; Manzano, C.; Pallero-Baena, M.; Navarro-Neila, S.; Téllez-Robledo, B.; Garcia-Mina, J.M.; Baigorri, R.; Gallego, F.J.; Del Pozo, J.C. D-Root: A System for Cultivating Plants with the Roots in Darkness or under Different Light Conditions. *Plant J.* **2015**, *84*, 244–255. [CrossRef]

27. Silva-Navas, J.; Moreno-Risueno, M.A.; Manzano, C.; Téllez-Robledo, B.; Navarro-Neila, S.; Carrasco, V.; Pollmann, S.; Gallego, F.J.; Del Pozo, J.C. Flavonols Mediate Root Phototropism and Growth through Regulation of Proliferation-to-Differentiation Transition. *Plant Cell* **2016**, *28*, 1372–1387. [CrossRef] [PubMed]
28. Silva-Navas, J.; Conesa, C.M.; Saez, A.; Navarro-Neila, S.; Garcia-Mina, J.M.; Zamarreño, A.M.; Baigorri, R.; Swarup, R.; del Pozo, J.C. Role of Cis-Zeatin in Root Responses to Phosphate Starvation. *New Phytol.* **2019**, *224*, 242–257. [CrossRef]
29. García-González, J.; Lacek, J.; Retzer, K. Dissecting Hierarchies between Light, Sugar and Auxin Action Underpinning Root and Root Hair Growth. *Plants* **2021**, *10*, 111. [CrossRef]
30. García-González, J.; Lacek, J.; Weckwerth, W.; Retzer, K. Exogenous Carbon Source Supplementation Counteracts Root and Hypocotyl Growth Limitations under Increased Cotyledon Shading, with Glucose and Sucrose Differentially Modulating Growth Curves. *Plant Signal. Behav.* **2021**, *16*, 1969818. [CrossRef]
31. Darwin, C.; Darwin, F. *The Power of Movement in Plants*; John Murray: London, UK, 1880. [CrossRef]
32. Mo, M.; Yokawa, K.; Wan, Y.; Baluska, F. How and Why Do Root Apices Sense Light under the Soil Surface? *Front. Plant Sci.* **2015**, *6*, 775. [CrossRef]
33. Retzer, K.; Akhmanova, M.; Konstantinova, N.; Malínská, K.; Leitner, J.; Petrášek, J.; Luschnig, C. Brassinosteroid Signaling Delimits Root Gravitropism via Sorting of the *Arabidopsis* PIN2 Auxin Transporter. *Nat. Commun.* **2019**, *10*, 1–15. [CrossRef] [PubMed]
34. Mishra, B.S.; Sharma, M.; Laxmi, A. Role of Sugar and Auxin Crosstalk in Plant Growth and Development. *Physiol. Plant* **2021**. [CrossRef] [PubMed]
35. Retzer, K.; Lacek, J.; Skokan, R.; Del Genio, C.I.; Vosolsobe˘, S.; Laňková, M.; Malínská, K.; Konstantinova, N.; Zažímalová, E.; Napier, R.M.; et al. Evolutionary Conserved Cysteines Function as Cis-Acting Regulators of *Arabidopsis* PIN-FORMED 2 Distribution. *Int. J. Mol. Sci.* **2017**, *18*, 2274. [CrossRef] [PubMed]
36. Van Gelderen, K.; Kang, C.; Paalman, R.; Keuskamp, D.; Hayes, S.; Pierik, R. Far-Red Light Detection in the Shoot Regulates Lateral Root Development through the HY5 Transcription Factor. *Plant Cell* **2018**, *30*, 101–116. [CrossRef] [PubMed]
37. Halat, L.S.; Gyte, K.; Wasteneys, G.O. Microtubule-Associated Protein CLASP Is Translationally Regulated in Light-Dependent Root Apical Meristem Growth. *Plant Physiol.* **2020**, *184*, 2154–2167. [CrossRef]
38. Laxmi, A.; Pan, J.; Morsy, M.; Chen, R. Light Plays an Essential Role in Intracellular Distribution of Auxin Efflux Carrier PIN2 in *Arabidopsis* Thaliana. *PLoS ONE* **2008**, *3*, e1510. [CrossRef]
39. Sassi, M.; Lu, Y.; Zhang, Y.; Wang, J.; Dhonukshe, P.; Blilou, I.; Dai, M.; Li, J.; Gong, X.; Jaillais, Y.; et al. COP1 Mediates the Coordination of Root and Shoot Growth by Light through Modulation of PIN1- and PIN2-Dependent Auxin Transport in *Arabidopsis*. *Development* **2012**, *139*, 3402–3412. [CrossRef]
40. Yokawa, K.; Koshiba, T.; Baluška, F. Light-Dependent Control of Redox Balance and Auxin Biosynthesis in Plants. *Plant Signal. Behav.* **2014**, *9*, e29522. [CrossRef]
41. Xu, W.; Ding, G.; Yokawa, K.; Baluška, F.; Li, Q.F.; Liu, Y.; Shi, W.; Liang, J.; Zhang, J. An Improved Agar-Plate Method for Studying Root Growth and Response of *Arabidopsis* Thaliana. *Sci. Rep.* **2013**, *3*, 1273. [CrossRef]
42. Atkinson, J.A.; Pound, M.P.; Bennett, M.J.; Wells, D.M. Uncovering the Hidden Half of Plants Using New Advances in Root Phenotyping. *Curr. Opin. Biotechnol.* **2019**, *55*, 1–8. [CrossRef]
43. Dyachok, J.; Zhu, L.; Liao, F.; He, J.; Huq, E.; Blancaflor, E.B. SCAR Mediates Light-Induced Root Elongation in *Arabidopsis* through Photoreceptors and Proteasomes. *Plant Cell* **2011**, *23*, 3610–3626. [CrossRef] [PubMed]
44. Aronne, G.; Muthert, L.W.F.; Izzo, L.G.; Romano, L.E.; Iovane, M.; Capozzi, F.; Manzano, A.; Ciska, M.; Herranz, R.; Medina, F.J.; et al. A Novel Device to Study Altered Gravity and Light Interactions in Seedling Tropisms. *Life Sci. Space Res.* **2022**, *32*, 8–16. [CrossRef]
45. Van Gelderen, K.; Kang, C.; Li, P.; Pierik, R. Regulation of Lateral Root Development by Shoot-Sensed Far-Red Light via HY5 Is Nitrate-Dependent and Involves the NRT2.1 Nitrate Transporter. *Front. Plant Sci.* **2021**, *12*, 660870. [CrossRef] [PubMed]
46. Barrada, A.; Montané, M.H.; Robaglia, C.; Menand, B. Spatial Regulation of Root Growth: Placing the Plant TOR Pathway in a Developmental Perspective. *Int. J. Mol. Sci.* **2015**, *16*, 19671–19697. [CrossRef]
47. Zhao, Y.; Wang, X.Q. The Hot Issue: TOR Signalling Network in Plants. *Funct. Plant Biol.* **2020**, *48*, 1–7. [CrossRef]
48. Wu, Y.; Shi, L.; Li, L.; Fu, L.; Liu, Y.; Xiong, Y.; Sheen, J. Integration of Nutrient, Energy, Light, and Hormone Signalling via TOR in Plants. *J. Exp. Bot.* **2019**, *70*, 2227–2238. [CrossRef]
49. Mase, K.; Tsukagoshi, H. Reactive Oxygen Species Link Gene Regulatory Networks during *Arabidopsis* Root Development. *Front. Plant Sci.* **2021**, *12*, 660274. [CrossRef]
50. Diaz-Vivancos, P.; De Simone, A.; Kiddle, G.; Foyer, C.H. Glutathione—Linking Cell Proliferation to Oxidative Stress. *Free. Radic. Biol. Med.* **2015**, *89*, 1154–1164. [CrossRef]
51. Wan, Y.; Jasik, J.; Wang, L.; Hao, H.; Volkmann, D.; Menzel, D.; Mancuso, S.; Baluška, F.; Lin, J. The Signal Transducer NPH3 Integrates the Phototropin1 Photosensor with PIN2-Based Polar Auxin Transport in *Arabidopsis* Root Phototropism. *Plant Cell* **2012**, *24*, 551–565. [CrossRef] [PubMed]
52. Velasquez, S.M.; Barbez, E.; Kleine-Vehn, J.; Estevez, J.M. Auxin and Cellular Elongation. *Plant Physiol.* **2016**, *170*, 1206–1215. [CrossRef]

53. Mangano, S.; Denita-Juarez, S.P.; Choi, H.-S.; Marzol, E.; Hwang, Y.; Ranocha, P.; Velasquez, S.M.; Borassi, C.; Barberini, M.L.; Aptekmann, A.A.; et al. Molecular Link between Auxin and ROS-Mediated Polar Growth. *Proc. Natl. Acad. Sci. USA* **2017**, *114*, 5289–5294. [CrossRef]
54. Eljebbawi, A.; Guerrero, Y.D.C.R.; Dunand, C.; Estevez, J.M. Highlighting Reactive Oxygen Species as Multitaskers in Root Development. *iScience* **2021**, *24*, 101978. [CrossRef]
55. Yokawa, K.; Kagenishi, T.; Baluška, F. UV-B Induced Generation of Reactive Oxygen Species Promotes Formation of BFA-Induced Compartments in Cells of *Arabidopsis* Root Apices. *Front. Plant Sci.* **2016**, *6*, 1162. [CrossRef]
56. Tsukagoshi, H.; Busch, W.; Benfey, P.N. Transcriptional Regulation of ROS Controls Transition from Proliferation to Differentiation in the Root. *Cell* **2010**, *143*, 606–616. [CrossRef] [PubMed]
57. Thomine, S.; Lanquar, V. Iron Transport and Signaling in Plants. In *Transporters and Pumps in Plant Signaling*; Geisler, M., Venema, K., Eds.; Springer: Berlin/Heidelberg, Germany, 2011; pp. 99–131. [CrossRef]
58. Shin, R.; Schachtman, D.P. Hydrogen Peroxide Mediates Plant Root Cell Response to Nutrient Deprivation. *Proc. Natl. Acad. Sci. USA* **2004**, *101*, 8827–8832. [CrossRef] [PubMed]
59. Conesa, C.M.; Saez, A.; Navarro-Neila, S.; de Lorenzo, L.; Hunt, A.G.; Sepúlveda, E.B.; Baigorri, R.; Garcia-Mina, J.M.; Zamarreño, A.M.; Sacristán, S.; et al. Alternative Polyadenylation and Salicylic Acid Modulate Root Responses to Low Nitrogen Availability. *Plants* **2020**, *9*, 251. [CrossRef] [PubMed]
60. Briggs, W.R.; Christie, J.M. Phototropins 1 and 2: Versatile Plant Blue-Light Receptors. *Trends Plant Sci.* **2002**, *7*, 204–210. [CrossRef]
61. Tsukagoshi, H. Control of Root Growth and Development by Reactive Oxygen Species. *Curr. Opin. Plant Biol.* **2016**, *29*, 57–63. [CrossRef]
62. Yamada, M.; Han, X.; Benfey, P.N. RGF1 Controls Root Meristem Size through ROS Signalling. *Nature* **2020**, *577*, 85–88. [CrossRef]
63. Ovecˇka, M.; Lang, I.; Baluška, F.; Ismail, A.; Illeš, P.; Lichtscheidl, I.K. Endocytosis and Vesicle Trafficking during Tip Growth of Root Hairs. *Protoplasma* **2005**, *226*, 39–54. [CrossRef]
64. Wasteneys, G.O.; Ambrose, J.C. Spatial Organization of Plant Cortical Microtubules: Close Encounters of the 2D Kind. *Trends Cell Biol.* **2009**, *19*, 62–71. [CrossRef] [PubMed]
65. Retzer, K.; Butt, H.; Korbei, B.; Luschnig, C. The Far Side of Auxin Signaling: Fundamental Cellular Activities and Their Contribution to a Defined Growth Response in Plants. *Protoplasma* **2014**, *251*, 731–746. [CrossRef]
66. Adamowski, M.; Friml, J. PIN-Dependent Auxin Transport: Action, Regulation, and Evolution. *Plant Cell* **2015**, *27*, 20–32. [CrossRef] [PubMed]
67. Gallei, M.; Luschnig, C.; Friml, J. Auxin Signalling in Growth: Schrödinger's Cat out of the Bag. *Curr. Opin. Plant Biol.* **2020**, *53*, 43–49. [CrossRef]
68. Semeradova, H.; Montesinos, J.C.; Benkova, E. All Roads Lead to Auxin: Post-Translational Regulation of Auxin Transport by Multiple Hormonal Pathways. *Plant Commun.* **2020**, *1*, 100048. [CrossRef] [PubMed]
69. Luschnig, C.; Vert, G. The Dynamics of Plant Plasma Membrane Proteins: PINs and Beyond. *Development* **2014**, *141*, 2924–2938. [CrossRef] [PubMed]
70. Zourelidou, M.; Absmanner, B.; Weller, B.; Barbosa, I.C.R.; Willige, B.C.; Fastner, A.; Streit, V.; Port, S.A.; Colcombet, J.; van Bentem, S.; et al. Auxin Efflux by PIN-FORMED Proteins Is Activated by Two Different Protein Kinases, D6 PROTEIN KINASE and PINOID. *eLife* **2014**, *3*, e02860. [CrossRef] [PubMed]
71. Löfke, C.; Luschnig, C.; Kleine-Vehn, J. Posttranslational Modification and Trafficking of PIN Auxin Efflux Carriers. *Mech. Dev.* **2013**, *130*, 82–94. [CrossRef]
72. Leitner, J.; Petrášek, J.; Tomanov, K.; Retzer, K.; Parˇezová, M.; Korbei, B.; Bachmair, A.; Zažímalová, E.; Luschnig, C. Lysine63-Linked Ubiquitylation of PIN2 Auxin Carrier Protein Governs Hormonally Controlled Adaptation of *Arabidopsis* Root Growth. *Proc. Natl. Acad. Sci. USA* **2012**, *109*, 8322–8327. [CrossRef]
73. Leyser, O. Auxin Signaling. *Plant Physiol.* **2018**, *176*, 465–479. [CrossRef]
74. Benková, E.; Michniewicz, M.; Sauer, M.; Teichmann, T.; Seifertová, D.; Jürgens, G.; Friml, J. Local, Efflux-Dependent Auxin Gradients as a Common Module for Plant Organ Formation. *Cell* **2003**, *115*, 591–602. [CrossRef]
75. Petrášek, J.; Mravec, J.; Bouchard, R.; Blakeslee, J.J.; Abas, M.; Seifertová, D.; Wis´niewska, J.; Tadele, Z.; Kubeš, M.; Cˇ ovanová, M.; et al. PIN Proteins Perform a Rate-Limiting Function in Cellular Auxin Efflux. *Science* **2006**, *312*, 914–918. [CrossRef] [PubMed]
76. De Smet, I. Lateral Root Initiation: One Step at a Time. *New Phytol.* **2012**, *193*, 867–873. [CrossRef]
77. Orman-Ligeza, B.; Parizot, B.; Gantet, P.P.; Beeckman, T.; Bennett, M.J.; Draye, X. Post-Embryonic Root Organogenesis in Cereals: Branching out from Model Plants. *Trends Plant Sci.* **2013**, *18*, 459–467. [CrossRef] [PubMed]
78. Bielach, A.; Hrtyan, M.; Tognetti, V.B. Plants under Stress: Involvement of Auxin and Cytokinin. *Int. J. Mol. Sci.* **2017**, *18*, 1427. [CrossRef]
79. Mroue, S.; Simeunovic, A.; Robert, H.S. Auxin Production as an Integrator of Environmental Cues for Developmental Growth Regulation. *J. Exp. Bot.* **2018**, *69*, 201–212. [CrossRef] [PubMed]
80. Monshausen, G.B.; Bibikova, T.N.; Messerli, M.A.; Shi, C.; Gilroy, S. Oscillations in Extracellular PH and Reactive Oxygen Species Modulate Tip Growth of *Arabidopsis* Root Hairs. *Proc. Natl. Acad. Sci. USA* **2007**, *104*, 20996–21001. [CrossRef]
81. Peer, W.A.; Jenness, M.K.; Murphy, A.S. Measure for Measure: Determining, Inferring and Guessing Auxin Gradients at the Root Tip. *Physiol. Plant.* **2014**, *151*, 97–111. [CrossRef]

82. Peer, W.A.; Cheng, Y.; Murphy, A.S. Evidence of Oxidative Attenuation of Auxin Signalling. *J. Exp. Bot.* **2013**, *64*, 2629–2639. [CrossRef]
83. Klíma, P.; Laňková, M.; Zažímalová, E. Inhibitors of Plant Hormone Transport. *Protoplasma* **2016**, *253*, 1391–1404. [CrossRef]
84. Steenackers, W.; Klíma, P.; Quareshy, M.; Cesarino, I.; Kumpf, R.P.; Corneillie, S.; Araújo, P.; Viaene, T.; Goeminne, G.; Nowack, M.K.; et al. Cis-Cinnamic Acid Is a Novel, Natural Auxin Efflux Inhibitor That Promotes Lateral Root Formation. *Plant Physiol.* **2017**, *173*, 552–565. [CrossRef]
85. Roychoudhry, S.; Kepinski, S. Auxin in Root Development. *Cold Spring Harb. Perspect. Biol.* **2021**, *13*, a039933. [CrossRef]
86. Schepetilnikov, M.; Ryabova, L.A. Auxin Signaling in Regulation of Plant Translation Reinitiation. *Front. Plant Sci.* **2017**, *8*, 1014. [CrossRef]
87. Dello Ioio, R.; Nakamura, K.; Moubayidin, L.; Perilli, S.; Taniguchi, M.; Morita, M.T.; Aoyama, T.; Costantino, P.; Sabatini, S. A Genetic Framework for the Control of Cell Division and Differentiation in the Root Meristem. *Science* **2008**, *322*, 1380–1384. [CrossRef] [PubMed]
88. Chapman, E.J.; Estelle, M. Mechanism of Auxin-Regulated Gene Expression in Plants. *Annu. Rev. Genet.* **2009**, *43*, 265–285. [CrossRef] [PubMed]
89. Ruzicka, K.; Simásková, M.; Duclercq, J.; Petrásek, J.; Zazímalová, E.; Simon, S.; Friml, J.; Van Montagu, M.C.E.; Benková, E. Cytokinin Regulates Root Meristem Activity via Modulation of the Polar Auxin Transport. *Proc. Natl. Acad. Sci. USA* **2009**, *106*, 4284–4289. [CrossRef]
90. Lv, B.; Tian, H.; Zhang, F.; Liu, J.; Lu, S.; Bai, M.; Li, C.; Ding, Z. Brassinosteroids Regulate Root Growth by Controlling Reactive Oxygen Species Homeostasis and Dual Effect on Ethylene Synthesis in *Arabidopsis*. *PLoS Genet.* **2018**, *14*, e1007144. [CrossRef]
91. Sakaguchi, J.; Matsushita, T.; Watanabe, Y. DWARF4 Accumulation in Root Tips Is Enhanced via Blue Light Perception by Cryptochromes. *Plant Cell Environ.* **2019**, *42*, 1615–1629. [CrossRef]
92. Pierik, R.; Fankhauser, C.; Strader, L.C.; Sinha, N. Architecture and Plasticity: Optimizing Plant Performance in Dynamic Environments. *Plant Physiol.* **2021**, *187*, 1029–1032. [CrossRef]
93. Yokawa, K.; Baluška, F. The TOR Complex: An Emergency Switch for Root Behavior. *Plant Cell Physiol.* **2016**, *57*, 14–18. [CrossRef] [PubMed]
94. Zandalinas, S.I.; Sengupta, S.; Fritschi, F.B.; Azad, R.K.; Nechushtai, R.; Mittler, R. The Impact of Multifactorial Stress Combination on Plant Growth and Survival. *New Phytol.* **2021**, *230*, 1034–1048. [CrossRef] [PubMed]
95. Fasano, R.; Gonzalez, N.; Tosco, A.; Dal Piaz, F.; Docimo, T.; Serrano, R.; Grillo, S.; Leone, A.; Inzé, D. Role of *Arabidopsis* UV RESISTANCE LOCUS 8 in Plant Growth Reduction under Osmotic Stress and Low Levels of UV-B. *Mol. Plant* **2014**, *7*, 773–791. [CrossRef] [PubMed]
96. Ghatak, A.; Chaturvedi, P.; Weckwerth, W. Cereal Crop Proteomics: Systemic Analysis of Crop Drought Stress Responses towards Marker-Assisted Selection Breeding. *Front. Plant Sci.* **2017**, *8*, 757. [CrossRef] [PubMed]
97. Ghatak, A.; Chaturvedi, P.; Nagler, M.; Roustan, V.; Lyon, D.; Bachmann, G.; Postl, W.; Schröfl, A.; Desai, N.; Varshney, R.K.; et al. Comprehensive Tissue-Specific Proteome Analysis of Drought Stress Responses in *Pennisetum Glaucum* (L.) R. Br. (Pearl Millet). *J. Proteom.* **2016**, *143*, 122–135. [CrossRef]
98. Ghatak, A.; Chaturvedi, P.; Bachmann, G.; Valledor, L.; Ramšak, Ž.; Bazargani, M.M.; Bajaj, P.; Jegadeesan, S.; Li, W.; Sun, X.; et al. Physiological and Proteomic Signatures Reveal Mechanisms of Superior Drought Resilience in Pearl Millet Compared to Wheat. *Front. Plant Sci.* **2020**, *11*, 600278. [CrossRef]
99. Piñeros, M.A.; Larson, B.G.; Shaff, J.E.; Schneider, D.J.; Falcão, A.X.; Yuan, L.; Clark, R.T.; Craft, E.J.; Davis, T.W.; Pradier, P.-L.; et al. Evolving Technologies for Growing, Imaging and Analyzing 3D Root System Architecture of Crop Plants. *J. Integr. Plant Biol.* **2016**, *58*, 230–241. [CrossRef]
100. Freschet, G.T.; Pagès, L.; Iversen, C.M.; Comas, L.H.; Rewald, B.; Roumet, C.; Klimešová, J.; Zadworny, M.; Poorter, H.; Postma, J.A.; et al. A Starting Guide to Root Ecology: Strengthening Ecological Concepts and Standardising Root Classification, Sampling, Processing and Trait Measurements. *New Phytol.* **2021**, *232*, 973–1122. [CrossRef]
101. Ghatak, A.; Schindler, F.; Bachmann, G.; Engelmeier, D.; Bajaj, P.; Brenner, M.; Fragner, L.; Varshney, R.K.; Subbarao, G.V.; Chaturvedi, P.; et al. Root Exudation of Contrasting Drought-Stressed Pearl Millet Genotypes Conveys Varying Biological Nitrification Inhibition (BNI) Activity. *Biol. Fertil. Soils* **2021**, *57*, 1–16. [CrossRef]
102. Yee, M.O.; Kim, P.; Li, Y.; Singh, A.K.; Northen, T.R.; Chakraborty, R. Specialized Plant Growth Chamber Designs to Study Complex Rhizosphere Interactions. *Front. Microbiol.* **2021**, *12*, 625752. [CrossRef]
103. Ma, L.; Shi, Y.; Siemianowski, O.; Yuan, B.; Egner, T.K.; Mirnezami, S.V.; Lind, K.R.; Ganapathysubramanian, B.; Venditti, V.; Cademartiri, L. Hydrogel-Based Transparent Soils for Root Phenotyping in Vivo. *Proc. Natl. Acad. Sci. USA* **2019**, *116*, 11063–11068. [CrossRef]
104. Downie, H.; Holden, N.; Otten, W.; Spiers, A.J.; Valentine, T.A.; Dupuy, L.X. Transparent Soil for Imaging the Rhizosphere. *PLoS ONE* **2012**, *7*, e44276. [CrossRef] [PubMed]

3.2. Original Research

3.2.1. Evolutionary Conserved Cysteines Function as cis-Acting Regulators of Arabidopsis PIN-FORMED2 Distribution

Authors: Katarzyna Retzer, Jozef Lacek, Roman Skokan, Charo I. del Genio, Stanislav Vosolsobě, Martina Laňková, Kateřina Malínská, Nataliia Konstantinova, Eva Zažímalová, Richard M. Napier, Jan Petrášek, Christian Luschnig

Summary:

Modulation of growth responses in plants is maintained by several tightly controlled mechanisms. Auxin as growth regulator helps to regulate growth and adaptation mechanisms by establishing concentration minima and maxima at specific tissues and organs in particular time. Plants developed multi-layered regulation of auxin transporters to establish required spatial and temporal distribution of auxin. This study focusses on post-translational modifications of root specific Arabidopsis PIN2 carrier. It is well-known that PIN proteins are regulated by phosphorylation and ubiquitination. We show functional implications of the two evolutionary conserved cysteines, which might be accessible to redox-status-controlled modification. We show that by exchanging these especially conserved cysteines for alanine we affect PIN2 mobility on the membrane which then affect the fine tuning of polar auxin transport.

My contribution: I contributed with planning and performing experiments primarily focusing on phenotyping and confocal microscopy, and furthermore, I was involved in evaluating the raw data and manuscript preparation.

International Journal of
Molecular Sciences

MDPI

Article

Evolutionary Conserved Cysteines Function as *cis*-Acting Regulators of *Arabidopsis* PIN-FORMED 2 Distribution

Katarzyna Retzer [1,2,†], Jozef Lacek [2,3,†], Roman Skokan [2,3], Charo I. del Genio [4,†], Stanislav Vosolsobe [3], Martina Lan˘ková [2], Kater˘ina Malínská [2], Nataliia Konstantinova [1], Eva Zažímalová [2], Richard M. Napier [4], Jan Petrášek [2,3,*] and Christian Luschnig [1,*]

1 Department of Applied Genetics and Cell Biology, University of Natural Resources and Life Sciences, Vienna (BOKU), Muthgasse 18, 1190 Wien, Austria; retzer@ueb.cas.cz (K.R.); nataliia.konstantinova@boku.ac.at (N.K.)
2 Institute of Experimental Botany of the Czech Academy of Sciences, Rozvojová 263, 165 02 Praha 6, Czech Republic; lacek@ueb.cas.cz (J.L.); skokan@ueb.cas.cz (R.S.); lankova@ueb.cas.cz (M.L.); malinska@ueb.cas.cz (K.M.); Zazimalova@ueb.cas.cz (E.Z.)
3 Department of Experimental Plant Biology, Faculty of Science, Charles University, Vinicna 5, 128 44 Prague 2, Czech Republic; stanislav.vosolsobe@natur.cuni.cz
4 School of Life Sciences, University of Warwick, Gibbet Hill Road, Coventry CV4 7AL, UK; the.paraw@gmail.com (C.I.d.G.); Richard.Napier@warwick.ac.uk (R.M.N.)
* Correspondence: petrasek@ueb.cas.cz (J.P.); christian.luschnig@boku.ac.at (C.L.); Tel.: +420-225-106-435 (J.P.); +43-1-47654-94130 (C.L.)
† These authors contributed equally to this work.

Received: 26 September 2017; Accepted: 26 October 2017; Published: 29 October 2017

Abstract: Coordination of plant development requires modulation of growth responses that are under control of the phytohormone auxin. PIN-FORMED plasma membrane proteins, involved in intercellular transport of the growth regulator, are key to the transmission of such auxin signals and subject to multilevel surveillance mechanisms, including reversible post-translational modifications. Apart from well-studied PIN protein modifications, namely phosphorylation and ubiquitylation, no further post-translational modifications have been described so far. Here, we focused on root-specific *Arabidopsis* PIN2 and explored functional implications of two evolutionary conserved cysteines, by a combination of *in silico* and molecular approaches. PIN2 sequence alignments and modeling predictions indicated that both cysteines are facing the cytoplasm and therefore would be accessible to redox status-controlled modifications. Notably, mutant *pin2*$^{C-A}$ alleles retained functionality, demonstrated by their ability to almost completely rescue defects of a *pin2* null allele, whereas high resolution analysis of pin2^{C-A} localization revealed increased intracellular accumulation, and altered protein distribution within plasma membrane micro-domains. The observed effects of cysteine replacements on root growth and PIN2 localization are consistent with a model in which redox status-dependent cysteine modifications participate in the regulation of PIN2 mobility, thereby fine-tuning polar auxin transport.

Keywords: Auxin; PIN proteins; plasma membrane protein sorting; protein mobility; intracellular distribution; root phenotype; *Arabidopsis*; protein modeling; SRRF

1. Introduction

Auxin, a versatile plant growth regulator, is involved in a multitude of developmental processes [1–3]. This versatility is largely dependent on a very flexible molecular machinery, mediating directional transport of the phytohormone throughout the entire organism [4–6]. Plasma membrane

localized PIN-FORMED (PIN) proteins, in particular, have been connected to the cellular efflux of the growth regulator, a critical step that defines directionality and rates of polar auxin transport and requires tight regulation [4,7].

Key to the function of PIN proteins at the plasma membrane is a stringent control of their localization, activity and abundance, which has been linked to specific cellular activities. PIN trafficking to and from the plasma membrane is mediated by evolutionary conserved elements of secretory and endocytic sorting machineries, essential for maintenance of and adjustments in PIN distribution. Exocytotic sorting occurs via the TGN (Trans Golgi network), and is dependent on ARF-GEF (ADP Ribosylation Factor–Guanine Nucleotide Exchange Factor) and exocyst complex activities. Plasma membrane-resident PIN proteins are subject to lateral diffusion processes, which is eventually followed by clathrin-dependent endocytic sorting to the TGN. From there, PINs appear to be either rerouted to the plasma membrane, or sorted towards late endosomes en route to the lytic vacuole [4,7].

Some PIN sorting decisions have been linked to reversible, post-translational protein modifications (PTMs), allowing for rapid adjustments in protein function. Phosphorylation of PIN proteins by members of the AGCVIII (cAMP dependent, cGMP dependent, and protein kinase C) protein kinase family has been implicated in the regulation of PIN activity as well as in the control of polar PIN localization at the plasma membrane [8–10]. Although it is not yet entirely resolved, how variations in PIN phosphorylation could mediate such responses, structure-function analyses of a number of conserved phosphorylation sites within the PIN central hydrophilic loop revealed their essential function in the regulation of PINs. Specifically, a set of evolutionary conserved serines, found in the N-terminal portion of the central loop domain, has been analyzed extensively and revealed divergent but overlapping roles of distinct phosphosites in polar sorting of PIN proteins and in the activation of PIN-mediated auxin transport across membrane boundaries [9].

Another signal, triggering endocytic sorting of plasma membrane cargo involves reversible covalent attachment of the small protein modifier ubiquitin [11,12]. Recognition of ubiquitylated cargo by distinct adaptor protein complexes triggers a cascade of downstream events, ultimately resulting in cargo delivery to and degradation in lytic vacuoles [13,14]. In case of PIN proteins, ubiquitylation has so far only been demonstrated for *Arabidopsis* PIN2, which is subject to decoration by K63-linked ubiquitin chains [15]. Abolishment of PIN2 ubiquitylation by mutagenesis of several potential ubiquitin attachment sites in the central loop domain caused deficiencies in the protein's endocytic sorting and functionality, underlining an essential role for ubiquitin-controlled sorting of PIN2 [15].

Next to phosphorylation and ubiquitylation of distinct amino acid side chains, proteinogenic cysteines are subject to a range of different modifications. Cysteines represent the principal target of Reactive Oxygen Species (ROS), with its sulfur atom allowing for several different oxidation states, causing disulfide bond formation, *S*-glutathionylation, or *S*-nitrosylation, to name just a few, with distinct effects on protein fate [16]. Recently, links between auxin and redox signaling [17] were established, as variations in the cellular redox balance, triggered by altered ROS levels, were found to affect auxin-controlled plant morphogenesis [18–20]. A key role in controlling the cellular redox status has been attributed to the NADPH-dependent thioredoxin/glutaredoxin (TRX/GRX) and the NADPH-dependent glutathione (GSH) systems, both in the context of preventing oxidative damage as well as in the modulation of redox signaling events [18]. Loss of enzymatic activities, required for regulation of GRX/TRX and/or GSH homeostasis, was found to cause striking developmental aberrations, with combinatorial effects on auxin-controlled development. This is indicated by phenotypes exhibited by an *Arabidopsis ntra ntrb cab* triple mutant, affected in *NTRA* and *NTRB* NADPH-dependent thioredoxin reductase as well as *GSH1* γ-glutamylcysteine synthetase, strikingly resembling mutants defective in polar auxin transport. Moreover, this mutant combination is characterized by a dramatic reduction in *PIN* transcript levels and protein abundance, which could be phenocopied by application of buthionine sulphoximine (BSO), a potent inhibitor of GSH biosynthesis [19,21]. Therefore, it appears plausible that reduced expression of PINs could

at least partially account for auxin-related phenotypes described for *ntra ntrb cab*. This hypothesis is supported by another study, demonstrating that *miao*, a leaky *GLUTHATIONE REDUCTASE 2* (*GR2*) loss-of-function allele, markedly interferes with expression of regulators of auxin responses, including *PLETHORA* transcriptional regulators and *PIN* auxin transport proteins [20]. Whether alterations in these mutants' redox status directly affect distribution and sorting of PIN proteins at a post-transcriptional level remains to be addressed.

Indirect evidence for post-transcriptional regulation of PINs by GSH and/or nitric oxide came from the characterization of an *Arabidopsis* mutant deficient in *S*-nitrosoglutathione reductase (*GSNOR*), catalyzing reduction of GSNO and thereby adjusting levels of *S*-nitrosylated proteins. Specifically, loss of *GSNOR1* in *gsnor1–3* results in severe developmental perturbations, signifying wide-ranging effects of increased protein *S*-nitrosylation [22,23]. Defects involve lowered sensitivity to auxin, indicated by diminished proteolytic turnover of an AXR3/IAA17 reporter protein in response to the hormone as well as reduced lateral root formation, when grown in the presence of synthetic auxin 2,4-D. Moreover, *gsno1–3* seedlings are characterized by a reduction in polar auxin transport, which coincides with diminished levels of PIN auxin transport proteins, similar to observations made for mutants affected in GSH/TRX/GRX homeostasis [23]. However, unlike the situation in *ntra ntrb cab*, PIN protein down-regulation in *gsnor1–3* is not correlated with a corresponding decrease in *PIN* transcript levels [19,23]. In addition, another article reported elevated nitric oxide (NO) levels to cause a reduction of PIN1 protein abundance, without significantly affecting its transcript levels, pointing towards an involvement of protein *S*-nitrosylation in the post-translational control of PIN proteins [24].

Analysis of *Arabidopsis* mutants impaired in GSH and/or NO homeostasis revealed pronounced alterations in PIN protein abundance. However, whether such changes in protein fate arise as a consequence of redox status-induced PTMs of PINs remains unknown. In a pilot approach, we therefore set out and explored the functional significance of highly conserved cysteines found in the PIN protein family, utilizing modeling approaches and site-directed mutagenesis of *Arabidopsis PIN2*. Our findings indicate that, whilst almost dispensable for functionality in root gravitropism, PIN2 cysteines impact on protein distribution, highlighting their potential contribution to the fine-tuning of polar auxin transport.

2. Results

2.1. PIN Proteins Share Conserved Cysteines that Contribute to Protein Functionality

To address the hypothesis that cysteines do function as *cis*-acting regulators of PIN protein function, we reasoned that such residues should exhibit a high degree of conservation within the PIN family. Multiple sequence alignments performed with *Arabidopsis* PINs revealed a variable number of cysteines encoded by the different members of the gene family. This variability ranged from eight residues found in the *PIN5* ORF (Open Reading Frame) to only two cysteines found in PIN2 (Figure 1A). Notably, these two cysteines are highly conserved in the *Arabidopsis PIN* gene family, which generally appears to be case for PINs encoded by Tracheophyta, including ferns and clubmosses (Figure 1B). Additional alignments performed with predicted canonical PINs from *Physcomitrella patens, Marchantia polymorpha* and additional sequences from Charoyphyta revealed that both cysteines are present in *Marchantia* and *Physcomitrella* PINs, indicative of a high degree of conservation in Embryophyta. In contrast, PIN representatives from charophyte green algae rarely contain both cysteines (Figure 1B).

Taken together, our analysis of PINs found in land plants demonstrates a high degree of evolutionary conservation of a few, distinct cysteines within the protein family.

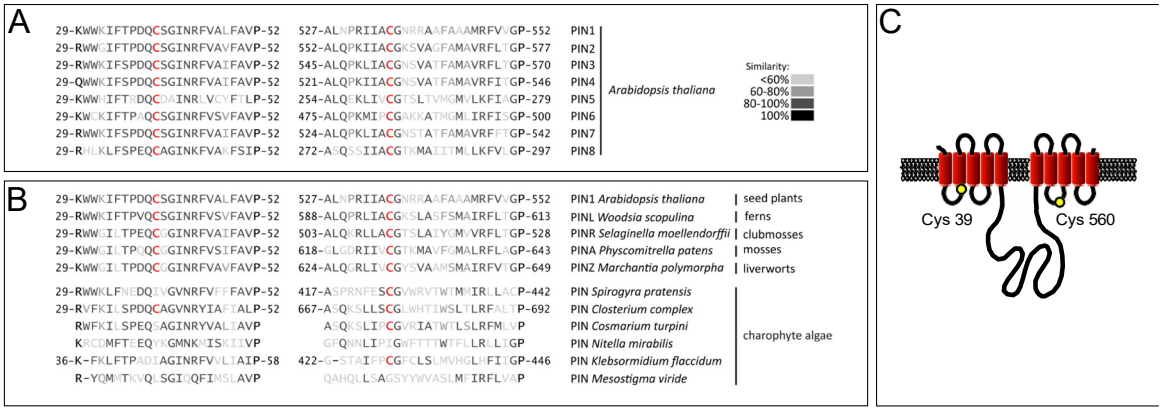

Figure 1. Conservation and predicted localization of conserved PIN cysteines. (**A**) Alignment of *Arabidopsis* PIN protein domains flanking conserved cysteines. Conserved cysteines are displayed in red; (B) Alignment of PIN protein domains flanking conserved cysteines, from representative Embryophyta and charophyte green algae. Conserved cysteines are displayed in red. Lack of indicated amino acid positions denotes incomplete sequences; (**C**) 2-D model displaying potential membrane conformation of PIN2. Red barrels represent predicted transmembrane helices, separated by loop domains (black lines). According to these predictions, both cysteines are facing the cytoplasm. The positions of Cys-39 in loop 1 and Cys-560 in loop 7 are indicated (yellow circles).

Among *Arabidopsis* PINs, PIN2 turned out to be unique, as it contains only those two cysteines that are highly conserved in PINs. As the case with any canonical PIN protein, PIN2 hydrophobicity plots indicated the presence of 10 transmembrane helices, which are organized as two blocks of five helices, separated by a central spacer region [25–27]. According to these predictions, Cys-39 would localize to the junction between loop 1 and helix 2, whereas Cys-560 would reside between helix 7 and 8. Considering that the PIN central loop region has been predicted to face the interior of the cell [28], then these topology predictions would indicate that both conserved cysteines localize to the cytoplasmic side of the plasma membrane (Figure 1C).

To obtain additional insights into PIN2 topology and accessibility of conserved cysteines, we performed an *in silico* modeling. However, due to the structural heterogeneity of full-length PIN2 (647 aa), we decided that rather than modeling it as a whole entity, it was more feasible to separate it into three constituting parts, and model each one individually, refining then the resulting structures via molecular dynamics (MD) simulations (see Material and Methods for protocol details). Because of the existing predictions of the protein structure [27], we considered the first part of the sequence as going from Met-1 to Arg-155, corresponding to the first cluster of transmembrane helices, the second part going from Gly-156 to Trp-495 and corresponding to the central loop, and the third part spanning from Arg-496 to Leu-647, corresponding to the second cluster of transmembrane helices.

To generate the initial models for the three parts, we used Modeller [29], producing several hundred structures, from which we selected the three best ones. Then, we refined these via MD simulations using AMBER (http://ambermd.org/) [30]. The procedures we followed are different for the loop and the helix clusters, since the latter are inside the cell membrane, and thus they are surrounded by lipids, rather than by water molecules. Concerning the loop, we solvated it explicitly, and then performed a two-step minimization of the structure: first, we minimized the position of water and ions around the protein fragment by constraining the atoms of the latter to their initial coordinates; then, we removed the constraints and minimized the whole system. Following minimization, we heated up the system with periodic boundary conditions at constant volume, and after the heating phase, we let it equilibrate at constant pressure for 1 ns. The behavior of temperature and energies (Figure 2) shows that equilibration of the loop is indeed reached over the time of these initial MD steps.

Finally, we extracted the lowest-energy conformation from the simulation trajectory and minimized it as described above.

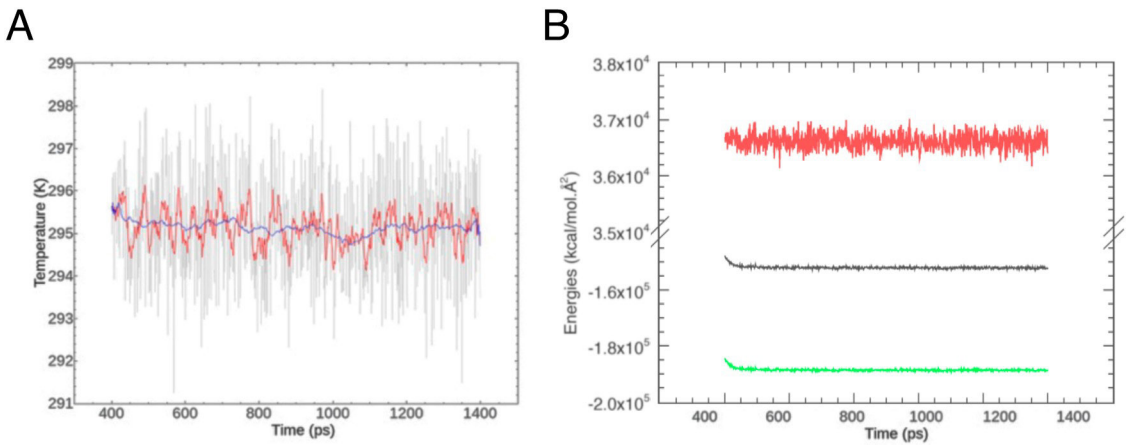

Figure 2. Equilibration of the PIN2 loop. (**A**) Behavior of system temperature over the equilibration period. The full raw data are in grey, while the red and blue lines show window averages over 10 and 100 ps, respectively; (**B**) Potential energy (green), kinetic energy (red) and total energy (black) of the system over the same period.

For the helix clusters (parts 1 and 3 of the protein), we employed implicit solvation to approximate the presence of a lipid bilayer as solvent of the protein fragments, which were treated individually and independently. The lipid environment was simulated by imposing a relative permittivity of the implicit solvent equal to 2.2, following the calculation before heating them and performing production runs of part 1 for a total of 41.4 ns and part 3 for a total of 30.1 ns. Temperature and energy plots (Figure 3A,B) show a good stability of the simulation over this time period. Then, we extracted the lowest energy conformations from the trajectories. To check the structural stability of these folded states, we aligned them with each individual frame of the whole simulation, computing a mass-weighted RMSD of the backbones. The results show that the selected conformation for part 1 is stable approximately over the last 20 ns, with an RMSD only occasionally greater than 2 Å and always close to 1 Å for the last 13 ns (Figure 3C). This suggests that no further secondary structure changes are likely to happen. The same conclusion can be drawn about part 3, with an RMSD fluctuating around an average of 1.3 Å for the duration of the production run.

Having obtained MD-refined models for the three regions of PIN2, we stitched them using UCSF Chimera (https://www.cgl.ucsf.edu/chimera/) [31], resulting in a single pdb file of the whole protein on which we performed a final refinement. To start this, we carried out a two-step minimization: first we constrained the positions of the atoms of the transmembrane regions, minimizing the conformation of the loop using the solvent relative permittivity of water; then, we restrained the resulting position of the loop and minimized the transmembrane domains with relative permittivity of the solvent equal to 2.2. To heat up the protein, we decided to constrain the helix clusters and let the loop move freely, since we expect that in the cell environment the rigidity of the loop is considerably smaller than that of the transmembrane domains. Subsequently, we let the loop equilibrate for 1 ns, before constraining it and equilibrating the conformation of the helix clusters for 1 ns. The final, globally equilibrated conformation was then minimized with the same two-step procedure described above.

The *in silico* modeling yielded a 3-D structure of the entire, translated PIN2 coding region (Figure 4A,B; Movie S1). Evidently, the calculated protein structure could represent a very useful tool, suitable for addressing PIN function in polar auxin transport. Here, we would like to point out that both cysteines are predicted to be positioned on the surface of modeled PIN2 (Figure 4A,B; Movie S1). If true, then such a protein configuration makes both cysteines accessible for interactions and modifications.

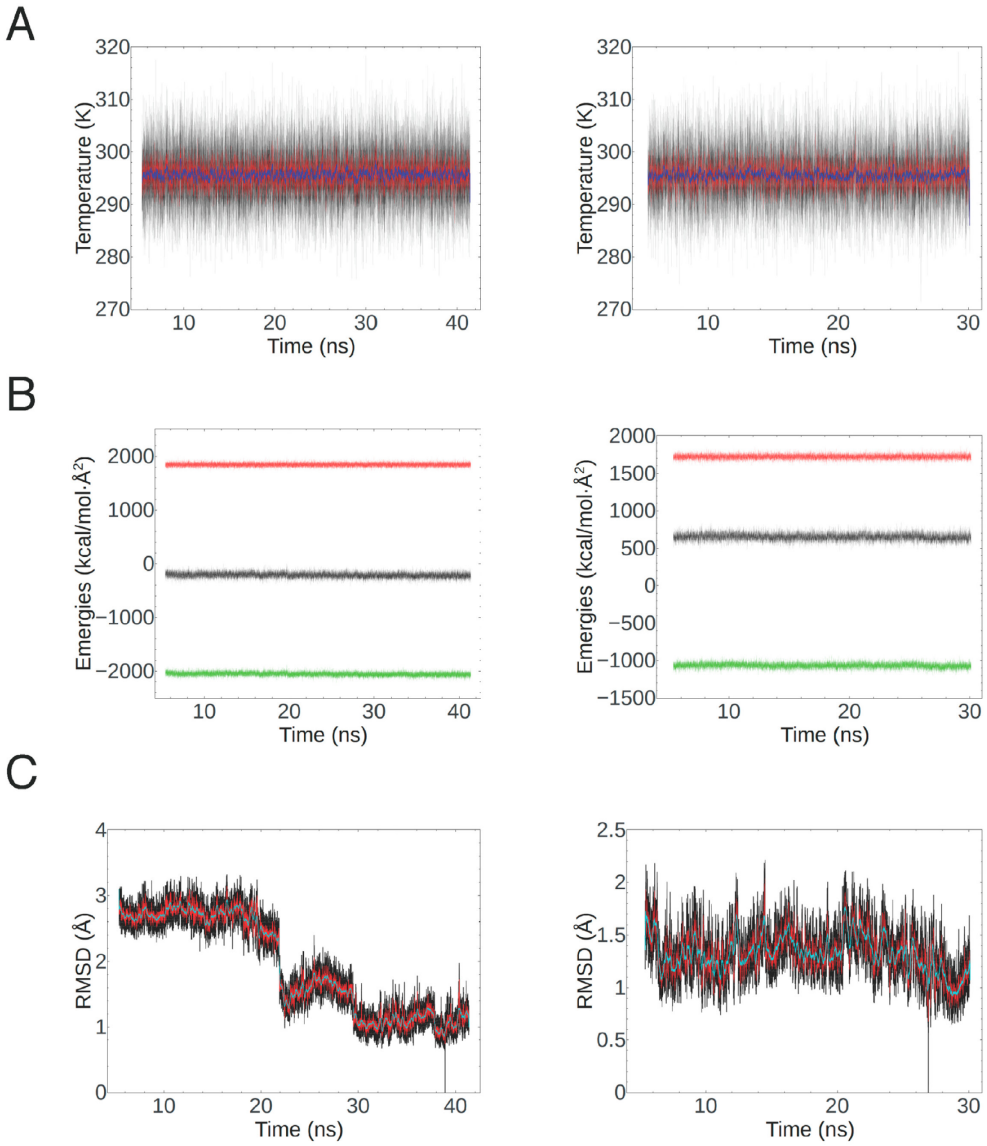

Figure 3. Equilibration and stability of the folded PIN2 helix clusters. (**A**) System temperature of part 1 (**left**) and part 3 (**right**) over the full production run. The raw data are in black, while the red and blue lines show window averages over 10 and 100 ps, respectively; (**B**) Potential energy (green), kinetic energy (red) and total energy (black) of part 1 (**left**) and of part 3 (**right**) over the same period as in (**A**); (C) RMSD of the lowest-energy conformation of part 1 (**left**) and part 3 (**right**) with respect to every other frame in the simulation, after alignment (black); the red and light blue lines are window averages over periods of 20 and 200 ps, respectively.

For a functional analysis of PIN2 cysteines, we initiated a site-directed mutagenesis approach, and replaced either Cys-39 or Cys-560 with an alanine residue. In addition, we generated a mutant *pin2*^{C39,560A} allele, in which both cysteines were replaced by alanines. These mutant alleles as well as a wild type copy of the *PIN2* ORF were fused to the *Arabidopsis PIN2* promoter and transformed into the root agravitropic *eir1-4* null allele of *PIN2,* in order to study functionality of *pin2*$^{C-A}$ alleles [15]. When grown on vertically oriented nutrient agar plates, no striking difference was observed between wild type controls and *eir1-4 PIN2::PIN2* seedlings, demonstrating that the transgene complements loss of endogenous *PIN2* [15]. Similarly, when comparing growth of vertically oriented *eir1-4 PIN2::PIN2* with *eir1-4 PIN2::pin2*^{C39A}, *eir1-4 PIN2::pin2*^{C560A} and *eir1-4 PIN2::pin2*^{C39,560A} seedlings, we did not observe any prominent differences in gravitropic root growth, which was indistinguishable from growth of

wild type Col-0 seedlings, indicating that *pin2*$^{C-A}$ alleles have retained functionality, sufficient for rescuing major *eir1-4* growth deficiencies (Figure 5A–F). Closer examination of root growth, however, revealed a reduction in root waviness for all three different *pin2*$^{C-A}$ alleles, when grown on the surface of vertically positioned agar medium (Figure 5A–E,G). Thus, whilst mutagenesis of cysteines does not interfere with overall PIN2 functionality in root gravitropism, these residues nonetheless appear critical for fine-tuning of directional root growth.

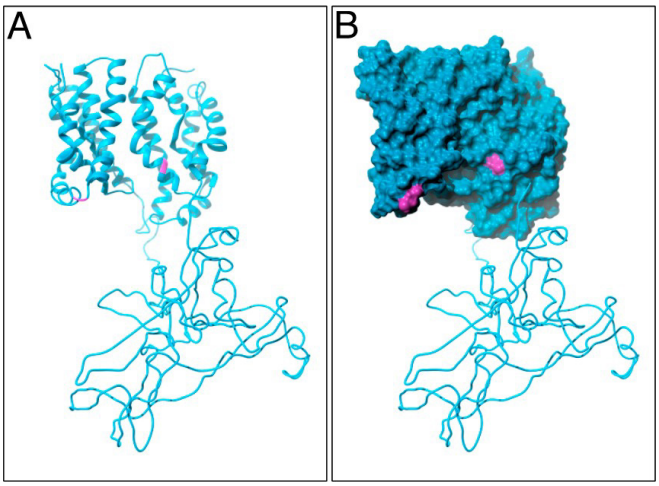

Figure 4. A 3-D model for PIN2: Ribbon diagram (**A**) and surface representation (**B**) of assembled 3-D structural predictions for PIN2. The position of both cysteines is labeled in pink. Rendering was performed within Chimera (https://www.cgl.ucsf.edu/chimera/) [31] using POV-Ray (http://www.povray.org/).

Pharmacological interference with GSH homeostasis by treatment of *Arabidopsis* seedlings with BSO resulted in pronounced defects in root development, which coincided with reduced expression of *PIN* genes [19,21]. In related experiments, we tested growth of *pin2*$^{C-A}$ alleles in response to BSO, which demonstrated increased root growth inhibition of *eir1-4 PIN2::pin2*^{C39A}, *eir1-4 PIN2::pin2*^{C560A} and *eir1-4 PIN2::pin2*^{C39,560A}, when germinated in presence of the drug (Figure 5H). Notably, this apparent hypersensitivity to BSO treatment, was visible, even when testing *pin2*^{C39,560A} completely lacking cysteines. This observation argues for additive effects of BSO-induced downregulation of GSH biosynthesis and Cys-to-Ala substitutions introduced into *pin2*$^{C-A}$ alleles. Whilst the nature of this interaction remains to be determined, it supports a role for the conserved cysteines in the regulation of PIN2 function.

Taken together, mutational analysis of PIN2 cysteines revealed their requirement for full functionality of the auxin transport protein. Nevertheless, expression of *pin2*$^{C-A}$ alleles is sufficient to rescue principal *eir1-4* growth deficiencies, indicating that these point mutations do not generally abolish PIN2 activity. Subtle growth deficiencies associated with *pin2*$^{C-A}$ alleles, would rather argue for a role of PIN2 redox control in the fine-tuning of adjustments in root growth.

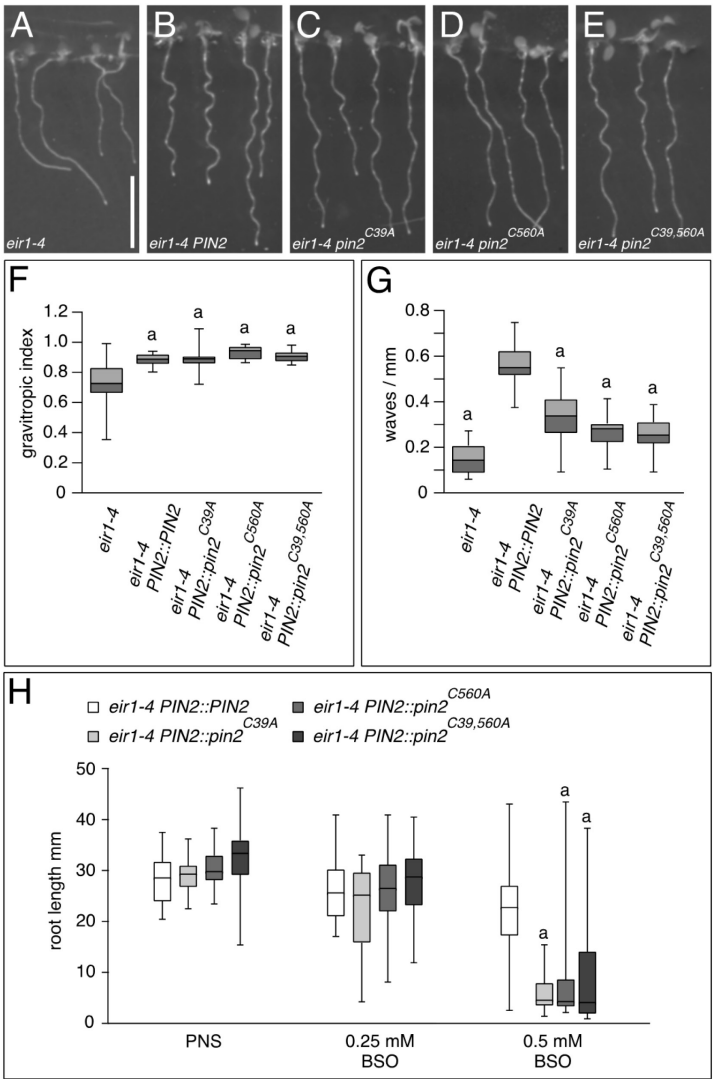

Figure 5. Growth of *pin2*$^{C-A}$ alleles. (**A**–**E**) Comparison of: *eir1-4* (**A**); *eir1-4 PIN2::PIN2* (**B**); *eir1-4 PIN2::pin2*^{C39A} (**C**); *eir1-4 PIN2::pin2*^{C560A} (**D**); and *eir1-4 PIN2::pin2*^{C39,560A} seedlings at 6 DAG. Size bar corresponds to 10 mm; (**F**) Box plot displaying the root gravitropic index of *eir1-4*, *eir1-4 PIN2::PIN2*, *eir1-4 PIN2::pin2*^{C39A}, *eir1-4 PIN2::pin2*^{C560A}, and *eir1-4 PIN2::pin2*^{C39,560A}, according to Grabov and colleagues [32] at 6 DAG. In total, 13–27 roots were tested for each genotype. "a" indicates a significant difference to *eir1-4* ($p < 0.01$), determined by One-way ANOVA with post-hoc Tukey HSD test. No significant differences were observed when comparing *eir1-4 PIN2::PIN2* to *eir1-4 PIN2::pin2*^{C39A}, *eir1-4 PIN2::pin2*^{C560A}, and *eir1-4 PIN2::pin2*^{C39,560A}. Whiskers represent the entire range of outliers obtained in the datasets; dark grey and light grey boxes display first and third quartiles, respectively. (**G**) Box plot, displaying the root waviness of *eir1-4*, *eir1-4 PIN2::PIN2*, *eir1-4 PIN2::pin2*^{C39A}, *eir1-4 PIN2::pin2*^{C560A}, and *eir1-4 PIN2::pin2*^{C39,560A} at 6 DAG, grown on vertically orientated agar (1.5% (*w*/*v*)) nutrient plates. In total, 21–27 roots were tested for each genotype. "a" indicates a significant difference to *eir1-4 PIN2::PIN2* ($p < 0.01$), determined by One-way ANOVA with post-hoc Tukey HSD test. Whiskers represent the entire range of outliers obtained in the datasets; dark grey and light grey boxes display first and third quartiles, respectively; (**H**) Box plot displaying the primary root length of *eir1-4 PIN2::PIN2*, *eir1-4 PIN2::pin2*^{C39A}, *eir1-4 PIN2::pin2*^{C560A}, and *eir1-4 PIN2::pin2*^{C39,560A} at 7 DAG, when germinated in presence of indicated concentrations of buthionine sulphoximine (BSO). In total, 20–32 seedlings were analyzed for each genotype "a" indicates a significant difference to *eir1-4 PIN2::PIN2* ($p < 0.01$), determined by One-way ANOVA with post-hoc Tukey HSD test. Whiskers represent the entire range of outliers obtained in the datasets.

2.2. Conserved Cysteines Are Determinants of PIN2 Intracellular Distribution

To test for possible consequences of *pin2*$^{C-A}$ mutations on intracellular distribution and sorting of PIN2, we generated Venus-tagged translational fusion constructs, which were then expressed in *eir1-4*. The resulting *eir1-4 PIN2::pin2*^{C39,560A}*:Venus* lines exhibited phenotypes similar to those of lines expressing untagged *pin2*$^{C-A}$ alleles (Figure 6A–C), and were subject to further expression analysis.

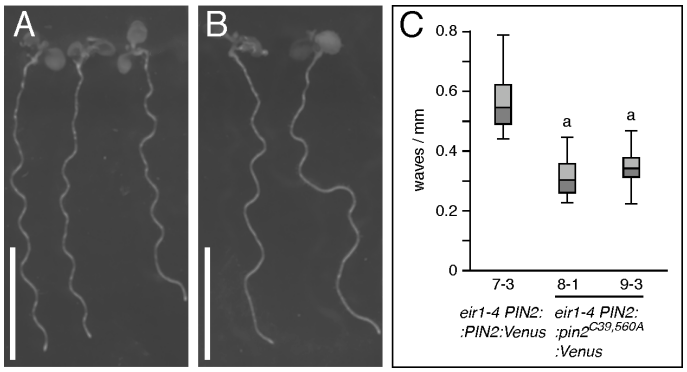

Figure 6. Analysis of *PIN2::pin2*^{C39,560A}*:Venus* lines. (**A**,**B**) Comparison of: *eir1-4 PIN2::PIN2:Venus* (**A**) and *eir1-4 PIN2::pin2*^{C39,560A}*:Venus* (**B**) seedlings at 6 DAG grown on vertically oriented nutrient plates. Size bars correspond to 10 mm; (**C**) Root waviness of *eir1-4 PIN2::PIN2:Venus* and two independent *eir1-4 PIN2::pin2*^{C39,560A}*Venus* lines at 6 DAG, grown on vertically orientated agar (1.5% (*w*/*v*)) nutrient plates. In total, 25–28 seedlings were tested for each genotype. "a" indicates a significant difference to *eir1-4 PIN2::PIN2:Venus* ($p < 0.01$), determined by One-way ANOVA with post-hoc Tukey HSD test. Whiskers represent the entire range of outliers obtained in the datasets; dark grey and light grey boxes display first and third quartiles, respectively.

Eir1-4 PIN2::pin2^{C39,560A}*:Venus* exhibited an expression pattern and polarly localized signals at the plasma membrane, similar to wild type PIN2:Venus (Figure 7A–D). However, when comparing subcellular distribution of PIN2:Venus and pin2^{C39,560A}:Venus protein in more detail, we observed an increase of intracellular signals in epidermal cells of *eir1-4 PIN2::pin2*^{C39,560A}*:Venus* seedlings (Figure 7E). This increase was apparent in trichoblast and atrichoblast cells of primary root meristems, indicative of modifications in intracellular distribution/sorting of the mutant PIN2 reporter protein (Figure 7F). Furthermore, when performing co-staining experiments with the endocytosed styryl dye FM4-64, we detected a prominent overlap in signal distribution, demonstrating that mutant pin2^{C39,560A}:Venus has a strong tendency to enter the endocytic sorting pathway, which might explain the increased intracellular accumulation of pin2^{C39,560A}:Venus signals (Figure 7G,H).

We reasoned that the apparent differences in intracellular distribution of PIN2:Venus and pin2^{C39,560A}:Venus signals highlight a requirement for the conserved cysteines in PIN protein traffic.

Models for PIN2 sorting in root epidermis cells predicted super-polar exocytotic sorting to the central section of the apical plasma membrane domain. A fraction of plasma membrane-targeted PIN2 was suggested to be subject to lateral diffusion, followed by clathrin-dependent endocytosis, initiated at the outermost edges of the apical domain. In contrast, another fraction of exocytosed PIN2 was described to accumulate in plasma membrane-associated clusters, exhibiting only limited mobility, when compared to the kinetics of other plasma membrane proteins [33,34]. This led to models in which the interplay between mobile vs. immobile PIN2 fractions at the plasma membrane could determine abundance, distribution and hence PIN2 activity in cellular auxin efflux [33]. We analyzed PIN2:Venus and pin2^{C39,560A}:Venus reporter protein signals at the plasma membrane of root epidermis cells by using conventional confocal microscopy. This analysis revealed discontinuities in signal distribution along the plasma membrane, which might reflect the occurrence of PIN2 signal aggregates (Figure 8A). Attempts to visualize these structures at higher resolution by super-resolution STED microscopy were

not successful, due to very prominent signal bleaching, specifically of pin2^{C39,560A}:Venus, and we therefore utilized an alternative high resolution approach.

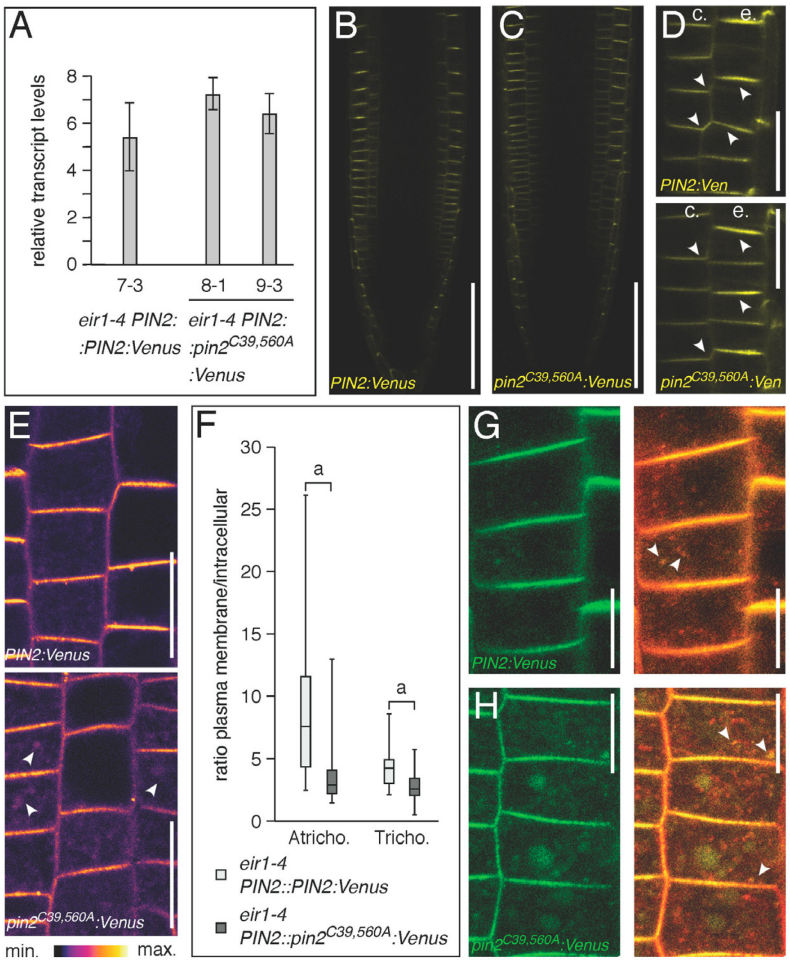

Figure 7. Expression pattern and localization of *PIN2::pin2*^{C39,560A}*:Venus* reporter lines. (**A**) Relative transcript levels of *PIN2::PIN2:Venus* and two *PIN2::pin2*^{C39,560A}*Venus* lines at 6 DAG. Two biological repetitions have been used for each sample, with transcripts normalized to expression of *EF1a* (At1g07940). Bars indicate standard deviations. One-way ANOVA with post-hoc Tukey HSD test demonstrated no significant differences in transcript levels (*PIN2::PIN2:Venus* vs. *PIN2::pin2*^{C39,560A}*Venus* 8-1, p = 0.1506725; *PIN2::PIN2:Venus* vs. *PIN2::pin2*^{C39,560A}*Venus* 9-3, p = 0.5558223); (**B**,**C**) Expression pattern (yellow coloration) in: *eir1-4 PIN2::PIN2:Venus* (**B**) and *eir1-4 PIN2::pin2*^{C39,560A}*Venus* (**C**) primary root meristems at 6 DAG is restricted to lateral root cap, epidermis and cortex cells; (**D**) Reporter signal localization in epidermis ("e") and cortical ("c") in *eir1-4 PIN2::PIN2:Venus* and *eir1-4 PIN2::pin2*^{C39,560A}*Venus* primary root meristem cells at 6 DAG. Arrowheads indicate polar localization of the reporter signals; (**E**) Comparison of signal distribution in *eir1-4 PIN2::PIN2:Venus* and *eir1-4 PIN2::pin2*^{C39,560A}*Venus* primary root meristem epidermis cells at 6 DAG; white arrowheads indicate intracellular reporter protein signals; (**F**) Signal quantification in *eir1-4 PIN2::PIN2:Venus* and *eir1-4 PIN2::pin2*^{C39,560A}*Venus* primary root meristem epidermis cells at 6 DAG. The ratio of reporter signal intensities at the plasma membrane compared to intracellular signals was determined in 36–57 trichoblast ("Tricho.") and atrichoblast ("Atricho.") cells for each sample. Two-tailed *t*-test analysis of resulting values demonstrated significant differences (p < 0.001, "a"); (**G**,**H**) Staining of *eir1-4 PIN2::PIN2:Venus* and *eir1-4 PIN2::pin2*^{C39,560A}*Venus* (green) with FM4-64 for 30 min in the dark, followed by visualization at the CLSM. White arrowheads indicate co-staining (yellow) in endocytosed compartments. Size bars: **B–D** = 50 µm; **E** = 20 µm; **G**,**H** = 10 µm.

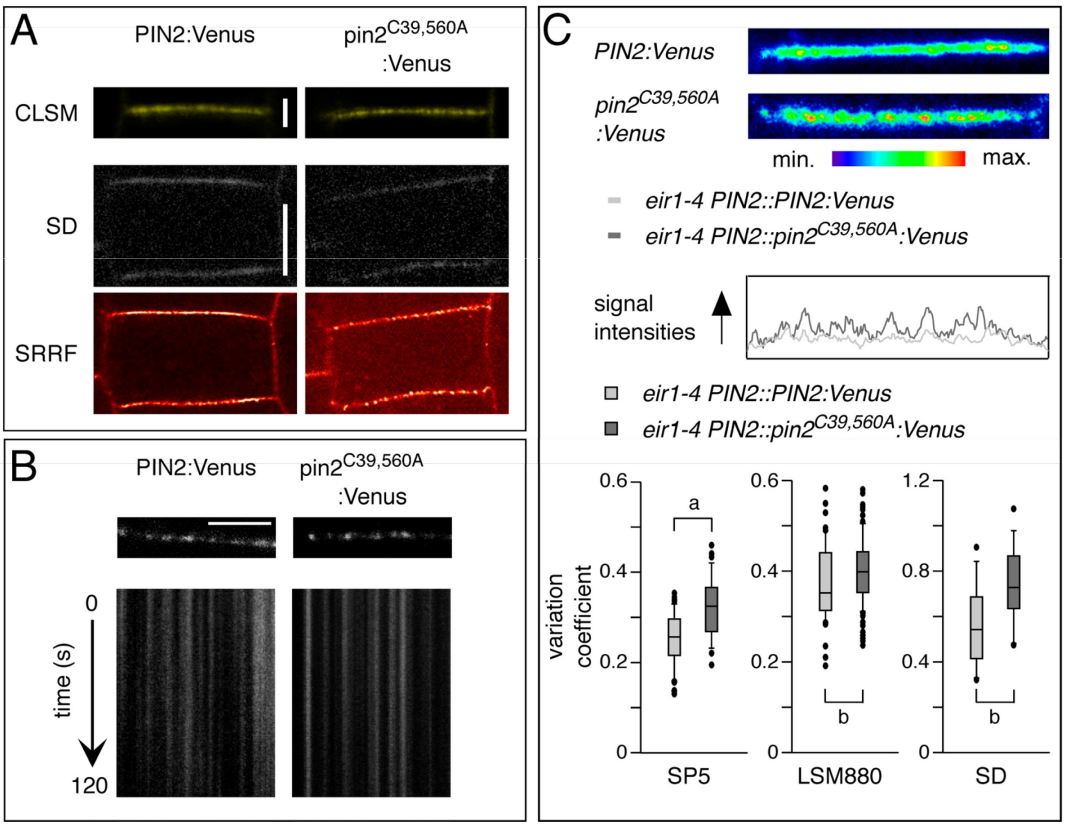

Figure 8. Distribution and mobility of PIN2-Venus reporter proteins. (**A**) Upper row: Comparison of PIN2:Venus (**left**) and pin2^{C39,560A}:Venus (**right**) signals at the plasma membrane of root epidermis cells, viewed by conventional CLSM imaging. Middle row: A single frame generated by fast SD scanning (50 ms exposition), displaying PIN2:Venus (**left**) and pin2^{C39,560A}:Venus (**right**) signals at the plasma membrane of root epidermis cells. Bottom row: SRRF algorithm applied to 100 frames generated by SD on the same sections as above. Scale bars 2 µm (CLSM) and 5 µm (SD); (**B**) Kymographs representing the fluorescence of PIN2:Venus (left) and pin2^{C39,560A}:Venus (right) signals over time. Scale bar 5 µm; (**C**) Top panel: Comparison of signal distribution in root epidermis plasma membrane domains of PIN2:Venus and pin2^{C39,560A}:Venus. Bottom panels: Box plots displaying PIN2:Venus and pin2^{C39,560A}:Venus signal intensity profiles at the plasma membrane calculated from CLSM (Leica SP5, Zeiss LSM880) and SD images. Ninety membranes from images generated by Leica SP5, 150 from Zeiss LSM880 and 40 membranes from SD images were used for these analyses. Two-tailed *t*-test analysis of resulting values demonstrated significant differences ($p < 0.001$, "a"; $p < 0.05$, "b").

The Super-Resolution Radial Fluctuations (SRRF) algorithm has been introduced recently, to allow for generation of high resolution images, with illumination intensity requirements orders of magnitude lower, than used by other super-resolution methods [35]. We made use of this approach, which allowed us a comparison of signal distribution and signal intensities in *eir1-4 PIN2::PIN2:Venus* and *eir1-4 PIN2::pin^{C39,560A}:Venus* root meristem cells, derived from frame sets generated by fast scanning with low laser power Spinning Disc (SD) confocal microscopy. This sub-diffraction analysis revealed distinct structures in the sub-nanometer size range in *eir1-4 PIN2::PIN2:Venus* and *eir1-4 PIN2::pin^{C39,560A}:Venus* root meristem cells (Figure 8A), likely reflecting PIN2 clusters that have been described earlier [33]. We then employed SD confocal microscopy and kymograph analysis to determine signal distribution over time. These experiments indicated very limited cluster movement when analyzing either wild type PIN2:Venus or pin2^{C39,560A}:Venus signals (Figure 8B). From that, we concluded that formation of static PIN2 clusters at the plasma membrane is not categorically obstructed by mutagenesis of PIN2 cysteines.

To assess the distribution of PIN2:Venus signal at the plasma membrane we decided to evaluate local fluctuations of fluorescence intensity in membranes of individual cells. The resulting values were used for calculating the coefficient of variation of signal intensity profiles along plasma membranes in PIN2:Venus and pin2^{C39,560A}:Venus lines. Notably, evaluation of these profiles revealed a prominent increase in the coefficient of variation in pin2^{C39,560A}:Venus signal intensities, when compared to the wild type protein. Higher signal variabilities point towards a less homogenous distribution of the mutant reporter protein at the plasma membrane, indicative of local alterations in protein distribution (Figure 8C). Thus, apart from the increased intracellular accumulation of pin2^{C39,560A}:Venus, Cys-to-Ala substitutions seemingly affect the pattern of PIN2 distribution within plasma membrane micro-domains, hinting at an overall altered mobility of the mutant protein.

3. Discussion

Timely and coordinated responses to environmental parameters are important for the survival of sessile organisms, well exemplified by the ability of higher plants to adapt to a wide range of growth conditions. At the molecular level, adaptations to variable conditions involve a diversity of PTMs, influencing distribution and mobility, steady state levels, conformation as well as activity of proteins. Specifically, modifications of cysteines play a decisive role in such post-translational control of proteins, and were found to be of general importance for all life on earth [16]. In this study, we tested the role of two conserved cysteines identified in the PIN family of auxin transport proteins, revealing a role in protein mobility and localization in plasma membrane micro-domains. Such altered PIN2 behavior could be attributed to modifications in protein topology, caused by the point mutations introduced, and would be consistent with a role of redox status-controlled cysteine modifications in the regulation of PIN2 mobility.

At present, crystal structure and overall configuration of PIN proteins are not known, which makes it difficult to draw conclusions solely based on the outcome of site-directed mutagenesis experiments, as described in this study. Conversely, aquaporin-type water channel proteins, represent extremely well characterized plasma membrane proteins, and have been subject to extensive analyses [36]. Notably, mutagenesis of a conserved cysteine found in plant PLASMA MEMBRANE INTRINSIC PROTEIN-(PIP)-type aquaporins had effects similar to those that we observed for mutant pin2^{C-A}. Specifically, a PIP Cys-to-Ser substitution did not significantly interfere with protein function, as it had no striking effects on protein sorting and protein activity, upon heterologous expression in oocytes. Moreover, formation of the biologically active, tetrameric PIP configuration remained unaffected by this mutation [37], questioning a contribution of the conserved cysteine to PIP maturation and oligomerization. Consistent with these findings, another study identified several transmembrane helix-localized residues as critical for intra- and inter-proteinogenic helix interactions, which turned out to be essential for PIP sorting to the plasma membrane and for formation of functional PIP protein tetramers [38]. Based on these observations, it appears that disulfide bond formation plays only subordinate roles in establishing functional PIP protein complexes.

By analogy to PIPs, our analysis of mutant pin2^{C-A} suggests that disulfide bond formation is not a principal prerequisite for activity of the auxin transport protein. This is indicated by the apparently polar localization of pin2^{C39,560A}:Venus, together with rather subtle root growth defects, associated with expression of *pin2*$^{C-A}$ alleles in a *pin2* null background. This contradicts a model, in which redox status-induced PTMs are quintessential for the regulation of PIN2 polar targeting. Rather, we conclude that PIN2 cysteine residues and potential redox signaling-controlled modifications contribute to association to specific plasma membrane domains, thereby influencing PIN2 sorting processes.

A report by Kleine–Vehn and colleagues [33] provided evidence for the existence of distinct PIN protein pools that can be found at plasma membrane domains. The majority of membrane-associated PIN2 appears to form protein aggregates, visible as irregularly shaped signal clusters with a limited tendency to move within the plasma membrane. In addition, another protein fraction was suggested to show higher mobility, which is primarily based on observations, demonstrating clathrin-dependent

PIN2 endocytosis at distal portions of the apical plasma membrane domain of root epidermis cells. The biological significance of such distinct PIN2 fractions and mechanisms that would control the equilibrium between such fractions, however, are not known [33].

PIN2 super-resolution SRRF analyses presented in this study, provides additional evidence for the existence of distinct PIN2 pools. This is supported by signal quantification, based on SRRF-generated images, together with SD analysis, demonstrating aggregations of immobile PIN2 signals for PIN2 wild type and pin2^{C39,560A} reporter lines. However, when determining intensity profiles by calculation of reporter protein signal scattering, we observed a prominent increase in the local variations of pin2^{C39,560A} signal intensities. These variabilities reflect adjustments in protein localization within plasma membrane micro-domains, potentially arising from an altered intramembranous mobility caused by Cys-to-Ala substitutions introduced into PIN2. We cannot categorically exclude a scenario, in which an altered protein conformation caused by the point mutations introduced, is solely responsible for the altered characteristics of pin2^{C39,560A}. Due to the differences in their side chains, replacement of cysteines by alanines might cause subtle changes in the overall structure of protein domains. This however, might also be true for serine, frequently used for mutational analysis of cysteine residues, and characterized by a hydroxyl group instead of a sulfhydryl group in its side chain. These side chains enable hydrogen bond formation between serines, when positioned in an adequate distance, thereby influencing protein conformation. A detailed biochemical analysis of PIN2 protein conformation and of potential redox status-controlled effects on PIN2 is required, to further address this issue.

Indirect support for redox status-dependent PIN protein modifications comes from experiments, demonstrating that variations in NO levels and protein *S*-nitrosylation exert strong effects on PIN abundance at the plasma membrane [22,23]. As a result, redox status-dependent variations in PIN distribution would modulate auxin flow, via controlling protein mobility in the plasma membrane. PIN2 thus could be subject to sorting control mechanisms, similar to those of *Arabidopsis* Salicylic Acid (SA) receptor *NONEXPRESSER OF PR GENES 1* (*NPR1*), which undergoes redox status-dependent protein redistribution in response to pathogens. NPR1, a regulator of plant systemic acquired resistance (SAR), resides in the cytoplasm and in the nucleus, where it functions as transcriptional co-regulator of *PR* genes [39]. Cytoplasmic sequestration depends on intermolecular disulfide bond formation between NPR1 monomers, which is promoted by *S*-nitrosylation of NPR1 [40]. Conversely, SA-induced reduction of NPR1 oligomers, facilitated by thioredoxins, results in nuclear accumulation of monomeric NPR1, where it modulates expression of defense-related genes [39–41]. This elegant mechanism integrates stimulus-dependent variations in redox signaling and plant defense responses via control of NPR1 conformation, and a related scenario could be envisioned for PIN2. By analogy to NPR1, redox status-induced structural changes of PIN2 could be induced by reversible cysteine modifications, which might influence conformation of the protein. This in turn, could transiently affect PIN2 mobility, followed by altered distribution in plasma membrane micro-domains and variations in endocytic protein sorting.

At this moment, we are still lacking conclusive experimental evidence for redox status-dependent PTMs directly controlling mobility and sorting of PIN2. Specifically, whilst some reports demonstrated dramatic effects of NO-signaling on post-transcriptional regulation of PIN protein abundance, it remains to be determined, whether or not PINs represent substrates for associated protein modifications [23,24]. This is also the case for our understanding of mechanisms, by which redox-controlled PTMs could affect mobility of proteins at the plasma membrane. A recent study suggested cross-talk between plant plasma membrane proteins and the cell wall as a determinant of protein mobility, and such cross-talk appears essential for correct sorting and localization of PIN proteins as well [34,42]. Adjustments in redox signaling could modify such hypothetical PIN2–cell wall interactions in a quantitative manner, thereby influencing PIN2 mobility and function at the plasma membrane.

Regardless of the hypothetical role of PIN2 cysteines in redox signaling, subtle phenotypes of *pin2*$^{C-A}$ alleles suggest that adjustments in the PIN2 redox status exert only limited effects on polar

auxin transport and root growth. These mild developmental modifications are in striking contrast to the severe auxin-related defects, described for mutants defective in the control of GSH and/or NO homeostasis [19,20,23]. Hence, it appears that transmission of redox signals that decide about *PIN* expression and activity depends on a combination of events [17,19,20,23,43]. Deciphering the interplay between such distinct redox status-controlled processes and how they might jointly shape auxin distribution and signaling events in the orchestration of plant development, remains a challenge for future research.

4. Materials and Methods

4.1. Plant Lines, Growth Conditions and Vector Construction

Plants were grown on $\frac{1}{2}\times$ Murashige Skoog medium, or on PNS plant nutrient agar plates (5 mM KNO_3, 2 mM $MgSO_4$, 2 mM $Ca(NO_3)_2$, 250 mM KPO_4, 70 µM H_3BO_3, 14 µM $MnCl_2$, 500 nM $CuSO_4$, 1 µM $ZnSO_4$, 200 nM Na_2MoO_4, 10 µM NaCl, 10 nM $CoCl_2$, 50 µM $FeSO_4$; pH adjusted to 5.7; supplemented with 1% (*w*/*v*) agar and 1% (*w*/*v*) sucrose; in a 16 h light/8 h dark regime at 22 °C). *PIN2::PIN2*, *PIN2::PIN2:Venus* and *eir1-4* have been described elsewhere [15,44]. For site-directed mutagenesis, we generated primers 5^t-GGGATATTCACACCGGACCAAGCTTCCGGTATAAACCG GTTGC-3^t and 5^t-CGAACCGGTTTATACCGGAAGCTTGGTCCGGTGTGAATATCC-3^t for mutagenesis of C39. As a template for PCR we made use of *PIN2::PIN2* and *PIN2::PIN2:Venus* binary vector constructs, as described previously. *Resulting pin2^{C39A}* candidate clones were confirmed by sequencing and subsequently subject to another round of site-directed mutagenesis, using primers 5^t-AACCAAAGATTATTGCGGCCGGAAAATCAGTAGCAGGG-3^t and 5^t-CCCTGCTACTGATTTTCCGGCCGCAATAATCTTTGGTT-3^t for replacement of C560. Resulting *pin2^{C39,560A}* candidate clones were confirmed by sequencing. For generation of *pin2^{C560A}*, PIN2::PIN2 and PIN2::PIN2:Venus binary vectors were used as template DNA. Flowering *Arabidopsis* plants were transformed by the floral dip method [45], using *Agrobacterium tumefaciens* strain GV3101/pMP90 [46]. Resulting T2 lines were confirmed for single transgene insertion sites and propagated to homozygosity for further analyses.

4.2. Microscopy

Spinning disk confocal microscopy was performed using spinning disc microscope Eclipse Ti-E (Nikon, Tokyo, Japan) with CSU-X1 SD unit (Yokogawa, Tokyo, Japan), 100× Plan-Apochromat objective (NA = 1.45 Oil) and a dual camera system. Time series for SRRF analysis were acquired with an EMCCD camera iXon3 897 (Andor Technology, Belfast, Northern Ireland) obtaining images with no averaging at 32 fps with a pixel size of 110 nm. Kymograph imaging was performed with a sCMOS camera Zyla (Andor Technology). Fluorescence signals were excited with a diode laser (488 nm; Agilent, Santa Clara, CA, USA) and fluorescence emission recorded using Semrock Brightline single-pass filters (Semrock, Rochester, NY, USA) for GFP or YFP. For kymograph analysis, a 120 s time series was taken for each image.

CLSM images were generated using Leica SP5 (Leica Microsystems, Wetzlar, Germany) and Zeiss LSM880 (Carl Zeiss, Jena, Germany) microscopes. For imaging, we used the following excitation conditions: 514 nm (Venus), 561 nm (FM4-64). For endocytic sorting studies, 5–6 day old seedlings were transferred from horizontally oriented nutrient plates into 6-well plates with liquid medium and incubated in presence of FM4-64 (Invitrogen, Waltham, MA, USA; working concentration 2 µM) for 30 min before CLSM visualization.

4.3. Homology Modeling and Molecular Dynamics

To find appropriate templates to model the three sequence parts, we submitted them to PSIPRED for analysis via GenTHREADER [47–50], which identified the sodium bile acid symporter from *Y. frederiksenii* (PDB code 4N7W) as a viable template for parts 1 and 3, and the capsid of the B19

parvovirus (PDB code 1S58) as a homologous structure for part 2. We then employed Modeller, a program that implements several methods to determine the structure of proteins via comparative modeling. These were obtained, using the "slow" library scheduler and the "very slow" annealing refinement, as these options provide the highest level of modeling accuracy. Each base model of part 2 was then refined via loop optimization 16 independent times, yielding a total of 1024 models for the central loop. Loop optimizations were also performed with the "very slow" annealing, and repeated twice for each of the 16 independent refinements. To choose the best models for each part, we considered the respective values of the Modeller objective function, the high-resolution discrete optimized protein energy (d atomic potential).

To prepare the input for the molecular dynamics simulations, we explicitly solvated part 2 of the protein in an octahedral box with a minimum allowed distance between solute atoms and box edges of 8 Å and the addition of 5 Cl^- counter-ions to neutralize the electric charge. To prepare the input for the molecular dynamics simulations, we explicitly solvated part 2 of the protein in an octahedral box with a minimum allowed distance between solute atoms and box edges of 8 Å and the addition of 5 Cl^- counter-ions to neutralize the electric charge. The model we used for implicit solvation of the transmembrane helix clusters (parts 1 and 3), as well as for the final, assembled protein, is the Generalized Born with volume corrections of Ref. [51], with further optimizations for H, C, N, O and S atoms in proteins as described in Ref. [52]. The topology parameters for the loop were prepared using the ff14SB force field for the protein fragment [53] and the TIP3P model for the water molecules [54]. For parts 1 and 3, and for the full protein, we used instead the ff14SBonlysc force field, which includes the backbone parameters of the ff99SB force field [55] with the side-chain parameters of the ff14SB [53], and which is known to yield the best results with the implicit solvation model we chose.

All minimization steps were automatically stopped when the RMS of the Cartesian components of the energy gradient became smaller than 0.05 kcal/(mol·Å^2). Whenever applied, positional constraints on the atoms were obtained by applying a harmonic potential, with force constant of 500 kcal/(mol·Å^2) for part 2, and 20 kcal/(mol·Å^2) for the full protein.

Heating was always carried out to a temperature of 295.15 K over a time of 400 ps with a time-step of 2 fs, constraining the bond length of the protein fragment with SHAKE [56] and that of water molecules, whenever present, with SETTLE [57]. The force constant for the harmonic potential restraints during heating of the full assembled protein was 20 kcal/(mol·Å^2).

During equilibration and production runs, temperature control was achieved via Langevin dynamics. The collision frequency was 2 ps^{-1} for the simulations of the three individual pieces, and 5 ps^{-1} for the final full protein, where we wanted to maintain a tighter thermal coupling.

For the simulations of part 2, long-range electrostatic interactions were evaluated via a particle-mesh Ewald procedure with a cutoff of 8 Å. The implicit solvent simulations were always carried out with an effectively infinite cutoff (larger than system size) for the non-bonded pair truncation and for the maximum atom distance to consider in the effective Born radii calculation, with the exception of the heating and loop equilibration steps for the assembled proteins, where we imposed a cutoff of 16 Å. In addition, during the implicit solvent simulations, forces dependent on effective radii derivatives and interactions over more than 8 Å were computed every two integration steps.

4.4. Data Acquisition and Processing

For root elongation assays, seedlings of each genotype were germinated on PNS in presence of the indicated drugs. After incubation on vertically positioned nutrient plates, seedlings were scanned and root length was determined, using ImageJ/Fiji software [58]. For root gravitropism and root waving assays, seedlings of each genotype were germinated on vertically oriented nutrient plates. Seedlings were scanned and resulting images used for determination of the gravity index [32] and root waves per root length. For assessment of reporter protein distribution, we determined relative grey values at the plasma membrane and in endocytic/vacuolar compartments, by using Fiji/ImageJ software [58].

Images acquired with Leica SP5, Zeiss LSM880 and spinning disc microscope were used to evaluate protein accumulation in membrane micro-domains. For the quantification of CLSM fluorescence at the plasma membrane, intensity profiles along individual membranes were generated with Zen Blue software (Zeiss). For each membrane, the coefficient of variation was calculated as the ratio of standard deviation to the mean florescence intensity, taking into account all fluorescence intensities of individual pixels. These coefficients of variation were used as measures for local fluctuations of fluorescence intensity in membranes of individual cells. Average values were depicted as box plots, their statistical significance was calculated using Two-tailed *t*-test or Mann-Whitney Rank Sum test in Sigma Plot (Systat, Chicago, IL, USA).

For SRRF analysis, the NanoJ-SRRF plugin for Fiji software was used [30]. Image stack of 100 SD image frames (frequency 32 fps) was grabbed with NIS elements 3.1 software (Nikon, Tokyo, Japan) in 14 bit color depth, image resolution 512 × 512 and pixel size 110 nm. Whole image stacks were converted to NanoJ file format and processed with SRRF analysis function with default values (ring radius 0.5, radiality magnification 5 and 6 axes in ring). No drift correction was needed, because there was no detectable growth and/or shift of cells during fast scanning. Resulting SRRF images with resolution 2560 × 2560 were obtained.

4.5. PIN Sequences and Alignments

PIN sequences from streptophyte algae were obtained from the NCBI SRA databases [59]. The sequence from *Klebsormidium flaccidum* was used as a query for tblastn search [60]. Short reads were assembled with CAP3 [61] and resulting contigs were subjected to further blastn searches against the respective SRA database to achieve additional sequence coverage. The obtained algal sequences were added to an alignment of representative land plant *PIN* sequences published previously [27] by means of the realigning MAFFT algorithm—add method with automatic parameter adjustment [62]. The degree of amino acid conservation reflected by the black–white color gradient was determined with the Geneious program (Blosum62 matrix; threshold set to 1).

4.6. Expression Analysis

RNA was isolated from 6-days old *Arabidopsis* seedlings using RNeasy Plant Mini kit (Qiagen, Hilden, Germany), treated with DNase I (Ambion, Waltham, MA, USA) and reverse transcribed using oligo-dT primers and M-MLV Reverse Transcriptase (Promega, Fitchburg, WI, USA). First strand cDNA was diluted 20× and qPCR was performed using the GoTaq® qPCR Master Mix (Promega) at 58 °C on a LightCycler 480 (Roche, Basel, Switzerland). The relative ratio of target gene expression was calculated using the equation: ratio = $(eff_{ref}{}^{CPr})/(eff_{target}{}^{CPt})$, with eff_{ref} representing PCR efficiency of the reference gene and eff_{target} representing PCR efficiency of the target gene. CPr and CPt represent crossing points of reference and target gene, respectively [63].

Primers pairs used for *PIN2* reporters were 5′-ATTGCTTAGGGCGATGTACG-3′ 5′-TAAT TGAACCAGCCGTCTCC-3′ as well as 5′-GGGGTGGTGCCCATCCTGGTCG-3′ 5′-CCTCGGCG CGGGTCTTGTAG-3′. For amplification of the reference gene *EF1a* (At1g07940) 5′-TGAGCACGCTCT TCTTGCTTTCA-3′ and 5′-GGTGGTGGCATCCATCTTGTTACA-3′ were used.

Supplementary Materials: Supplementary materials can be found at http://www.mdpi.com/1422-0067/18/11/2274/s1.

Acknowledgments: This research was supported by grants from the FWF (Austrian Science Fund, P25931 to Christian Luschnig), Czech Science Foundation (P305/11/0797, to Eva Zažímalová), MEYS CR (LO1417, Roman Skokan, Stanislav Vosolsobě, Jan Petrášek), EU Operational Program Prague—Competitiveness (CZ.2.16/3.1.00/21519) and European Regional Development Fund-Project "CERIT Scientific Cloud" (CZ.02.1.01/0.0/0.0/16_013/0001802). Katarzyna Retzer was funded by a Post-Doctoral Fellowship PPLZ from the Czech Academy of Sciences and by a Docfforte fellowship from the Austrian Academy of Sciences. We thank Jan Malinsky for support with the analysis of PIN2 reporter signal distribution, and Jonáš Vlasák and Takudzwa Manangazira for their help with microscopy. Finally, we would like to thank Lindy Abas for advice and inspiring discussions, specifically during early phases of this work.

Author Contributions: Katarzyna Retzer, Jozef Lacek, Martina Laňková, Nataliia Konstantinova and Christian Luschnig generated and analyzed plant lines; Katarzyna Retzer, Jozef Lacek, Kateřina Malínská, Jan Petrášek and Christian Luschnig determined protein localization; Roman Skokan and Stanislav Vosolsobě did the protein alignments; Charo I. del Genio generated the PIN2 model; Katarzyna Retzer, Eva Zažímalová, Richard M. Napier, Jan Petrášek and Christian Luschnig conceived experiments; and Katarzyna Retzer, Charo I. del Genio, Richard M. Napier, Jan Petrášek and Christian Luschnig wrote the manuscript.

Conflicts of Interest: No conflict of interest is declared by the authors.

References

1. Lavy, M.; Estelle, M. Mechanisms of auxin signaling. *Development* **2016**, *143*, 3226–3229. [CrossRef] [PubMed]
2. Enders, T.A.; Strader, L.C. Auxin activity: Past, present, and future. *Am. J. Bot.* **2015**, *102*, 180–196. [CrossRef] [PubMed]
3. Leyser, O. Auxin signaling. *Plant Physiol.* **2017**. [CrossRef] [PubMed]
4. Adamowski, M.; Friml, J. PIN-dependent auxin transport: Action, regulation, and evolution. *Plant Cell* **2015**, *27*, 20–32. [CrossRef] [PubMed]
5. Borghi, L.; Kang, J.; Ko, D.; Lee, Y.; Martinoia, E. The role of ABCG-type ABC transporters in phytohormone transport. *Biochem. Soc. Trans.* **2015**, *43*, 924–930. [CrossRef] [PubMed]
6. Zazimalova, E.; Murphy, A.S.; Yang, H.; Hoyerova, K.; Hosek, P. Auxin transporters—Why so many? *Cold Spring Harb Perspect Biol* **2010**, *2*, a001552. [CrossRef] [PubMed]
7. Luschnig, C.; Vert, G. The dynamics of plant plasma membrane proteins: PINs and beyond. *Development* **2014**, *141*, 2924–2938. [CrossRef] [PubMed]
8. Huang, F.; Zago, M.K.; Abas, L.; van Marion, A.; Galvan-Ampudia, C.S.; Offringa, R. Phosphorylation of conserved PIN motifs directs *Arabidopsis* PIN1 polarity and auxin transport. *Plant Cell* **2010**, *22*, 1129–1142. [CrossRef] [PubMed]
9. Zourelidou, M.; Absmanner, B.; Weller, B.; Barbosa, I.C.; Willige, B.C.; Fastner, A.; Streit, V.; Port, S.A.; Colcombet, J.; de la Fuente van Bentem, S.; et al. Auxin efflux by PIN-FORMED proteins is activated by two different protein kinases, D6 PROTEIN KINASE and PINOID. *Elife* **2014**, *3*. [CrossRef] [PubMed]
10. Michniewicz, M.; Zago, M.K.; Abas, L.; Weijers, D.; Schweighofer, A.; Meskiene, I.; Heisler, M.G.; Ohno, C.; Zhang, J.; Huang, F.; et al. Antagonistic regulation of PIN phosphorylation by PP2A and PINOID directs auxin flux. *Cell* **2007**, *130*, 1044–1056. [CrossRef] [PubMed]
11. Korbei, B.; Luschnig, C. Plasma membrane protein ubiquitylation and degradation as determinants of positional growth in plants. *J. Integr. Plant Biol.* **2013**, *55*, 809–823. [CrossRef] [PubMed]
12. Isono, E.; Kalinowska, K. ESCRT-dependent degradation of ubiquitylated plasma membrane proteins in plants. *Curr. Opin. Plant Biol.* **2017**, *40*, 49–55. [CrossRef] [PubMed]
13. Korbei, B.; Moulinier-Anzola, J.; De-Araujo, L.; Lucyshyn, D.; Retzer, K.; Khan, M.A.; Luschnig, C. *Arabidopsis* TOL proteins act as gatekeepers for vacuolar sorting of PIN2 plasma membrane protein. *Curr. Biol.* **2013**, *23*, 2500–2505. [CrossRef] [PubMed]
14. Nagel, M.K.; Kalinowska, K.; Vogel, K.; Reynolds, G.D.; Wu, Z.X.; Anzenberger, F.; Ichikawa, M.; Tsutsumi, C.; Sato, M.H.; Kuster, B.; et al. *Arabidopsis* SH3P2 is an ubiquitin-binding protein that functions together with ESCRT-I and the deubiquitylating enzyme AMSH3. *Proc. Natl. Acad. Sci. USA* **2017**, *114*, E7197–E7204. [CrossRef] [PubMed]
15. Leitner, J.; Petrasek, J.; Tomanov, K.; Retzer, K.; Parezova, M.; Korbei, B.; Bachmair, A.; Zazimalova, E.; Luschnig, C. Lysine63-linked ubiquitylation of PIN2 auxin carrier protein governs hormonally controlled adaptation of *Arabidopsis* root growth. *Proc. Natl. Acad. Sci. USA* **2012**, *109*, 8322–8327. [CrossRef] [PubMed]
16. Giles, N.M.; Watts, A.B.; Giles, G.I.; Fry, F.H.; Littlechild, J.A.; Jacob, C. Metal and redox modulation of cysteine protein function. *Chem. Biol.* **2003**, *10*, 677–693. [CrossRef]
17. Xia, X.J.; Zhou, Y.H.; Shi, K.; Zhou, J.; Foyer, C.H.; Yu, J.Q. Interplay between reactive oxygen species and hormones in the control of plant. *J. Exp. Bot.* **2015**, *66*, 2839–2856. [CrossRef] [PubMed]
18. Rouhier, N.; Cerveau, D.; Couturier, J.; Reichheld, J.P.; Rey, P. Involvement of thiol-based mechanisms in plant development. *Biochim. Biophys. Acta* **2015**, *1850*, 1479–1496. [CrossRef] [PubMed]
19. Bashandy, T.; Guilleminot, J.; Vernoux, T.; Caparros-Ruiz, D.; Ljung, K.; Meyer, Y.; Reichheld, J.P. Interplay between the NADP-linked thioredoxin and glutathione systems in *Arabidopsis* auxin signaling. *Plant Cell* **2010**, *22*, 376–391. [CrossRef] [PubMed]

20. Yu, X.; Pasternak, T.; Eiblmeier, M.; Ditengou, F.; Kochersperger, P.; Sun, J.; Wang, H.; Rennenberg, H.; Teale, W.; Paponov, I.; et al. Plastid-localized glutathione reductase2-regulated glutathione redox status is essential for *Arabidopsis* root apical meristem maintenance. *Plant Cell* **2013**, *25*, 4451–4468. [CrossRef] [PubMed]
21. Koprivova, A.; Mugford, S.T.; Kopriva, S. *Arabidopsis* root growth dependence on glutathione is linked to auxin transport. *Plant Cell Rep.* **2010**, *29*, 1157–1167. [CrossRef] [PubMed]
22. Feechan, A.; Kwon, E.; Yun, B.W.; Wang, Y.; Pallas, J.A.; Loake, G.J. A central role for S-nitrosothiols in plant disease resistance. *Proc. Natl. Acad. Sci. USA* **2005**, *102*, 8054–8059. [CrossRef] [PubMed]
23. Shi, Y.F.; Wang, D.L.; Wang, C.; Culler, A.H.; Kreiser, M.A.; Suresh, J.; Cohen, J.D.; Pan, J.; Baker, B.; Liu, J.Z. Loss of GSNOR1 function leads to compromised auxin signaling and polar auxin transport. *Mol. Plant* **2015**, *8*, 1350–1365. [CrossRef] [PubMed]
24. Fernandez-Marcos, M.; Sanz, L.; Lewis, D.R.; Muday, G.K.; Lorenzo, O. Nitric oxide causes root apical meristem defects and growth inhibition while reducing PIN-FORMED 1 (PIN1)-dependent acropetal auxin transport. *Proc. Natl. Acad. Sci. USA* **2011**, *108*, 18506–18511. [CrossRef] [PubMed]
25. Luschnig, C.; Gaxiola, R.A.; Grisafi, P.; Fink, G.R. EIR1, a root-specific protein involved in auxin transport, is required for gravitropism in *Arabidopsis thaliana*. *Genes Dev.* **1998**, *12*, 2175–2187. [CrossRef] [PubMed]
26. Krecek, P.; Skupa, P.; Libus, J.; Naramoto, S.; Tejos, R.; Friml, J.; Zazimalova, E. The PIN-FORMED (PIN) protein family of auxin transporters. *Genome Biol.* **2009**, *10*, 249. [CrossRef] [PubMed]
27. Bennett, T.; Brockington, S.F.; Rothfels, C.; Graham, S.W.; Stevenson, D.; Kutchan, T.; Rolf, M.; Thomas, P.; Wong, G.K.; Leyser, O.; et al. Paralogous radiations of PIN proteins with multiple origins of noncanonical PIN structure. *Mol. Biol. Evol.* **2014**, *31*, 2042–2060. [CrossRef] [PubMed]
28. Nodzynski, T.; Vanneste, S.; Zwiewka, M.; Pernisova, M.; Hejatko, J.; Friml, J. Enquiry into the topology of plasma membrane-localized PIN auxin transport components. *Mol. Plant* **2016**, *9*, 1504–1519. [CrossRef] [PubMed]
29. Sali, A.; Blundell, T.L. Comparative protein modelling by satisfaction of spatial restraints. *J. Mol. Biol.* **1993**, *234*, 779–815. [CrossRef] [PubMed]
30. Case, D.A.; Cerutti, D.S.; Cheatham, I.T.E.; Darden, T.A.; Duke, R.E.; Giese, T.J.; Gohlke, H.; Goetz, A.W.; Greene, D.; Homeyer, N.; et al. *AMBER 2017*; University of California: San Francisco, CA, USA, 2017.
31. Pettersen, E.F.; Goddard, T.D.; Huang, C.C.; Couch, G.S.; Greenblatt, D.M.; Meng, E.C.; Ferrin, T.E. UCSF chimera—A visualization system for exploratory research and analysis. *J. Comput. Chem.* **2004**, *25*, 1605–1612. [CrossRef] [PubMed]
32. Grabov, A.; Ashley, M.K.; Rigas, S.; Hatzopoulos, P.; Dolan, L.; Vicente-Agullo, F. Morphometric analysis of root shape. *New Phytol.* **2005**, *165*, 641–651. [CrossRef] [PubMed]
33. Kleine-Vehn, J.; Wabnik, K.; Martiniere, A.; Langowski, L.; Willig, K.; Naramoto, S.; Leitner, J.; Tanaka, H.; Jakobs, S.; Robert, S.; et al. Recycling, clustering, and endocytosis jointly maintain PIN auxin carrier polarity at the plasma membrane. *Mol. Syst. Biol.* **2011**, *7*, 540. [CrossRef] [PubMed]
34. Martiniere, A.; Lavagi, I.; Nageswaran, G.; Rolfe, D.J.; Maneta-Peyret, L.; Luu, D.T.; Botchway, S.W.; Webb, S.E.; Mongrand, S.; Maurel, C.; et al. Cell wall constrains lateral diffusion of plant plasma-membrane proteins. *Proc. Natl. Acad. Sci. USA* **2012**, *109*, 12805–12810. [CrossRef] [PubMed]
35. Gustafsson, N.; Culley, S.; Ashdown, G.; Owen, D.M.; Pereira, P.M.; Henriques, R. Fast live-cell conventional fluorophore nanoscopy with ImageJ through super-resolution radial fluctuations. *Nat. Commun.* **2016**, *7*, 12471. [CrossRef] [PubMed]
36. Chevalier, A.S.; Chaumont, F. Trafficking of plant plasma membrane aquaporins: Multiple regulation levels and complex sorting signals. *Plant Cell Physiol.* **2015**, *56*, 819–829. [CrossRef] [PubMed]
37. Bienert, G.P.; Cavez, D.; Besserer, A.; Berny, M.C.; Gilis, D.; Rooman, M.; Chaumont, F. A conserved cysteine residue is involved in disulfide bond formation between plant plasma membrane aquaporin monomers. *Biochem. J.* **2012**, *445*, 101–111. [CrossRef] [PubMed]
38. Yoo, Y.J.; Lee, H.K.; Han, W.; Kim, D.H.; Lee, M.H.; Jeon, J.; Lee, D.W.; Lee, J.; Lee, Y.; Lee, J.; et al. Interactions between transmembrane helices within monomers of the aquaporin AtPIP2;1 play a crucial role in tetramer formation. *Mol. Plant* **2016**, *9*, 1004–1017. [CrossRef] [PubMed]
39. Mou, Z.; Fan, W.; Dong, X. Inducers of plant systemic acquired resistance regulate NPR1 function through redox changes. *Cell* **2003**, *113*, 935–944. [CrossRef]

40. Tada, Y.; Spoel, S.H.; Pajerowska-Mukhtar, K.; Mou, Z.; Song, J.; Wang, C.; Zuo, J.; Dong, X. Plant immunity requires conformational changes [corrected] of NPR1 via S-nitrosylation and thioredoxins. *Science* **2008**, *321*, 952–956. [CrossRef] [PubMed]
41. Wu, Y.; Zhang, D.; Chu, J.Y.; Boyle, P.; Wang, Y.; Brindle, I.D.; De Luca, V.; Despres, C. The *Arabidopsis* NPR1 protein is a receptor for the plant defense hormone salicylic acid. *Cell Rep.* **2012**, *1*, 639–647. [CrossRef] [PubMed]
42. Feraru, E.; Feraru, M.I.; Kleine-Vehn, J.; Martiniere, A.; Mouille, G.; Vanneste, S.; Vernhettes, S.; Runions, J.; Friml, J. PIN polarity maintenance by the cell wall in *Arabidopsis*. *Curr. Biol.* **2011**, *21*, 338–343. [CrossRef] [PubMed]
43. Mittler, R.; Vanderauwera, S.; Suzuki, N.; Miller, G.; Tognetti, V.B.; Vandepoele, K.; Gollery, M.; Shulaev, V.; Van Breusegem, F. ROS signaling: The new wave? *Trends Plant Sci.* **2011**, *16*, 300–309. [CrossRef] [PubMed]
44. Abas, L.; Benjamins, R.; Malenica, N.; Paciorek, T.; Wisniewska, J.; Moulinier-Anzola, J.C.; Sieberer, T.; Friml, J.; Luschnig, C. Intracellular trafficking and proteolysis of the *Arabidopsis* auxin-efflux facilitator PIN2 are involved in root gravitropism. *Nat. Cell Biol.* **2006**, *8*, 249–256. [CrossRef] [PubMed]
45. Clough, S.J.; Bent, A.F. Floral dip: A simplified method for Agrobacterium-mediated transformation of *Arabidopsis thaliana*. *Plant J.* **1998**, *16*, 735–743. [CrossRef] [PubMed]
46. Koncz, C.; Schell, J. The promoter of Tl-DNA gene 5 controls the tissue-specific expression of chimeric genes carried by a novel type of Agrobacterium binary vector. *Mol. Gen. Genet.* **1986**, *204*, 383–396. [CrossRef]
47. Jones, D.T. GenTHREADER: An efficient and reliable protein fold recognition method for genomic sequences. *J. Mol. Biol.* **1999**, *287*, 797–815. [CrossRef] [PubMed]
48. Jones, D.T. Protein secondary structure prediction based on position-specific scoring matrices. *J. Mol. Biol.* **1999**, *292*, 195–202. [CrossRef] [PubMed]
49. McGuffin, L.J.; Jones, D.T. Improvement of the GenTHREADER method for genomic fold recognition. *Bioinformatics* **2003**, *19*, 874–881. [CrossRef] [PubMed]
50. Lobley, A.; Sadowski, M.I.; Jones, D.T. pGenTHREADER and pDomTHREADER: New methods for improved protein fold recognition and superfamily discrimination. *Bioinformatics* **2009**, *25*, 1761–1767. [CrossRef] [PubMed]
51. Mongan, J.; Simmerling, C.; McCammon, J.A.; Case, D.A.; Onufriev, A. Generalized Born model with a simple, robust molecular volume correction. *J. Chem. Theory Comput.* **2007**, *3*, 156–169. [CrossRef] [PubMed]
52. Nguyen, H.; Roe, D.R.; Simmerling, C. Improved generalized born solvent model parameters for protein simulations. *J. Chem. Theory Comput.* **2013**, *9*, 2020–2034. [CrossRef] [PubMed]
53. Maier, J.A.; Martinez, C.; Kasavajhala, K.; Wickstrom, L.; Hauser, K.E.; Simmerling, C. ff14SB: Improving the accuracy of protein side chain and backbone parameters from ff99SB. *J. Chem. Theory Comput.* **2015**, *11*, 3696–3713. [CrossRef] [PubMed]
54. Jorgensen, W.L.; Chandrasekhar, J.; Madura, J.D.; Impey, R.W.; Klein, M.L. Comparison of simple potential functions for simulating liquid water. *J. Chem. Phys.* **1983**, *79*, 926–935. [CrossRef]
55. Hornak, V.; Abel, R.; Okur, A.; Strockbine, B.; Roitberg, A.; Simmerling, C. Comparison of multiple amber force fields and development of improved protein backbone parameters. *Proteins* **2006**, *65*, 712–725. [CrossRef] [PubMed]
56. Ryckaert, J.P.; Ciccotti, G.; Berendsen, H.J.C. Numerical-integration of Cartesian equations of motion of a system with constraints—Molecular-dynamics of N-alkanes. *J. Comput. Phys.* **1977**, *23*, 327–341. [CrossRef]
57. Miyamoto, S.; Kollman, P.A. Settle—An analytical version of the Shake and Rattle algorithm for rigid water models. *J. Comput. Chem.* **1992**, *13*, 952–962. [CrossRef]
58. Schindelin, J.; Arganda-Carreras, I.; Frise, E.; Kaynig, V.; Longair, M.; Pietzsch, T.; Preibisch, S.; Rueden, C.; Saalfeld, S.; Schmid, B.; et al. Fiji: An open-source platform for biological-image analysis. *Nat. Methods* **2012**, *9*, 676–682. [CrossRef] [PubMed]
59. Leinonen, R.; Sugawara, H.; Shumway, M.; International Nucleotide Sequence Database Collaboration. The sequence read archive. *Nucleic Acids Res.* **2011**, *39*, D19–D21. [CrossRef] [PubMed]
60. Camacho, C.; Coulouris, G.; Avagyan, V.; Ma, N.; Papadopoulos, J.; Bealer, K.; Madden, T.L. BLAST+: Architecture and applications. *BMC Bioinform.* **2009**, *10*, 421. [CrossRef] [PubMed]
61. Huang, X.; Madan, A. CAP3: A DNA sequence assembly program. *Genome Res.* **1999**, *9*, 868–877. [CrossRef] [PubMed]

62. Katoh, K.; Standley, D.M. MAFFT multiple sequence alignment software version 7: Improvements in performance and usability. *Mol. Biol. Evol.* **2013**, *30*, 772–780. [CrossRef] [PubMed]
63. Hellemans, J.; Mortier, G.; de Paepe, A.; Speleman, F.; Vandesompele, J. qBase relative quantification framework and software for management and automated analysis of real-time quantitative PCR data. *Genome Biol.* **2007**, *8*, R19. [CrossRef] [PubMed]

3.2.2. Dissecting Hierarchies between Light, Sugar and Auxin Action Underpinning Root and Root Hair Growth

Authors: Judith Garcia-Gonzales†, Jozef Lacek†, Katarzyna Retzer

† contributed equally

Summary:

Direct root illumination and sugar supplementation can mask phenotypes and cause changes in root growth traits. Auxin signaling is crucial to establishing several root traits including total root length, gravitropic adaptation, root hair initiation and elongation. Biosynthesis and transport of auxin within root is affected by direct root illumination and sugar supplementation. This study shows the extent of combined effect of light and sucrose on root length, root hair emergence and elongation. In the case of root length, we can prove antagonistic effect between light, which is reducing root length, and sucrose, which is masking this effect, although only partially. In mutants with loss of PIN2 function the additive effect of sucrose is negated. Light and sucrose stimulate outgrowth and length of root hairs. Sucrose in environment without direct root illumination increase randomization of root growth direction. With this study, we attempted to differentiate and define the roles of auxin transport (via PIN2), direct root illumination and sucrose supplementation on establishing basic root traits.

My contribution: As joint first author, I have actively contributed to designing and performing phenotypical experiments, and manuscript preparation.

plants

MDPI

Article

Dissecting Hierarchies between Light, Sugar and Auxin Action Underpinning Root and Root Hair Growth

Judith García-González [1,2,†], Jozef Lacek [1,†] and Katarzyna Retzer [1,*]

[1] Laboratory of Hormonal Regulations in Plants, Institute of Experimental Botany, Czech Academy of Sciences, 165 02 Prague, Czech Republic; garciago.judith@gmail.com (J.G.-G.); jozeflacek9@gmail.com (J.L.)
[2] Department of Experimental Plant Biology, Faculty of Science, Charles University, 128 00 Prague, Czech Republic
* Correspondence: retzer@ueb.cas.cz
† Those authors contributed equally to this work.

Abstract: Plant roots are very plastic and can adjust their tissue organization and cell appearance during abiotic stress responses. Previous studies showed that direct root illumination and sugar supplementation mask root growth phenotypes and traits. Sugar and light signaling where further connected to changes in auxin biosynthesis and distribution along the root. Auxin signaling underpins almost all processes involved in the establishment of root traits, including total root length, gravitropic growth, root hair initiation and elongation. Root hair plasticity allows maximized nutrient uptake and therefore plant productivity, and root hair priming and elongation require proper auxin availability. In the presence of sucrose in the growth medium, root hair emergence is partially rescued, but the full potential of root hair elongation is lost. With our work we describe a combinatory study showing to which extent light and sucrose are antagonistically influencing root length, but additively affecting root hair emergence and elongation. Furthermore, we investigated the impact of the loss of PIN-FORMED2, an auxin efflux carrier mediating shootward auxin transporter, on the establishment of root traits in combination with all growth conditions.

Keywords: PIN-FORMED2; shootward auxin transport; root growth; root hair; sugar; sucrose; dark grown roots; light grown roots; root hair elongation; total root length; gravitropic index

Citation: García-González, J.; Lacek, J.; Retzer, K. Dissecting Hierarchies between Light, Sugar and Auxin Action Underpinning Root and Root Hair Growth. *Plants* **2021**, *10*, 111. https://doi.org/10.3390/plants10010111

Received: 6 December 2020
Accepted: 5 January 2021
Published: 7 January 2021

1. Introduction

1.1. Root Trait Establishment Is Highly Plastic and Depends on Growth Conditions

Plants are divided into above- (shoot) and under-ground (root) organs, and each part has a specific role in capturing the crucial components to ensure plant mass production and health. Both parts of the plant are in constant communication with each other and exchange growth substances, also known as phytohormones, and nutrients (light energy converted to sugar from shoot to root, water and minerals from root to shoot). External signals upon environmental changes are perceived at the cell surface and trigger changes in plant architecture [1–3]. Plant roots are very plastic and can adjust their tissue organization and cell appearance during abiotic stress responses [4]. The root consists of a meristematic zone that continually delivers new cells, and its activity arrests when the environmental conditions are not beneficial for the plant. After leaving the division zone, cells pass through the transition and elongation zone towards the differentiation zone, whereby they are maturing and primed according to the growth conditions of the root and the shoot, which are connected through signaling cascades with each other [5–8]. Root length is defined by the balance between cell proliferation and cell elongation [1,4]. Roots expand and change their architecture, by forming lateral roots and root hairs, to anchor the plant in the soil and enlarge their surface [1,3,4]. Especially root hairs contribute to an efficient uptake of water and nutrients to maximize plant productivity and their outgrowth is highly regulated by environmental conditions [1,2].

1.2. Root Growth Is Orchestrated through Interwoven Signaling Cascades

Plant growth's plasticity, especially the proliferation rate, depends significantly on carbohydrates gained over photosynthesis [8,9]. However, depending on the wavelength, light is also triggering fast-growth processes over asymmetric auxin distribution to change cell elongation behavior [3] and the root is negatively phototropic, which results in growth away from the light source [1,3]. Roots have evolved a finely interwoven network of signaling cascades to adapt to environmental changes, including tight crosstalk between auxin, sugar, and light signaling to balance root growth toward beneficial surroundings but away from harmful influences [1,2,10,11]. Cell elongation processes in the root allow fast growth or to enlarge root surface through root hair outgrowth, both events are highly dependent on sufficient shootward auxin transport along the epidermis [12–15]. Interference with proper auxin distribution was reported to impact root architecture [16] and to negatively impact gravitropic responses [17]. The root of *Arabidopsis thaliana* is an established model system to study molecular processes underpinning plant growth adaptation upon changing environmental conditions [1,10,18–22]. All root growth aspects are highly dependent on fine-tuned, active polar auxin distribution through the root tip followed by auxin signaling orchestrating cellular responses [3,11,23–26]. The auxin efflux transporter PIN-FORMED2 (PIN2) orchestrates root growth but is itself regulated on transcriptional through to the post-translational level by external factors such as nutrient availability or light [26–30]. PIN2 abundance and subcellular distribution are dependent on light growth conditions for both the root and the shoot [25,29,30]. Auxin gradients in the root epidermis, which rise from the meristem towards the elongation zone, are crucial to prime trichoblast cells (root hair cells) [31–34]. Mutants of key players of auxin signaling and transport show severe root hair morphology, spacing, and length phenotypes [15,35–37].

1.3. Direct Root Illumination Triggers Stress Responses and Inhibits Root Growth

Arabidopsis thaliana is one of the most studied model plants, especially in terms of cell biology. Few day-old seedlings grown on agar medium in plates became standard test objects and germination on medium allows easy and clean accessibility of the plants for molecular approaches and microscopy. It is known for over a century that plant roots are negatively phototropic, aiming to grow away from a light source [3,10]. However, only over the past decade, biochemical, genetical, and molecular studies reveal the striking impact of direct root illumination on the establishment of the root system architecture [1,21,22,38–40]. Direct root illumination triggers stress responses in the root tip, which result in changes of cell fate establishment, including meristem activity, the transition to the elongation zone, and root hair growth [1,21,22]. Root growth differs under direct root illumination among others because of the elevated production of reactive oxygen species, which modulate growth responses on cellular level in the meristem and root hairs [22,38]. In the study of Silva-Navas et al. 2015, the lab introduces a simple and reproducible solution to cover the plates partially with a black box, the D-root system, which allows the cultivation of seedlings in a way that the shoot is exposed to light, but the root is covered [1]. The dark-grown roots (DGR), in comparison to light-grown roots (LGR), show longer roots due to a more active meristem, the number of lateral roots, differential response to hormonal crosstalk, less dramatic phenotypes to additive stress treatment, and altered root hair plasticity [1,21,22].

1.4. Sucrose Supplementation to the Growth Medium Triggers Auxin Biosynthesis and Results in Altered Root Trait Establishment

Another widely used cultivation protocol includes the addition of 1% sucrose to the growth medium, often half strength Murashige and Skoog (MS) medium solidified with 1% agar. Studies investigating the role of sugar supplementation to the plant growth medium revealed that it enhances indole-3 acetic acid (IAA) biosynthesis and responses in the root, which is the main naturally-occurring auxin in plants [9,41]. Furthermore, glucose in the medium altered several root traits, which are commonly used to evaluate the impact of

auxin-mediated plant growth responses, including total root length, root hair growth (root hair growth), and gravitropic index [41]. Exogenously applied glucose interferes with auxin signaling and transport, which changed total root length, number root hair, and root growth direction [41]. Endogenous sugars, produced upon photosynthesis in the cotyledons, trigger long-distance signaling cascades to modulate root meristem activity in young seedlings [42].

1.5. Experimental Design to Dissect the Influence of Common Growth Conditions on Root Trait Establishment

Here, we describe a timely attempt to dissect the hierarchy of light, sugar and auxin during the growth of roots shaded from direct illumination (Figure 1A). To investigate the interplay of light and sugar we first compared total root length, root hair growth, and gravitropic index (Figure 1B,C) of an established line, expressing wild type levels of the auxin efflux carrier PIN-FORMED2 fused to the yellow fluorescent protein VENUS (PIN2:VEN), driven by the PIN2 promoter [43]. We examined the seedlings seven days after germination (DAG) under four growth conditions, namely DGR with and without 1% sucrose added to half strength MS, and LGR with and without sucrose (Figure 1A). To understand to which extent shootward auxin transport, mediated by PIN2, is involved in the establishment of the chosen root growth traits under the four growth conditions, we compared *eir1-4 PIN2::PIN2:VEN* with the established *pin2* mutant *eir1-4* (SALK_091142) (Figure 1A). Representative pictures of the seedlings grown under all growth conditions are summarized in the Figure S1A and representative pictures of the root hair outgrowth are available in the Figure S1B.

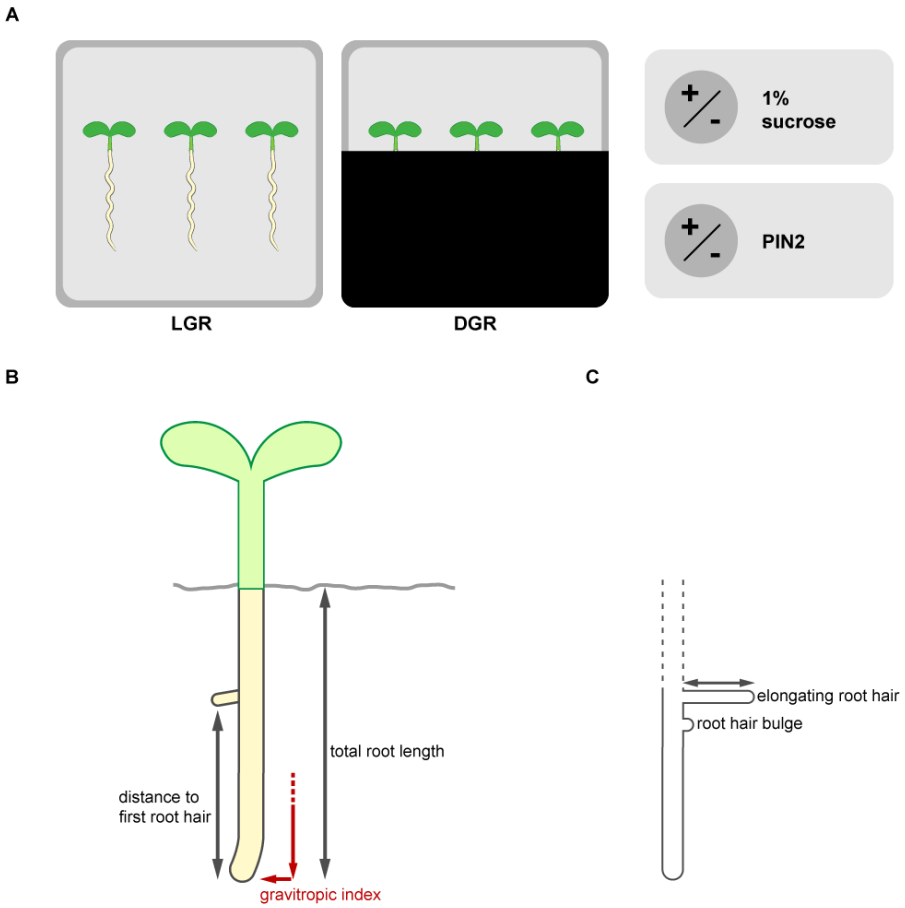

Figure 1. Outline of the experiments. (**A**) To understand the impact of standard lab growth conditions on the outcome of phenotyping experiments we analyzed root traits of seven days old seedlings combining differential root illumination status and sucrose supplementation to the growth medium.

To study the influence of direct root illumination the roots were grown in a square petri dish with exposed roots (light grown roots, LGR) and compared to roots grown shaded from light by using the D-root system. The D-root system is a box covering the square plate partially, which allows to grow seedlings with shaded roots, but the shoot stays illuminated, and was introduced by Silva-Navas et al., 2015. To understand the impact of sucrose in the growth medium in combination with altered root illumination status, the seedlings were grown on a commonly used standard medium (half strength MS medium with 1% agar) supplemented with or without 1% sucrose. Sugar supplementation was previously described to enhance the energy level and auxin biosynthesis, which alters root growth. Because shootward auxin transport, mediated by the auxin efflux carrier PIN-FORMED2 (PIN2) in the root tip, is known to be crucial for the establishment of the traits of interest, *Arabidopsis thalilana* lines expressing (*eir1-4 PIN2::PIN2:VEN*) or not expressing (*eir1-4*) PIN2 were compared. Representative pictures of the seedlings grown under all growth conditions are summarized in the Figure S1. (**B**) Root growth traits of the primary root were evaluated (total root length, appearance of the first root hair and gravitropic index). (**C**) Root illumination status, sucrose availability and shootward auxin transport mediated by PIN2 were individually already published to influence root hair emerge and elongation immensely. Therefore, we evaluated the amount of emerged root hairs (bulges and elongated), the percentage of elongated root hairs and root hair length of the elongated root hairs under all growth conditions along the first two mm of the root tip. Representative pictures of the root tips and root hair outgrowth are summarized in the Figure S1.

2. Results

2.1. Direct Root Illumination and Sucrose Supplementation Influence Total Root Length Growth Antagonistically

The majority of published studies, including those addressing how light, sugar and auxin signaling is modulating root growth, were performed on roots continuously exposed to light, sometimes followed by a shift of the whole seedling to darkness, or on roots of etiolated seedlings. The root is negatively phototropic and direct illumination enhances stress responses that interfere with root growth and responses [21]. Furthermore, the establishment of root traits are also modulated by signals obtained from above ground signals [3]. Root length depends highly on the meristem activity of the root, which is regulated by various signaling cascades integrating environmental signals and availability of resources [1,8]. The D-root system prevents direct illumination of the root and thereby reduces stress responses in the root tip and this results in a higher proliferation rate, the total root length is longer in DGR [1,21]. First we compared if the chosen reporter line *eir1-4 PIN2::PIN2:VEN* responded in the same way as the wild type line *Col-0* used in the original paper introducing the D-root system [1]. We measured total root length of *eir1-4 PIN2::PIN2:VEN* seven DAG grown on half strength MS medium containing 1% sucrose under DGR and LGR conditions, and we observed the expected significant root length difference between the root illumination regimes, with DGR being 19.53 ± SE 0.73/SD 6.49 mm long and LGR 16.71 ± SE 0.69/SD 5.42 mm (Figure 2A).

The composition of growth media immensely influences cell fate and root architecture and because sugar triggers signaling cascades which have an impact on root growth and adaptation processes it is therefore often omitted [41,44]; we compared total root length of *eir1-4 PIN2::PIN2:VEN* seedlings grown seven DAG on medium without sucrose supplementation to understand the impact of sucrose in relation to the used light regimes. Without sucrose the significant difference of total root length was gone between DGR, 15.72 ± SE 0.72/SD 5.74 mm, and LGR, 14.83 ± SE 0.74/SD 5.94 mm (Figure 2A). When we compared the relative total root length upon individual root illumination conditions depending on sucrose supplementation, DGR roots showed a significant difference of total root length (Figure 2B), whereas the difference of LGR is less pronounced (Figure 2C). In conclusion, total root length is inhibited by direct illumination of the root, as it was already described [1]. Furthermore, sucrose has a significant influence by boosting total root length of DGR, indicating that light acts antagonistically to sucrose promoting effect on root length.

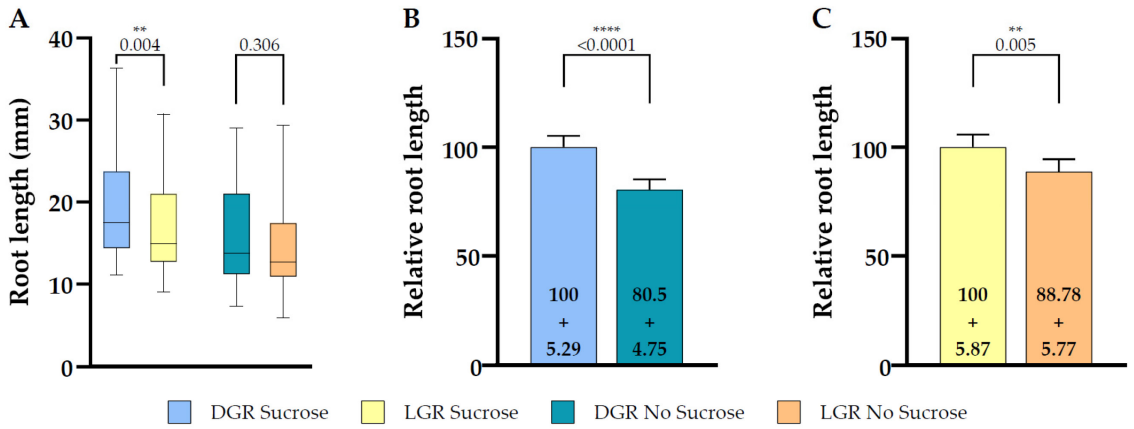

Figure 2. Total root length comparison between dark and light grown 7 DAG *eir1-4 PIN2::PIN2:VENUS* roots in dependence of sucrose supplementation. (**A**) Quantitative analysis of total root length of dark or light grown roots are shown for plants grown on half strength MS medium supplemented with 1% sucrose or without sucrose. (**B**,**C**) Relative root length comparison of seedlings grown under the same root illumination regime, either grown on half strength MS medium supplemented or not supplemented with sucrose, (**B**) for dark grown roots or (**C**) light grown roots (relative length + SE is shown). Differences were assessed by the Mann–Whitney U Test comparing (**A**) dark and light grown roots and (**B**,**C**) plants grown on half strength MS with and without 1% sucrose. p-values are depicted for each comparison (** $p < 0.01$, **** $p < 0.0001$). n = 61–79 roots.

2.2. Loss of PIN2 Results in Shorter Roots and Counteracts Sucrose Induced Growth Boost of Dark Grown Roots

To understand the impact on total root length of shootward, actively regulated polar auxin transport by PIN2, we compared root length of the PIN2 knockout mutant *eir1-4* under all four growth conditions (Figure 3A). The difference of total root length of DGR seedlings grown on sucrose supplemented medium was less pronounced compared to *eir1-4 PIN2::PIN2:VEN* (Figure 3A; Figure 4), DGR, 17.33 ± SE 0.93/SD 5.52 mm, and LGR, 14.67 ± SE 0.93/SD 5.67 mm. Again, we didn't observe any significant difference of *eir1-4* seedlings grown on sucrose-free medium between DGR, 15.31 ± SE 0.94/SD 5.48 mm and LGR, 13.71 ± SE 1.03/SD 6.18 mm (Figure 3A).

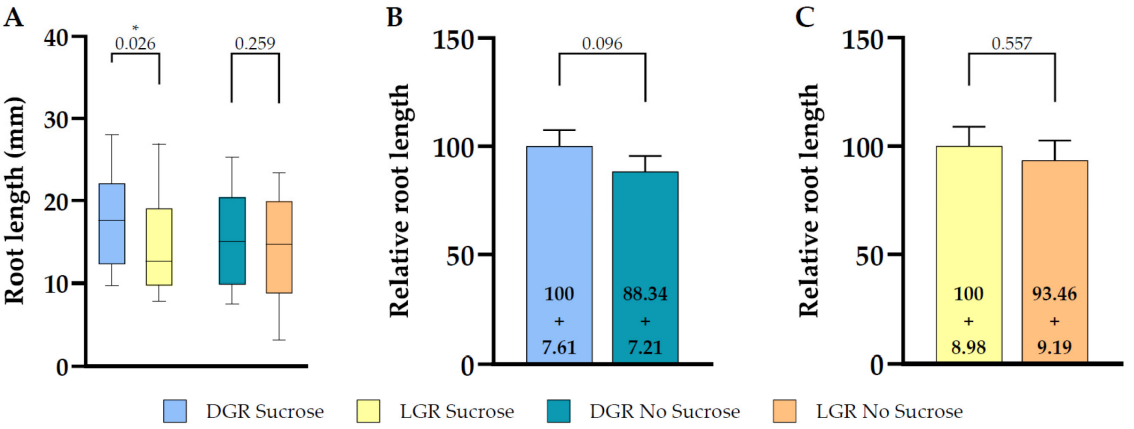

Figure 3. Root length comparison between dark and light grown 7 DAG *eir1-4* roots in dependence of sucrose supplementation. (**A**) Quantitative analysis of root length of dark or light grown roots are shown for plants grown on half strength MS medium supplemented with 1% sucrose or without sucrose. Relative total root length comparison of seedlings grown under the same root illumination regime, either grown on half strength MS medium supplemented or not supplemented with sucrose, (**B**) for dark grown roots (**C**) light grown roots (relative length + SE is shown). Differences were assessed by Mann–Whitney U Test comparing (**A**) dark and light grown roots and (**B**,**C**) plants grown on half strength MS with and without 1% sucrose. p-values are depicted for each comparison (* $p < 0.05$). n = 34–37 roots.

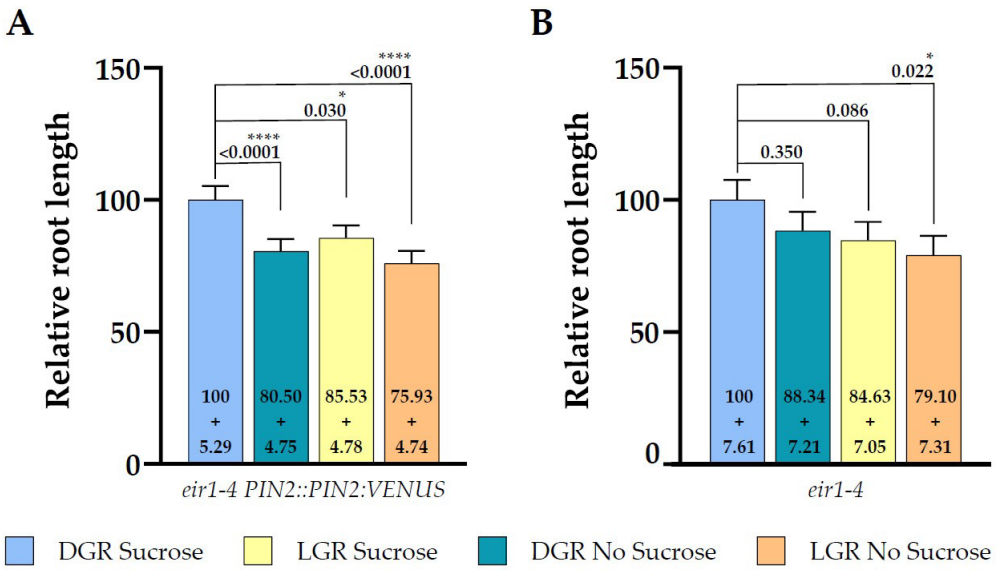

Figure 4. Root length comparison of both lines under all growth conditions relative to dark grown roots germinated on half strength MS supplemented with 1% sucrose. Data shown for (**A**) *eir1-4 PIN2::PIN2:VENUS* and (**B**) *eir1-4* (relative length + SE is shown). Kruskal–Wallis test with Dunn's post hoc test was used to determine statistical significance. Dark grown roots grown on half strength MS medium supplemented with 1% sucrose were used as reference for the statistical analysis. *p*-values are depicted in each plot (* $p < 0.05$, **** $p < 0.0001$). *eir1-4 PIN2::PIN2:VENUS* n = 61–79 roots; *eir1-4* n = 34–37 roots.

When we compared the relative root length ratios within one root illumination regime depending on supplementation, we couldn't observe any statistically significant change of total root length for *eir1-4* grown on sucrose (Figure 3B) or without (Figure 3C). This is contrasting to the results obtained for *eir1-4 PIN2::PIN2:VEN*, which showed a clear difference of total root length between DGR from sucrose supplemented medium compared to sucrose free medium (Figure 2B). The loss of PIN2 results in overall shorter roots, and dramatically impairs the enhancing effect of sucrose on root length of DGR (Figure 4). Taken together, PIN2 dependent shootward distribution of auxin contributes positive to root length, and the loss of PIN2 resulted in shorter roots under all growth conditions, which correlates with published data showing that *pin2* mutants have a less active meristem and therefore shorter roots [45,46].

2.3. Differential Root Illumination Influences the Number of Emerging Root Hairs, and Sucrose Enhances Root Hair Length of eir1-4 PIN2::PIN2:VEN

Root hair establishment and polar outgrowth is very plastic and sensitively enhanced or inhibited by hormonal and secondary messenger signaling, which are responding to exogenous signals balanced against available resources of the plant [2,32,47]. Direct root illumination negatively correlates with the plasticity of root hairs under phosphate deficient growth conditions [22]. When grown on sucrose supplemented half strength MS medium, LGR possess longer root hairs close to the meristem, which was suggested to result from elevated stress responses in the root tip [1]. We compared the impact of sucrose in combination of the root illumination regime on root hair outgrowth and measured the distance between the bottom of the root columella and the first visible root hair bulge, which is defining the end of the elongation zone of the root, and the beginning of the differentiation zone. *Eir1-4 PIN2::PIN2:VEN* showed no statistically significant change in the length of the meristem and elongation zone combined depending on the growth conditions (Figure 5A), LGR with sucrose 929.6 ± SE 91.87/SD 304.7 µm; LGR without sucrose 950.4 ± SE 43.62/SD 123.4 µm; DGR with sucrose 1043 ± SE 49.13/SD 96.66 µm and DGR without sucrose 971.9 ± SE 56.25/SD 159.25 µm. Further detailed determina-

tion of meristem and elongation zone length, cell number, and cell volume will allow to understand if there is a change of root zonation establishment depending of light and sucrose perception. We further focused on the evaluation of root hair traits, and measured the number of all root hairs emerging, as bulges and elongated, along the first 2 mm of the root tip. We measured for DGR, independent on sucrose supplementation, the lowest number of root hairs (6 ± SE 0.93/SD 2.45 for DGR with sucrose, and 5.75 ± SE 1.07/SD 3.01 for DGR without sucrose; Figure 5B), whereas direct root illumination triggered the appearance of root hairs clearly, with no significant enhancement upon sucrose supplementation (14.50 ± SE 2.44/SD 8.46 for LGR with sucrose, and 9.25 ± SE 0.98/SD 2.77 for LGR without sucrose; Figure 5B).

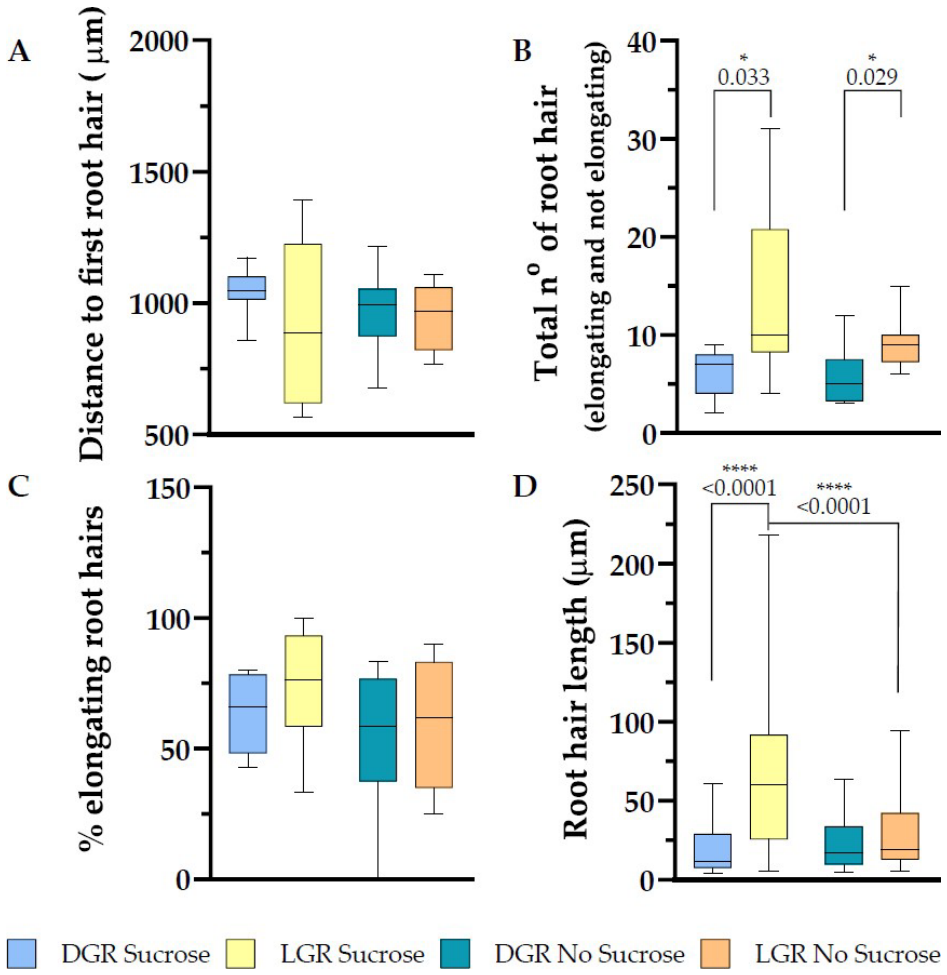

Figure 5. Root hair trait evaluation along the first 2 mm of the root tip of 7 DAG *eir1-4 PIN2::PIN2:VENUS* plants. Depicted are (**A**) the distance from the root tip to the first emerging root hair, (**B**) total amount of root hairs (bulges and elongated), (**C**) in percentage how many root hairs elongated and (**D**) root hair length. (**A–D**) Root hair traits were evaluated from dark and light grown roots, grown either on half strength MS medium supplemented with 1% sucrose or without sucrose. Roots measured: n = 7–12. Root hairs measured: 25–122. Student's t-test (total number of root hairs and distance to first root hair) or Mann–Whitney U test (% of elongating root hairs and root hair length) was used to perform statistical analysis for the following comparisons: LGR sucrose vs. LGR no sucrose; DGR sucrose vs. DGR no sucrose; LGR sucrose vs. DGR sucrose; LGR no sucrose vs. DGR no sucrose. p-values for statistically significant comparisons are depicted in each plot (* $p < 0.05$, **** $p < 0.0001$).

We evaluated root hair elongation of *eir1-4 PIN2::PIN2:VEN* under all four growth conditions and couldn't detect a significant difference of the percentage of elongating root

hairs, LGR with sucrose 75.20 ± SE 5.99/SD 20.73 %; LGR without sucrose 59.54 ± SE 11.85/SD 24 %; DGR with sucrose 63.8 ± SE 7.53/SD 15.85 % and DGR without sucrose 53.75 ± SE 9.66/SD 27.34 % (Figure 5C). In the study of Silva-Navas et al., 2015 they described that in Col-0 the root hair closer to the meristem were longer under direct root illumination, when using sucrose supplemented medium, we observed the same pattern for *eir1-4 PIN2::PIN2:VEN*, LGR with sucrose 66.29 ± SE 4.16/SD 49.98 µm, and DGR with sucrose 20.47 ± SE 3.31/SD 16.54 µm (Figure 5D). Without sucrose supplementation, the root hair length for LGR 28.37 ± SE 3.26/SD 21.88 µm, was not significantly different to DGR, 23.16 ± SE 3.22/SD 16.43 µm (Figure 5D). Taken together, without any further additive stress treatment, direct root illumination results in elevated root hair emergence, independent on sucrose supplementation, whereas sucrose supplementation triggers an increase in root hair length of LGR, but not upon the other three growth conditions.

2.4. Root Hair Outgrowth of eir1-4 Is Strongly Inhibited on Sucrose Free Medium

Root hair initiation and elongation depend on proper auxin distribution and signaling along the root and in the individual root hair [15,48,49]. To evaluate the impact of PIN2 action in relation to root illumination and sucrose supplementation, we measured the differences in root hair appearance, number, and percentage of elongating root hairs of root tips 2 mm shootward. Consistent with published data [15,32], root hair appearance and elongation are altered in *eir1-4* compared to *eir1-4 PIN2::PIN2:VEN* control line, which expresses PIN2 at wild type levels. Root hairs appeared further away from the root tip in the mutant compared to *eir1-4 PIN2::PIN2:VEN*, LGR with sucrose 1216 ± SE 74.08/SD 277.2 mm, LGR without sucrose 1321 ± SE 126.3/SD 357.3 mm, DGR with sucrose 1196 ± SE 101.3/SD 286.5 mm, and DGR without sucrose 1553 ± SE 138.4/SD 391.5 mm (Figure 6A). The amount of emerging root hairs dropped along the first 2 mm of root tip in comparison to *eir1-4 PIN2::PIN2:VEN*, which was further more evident when sucrose was omitted in the growth medium, LGR with sucrose 5.14 ± SE 0.79/SD 2.96, LGR without sucrose 2.75 ± SE 1.03/SD 2.92, DGR with sucrose 7.38 ± SE 1.21/SD 3.42, and DGR without sucrose 1.75 ± SE 0.70/SD 1.98 (Figure 6B). *Eir 1–4* responded differently if compared to *eir1-4 PIN2::PIN2:VEN* that showed upon direct illumination a higher emergence of root hairs compared to the DGR. *Eir1-4* didn't show a difference regarding root hair amount upon different light regimes, supporting published studies stating that root hair outgrowth in general, and further under light stress, is auxin dependent [1,15].

Root hair elongation of *eir1-4* changed compared to *eir1-4 PIN2::PIN2:VEN*, regarding the significant difference of the elongation rate depending on sucrose supplementation to the growth medium. *Eir1-4* showed a statistically relevant drop of the percentage of elongating root hairs when sucrose was omitted in the medium, LGR with sucrose 60.98 ± SE 9.06/SD 33.90 %; LGR without sucrose 25.06 ± SE 12.53/SD 35.43%; DGR with sucrose 70.88 ± SE 4.89/SD 13.85 % and DGR without sucrose 22.71 ± SE 11.61/SD 32.83% (Figure 6C). Further studies are imminent to dissect at which developmental stage of the root and to which extent sucrose is triggering root hair growth. From former studies, it can be deduced that sucrose is enhancing auxin biosynthesis in the root tip [9,41], and 1% sucrose elevates levels of IAA by three-fold [9], whereby auxin is required to prime root hair cell fate long before they reach the differentiation zone [15]. Although sucrose is enhancing root hair emergence, root hair length was not promoted further at LGR, contrary to data obtained for *eir1-4 PIN2::PIN2:VEN*. Root hair length for the other three conditions resembled for *eir1-4* values of *eir1-4 PIN2::PIN2:VEN*. The root hair length was for LGR with sucrose 35.28 ± SE 4.37/SD 29.30 µm, LGR without sucrose 22.05 ± SE 6.11/SD 22.84 µm, DGR with sucrose 44.04 ± SE 4.07/SD 24.75 µm, and DGR without sucrose 32.29 ± SE 8.30/SD 1.97 µm (Figure 5D). Taken together, PIN2 modulated shootward auxin transport is crucial to initiate and promote root hair growth, which is consistent with published data. *Eir1-4* root hair phenotypes can be partially rescued by sucrose supplementation, as root hair emerge of DGR was significantly enhanced, and sucrose is slightly shifting the ration from root hair bulges towards elongated root hairs, but the elongation potential as seen for

eir1-4 PIN2::PIN2:VEN is lost. Root hairs of LGR grown on sucrose supplemented medium elongate more than three times longer in average compared to DGR grown on sucrose supplemented medium (Table S3).

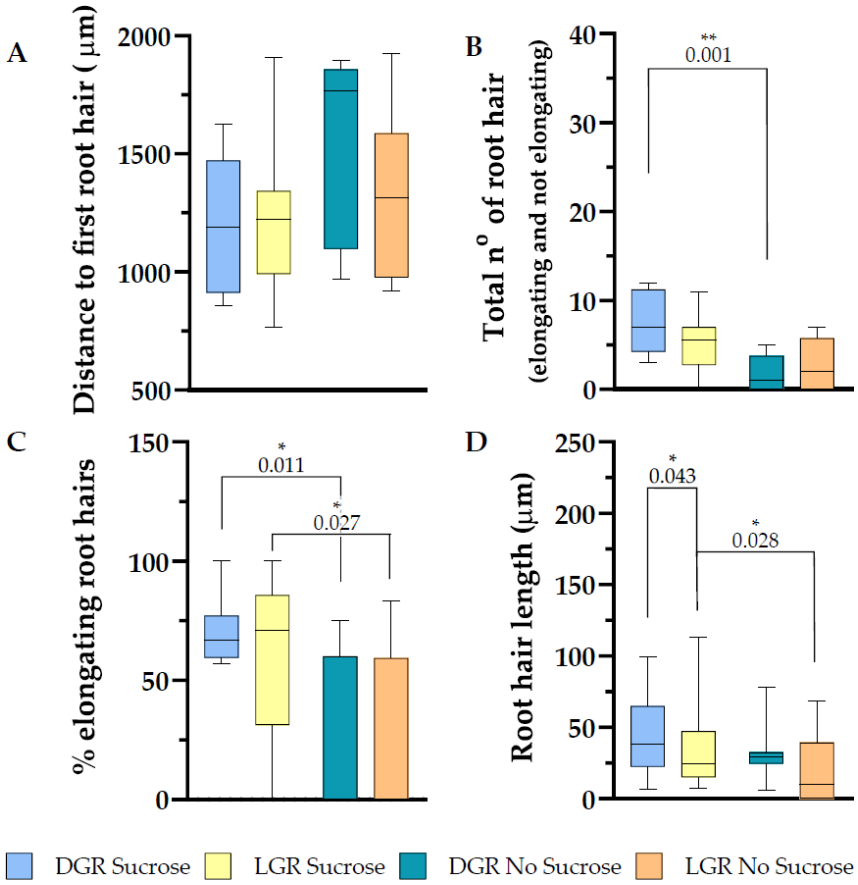

Figure 6. Root hair trait evaluation along the first 2 mm of the root tip of *eir1-4* plants. Depicted are (**A**) the distance from the root tip to the first emerging root hair, (**B**) total amount of root hairs (bulges and elongated), (**C**) in percentage how many root hairs elongated and (**D**) root hair length. (**A–D**) Root hair traits were evaluated from dark and light grown roots, grown either on half strength MS supplemented with 1% sucrose or without sucrose. Roots measured: n = 8–14. Root hairs measured: 7–45. Student's t-test (total number of root hairs and distance to first root hair) or Mann–Whitney U test (% of elongating root hairs and root hair length) was used to perform statistical analysis for the following comparisons: LGR sucrose vs. LGR no sucrose; DGR sucrose vs. DGR no sucrose; LGR sucrose vs. DGR sucrose; LGR no sucrose vs. DGR no sucrose. p-values for statistically significant comparisons are depicted in each plot. (* $p < 0.05$, ** $p < 0.01$)

2.5. Sucrose Supplementation Results in More Randomized Vertical Growth of eir1-4 PIN2::PIN2:VEN Independent on Root Illumination, but only in DGR for eir1-4

Previously, glucose was reported to lead to randomized root growth, with a stronger deviation from vertical compared to roots grown on medium without sucrose supplementation [41]. Furthermore, upon glucose addition to the growth medium PIN2:GFP was stabilized on lateral PMs and enhanced shootward auxin transport was measured, probably interfering with the fine-tuning of growth along the gravity vector [41]. Increased root tip growth deviation from vertical can is visible in decreased values of the vertical growth index, in our study named gravitropic index [50]. Our analysis of the gravitropic index of *eir1-4 PIN2::PIN2:VEN* roots showed that sucrose is like glucose leading to a small, but highly significant randomization of root growth, which is not dependent on the root illumination regime, LGR with sucrose 0.95 ± SE 0.003/SD 0.03; LGR without sucrose 0.97 ± SE 0.002/SD 0.01; DGR with sucrose 0.94 ± SE 0.003/SD 0.023; and DGR without

sucrose 0.97 ± SE 0.001/SD 0.01 (Figure 7A). In the case of the agravitropic *eir1-4*, we could only measure a small statistically significant difference of the gravitropic index for DGR, with sucrose 0.68 ± SE 0.038/SD 0.23; without sucrose 0.83 ± SE 0.018/SD 0.11, whereas there was no difference for LGR, with sucrose 0.79 ± SE 0.027/0.17; without sucrose 0.82 ± SE 0.023/SD 0.14 (Figure 7B).

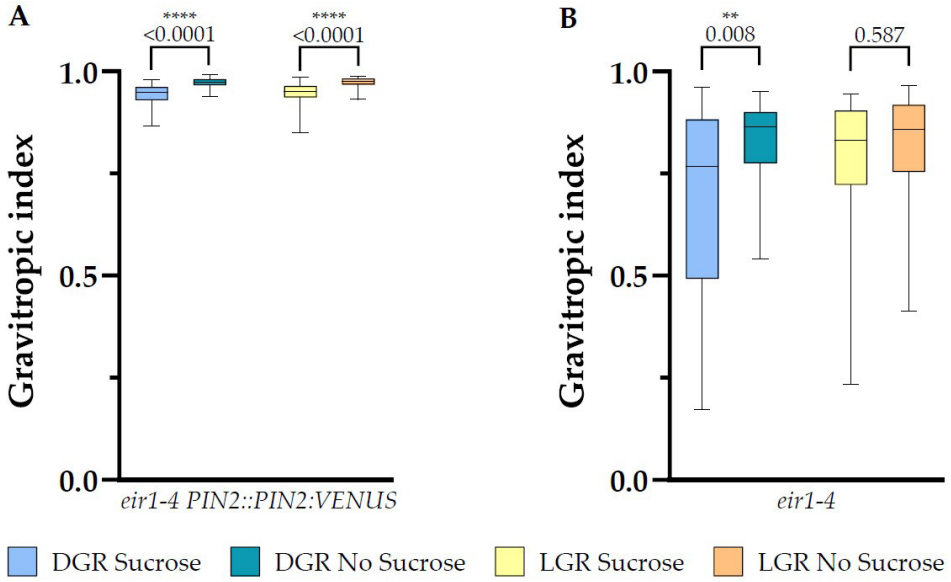

Figure 7. Root gravitropic index analysis of 7 DAG plants. Shown are gravitropic index data plots for (**A**) *eir1-4 PIN2::PIN2:VENUS* and (**B**) *eir1-4* plants grown on half strength MS medium either supplemented with 1% sucrose or without sucrose, of dark, respectively light grown roots. Differences were assessed by. Mann–Whitney *U* test was used to perform statistical analysis comparing plants grown on half strength MS medium with and without 1% sucrose supplementation under specific root illumination conditions (dark and light). *p*-values are depicted for each comparison (** $p < 0.01$, **** $p < 0.0001$). *eir1-4 PIN2::PIN2:VENUS* n = 61–79 roots; *eir1-4* n = 34–37 roots.

3. Discussion

Previously published studies linked the root illumination status and sucrose supplementation of the growth medium to altered root trait establishment, including differences in total root length and root hair outgrowth [1,25,41]. The establishment of those root traits depends strongly on fine-tuned polar auxin distribution, mediated by the auxin efflux carrier PIN2, through the root tip and availability of resources delivering energy to maintain proper root growth, in correlation to exogenous stimuli, like changing illumination or nutrition levels [3,11,23,25,26]. With this study, we present a first attempt to dissect the interplay between shootward transported auxin by PIN2, illumination status of the root and sucrose supplementation to the growth medium to mediate root growth and root hair outgrowth. A summary of all data is available in the Tables S1 and S2. Additionally, we calculated the changes of the measured root traits in percentage compared to DGR *eir1-4 PIN2::PIN2:VEN* grown on medium supplemented with sucrose and summarized them in the Table S3. Overall, our observations showed that sugar supplementation and continuous illumination of the root have an antagonistic effect on root length but an additive effect on root hair outgrowth. DGR showed more obvious difference of total root length depending on sucrose availability compared to LGR. The *pin2* mutant showed a similar sensitivity towards root illumination regime, but the total root length difference between DGR and LGR grown on sucrose was less pronounced compared to the control line, and total root length of the mutant was shorter upon all four growth conditions.

Root hair abundance and length are essential root traits to maximize nutrient uptake and therefore plant productivity, and depend on the transduction of environmental signals through the whole plant body towards the root tip [32,51]. Tubular root hair outgrowth

from the epidermis is an example of the planar and polar elongation of a cell and is regulated by various extra- and intracellular signaling events, highly depending on fine-tuned establishment of auxin gradients along the root tip [15]. The distribution of auxin is orchestrated in response to environmental stimuli in an active, directed (polar), cell-to-cell mediated way to define the spacing, abundance, and length of root hairs [32]. Direct, continuous illumination of the root induce stress responses [21] and auxin, light, and sugar signaling interfere with each other in a complex network to modulate meristem activity and root hair development [2]. Therefore, so far, most studies connecting light, sugar and auxin signaling underpinning root hair growth were done by evaluating constantly illuminated roots. This study dissects for the first time, the impact of shading the root from direct illumination in relation to sucrose levels and PIN2 loss during root hair outgrowth. Our results show that direct root illumination of *eir 1-4 PIN2::PIN2:VEN* results in a higher number of root hairs for LGR compared to DGR, independent on the availability of sucrose, but only root hairs of LGR grown on sucrose supplemented medium showed an extended ability for elongation. This ability was lost in *eir1-4*, accompanied by a drastic reduction of root hair emergence, especially if sucrose was omitted in the growth medium, independent on the root illumination status. Taken together, upon PIN2 action direct root illumination results in elevated root hair emergence, independent on sucrose supplementation, whereas sucrose supplementation triggers root hair length of LGR, but it doesn't for the other three growth conditions. In contrast, when PIN2 activity is lost, sucrose is partially elevating root hair emergence, but not root hair elongation. This indicates that sucrose supports trichoblast priming and partially root hair elongation, but shootward auxin delivery to the individual trichoblast is necessary to enhance its tip elongation. These results correlate with the published data that show that sugar is enhancing auxin biosynthesis in the root [9], but it also shows that for efficient root hair elongation on-point delivery of auxin to the individual root hair is crucial [32,51]. When shootward auxin transport is reduced root hairs fail to elongate, which was shown for the knockout *pin2* mutant [32,51]. Taken together, our data imply that shootward, PIN2 mediated auxin transport is crucial to implement light and sucrose mediated responses to orchestrate root hair elongation plasticity, whereas trichoblast priming is triggered also without PIN2 activity upon light stress in the presence of sucrose. The characterization of the deviation of root growth away from vertical of *eir1-4 PIN2::PIN2:VEN*, showed that sucrose is leading to a small, but highly significant randomization of the root growth direction, which is not dependent on the illumination regime of the root. This result correlates with the published study of Mishra et al., 2009, where they showed that glucose supplementation leads to randomized root growth in comparison to seedlings grown on sugar free medium, and further that glucose stabilized PIN2:GFP at the lateral PMs of some cells and enhanced shootward auxin transport towards the elongation zone, thereby linking sucrose signaling to auxin responses [41]. In contrast to *eir1-4 PIN2::PIN2:VEN*, *eir1-4*, which represents an agravitropic mutant [52], showed only a minor change of the gravitropic index of DGR depending on the availability of sucrose, but we couldn't measure a significant difference for LGR. Further evaluation of changes on cellular and subcellular level are required to dissect the molecular network connecting auxin, sugar, and light signaling cascades, which are involved in root and root hair growth regulation, root zone establishment, and switch between cell proliferation and elongation.

4. Materials and Methods

4.1. Plant Material and Growth Conditions

Seed stocks *eir1-4 PIN2::PIN2:VENUS* and *eir1-4* were obtained from Christian Luschnig, University of Natural Resources and Life Sciences, Vienna, Austria. Seeds were surface sterilized using 50% (*v*/*v*) bleach and 0.1% Tween20 (Sigma-Aldrich, Darmstadt, Germany) for 5 min and then rinsed three times with sterile water. The seeds were plated on 0.5× Murashige and Skoog (Sigma) medium, solidified with 1% agar (Sigma) and adjusted to pH 6.0 by KOH. The medium was supplemented by 1% sucrose (Merck-Millipore, Darm-

stadt, Germany), or was left sugar free to test the impact of sugar on root growth. Half of the plates were covered by the D-root system [1] to investigate the impact of direct root illumination on root growth. The seeds were plated and stratified at 4 ˚C for two days before germination. The plates were positioned vertically, 45 ˚C from vertical, at 22 ˚C and 100 µmol/sec/m^2 light intensity, in a climate control growth room with long day conditions (16h light, 8h dark).

4.2. Measurement of Root Length, Root Hair Traits and Gravitropic Index

After seven DAG the plates were scanned and total root length and gravitropic index were evaluated by using the ImageJ program from NIH. The gravitropic index was calculated according to [50]. Root tip bright field pictures for the evaluation of root hair traits were taken under the Zeiss880 microscope using the 20× objective and grabbing 3 × 9 tiles under 2× zoom, to capture 2 cm of the root tip. The root hair traits were also evaluated by using Image J. Distance to first root hair was calculated from the root tip to the first emerging root hair. Elongating root hairs were only taken into consideration when root hair length was measured. A summary of all average values with standard error and standard deviation is added in the Supplementary Tables S1 and S2). Statistical significance was assessed through unpaired Student's *t*-tests for comparisons between two conditions (normally distributed data, GraphPad Prism QuickCalcs was used https://www.graphpad.com/quickcalcs/ttest1/) or Mann–Whitney *U* test (not normally distributed data, online tool—https://www.statskingdom.com/170median_mann_whitney.html); when more groups were evaluated against a control, Kruskal–Wallis test with Dunn's post hoc test (online tool—https://astatsa.com/KruskalWallisTest/) was done. A summary of all average values with standard error and standard deviation is added in the Supplementary Figure S1.

Supplementary Materials: The following are available online at https://www.mdpi.com/2223-7747/10/1/111/s1, Figure S1A: example pictures of seedlings of all growth conditions, Figure S1B: example pictures of root hair outgrowth of all growth conditions, Table S1: descriptive statistics of analyzed root parameters, Table S2: descriptive statistics of analyzed root hair parameters, Table S3: comparison of all values relative to DGR with sucrose. Table S4: Raw data presented in this study.

Author Contributions: Conceptualization, K.R.; methodology, K.R. and J.L.; validation, K.R. and J.L.; formal analysis, J.G.-G.; investigation, K.R. and J.L.; resources, K.R.; data curation, K.R. and J.L.; writing—original draft preparation, K.R. and J.G.-G.; writing—review and editing, K.R., J.G.-G. and J.L.; visualization, J.G.-G. and K.R.; supervision, K.R.; project administration, K.R.; funding acquisition, K.R. All authors have read and agreed to the published version of the manuscript.

Funding: This research was funded by the Ministry of Education, Youth and Sports of Czech Republic from European Regional Development Fund 'Centre for Experimental Plant Biology': Project no. CZ.02.1.01/0.0/0.0/16_019/0000738 and the Czech Science Foundation (19-13375Y). The IEB CAS Imaging facility is supported by EU OPPC CZ.2.16/3.1.00/21519 and MEYS Czech Republic CZ.02.1.01/0.0/0.0/16_013/0001775.

Institutional Review Board Statement: Not applicable.

Informed Consent Statement: Not applicable.

Data Availability Statement: The data presented in this study are available in the Supplemental Table S4.

Acknowledgments: The authors would like to thank Christian Luschnig, Jan Petrášek and Felipe dos Santos Maraschin for constructive comments, and Christian Luschnig for providing *eir1-4 PIN2::PIN2:VENUS* and *eir1-4* seeds.

Conflicts of Interest: The authors declare no conflict of interest. The funders had no role in the design of the study; in the collection, analyses, or interpretation of data; in the writing of the manuscript, or in the decision to publish the results.

References

1. Silva-Navas, J.; Moreno-Risueno, M.A.; Manzano, C.; Pallero-Baena, M.; Navarro-Neila, S.; Téllez-Robledo, B.; Garcia-Mina, J.M.; Baigorri, R.; Gallego, F.J.; Del Pozo, J.C. D-Root: A System for Cultivating Plants with the Roots in Darkness or under Different Light Conditions. *Plant J.* **2015**, *84*, 244–255. [CrossRef]
2. Barrada, A.; Montané, M.H.; Robaglia, C.; Menand, B. Spatial Regulation of Root Growth: Placing the Plant TOR Pathway in a Developmental Perspective. *Int. J. Mol. Sci.* **2015**, *196*, 19671–19697. [CrossRef]
3. Van Gelderen, K.; Kang, C.; Pierik, R. Light Signaling, Root Development, and Plasticity. *Plant Physiol.* **2018**, *176*, 1049–1060. [CrossRef]
4. Korver, R.A.; Koevoets, I.T.; Testerink, C. Out of Shape during Stress: A Key Role for Auxin. *Trends Plant Sci.* **2018**, *23*, 783–793. [CrossRef] [PubMed]
5. Kleine-Vehn, J.; Leitner, J.; Zwiewka, M.; Sauer, M.; Abas, L.; Luschnig, C.; Friml, J. Differential Degradation of PIN2 Auxin Efflux Carrier by Retromer-Dependent Vacuolar Targeting. *Proc. Natl. Acad. Sci. USA* **2008**, *105*, 17812–17817. [CrossRef] [PubMed]
6. Gallei, M.; Luschnig, C.; Friml, J. Auxin Signalling in Growth: Schrödinger's Cat out of the Bag. *Curr. Opin. Plant Biol.* **2020**, *53*, 43–49. [CrossRef]
7. Qi, J.; Greb, T. Cell Polarity in Plants: The Yin and Yang of Cellular Functions. *Curr. Opin. Plant Biol.* **2017**, *35*, 105–110. [CrossRef] [PubMed]
8. Bailey-Serres, J.; Pierik, R.; Ruban, A.; Wingler, A. The Dynamic Plant: Capture, Transformation, and Management of Energy. *Plant Physiol.* **2018**. [CrossRef]
9. Sairanen, I.; Novák, O.; Pe˘nc˘ík, A.; Ikeda, Y.; Jones, B.; Sandberg, G.; Ljung, K. Soluble Carbohydrates Regulate Auxin Biosynthesis via PIF Proteins in Arabidopsis. *Plant Cell* **2013**, *24*, 4907–4916. [CrossRef]
10. Retzer, K.; Korbei, B.; Luschnig, C. Auxin and Tropisms. In *Auxin and Its Role in Plant Development*; Springer: Vienna, Austria, 2014. [CrossRef]
11. Retzer, K.; Akhmanova, M.; Konstantinova, N.; Malínská, K.; Leitner, J.; Petrášek, J.; Luschnig, C. Brassinosteroid Signaling Delimits Root Gravitropism via Sorting of the Arabidopsis PIN2 Auxin Transporter. *Nat. Commun.* **2019**, *10*, 1–15. [CrossRef]
12. Pierik, R.; Testerink, C. The Art of Being Flexible: How to Escape from Shade, Salt, and Drought1. *Plant Physiol.* **2014**, *166*, 5–22. [CrossRef]
13. De Smet, I. Lateral Root Initiation: One Step at a Time. *New Phytol.* **2012**, *193*, 867–873. [CrossRef] [PubMed]
14. Orman-Ligeza, B.; Parizot, B.; Gantet, P.P.; Beeckman, T.; Bennett, M.J.; Draye, X. Post-Embryonic Root Organogenesis in Cereals: Branching out from Model Plants. *Trends Plant Sci.* **2013**, *18*, 459–467. [CrossRef] [PubMed]
15. Leyser, O. Auxin Signaling. *Plant Physiol.* **2018**. [CrossRef] [PubMed]
16. Lavenus, J.; Goh, T.; Roberts, I.; Guyomarc'h, S.; Lucas, M.; De Smet, I.; Fukaki, H.; Beeckman, T.; Bennett, M.; Laplaze, L. Lateral Root Development in Arabidopsis: Fifty Shades of Auxin. *Trends Plant Sci.* **2013**, *18*, 450–458. [CrossRef] [PubMed]
17. Baldwin, K.L.; Strohm, A.K.; Masson, P.H. Gravity Sensing and Signal Transduction in Vascular Plant Primary Roots. *Am. J. Bot.* **2013**, *100*, 126–142. [CrossRef] [PubMed]
18. Band, L.R.; Wells, D.M.; Larrieu, A.; Sun, J.; Middleton, A.M.; French, A.P.; Brunoud, G.; Sato, E.M.; Wilson, M.H.; Per´et, B.; et al. Root Gravitropism Is Regulated by a Transient Lateral Auxin Gradient Controlled by a Tipping-Point Mechanism. *Proc. Natl. Acad. Sci. USA* **2012**, *109*, 4668–4673. [CrossRef]
19. Scheuring, D.; Löfke, C.; Krüger, F.; Kittelmann, M.; Eisa, A.; Hughes, L.; Smith, R.S.; Hawes, C.; Schumacher, K.; Kleine-Vehn, J. Actin-Dependent Vacuolar Occupancy of the Cell Determines Auxin-Induced Growth Repression. *Proc. Natl. Acad. Sci. USA* **2016**, *113*, 452–457. [CrossRef]
20. Liu, M.; Chen, Y.; Chen, Y.; Shin, J.-H.; Mila, I.; Audran, C.; Zouine, M.; Pirrello, J.; Bouzayen, M. The Tomato Ethylene Response Factor Sl-ERF.B3 Integrates Ethylene and Auxin Signaling via Direct Regulation of Sl-Aux/IAA27. *New Phytol.* **2018**, *219*, 631–640. [CrossRef]
21. Silva-Navas, J.; Moreno-Risueno, M.A.; Manzano, C.; Téllez-Robledo, B.; Navarro-Neila, S.; Carrasco, V.; Pollmann, S.; Gallego, F.J.; Del Pozo, J.C. Flavonols Mediate Root Phototropism and Growth through Regulation of Proliferation-to-Differentiation Transition. *Plant Cell* **2016**, *28*, 1372–1387. [CrossRef]
22. Silva-Navas, J.; Conesa, C.M.; Saez, A.; Navarro-Neila, S.; Garcia-Mina, J.M.; Zamarreño, A.M.; Baigorri, R.; Swarup, R.; del Pozo, J.C. Role of Cis-Zeatin in Root Responses to Phosphate Starvation. *New Phytol.* **2019**, *224*, 242–257. [CrossRef] [PubMed]
23. Retzer, K.; Lacek, J.; Skokan, R.; Del Genio, C.I.; Vosolsobe˘, S.; Laňková, M.; Malínská, K.; Konstantinova, N.; Zažímalová, E.; Napier, R.M.; et al. Evolutionary Conserved Cysteines Function as Cis-Acting Regulators of Arabidopsis PIN-FORMED 2 Distribution. *Int. J. Mol. Sci.* **2017**, *18*, 2274. [CrossRef] [PubMed]
24. Tomanov, K.; Luschnig, C.; Bachmair, A. Ubiquitin Lys 63 Chains-Second-Most Abundant, but Poorly Understood in Plants. *Front. Plant Sci.* **2014**, *5*, 15. [CrossRef] [PubMed]
25. Halat, L.S.; Gyte, K.; Wasteneys, G.O. Microtubule-Associated Protein CLASP Is Translationally Regulated in Light-Dependent Root Apical Meristem Growth. *Plant Physiol.* **2020**. [CrossRef]
26. Ötvös, K.; Marconi, M.; Vega, A.; O' Brien, J.; Johnson, A.; Abualia, R.; Antonielli, L.; Montesinos, J.C.; Zhang, Y.; Tan, S.; et al. Modulation of Root Growth by Nutrient-Defined Fine-Tuning of Polar Auxin Transport. *bioRxiv* **2020**. [CrossRef]

27. Tan, S.; Zhang, X.; Kong, W.; Yang, X.L.; Molnár, G.; Vondráková, Z.; Filepová, R.; Petrášek, J.; Friml, J.; Xue, H.W. The Lipid Code-Dependent Phosphoswitch PDK1–D6PK Activates PIN-Mediated Auxin Efflux in Arabidopsis. *Nat. Plants* **2020**, 1–14. [CrossRef]
28. Korbei, B.; Moulinier-Anzola, J.; De-Araujo, L.; Lucyshyn, D.; Retzer, K.; Khan, M.A.; Luschnig, C. Arabidopsis TOL Proteins Act as Gatekeepers for Vacuolar Sorting of PIN2 Plasma Membrane Protein. *Curr. Biol.* **2013**, *23*, 2500–2505. [CrossRef]
29. Laxmi, A.; Pan, J.; Morsy, M.; Chen, R. Light Plays an Essential Role in Intracellular Distribution of Auxin Efflux Carrier PIN2 in Arabidopsis Thaliana. *PLoS ONE* **2008**, *3*, e1510. [CrossRef]
30. Sassi, M.; Lu, Y.; Zhang, Y.; Wang, J.; Dhonukshe, P.; Blilou, I.; Dai, M.; Li, J.; Gong, X.; Jaillais, Y.; et al. COP1 Mediates the Coordination of Root and Shoot Growth by Light through Modulation of PIN1- and PIN2-Dependent Auxin Transport in Arabidopsis. *Development* **2012**, *139*, 3402–3412. [CrossRef]
31. Dolan, L.; Duckett, C.M.; Grierson, C.; Linstead, P.; Schneider, K.; Lawson, E.; Dean, C.; Poethig, S.; Roberts, K. Clonal Relationships and Cell Patterning in the Root Epidermis of Arabidopsis. *Development* **1994**, *120*, 2465–2474.
32. Grierson, C.; Nielsen, E.; Ketelaarc, T.; Schiefelbein, J. Root Hairs. *Arab. Book/Am. Soc. Plant Biol.* **2014**, *12*, e0172. [CrossRef] [PubMed]
33. Salazar-Henao, J.E.; Schmidt, W. An Inventory of Nutrient-Responsive Genes in Arabidopsis Root Hairs. *Front. Plant Sci.* **2016**, *7*, 237. [CrossRef] [PubMed]
34. Lee, R.D.-W.; Cho, H.-T. Auxin, the Organizer of the Hormonal/Environmental Signals for Root Hair Growth. *Front. Plant Sci.* **2013**, *4*, 448. [CrossRef] [PubMed]
35. Park, E.; Nebenführ, A. Cytoskeleton and Root Hair Growth. In *The Plant Cytoskeleton*; Springer: New York, NY, USA, 2011. [CrossRef]
36. Grebe, M.; Friml, J.; Swarup, R.; Sandberg, G.; Terlou, M.; Palme, K.; Bennett, M.J.; Scheres, B. Cell Polarity Signaling in Arabidopsis Involves a BFA-Sensitive Auxin Influx Pathway. *Curr. Biol.* **2002**, *12*, 329–334. [CrossRef]
37. Grebe, M. Ups of and Downs of Tissue and Planar Polarity in Plants. *BioEssays* **2004**, *26*, 719–729. [CrossRef] [PubMed]
38. Yokawa, K.; Fasano, R.; Kagenishi, T.; Baluška, F. Light as Stress Factor to Plant Roots—Case of Root Halotropism. *Front. Plant Sci.* **2014**, *5*, 718. [CrossRef]
39. Mo, M.; Yokawa, K.; Wan, Y.; Baluska, F. How and Why Do Root Apices Sense Light under the Soil Surface? *Front. Plant Sci.* **2015**, *6*, 775. [CrossRef]
40. Wan, Y.; Yokawa, K.; Baluška, F. Arabidopsis Roots and Light: Complex Interactions. *Mol. Plant* **2019**, *12*, 1428–1430. [CrossRef]
41. Mishra, B.S.; Singh, M.; Aggrawal, P.; Laxmi, A. Glucose and Auxin Signaling Interaction in Controlling Arabidopsis Thaliana Seedlings Root Growth and Development. *PLoS ONE* **2009**, *4*, e4502. [CrossRef]
42. Kircher, S.; Schopfer, P. Photosynthetic Sucrose Acts as Cotyledon-Derived Long-Distance Signal to Control Root Growth during Early Seedling Development in Arabidopsis. *Proc. Natl. Acad. Sci. USA* **2012**, *109*, 11217–11221. [CrossRef]
43. Leitner, J.; Petrášek, J.; Tomanov, K.; Retzer, K.; Parˇezová, M.; Korbei, B.; Bachmair, A.; Zažímalová, E.; Luschnig, C. Lysine63-Linked Ubiquitylation of PIN2 Auxin Carrier Protein Governs Hormonally Controlled Adaptation of Arabidopsis Root Growth. *Proc. Natl. Acad. Sci. USA* **2012**, *109*, 8322–8327. [CrossRef] [PubMed]
44. Singh, A.P.; Fridman, Y.; Friedlander-Shani, L.; Tarkowska, D.; Strnad, M.; Savaldi-Goldstein, S. Activity of the Brassinosteroid Transcription Factors BRASSINAZOLE RESISTANT1 and BRASSINOSTEROID INSENSITIVE1-ETHYL METHANESULFONATE-SUPPRESSOR1/BRASSINAZOLE RESISTANT2 Blocks Developmental Reprogramming in Response to Low Phosphate Availability. *Plant Physiol.* **2014**, *166*, 678–688. [CrossRef] [PubMed]
45. Billou, I.; Xu, J.; Wildwater, M.; Willemsen, V.; Paponov, I.; Frimi, J.; Heldstra, R.; Aida, M.; Palme, K.; Scheres, B. The PIN Auxin Efflux Facilitator Network Controls Growth and Patterning in Arabidopsis Roots. *Nature* **2005**, *433*, 39–44. [CrossRef] [PubMed]
46. Vieten, A.; Vanneste, S.; Wisniewska, J.; Benková, E.; Benjamins, R.; Beeckman, T.; Luschnig, C.; Friml, J. Functional Redundancy of PIN Proteins Is Accompanied by Auxin-Dependent Cross-Regulation of PIN Expression. *Development* **2005**, *132*, 4521–4531. [CrossRef] [PubMed]
47. Nukarinen, E.; Ngele, T.; Pedrotti, L.; Wurzinger, B.; Mair, A.; Landgraf, R.; Börnke, F.; Hanson, J.; Teige, M.; Baena-Gonzalez, E.; et al. Quantitative Phosphoproteomics Reveals the Role of the AMPK Plant Ortholog SnRK1 as a Metabolic Master Regulator under Energy Deprivation. *Sci. Rep.* **2016**, *6*, 31697. [CrossRef]
48. Menand, B.; Yi, K.; Jouannic, S.; Hoffmann, L.; Ryan, E.; Linstead, P.; Schaefer, D.G.; Dolan, L. An Ancient Mechanism Controls the Development of Cells with a Rooting Function in Land Plants. *Science* **2007**, *316*, 1477–1480. [CrossRef]
49. Datta, S.; Prescott, H.; Dolan, L. Intensity of a Pulse of RSL4 Transcription Factor Synthesis Determines Arabidopsis Root Hair Cell Size. *Nat. Plants* **2015**, *1*, 1–6. [CrossRef]
50. Grabov, A.; Ashley, M.K.; Rigas, S.; Hatzopoulos, P.; Dolan, L.; Vicente-Agullo, F. Morphometric Analysis of Root Shape. *New Phytol.* **2005**, *165*, 641–652. [CrossRef]
51. Müller, M.; Schmidt, W. Environmentally Induced Plasticity of Root Hair Development in Arabidopsis. *Plant Physiol.* **2004**, *134*, 409–419. [CrossRef]
52. Luschnig, C.; Gaxiola, R.A.; Grisafi, P.; Fink, G.R. EIR1, a Root-Specific Protein Involved in Auxin Transport, Is Required for Gravitropism in Arabidopsis Thaliana. *Genes Dev.* **1998**, *12*, 2175–2187. [CrossRef]

3.2.3. Throttling Growth Speed: Evaluation of aux1-7 Root Growth Profile by Combining D-Root system and Root Penetration Assay

Authors: Judith Garcia-Gonzales†, Jozef Lacek†, Wolfram Weckwerth, Katarzyna Retzer

† contributed equally

Summary:

Control of root growth is the key in maintaining proper adaptation to environment. Root growth is affected by countless stimuli to which it must adapt. Therefore, it's very difficult to untangle several adaptation mechanisms from each other during experiments. In this study we focused on analyzing the ability of Columbia 0 and AUXIN RESISTANT 1 (AUX1) plants to adapt to mechano-stimulus. Penetration essay was used as the main method in this study with combination of D-root system. We show that aux1 mutant has difficulties to penetrate 1% agar media due to its inability to organize cell layers within elongation zone. These are necessary to establish rotation/throttling movement of root, which may be required to efficiently penetrate the media. Randomization of root growth is significantly higher in aux1 mutant and all gravitropic experiments confirmed that the mutant is unable to adapt to gravity vector change. We also observed that while Columbia 0 reduces its growth speed while adapting to change of gravity vector, aux1 is growing unaffected.

My contribution: As joint first author, I contributed to designing and performing phenotypic experiments.

plants

MDPI

Article

Throttling Growth Speed: Evaluation of *aux1-7* Root Growth Profile by Combining D-Root system and Root Penetration Assay

Judith García-González [1,2,†], Jozef Lacek [1,2,†], Wolfram Weckwerth [3,4] and Katarzyna Retzer [1,*]

1 Laboratory of Hormonal Regulations in Plants, Institute of Experimental Botany, Czech Academy of Sciences, 165 02 Prague, Czech Republic; garciago.judith@gmail.com (J.G.-G.); lacek@ueb.cas.cz (J.L.)
2 Department of Experimental Plant Biology, Faculty of Science, Charles University, 128 00 Prague, Czech Republic
3 Department of Functional and Evolutionary Ecology, Molecular Systems Biology (MoSys), Faculty of Life Sciences, University of Vienna, Djerassiplatz 1, 1030 Wien, Austria; wolfram.weckwerth@univie.ac.at
4 Vienna Metabolomics Center (VIME), University of Vienna, Djerassiplatz 1, 1030 Wien, Austria
* Correspondence: retzer@ueb.cas.cz
† These authors contributed equally to this work.

Abstract: Directional root growth control is crucial for plant fitness. The degree of root growth deviation depends on several factors, whereby exogenous growth conditions have a profound impact. The perception of mechanical impedance by wild-type roots results in the modulation of root growth traits, and it is known that gravitropic stimulus influences distinct root movement patterns in concert with mechanoadaptation. Mutants with reduced shootward auxin transport are described as being numb towards mechanostimulus and gravistimulus, whereby different growth conditions on agar-supplemented medium have a profound effect on how much directional root growth and root movement patterns differ between wild types and mutants. To reduce the impact of unilateral mechanostimulus on roots grown along agar-supplemented medium, we compared the root movement of Col-0 and *auxin resistant 1-7* in a root penetration assay to test how both lines adjust the growth patterns of evenly mechanostimulated roots. We combined the assay with the D-root system to reduce light-induced growth deviation. Moreover, the impact of sucrose supplementation in the growth medium was investigated because exogenous sugar enhances root growth deviation in the vertical direction. Overall, we observed a more regular growth pattern for Col-0 but evaluated a higher level of skewing of *aux1-7* compared to the wild type than known from published data. Finally, the tracking of the growth rate of the gravistimulated roots revealed that Col-0 has a throttling elongation rate during the bending process, but *aux1-7* does not.

Keywords: AUXIN-RESISTANT 1; AUX1; directional root growth; gravitropic response; mechanostimulus; mechanoadaptation; root skewing; root elongation rate; D-root system; root penetration assay

Citation: García-González, J.; Lacek, J.; Weckwerth, W.; Retzer, K. Throttling Growth Speed: Evaluation of *aux1-7* Root Growth Profile by Combining D-Root system and Root Penetration Assay. *Plants* **2022**, *11*, 650. https://doi.org/10.3390/plants11050650

Academic Editor: Helene Robert Boisivon

Received: 22 January 2022
Accepted: 25 February 2022
Published: 27 February 2022

1. Introduction

Roots have evolved to grow in darkness and surrounded by soil along the gravity vector [1–4]. They adapt their growth direction and rate to their ever-changing environment, which includes changes in soil density or nutrient availability [5,6]. The root tip senses the pressure of a more compact soil and either adjusts the root thickness to penetrate it or changes the direction of growth [5,7]. Under drought conditions, the soil becomes more compact, and in addition to the limiting effects on root growth itself, mechanical impedance also restricts shoot growth, probably by increasing energy consumption [6]. Therefore, it is of agronomic importance to understand how these growth adaptations are modulated [8–10]. As recently described by Taylor et al. [6], root movement efficiency is

fundamental to plant survival, but it is a complexly regulated collection of growth traits that are orchestrated by the interplay of multiple signaling pathways [6]. In addition to continuous growth along the gravitropic vector and the modulation of root system architecture to ensure efficient nutrient uptake, roots change their growth pattern form circumnutation to strict penetration depending on soil compaction [5,11–13]. This requires appropriate mechanostimulus perception, followed by signal transmission and mechanoadaptation [5,6,14,15]. The importance of orchestrated shootward auxin distribution along the root epidermis between the meristem and differentiation zone for the efficient modulation of root growth has been demonstrated repeatedly [3,4,16–28]. In 1990, Okada and Shimura [29] identified six *Arabidopsis thaliana* mutants with an apparent wavy phenotype, including the loss of function of a plasma membrane-located auxin influx carrier, AUXIN RESISTANT 1 (AUX1) [16,25,28–34]. The adaptation of root growth patterns is often studied by observing seedlings growing on an agar-enriched medium [35,36]. By increasing the percentage of agar in the growth medium and inclining the plates, the root tip experiences more pressure on the contact side between the root and the medium, which results in a wavy root growth pattern [7,26,35]. A loss of AUX1 also leads to root agravitropism and to a loss of perception of mechanical stress [7,25]. In addition, AUX1 is critical for the efficient circumnutation of rice roots through the soil [6]. AUX1 activity has been calculated as being able to enable the shootward auxin gradient, which is considered to orchestrate the spatial and temporal modulation of cell expansion in the elongation zone, to be established 10–20 times faster [16,24,25,28]. Because the root responds to mechanical stress by reducing its elongation rate and cell length, which likely allows for an increase in the root diameter to ensure better soil penetration, we speculated that AUX1 loss may negatively affect root velocity adaptation in response to mechanical impediment [37].

2. Results

2.1. Introducing the Combination of D-Rootsystem and Root Penetration Assay to Study Directional Root Growth Adaptation

Previously published studies have shown that wild-type roots reduce their growth rate when confronted with obstacles, whereas the *aux1* mutant shows no reduction in its root growth rate under mechanical stress conditions [7]. The experiments were performed on seedlings with their roots exposed to light during cultivation and growth along the medium's surface. It is known that direct illumination, the stiffness of the agar supplemented medium, and the angle between the root tip and the presence of obstacles influence the modulation of directional root growth [4,7,26,35,38–41]. Therefore, we wondered how the *aux1* mutant would respond to uniformly applied mechanical stress compared to the wild type, and performed a so-called root penetration assay [42]. Furthermore, we complemented the root penetration assay with the D-root system, a device that allows to study roots that are shaded from direct root illumination (Figure 1). Recently, we published research that indicated that direct root illumination and sugar supplementation additively enhance the deviation of directional root growth, with sugar supplementation having a greater impact [39]. Direct root illumination triggers the so-called light escape mechanism, root elongation, but inhibits root meristem activity. Exogenous sucrose supplementation results in a more pronounced elongation and proliferation rate [43–47]. By stimulating the roots uniformly, reducing direct illumination, and testing the effect of sucrose supplementation, we aim to establish an experimental setup to analyze to what extent AUX1-mediated shootward auxin transport underpins the gravitropic response compared to mechanoadaptation.

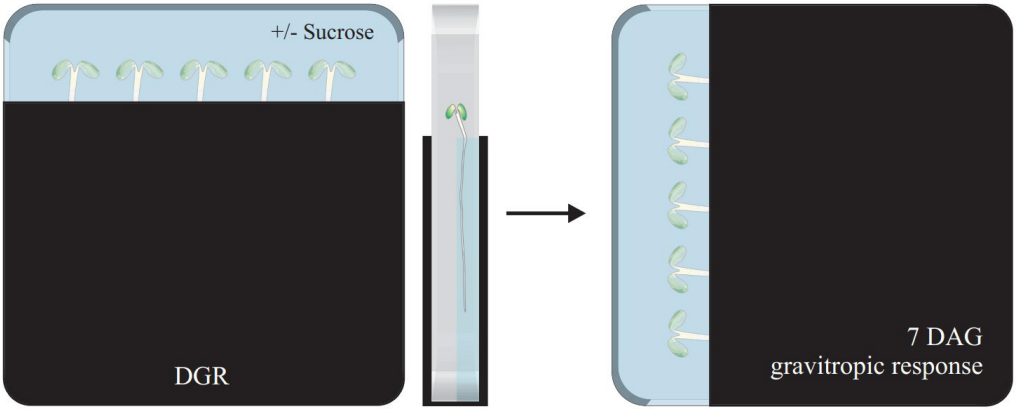

Figure 1. Schematic representation of the experimental setup. Briefly, seeds were placed on top of an agar layer unsupplemented or supplemented with sucrose. Plates were kept in the D–root system, allowing seedlings to grow with shaded roots for seven days. Primary root parameters (e.g., penetration frequency, root length, vertical growth index, straightness, and skewing angle) and gravitropic response were measured after a 90° turn. DGR: dark-grown root, DAG: days after germination.

2.2. Loss of AUX1 Results in Reduced Growth Medium Penetration Efficiency

Primarily, we compared the ability of the *aux1-7* and Col-0 roots to grow into $\frac{1}{2}$ MS medium supplemented with 1% agar, with and without the addition of 1% sucrose. We removed a part of the medium to place the seeds on top of it and scanned the plates seven days after germination to evaluate the root penetration efficiency (Figure 2A,B).

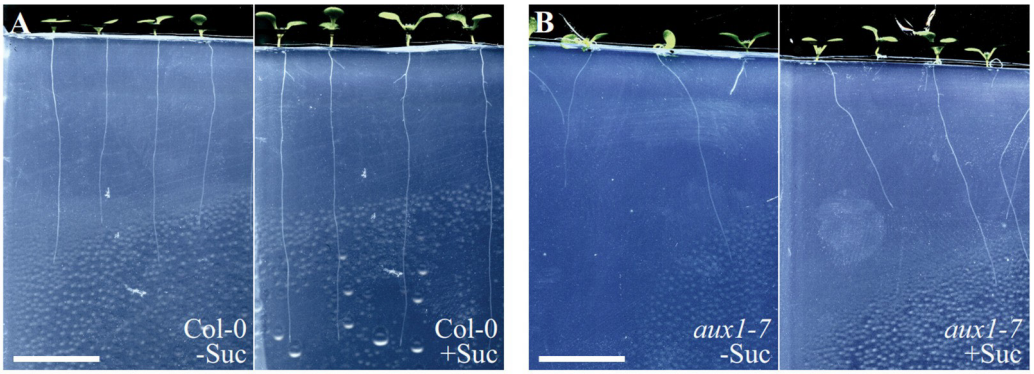

Figure 2. Representative images of seven DAG (**A**) Col-0 and (**B**) *aux1-7* seedlings grown in agar that had been unsupplemented or supplemented with sucrose. Scale bar = 10 mm.

The addition of sucrose did not significantly change the root penetration frequency in either line (Figure 3A). However, compared to the wild type, only a fraction of the *aux1-7* roots (27.17% without and 28.89% with sucrose) succeeded in growing into the growth medium (Figure 3A). This suggests that the mutant struggles to grow into soil with increased compactness under the surface-exposed roots, consistent with the recently published study, which shows that AUX1 is critical for the efficient modulation of root movement [6]. Therefore, we examined the root morphology of the Col-0 roots that successfully penetrated the agar-supplemented medium and compared it to the *aux1-7* roots after staining them with the vacuolar stain BCECF-AM to visualize the individual cells. We found that every Col-0 root performs a twisting movement at the position of the root elongation zone, whereas *aux1-7* fails to organize its root shape at the elongation zone in the same manner (Figure 3B). We suppose that when *aux1-7* roots fail to orchestrate the spatial and temporal modulation of the elongation zone, it also has diminished ability

to drill into the growth medium, which correlates with the low penetration efficiency compared to the Col-0 roots.

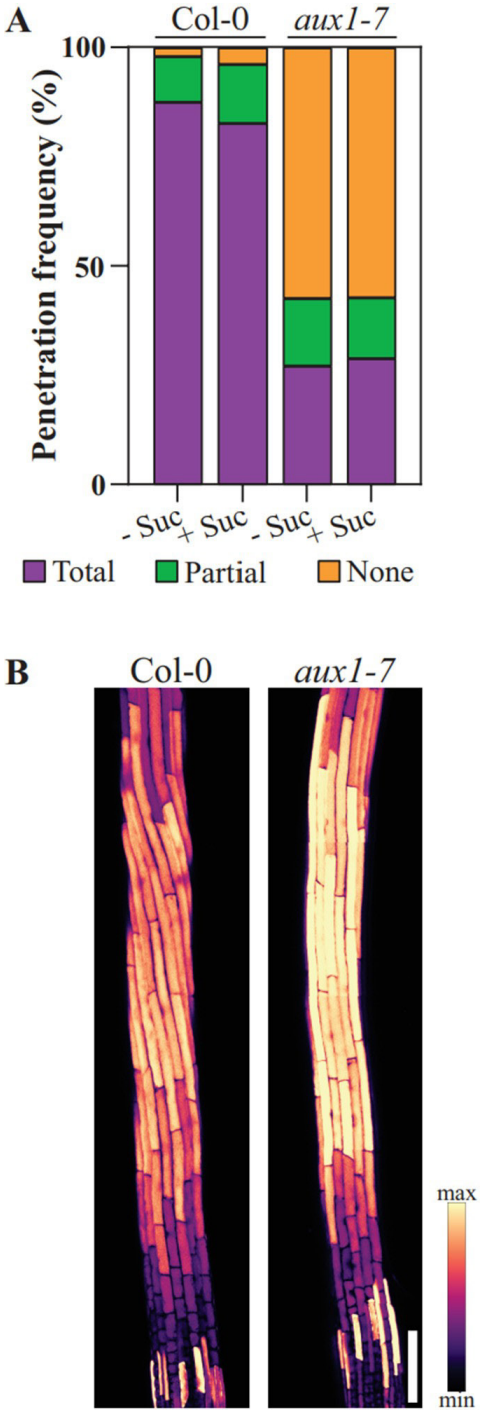

Figure 3. (**A**) Penetration frequency of seedlings grown in agar. Three categories were considered: no penetration (None), total penetration (Total; entire root embedded in the agar), and partial penetration (Partial; only part of the root can grow into the agar) (n = 42–57 roots). (**B**). Vacuole visualization in *Arabidopsis* roots with focus on the elongation zone. Staining with BCECF-AM was performed to distinguish individual root cells.

2.3. Loss of AUX1 Expectedly Results in an Uncoordinated Root Growth Pattern When Grown in Medium

To test whether growth in medium enriched with 1% agar alters the already known growth differences between Col-0 and *aux1* mutants, we measured the total root length, root skewing angle, gravitropic index (GI), and straightness, which is also known as waviness. The total length of the primary root was used to reflect root growth efficiency [48]. When grown on medium, supplementing the medium with sucrose results in longer roots by increasing the cell proliferation rate [39,46]. Col-0 shows a significant increase in root length between the mediums with and without sucrose supplementation (Figure 4A). *aux1-7* grows shorter roots compared to Col-0, and sucrose supplementation does not result in a significant difference in root length, likely due to less auxin transport to the root meristem [16,28].

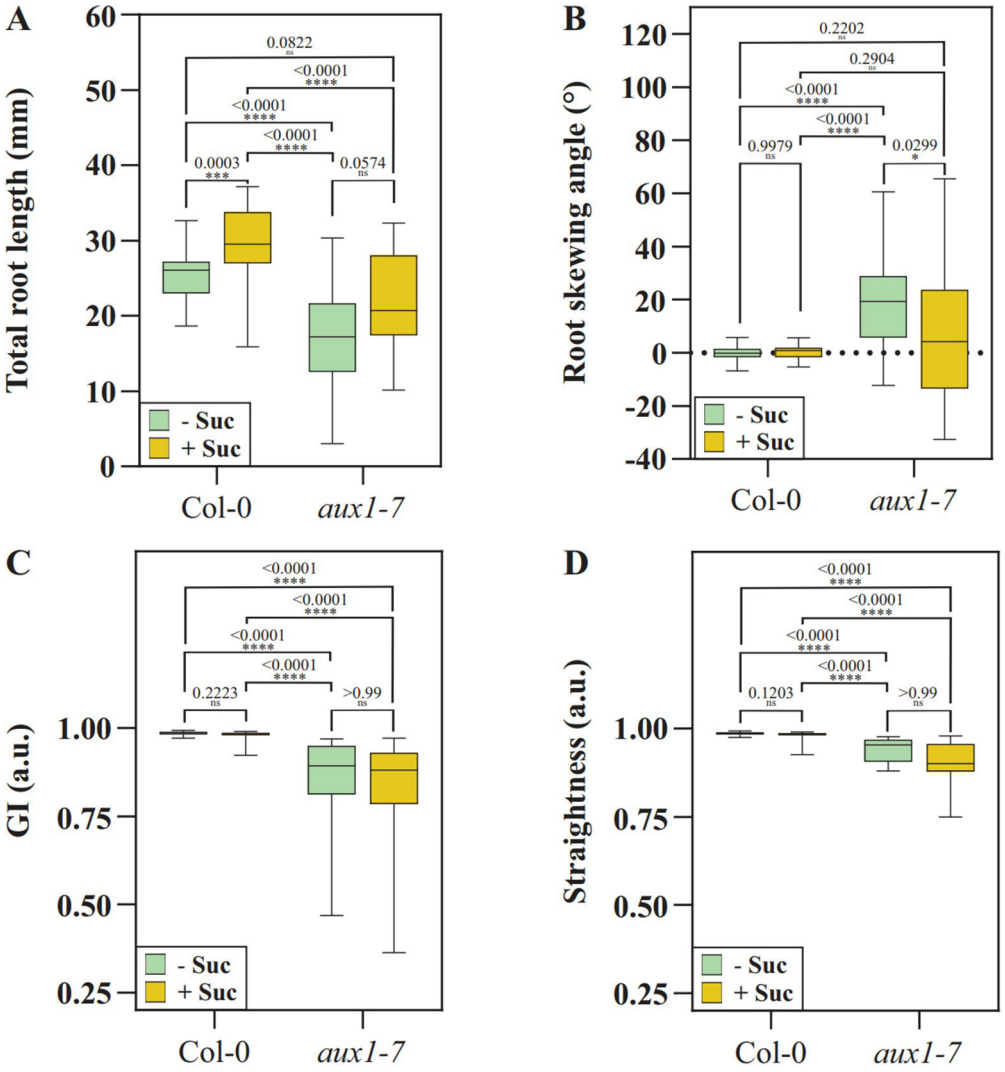

Figure 4. Analysis of root growth parameters: (**A**) root length, (**B**) skewing angle, (**C**) gravitropic index (GI), and (**D**) straightness. Only roots that showed total penetration into the medium were considered for analysis (Col-0, n = 38–50 roots; *aux1-7*, n = 15–16 roots). Statistical analysis: data normality was assessed through the Shapiro–Wilk test. Normally distributed data were analyzed with a One-Way ANOVA and Tukey's post hoc multiple comparison test. Not normally distributed data were analyzed via a Kruskal–Wallis test followed by Dunn's multiple comparison test. * $p < 0.05$; *** $p < 0.001$; **** $p < 0.0001$.

The root skewing angle reflects the slanted deviation of the root from the direction of gravity, something that *aux1* mutants have been previously described to do when grown exposed to light along a sugar-enriched growth medium [49,50]. In the current setup, Col-0 roots grow along the gravity vector in a less deviated manner compared to previously described experiments where the roots grew along the medium, and show no significant differences in the skewing angle and GI were found, regardless of supplementation (Figure 4B,C). Our previously published work showed that when roots are grown on the medium surface, there is a significant difference in the GI in response to the root illumination and sucrose supplementation status. We suspect that an uniformly perceived mechanical stimulus by wild-type roots that have grown into a medium limits the sugar-enhanced deviation from the vertical direction [27,39,46,51,52]. On the other hand, the *aux1-7* roots show a wider range of root skewing angles, while the difference between sucrose-enriched and non-enriched medium is small but still significantly relevant (Figure 4B). The deviation from the vertical direction is higher for *aux1-7* than it is for Col-0 in our penetration experiment (Figure 4C). We conclude that the directional growth of Col-0 deviates less because the roots grow in the dark and because the uniformly experienced mechanical stimulus limits the growth deviation, but *aux1-7* does not adapt to the mechanostimulus, which also correlates to the diminished ability to orchestrate the twisting movement at the position of the elongation zone (Figure 3A).

The wavy growth pattern, also referred to as straightness, reflects the ability of the root to respond to mechanic impedance [21,35,42,53]. Higher values for straightness indicate less curvature, fewer waves are formed, and lower values indicate more curvature [53]. Mutants with reduced shootward auxin transport were initially identified as roots lacking a wave pattern formation [26]. Published studies have described that Col-0 roots, when grown along the surface of a medium and with an increased plate inclination, exhibit a denser wave pattern that is further enhanced by the addition of sugar [26,35]. As in the case of GI, Col-0 roots show no significant difference in their waviness regardless of sucrose supplementation when embedded in the growth medium, and *aux1-7* roots show an expected uncoordinated growth pattern, resulting in a reduced straightness value (Figure 4D). Overall, the supplementation of $\frac{1}{2}$ MS with 1% agar does not result in the growth medium having a high stiffness, meaning that root growth would be more impaired compared to the root growth along the medium, and the growth discrepancies between Col-0 and *aux1-7* described earlier are still present. We observed the largest differences in Col-0 when comparing the evaluated data with previously published differences in growth patterns that were associated with mechanosensing and adaptation depending on sugar supplementation [4,27,39,46,51,52].

2.4. Col-0 Roots Throttle Elongation Speed during Gravitropic Response, but Not aux1-7

The loss of AUX1 results in agravitropic root growth and no gravitropic response, whereby the data were obtained from roots growing while exposed to light and along the surface of the medium's surface [16,25,28,32,34]. We tested the gravitropic response of Col-0 and *aux1-7* roots in a combined D-root system and using a root penetration test approach. As expected and previously published, we tracked a pronounced bending curve over time for Col-0 and no response for *aux1-7* (Figure 5A).

The maximum projection of the time-lapse images that we took every 30 min for four hours illustrates the form and growth rate of the bent root tips (Figure 5A). To quantify, if sucrose supplementation alters the bending efficiency of the roots when they grow into the agar, we analyzed the final root tip angle 240 min after gravistimulation, and it was determined that this was not the case (Figure 5B). However, regardless of the addition of sucrose, we observed that Col-0 limits the root growth rate during the bending process over time, while *aux1-7* roots continue to elongate at an almost constant rate (Figure 6). This is not surprising, as Fendrych et al. [24] have shown that cell elongation in roots is inhibited by exogenous auxin application and that this response requires the action of AUX1 [24,54]. This lack of the AUX1-dependent control of the root growth rate of individual cells in

response to exogenously occurring signals may explain why *aux1* roots exhibit reduced root elongation control and diminished organization in the elongation zone (Figure 3B).

After losing the ability to modulate the elongation zone and the lack of throttling growth speed during the root bending process upon gravitropic stimulation, *aux1-7* roots do not respond to the gravitropic stimulus (Figure 7). Supplementing the growth medium with sucrose increases the growth distance over time (Figure 6), resulting in the bending angle of Col-0 grown in medium supplemented with sucrose is larger compared to that of roots grown on medium that had not been supplemented with sucrose (Figures 5A and 7). Nevertheless, in both media, Col-0 is bends efficiently, whereas the *aux1-7* roots continue to grow in completely straight manner upon gravitropic stimulus (Figures 5B and 7).

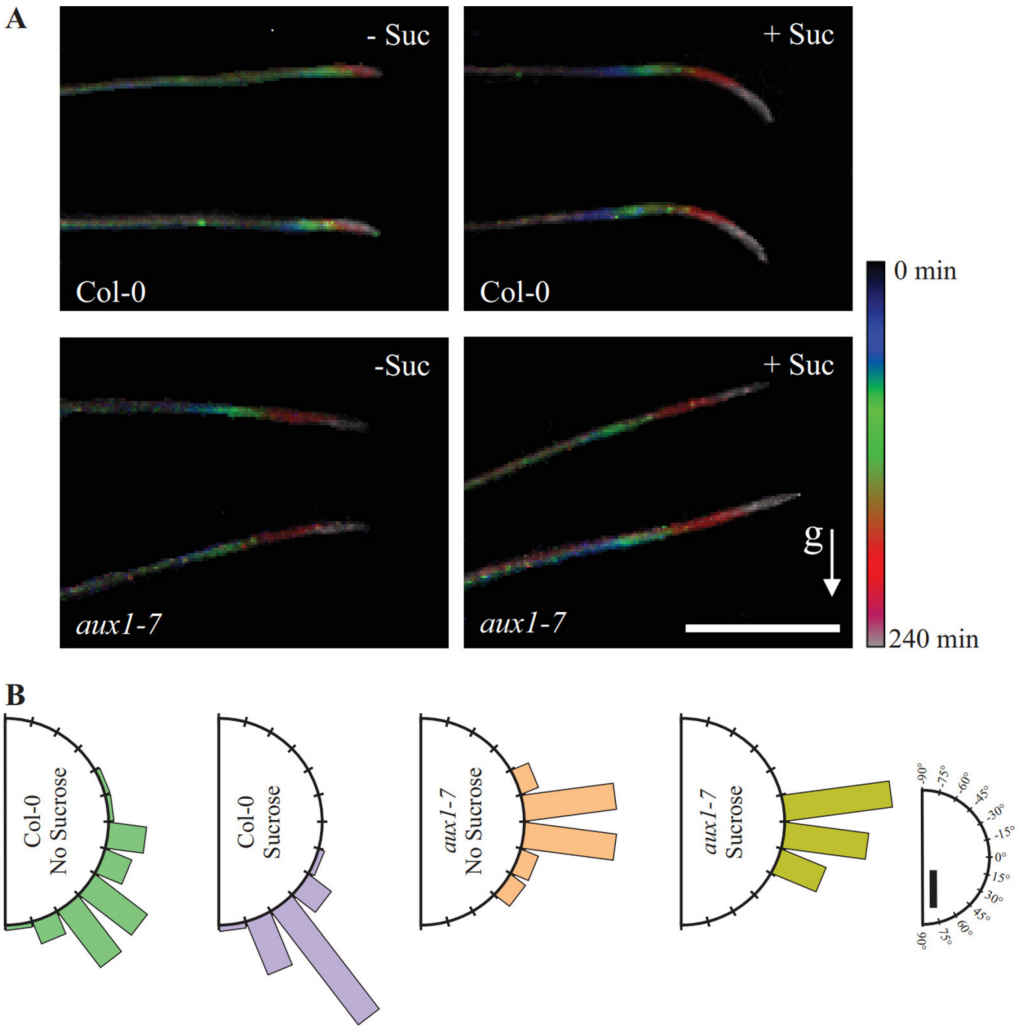

Figure 5. Gravitropic bending analysis. (**A**) Maximum projection of time-lapse imaging of root bending in unsupplemented and sucrose supplemented wild-type and *aux1-7* medium. Scalebar = 2 mm. Root imaging was carried out at time 0 (dark blue), 15, 30, 60, 120, 180, and 240 (light pink) minutes after turning the plates 90 degrees. (**B**) Root tip angle 240 min after gravistimulation. Roots were assigned to 15° sectors in a gravitropism diagram, and the percentage of roots belonging to each sector is represented by bars. Scalebar = 20%. (Col-0, n = 42–51 roots; *aux1-7*, n = 13–20 roots).

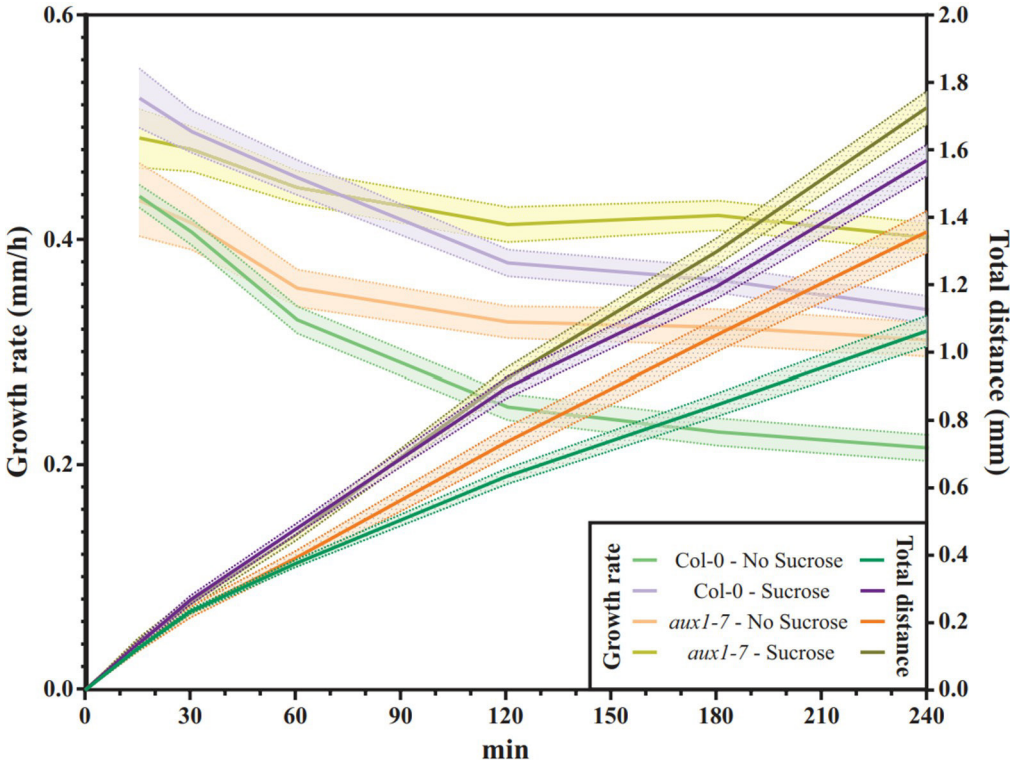

Figure 6. Root growth rates (left axis) compared to total growth distance (right axis) of 7DAG roots from the moment of gravistimulation over a period of four hours. Scans of the plates turned 90° were taken every 30 min, and the growth rate during the Col-0's bending process compared to *aux1-7's* was evaluated depending on sucrose supplementation (Col-0, n = 42–51 roots; *aux1-7*, n = 13–20 roots).

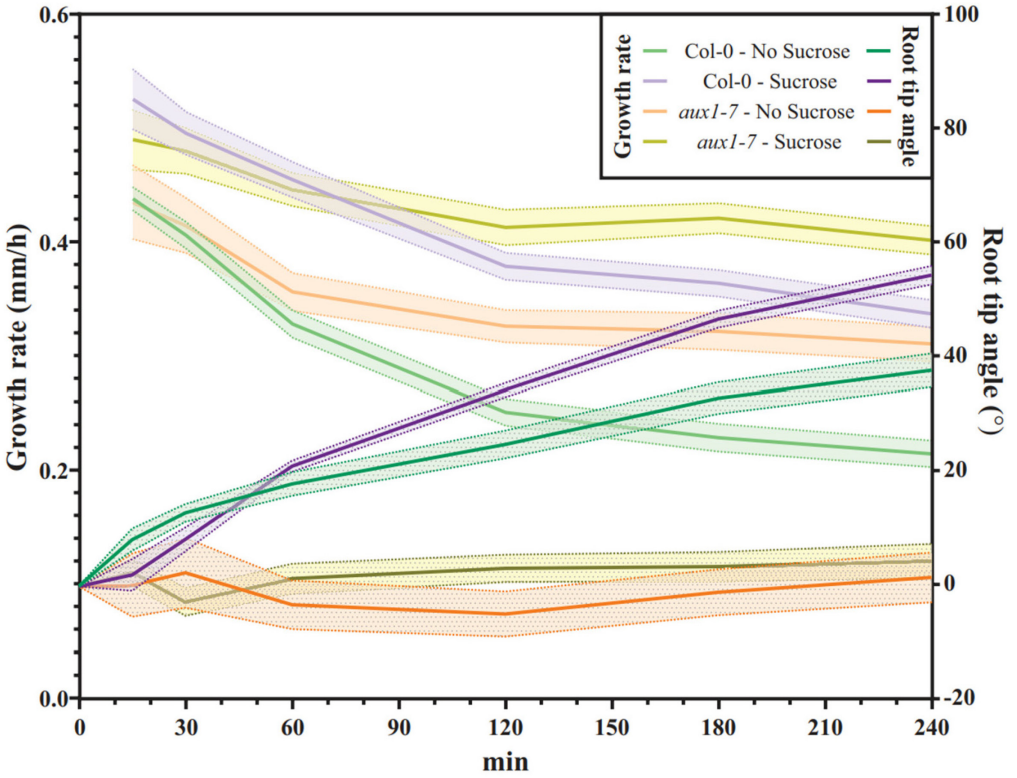

Figure 7. Time course of root bending upon gravistimulation of Col-0 and *aux1-7* 7DAG seedlings grown in agar with covered roots with or without sucrose supplementation. Root growth rates (left axis) versus root rip angles (right axis) are shown. (Col-0, n = 42–51 roots; *aux1-7*, n = 13–20 roots).

3. Discussion

Plant productivity and survival depend on efficient root growth in the soil. Roots have evolved to adapt and correct their architecture, volume, and directional root growth to ensure that enough water and nutrients are taken up to nourish the entire plant. For course direction, to avoid toxic compounds or obstacles, several signaling pathways are interwoven to initiate root growth adaptation.

Directional root growth adaptation is often studied by observing seedlings growing on agar-enriched medium [35,36]. By increasing the agar content and inclining the plates, the root tips experience more pressure and respond with a wavy root growth pattern [26]. Moreover, the addition of sucrose leads to increased deviation from vertical growth and from the straightness of the root when the roots grow along the medium [27,51,52]. The wavy pattern of the roots growing along the growth medium is orchestrated by multiple signaling pathways in the root tip, including mixed responses to gravisensing and mechanosensing [55]. Rutherford and Masson [56] proposed that thigmotropism is the cause of waviness and described that the changes in the symmetry at each half-wave occurs in response to gravity and mechanical impedance, with direction and force only varying for the mechanical stimulus, depending on the properties of the growth medium [56–59]. Gravity remains constant, and only the position of the plant can change relative to its source. Therefore, taller plants have evolved to grow their aboveground organs away (negative gravitropism) and their belowground organs along the gravitropic vector (positive gravitropism) [3,15,55,60–62].

With this study, we aimed to investigate the extent to which AUX1 activity maintains directional root growth under more natural growth conditions, namely omitting direct root illumination, sucrose supplementation, by combining the D-root system and the root penetration test. We chose the D-root system with and without sucrose supplementation because of the negative effects of direct root illumination and sugar supplementation shown in recently published studies [39,46]. Direct light illumination and exogenous sugar additively enhance the root growth that deviates from the vertical direction [39]. In addition, we chose to use the penetration test to uniformly expose the entire root to the same mechanostimulus intensity. In this way, we limited unnecessary exogenous stimuli by avoiding directional root illumination responding to uneven mechanostimuli and unnatural sucrose signaling in the case of plates without added sucrose.

Overall, we found a similar response in total root length growth and response to gravitropic stimulus as a function of the sucrose addition for Col-0 when the roots were grown in medium compared to published data for roots grown along surface of the medium. However, in contrast to the known data, we did not observe differential deviation from the vertical direction or increased waving of the Col-0 roots, which is generally observed in wild-type roots grown along a sucrose-enriched medium [27,47,52]. This is likely due to the ability of the wild-type roots to perform a twisting movement at the position of the elongation zone, which we could observe because the roots in our penetration assay are embedded in the medium and therefore are uniformly mechanostimulated but not impaired in the execution of their three-dimensional movement. The *aux1-7* roots do not show the same ability to modulate the elongation zone, which not only correlates with their reduced penetration ability and is further reflected in the loss of orchestrating directional root growth in general. Surprisingly *aux1-7* roots showed an unexpectedly high degree of skewness in the penetration assay, consistent with the recently suggested numbness of *aux1* mutants to mechanostimuli [7]. In addition, *aux1-7* root show a very low penetration frequency, with approximately 28% roots grown into the medium of all germinated seedlings, reflecting the importance of AUX1 as a mediator for efficient root movement [6]. Finally, when we tracked root growth during the bending assay, we found that *aux1-7* did not restrict the rate of root elongation compared to Col-0. Both lines responded as expected during the bending test and similarly to published results from roots grown on medium. The loss of root growth rate control in *aux1-7* is consistent with the observations of Fendrych et al. [24], who showed that AUX1 is required to limit

root elongation upon exogenous auxin supplementation [24,63]. In summary, our results show that the combination of the D-root system and penetration assay using 1% agar-enriched $\frac{1}{2}$ MS medium allows directional root growth to be observed while also reducing unnecessary interfering exogenous stimuli.

4. Materials and Methods

4.1. Plant Material and Growth Conditions

Col-0 and *aux1-7* seed stocks [32] were obtained from the Laboratory of Hormonal Regulations in Plants, Institute of Experimental Botany, Czech Academy of Sciences. Seeds were surface sterilized using 50% (*v*/*v*) bleach and 0.1% Tween20 (Sigma-Aldrich, Darmstadt, Germany) for 5 min and were then rinsed three times with sterile water. The seeds were plated on $\frac{1}{2}$ Murashige and Skoog (Sigma) medium, solidified with 1% agar (Sigma), and adjusted to pH 6.0 by KOH. The medium was supplemented with either 1% sucrose (Merck-Millipore, Darmstadt, Germany) or was left without sugar [39]. To stimulate the roots to grow into the medium, its upper part at the border of the D-root system [38] was removed, and the seeds were placed on top [42]. The seeds were plated and stratified at 4 °C for two days before germination. The plates were positioned inclined at 45° from the vertical direction, at 22 °C and with a light intensity of 100 µmol/s/m^2, in a climate-controlled growth room with long day conditions (16 h light, 8 h dark).

4.2. Root Parameter and Bending Analysis

Plate scans of seven-day-old *Arabidopsis thaliana* seedlings grown with covered roots were analyzed using the freely available ImageJ software. The root gravitropic index, straightness, and skewing angle were calculated according to Grabov et al. [53]. The skewing angle was determined based on the frontal orientation of the plates.

For the bending assay, 7DAG plants grown with covered roots were turned 90 degrees and were scanned at specific timepoints (0, 15, 30, 60, 90, 120, 180, 240 min). Images were aligned, and root tip coordinates were obtained using ImageJ. Data manipulation to determine the root tip angle and root growth rate was carried out using Microsoft Excel.

Statistical analysis and visual representation of the data were performed using GraphPad Prism. Normality was assessed via the Shapiro–Wilk test. Normally distributed data were evaluated with a One-Way ANOVA and Tukey's post hoc multiple comparison test; not normally distributed data were analyzed with the non-parametric Kruskal–Wallis test followed by Dunn's multiple comparison test.

Imaging was performed on five-day-old seedlings with roots grown in agar-supplemented medium without sugar supplementation, that had been shaded from direct light illumination, and that had been stained with BCECF-AM (10 µM, 60 min). The seedlings were placed on medium in a chambered coverslip, and pictures were taken with a Zeiss LSM880 laser scanning microscope in a horizontal setup that enabled the samples to be placed vertically using the objective 20×, at the Imaging Facility of the Institute of Experimental Botany AS CR.

Supplementary Materials: The following supporting information can be downloaded at: https://www.mdpi.com/article/10.3390/plants11050650/s1, Table S1: raw data.

Author Contributions: Conceptualization, K.R.; methodology, K.R. and J.L.; validation, K.R. and J.L.; formal analysis, J.G.-G.; investigation, K.R. and J.L.; resources, K.R.; data curation, K.R. and J.L.; writing—original draft preparation, K.R. and J.G.-G.; writing—review and editing, W.W., K.R., J.G.-G. and J.L.; visualization, J.G.-G. and K.R.; supervision, K.R.; project administration, K.R.; funding acquisition, K.R. All authors have read and agreed to the published version of the manuscript.

Funding: This research was funded by the Ministry of Education, Youth and Sports of Czech Republic from European Regional Development Fund 'Centre for Experimental Plant Biology': Project no. CZ.02.1.01/0.0/0.0/16_019/0000738.

Institutional Review Board Statement: Not applicable.

Informed Consent Statement: Not applicable.

Data Availability Statement: The data presented in this study are available in Supplemental Table S1.

Acknowledgments: The authors would like to thank Jan Hejátko and Jan Petrášek for their constructive comments. We acknowledge the Imaging Facility at the Institute of Experimental Botany AS CR supported by the MEYS CR (LM2018129 Czech-BioImaging) and IEB AS CR.

Conflicts of Interest: The authors declare no conflict of interest. The funders had no role in the design of the study; in the collection, analyses, or interpretation of data; in the writing of the manuscript; or in the decision to publish the results.

References

1. Swarup, R.; Bennett, M.J. Root Gravitropism. In *Annual Plant Reviews: Root Development*; Blackwell Publishing: Oxford, UK, 2009. [CrossRef]
2. Retzer, K.; Korbei, B.; Luschnig, C. Auxin and Tropisms. In *Auxin and Its Role in Plant Development*; Springer: Berlin/Heidelberg, Germany, 2014. [CrossRef]
3. Vandenbrink, J.P.; Kiss, J.Z. Plant responses to gravity. *Semin. Cell Dev. Biol.* **2019**, *92*, 122–125. [CrossRef]
4. Lacek, J.; García-González, J.; Weckwerth, W.; Retzer, K. Lessons Learned from the Studies of Roots Shaded from Direct Root Illumination. *Int. J. Mol. Sci.* **2021**, *22*, 12784. [CrossRef] [PubMed]
5. Kolb, E.; Legué, V.; Bogeat-Triboulot, M.-B. Physical root–soil interactions. *Phys. Biol.* **2017**, *14*, 065004. [CrossRef] [PubMed]
6. Taylor, I.; Lehner, K.; McCaskey, E.; Nirmal, N.; Ozkan-Aydin, Y.; Murray-Cooper, M.; Jain, R.; Hawkes, E.W.; Ronald, P.C.; Goldman, D.I.; et al. Mechanism and function of root circumnutation. *Proc. Natl. Acad. Sci. USA* **2021**, *118*, e2018940118. [CrossRef] [PubMed]
7. Okamoto, T.; Takatani, S.; Motose, H.; Iida, H.; Takahashi, T. The root growth reduction in response to mechanical stress involves ethylene-mediated microtubule reorganization and transmembrane receptor-mediated signal transduction in Arabidopsis. *Plant Cell Rep.* **2021**, *40*, 575–582. [CrossRef] [PubMed]
8. Jacobsen, A.G.R.; Jervis, G.; Xu, J.; Topping, J.F.; Lindsey, K. Root growth responses to mechanical impedance are regulated by a network of ROS, ethylene and auxin signalling in Arabidopsis. *New Phytol.* **2021**, *231*, 225–242. [CrossRef]
9. Tojo, H.; Nakamura, A.; Ferjani, A.; Kazama, Y.; Abe, T.; Iida, H. A Method Enabling Comprehensive Isolation of Arabidopsis Mutants Exhibiting Unusual Root Mechanical Behavior. *Front. Plant Sci.* **2021**, *12*, 646404. [CrossRef]
10. Potocka, I.; Szymanowska-Pułka, J. Morphological responses of plant roots to mechanical stress. *Ann. Bot.* **2018**, *122*, 711–723. [CrossRef]
11. Del Dottore, E.; Mondini, A.; Sadeghi, A.; Mattoli, V.; Mazzolai, B. An efficient soil penetration strategy for explorative robots inspired by plant root circumnutation movements. *Bioinspir. Biomim.* **2017**, *13*, 015003. [CrossRef]
12. Mishra, A.K.; Tramacere, F.; Guarino, R.; Pugno, N.M.; Mazzolai, B. A study on plant root apex morphology as a model for soft robots moving in soil. *PLoS ONE* **2018**, *13*, e0197411. [CrossRef]
13. Tedone, F.; del Dottore, E.; Palladino, M.; Mazzolai, B.; Marcati, P. Optimal control of plant root tip dynamics in soil. *Bioinspir. Biomim.* **2020**, *15*, 056006. [CrossRef] [PubMed]
14. Najrana, T.; Sanchez-Esteban, J. Mechanotransduction as an Adaptation to Gravity. *Front. Pediatr.* **2016**, *4*, 140. [CrossRef] [PubMed]
15. Darwin, C.; Darwin, F. *The Power of Movement in Plants*; John Murray: London, UK, 1880. [CrossRef]
16. Singh, G.; Retzer, K.; Vosolsobe˘, S.; Napier, R. Advances in Understanding the Mechanism of Action of the Auxin Permease AUX1. *Int. J. Mol. Sci.* **2018**, *19*, 3391. [CrossRef] [PubMed]
17. Halat, L.; Gyte, K.; Wasteneys, G. The Microtubule-Associated Protein CLASP Is Translationally Regulated in Light-Dependent Root Apical Meristem Growth. *Plant Physiol.* **2020**, *184*, 2154–2167. [CrossRef] [PubMed]
18. Ötvös, K.; Marconi, M.; Vega, A.; O'Brien, J.; Johnson, A.; Abualia, R.; Antonielli, L.; Montesinos, J.C.; Zhang, Y.; Tan, S.; et al. Modulation of plant root growth by nitrogen source-defined regulation of polar auxin transport. *EMBO J.* **2021**, *40*, e106862. [CrossRef] [PubMed]
19. Benková, E.; Michniewicz, M.; Sauer, M.; Teichmann, T.; Seifertová, D.; Jürgens, G.; Friml, J. Local, Efflux-Dependent Auxin Gradients as a Common Module for Plant Organ Formation. *Cell* **2003**, *115*, 591–602. [CrossRef]
20. Petraášek, J.; Friml, J. Auxin transport routes in plant development. *Development* **2009**, *136*, 2675–2688. [CrossRef]
21. Retzer, K.; Lacek, J.; Skokan, R.; del Genio, C.I.; Vosolsobe˘, S.; Laňková, M.; Malínská, K.; Konstantinova, N.; Zažímalová, E.; Napier, R.M.; et al. Evolutionary Conserved Cysteines Function as cis-Acting Regulators of Arabidopsis PIN-FORMED 2 Distribution. *Int. J. Mol. Sci.* **2017**, *18*, 2274. [CrossRef]
22. Lacek, J.; Retzer, K.; Luschnig, C.; Zazimalova, E. *Polar Auxin Transport*; Wiley Online Library, eLS: Hoboken, NJ, USA, 2017; pp. 1–11. Available online: https://onlinelibrary.wiley.com/doi/10.1002/9780470015902.a0020116.pub2 (accessed on 10 January 2022).
23. Retzer, K.; Akhmanova, M.; Konstantinova, N.; Malínská, K.; Leitner, J.; Petrasek, J.; Luschnig, C. Brassinosteroid signaling delimits root gravitropism via sorting of the Arabidopsis PIN2 auxin transporter. *Nat. Commun.* **2019**, *10*, 5516. [CrossRef]

24. Fendrych, M.; Akhmanova, M.; Merrin, J.; Glanc, M.; Hagihara, S.; Takahashi, K.; Uchida, N.; Torii, K.U.; Friml, J. Rapid and reversible root growth inhibition by TIR1 auxin signalling. *Nat. Plants* **2018**, *4*, 453–459. [CrossRef]
25. Swarup, R.; Kramer, E.; Perry, P.; Knox, K.; Leyser, O.; Haseloff, J.; Beemster, G.; Bhalerao, R.; Bennett, M. Root gravitropism requires lateral root cap and epidermal cells for transport and response to a mobile auxin signal. *Nat. Cell Biol.* **2005**, *7*, 1057–1065. [CrossRef] [PubMed]
26. Okada, K.; Ueda, J.; Komaki, M.K.; Bell, C.J.; Shimura, Y. Requirement of the Auxin Polar Transport System in Early Stages of Arabidopsis Floral Bud Formation. *Plant Cell* **1991**, *3*, 677–684. [CrossRef] [PubMed]
27. Mishra, B.S.; Sharma, M.; Laxmi, A. Role of sugar and auxin crosstalk in plant growth and development. *Physiol. Plant.* **2021**, *174*, e13546. [CrossRef] [PubMed]
28. Swarup, R.; Bhosale, R. Developmental Roles of AUX1/LAX Auxin Influx Carriers in Plants. *Front. Plant Sci.* **2019**, *10*, 1306. [CrossRef]
29. Okada, K.; Shimura, Y. Reversible Root Tip Rotation in Arabidopsis Seedlings Induced by Obstacle-Touching Stimulus. *Science* **1990**, *250*, 274–276. [CrossRef] [PubMed]
30. Hammes, U.Z.; Murphy, A.S.; Schwechheimer, C. Auxin Transporters—A Biochemical View. *Cold Spring Harb. Perspect. Biol.* **2021**, *14*, a039875. [CrossRef] [PubMed]
31. Geisler, M.M. A Retro-Perspective on Auxin Transport. *Front. Plant Sci.* **2021**, *12*, 756968. [CrossRef] [PubMed]
32. Swarup, R.; Kargul, J.; Marchant, A.; Zadik, D.; Rahman, A.; Mills, R.; Yemm, A.; May, S.; Williams, L.; Millner, P.; et al. Structure-Function Analysis of the Presumptive Arabidopsis Auxin Permease AUX1. *Plant Cell* **2004**, *16*, 3069–3083. [CrossRef] [PubMed]
33. Westermann, J.; Streubel, S.; Franck, C.M.; Lentz, R.; Dolan, L.; Boisson-Dernier, A. An Evolutionarily Conserved Receptor-like Kinases Signaling Module Controls Cell Wall Integrity during Tip Growth. *Curr. Biol.* **2019**, *29*, 3899–3908.e3. [CrossRef]
34. Marchant, A.; Kargul, J.; May, S.; Muller, P.; Delbarre, A.; Perrot-Rechenmann, C.; Bennett, M. AUX1 regulates root gravitropism in Arabidopsis by facilitating auxin uptake within root apical tissues. *EMBO J.* **1999**, *18*, 2066–2073. [CrossRef]
35. Roy, R.; Bassham, D.C. Root growth movements: Waving and skewing. *Plant Sci.* **2014**, *221–222*, 42–47. [CrossRef]
36. Yan, J.; Wang, B.; Zhou, Y.; Hao, S. Resistance from agar medium impacts the helical growth of Arabidopsis primary roots. *J. Mech. Behav. Biomed. Mater.* **2018**, *85*, 43–50. [CrossRef] [PubMed]
37. Wilson, A.J.; Robards, A.W.; Goss, M. Effects of Mechanical Impedance on Root Growth in Barley, *Hordeum vulgare* L.: II. Effects on Cell Development in Seminal Roots. *J. Exp. Bot.* **1977**, *28*, 1216–1227. [CrossRef]
38. Silva-Navas, J.; Moreno-Risueno, M.A.; Manzano, C.; Pallero-Baena, M.; Navarro-Neila, S.; Téllez-Robledo, B.; Garcia-Mina, J.M.; Baigorri, R.; Gallego, F.J.; del Pozo, J.C. D-Root: A system for cultivating plants with the roots in darkness or under different light conditions. *Plant J.* **2015**, *84*, 244–255. [CrossRef] [PubMed]
39. García-González, J.; Lacek, J.; Retzer, K. Dissecting Hierarchies between Light, Sugar and Auxin Action Underpinning Root and Root Hair Growth. *Plants* **2021**, *10*, 111. [CrossRef]
40. Wan, Y.; Yokawa, K.; Baluška, F. Arabidopsis Roots and Light: Complex Interactions. *Mol. Plant* **2019**, *12*, 1428–1430. [CrossRef]
41. Miotto, Y.; da Costa, C.T.; Offringa, R.; Kleine-Vehn, J.; dos Santos Maraschin, F. Effects of Light Intensity on Root Development in a D-Root Growth System. *Front. Plant Sci.* **2021**, *12*, 778382. [CrossRef]
42. Yan, J.; Wang, B.; Zhou, Y. A root penetration model of *Arabidopsis thaliana* in phytagel medium with different strength. *J. Plant Res.* **2017**, *130*, 941–950. [CrossRef]
43. Wu, Y.; Shi, L.; Li, L.; Fu, L.; Liu, Y.; Xiong, Y.; Sheen, J. Integration of nutrient, energy, light, and hormone signalling via TOR in plants. *J. Exp. Bot.* **2019**, *70*, 2227–2238. [CrossRef]
44. Stevenson, C.C.; Harrington, G.N. The impact of supplemental carbon sources on *Arabidopsis thaliana* growth, chlorophyll content and anthocyanin accumulation. *Plant Growth Regul.* **2009**, *59*, 255–271. [CrossRef]
45. Kircher, S.; Schopfer, P. Photosynthetic sucrose acts as cotyledon-derived long-distance signal to control root growth during early seedling development in Arabidopsis. *Proc. Natl. Acad. Sci. USA* **2012**, *109*, 11217–11221. [CrossRef] [PubMed]
46. García-González, J.; Lacek, J.; Weckwerth, W.; Retzer, K. Exogenous carbon source supplementation counteracts root and hypocotyl growth limitations under increased cotyledon shading, with glucose and sucrose differentially modulating growth curves. *Plant Signal. Behav.* **2021**, *16*, 1969818. [CrossRef] [PubMed]
47. Raya-González, J.; López-Bucio, J.S.; Prado-Rodríguez, J.C.; Ruiz-Herrera, L.F.; Guevara-García, Á.A.; López-Bucio, J. The MEDIATOR genes MED12 and MED13 control Arabidopsis root system configuration influencing sugar and auxin responses. *Plant Mol. Biol.* **2017**, *95*, 141–156. [CrossRef] [PubMed]
48. De Pessemier, J.; Chardon, F.; Juraniec, M.; Delaplace, P.; Hermans, C. Natural variation of the root morphological response to nitrate supply in *Arabidopsis thaliana*. *Mech. Dev.* **2013**, *130*, 45–53. [CrossRef] [PubMed]
49. Hu, Y.; Omary, M.; Hu, Y.; Doron, O.; Hoermayer, L.; Chen, Q.; Megides, O.; Chekli, O.; Ding, Z.; Friml, J.; et al. Cell kinetics of auxin transport and activity in Arabidopsis root growth and skewing. *Nat. Commun.* **2021**, *12*, 1657. [CrossRef] [PubMed]
50. Yang, X.; Wang, B.; Farris, B.; Clark, G.; Roux, S.J. Modulation of Root Skewing in Arabidopsis by Apyrases and Extracellular ATP. *Plant Cell Physiol.* **2015**, *56*, 2197–2206. [CrossRef] [PubMed]
51. Mishra, B.S.; Singh, M.; Aggrawal, P.; Laxmi, A. Glucose and Auxin Signaling Interaction in Controlling *Arabidopsis thaliana* Seedlings Root Growth and Development. *PLoS ONE* **2009**, *4*, e4502. [CrossRef]

52. Singh, M.; Gupta, A.; Laxmi, A. Striking the Right Chord: Signaling Enigma during Root Gravitropism. *Front. Plant Sci.* **2017**, *8*, 1304. [CrossRef]
53. Grabov, A.; Ashley, M.; Rigas, S.; Hatzopoulos, P.; Dolan, L.; Vicente-Agullo, F. Morphometric analysis of root shape. *New Phytol.* **2005**, *165*, 641–652. [CrossRef]
54. Pilet, P.E.; Elliott, M.C.; Moloney, M.M. Endogenous and exogenous auxin in the control of root growth. *Planta* **1979**, *146*, 405–408. [CrossRef]
55. Lopez, D.; Tocquard, K.; Venisse, J.-S.; Legué, V.; Roeckel-Drevet, P. Gravity sensing, a largely misunderstood trigger of plant orientated growth. *Front. Plant Sci.* **2014**, *5*, 610. [CrossRef] [PubMed]
56. Rutherford, R.; Masson, P.H. *Arabidopsis thaliana* sku Mutant Seedlings Show Exaggerated Surface-Dependent Alteration in Root Growth Vector. *Plant Physiol.* **1996**, *111*, 987–998. [CrossRef]
57. Thompson, M.V.; Holbrook, N.M. Root-Gel Interactions and the Root Waving Behavior of Arabidopsis. *Plant Physiol.* **2004**, *135*, 1822–1837. [CrossRef]
58. Migliaccio, F.; Tassone, P.; Fortunati, A. Circumnutation as an autonomous root movement in plants. *Am. J. Bot.* **2013**, *100*, 4–13. [CrossRef] [PubMed]
59. Moulia, B.; Fournier, M. The power and control of gravitropic movements in plants: A biomechanical and systems biology view. *J. Exp. Bot.* **2009**, *60*, 461–486. [CrossRef] [PubMed]
60. Friml, J. Fourteen Stations of Auxin. *Cold Spring Harb. Perspect. Biol.* **2021**, *14*, a039859. [CrossRef]
61. Konstantinova, N.; Korbei, B.; Luschnig, C. Auxin and Root Gravitropism: Addressing Basic Cellular Processes by Exploiting a Defined Growth Response. *Int. J. Mol. Sci.* **2021**, *22*, 2749. [CrossRef]
62. Band, L.R.; Wells, D.M.; Larrieu, A.; Sun, J.; Middleton, A.M.; French, A.P.; Brunoud, G.; Sato, E.M.; Wilson, M.H.; Péret, B.; et al. Root gravitropism is regulated by a transient lateral auxin gradient controlled by a tipping-point mechanism. *Proc. Natl. Acad. Sci. USA* **2012**, *109*, 4668–4673. [CrossRef]
63. Retzer, K.; Singh, G.; Napier, R.M. It starts with TIRs. *Nat. Plants* **2018**, *4*, 410–411. [CrossRef]

3.2.4. Arp2/3 Complex Is Required for Auxin-Driven Cell Expansion Through Regulation of Auxin Transporter Homeostasis

Authors: Judith Garcia-Gonzales, Štepánka Kebrlová, Matěj Semerák, Jozef Lacek, Innu Kotannal Baby, Jan Petrášek, Kateřina Schwarzerová

Summary:

Arp2/3 complex is involved in many stages of plant development. In our study we focused on expression patterns of subunits of the complex. Since it's a complex we expected and proved similar expression patterns of all studied subunits. As prominent expression pattern was found vascular tissues and mutants of the complex are affected in vascular tissues, we can suggest that Arp2/3 complex has an important role in establishing vascular tissues. Previous work on the complex shows auxin-related phenotypes including reduction of auxin transporter abundance. We proved that auxin can induce expression of two subunits of Arp2/3 complex, i.e. ARPC3 and ARPC4. We studied interplay between Arp2/3 and auxin in pavement cells. We detected decreased cell shape complexity in both Arp2/3 mutants, and conditions with increased auxin levels. Interestingly, the mutant still reacted to addition of auxin, hinting partially in cell lobe formation. We also show altered metabolism of auxin in Arp2/3 mutants in pavement cells: We detected increase in auxin indole-3-acetic acid and higher concentration of its inactive metabolites. Altered distribution of the auxin efflux-carrier PIN3 was detected with presence of vacuolar fragmentation suggesting role of Arp2/3 complex in endomembrane function and trafficking.

My contribution: I contributed by performing experiments and analyzing measurements of hormonal content and occurrence of native auxin metabolites.

frontiers in Plant Science

ORIGINAL RESEARCH
published: 28 April 2020
doi: 10.3389/fpls.2020.00486

Arp2/3 Complex Is Required for Auxin-Driven Cell Expansion Through Regulation of Auxin Transporter Homeostasis

Judith García-González[1], Štěpánka Kebrlová[1], Mateˇj Semerák[1], Jozef Lacek[1,2], Innu Kotannal Baby[1], Jan Petrášek[1] and Katerˇina Schwarzerová[1]**

[1] Department of Experimental Plant Biology, Faculty of Science, Charles University, Prague, Czechia, [2] Institute of Experimental Botany, Czech Academy of Sciences, Prague, Czechia

The Arp2/3 complex is an actin nucleator shown to be required throughout plant morphogenesis, contributing to processes such as cell expansion, tissue differentiation or cell wall assembly. A recent publication demonstrated that plants lacking functional Arp2/3 complex also present defects in auxin distribution and transport. This work shows that Arp2/3 complex subunits are predominantly expressed in the provasculature, although other plant tissues also show promoter activity (e.g., cotyledons, apical meristems, or root tip). Moreover, auxin can trigger subunit expression, indicating a role of this phytohormone in mediating the complex activity. Further investigation of the functional interaction between Arp2/3 complex and auxin signaling also reveals their cooperation in determining pavement cell shape, presumably through the role of Arp2/3 complex in the correct auxin carrier trafficking. Young seedlings of *arpc5* mutants show increased auxin-triggered proteasomal degradation of DII-VENUS and altered PIN3 distribution, with higher levels of the protein in the vacuole. Closer observation of vacuolar morphology revealed the presence of a more fragmented vacuolar compartment when Arp2/3 function is abolished, hinting a generalized role of Arp2/3 complex in endomembrane function and protein trafficking.

Keywords: actin, cytoskeleton, auxin, cell expansion, Arp2/3 complex

OPEN ACCESS

Edited by:
Taras P. Pasternak, University of Freiburg, Germany

Reviewed by:
Vasilina Kovrizhnykh, Russian Academy of Sciences, Russia
Jaideep Mathur, University of Guelph, Canada

**Correspondence:*
Judith García-González
garciago.judith@gmail.com
Katerˇina Schwarzerová
schwarze@natur.cuni.cz

Specialty section:
This article was submitted to Plant Cell Biology, a section of the journal Frontiers in Plant Science

Received: 13 January 2020
Accepted: 31 March 2020
Published: 28 April 2020

Citation:
García-González J, Kebrlová Š, Semerák M, Lacek J, Kotannal Baby I, Petrášek J and Schwarzerová K (2020) Arp2/3 Complex Is Required for Auxin-Driven Cell Expansion Through Regulation of Auxin Transporter Homeostasis. Front. Plant Sci. 11:486. doi: 10.3389/fpls.2020.00486

INTRODUCTION

The Arp2/3 complex is a conserved actin nucleator consisting of two actin-related proteins (ARP2 and ARP3) and five other complex-specific subunits (ARPC1 to ARPC5) (Welch et al., 1997). In plants, its mutation has been shown to affect the development of complex cell shapes such as trichomes and pavement cells (Le et al., 2003, 2006; Mathur et al., 2003a,b; Schwab et al., 2003; Saedler et al., 2004; Djakovic et al., 2006). Whereas the role of Arp2/3 complex in trichome shape development is the polarization of actin filaments for proper cell wall building (Yanagisawa et al., 2015), the role of Arp2/3 complex in pavement cell shape determination is not fully understood. Previous analysis has shown expression of ARP2 in all plant tissues with predominant expression in vascular tissues (Klahre and Chua, 1999). However, little is known about the expression of the other subunits and which factors affect it.

Correct cell shape formation requires the coordinated functioning of the cytoskeleton and hormone signaling. Auxin has been shown to be a major hormone involved in cell shape and patterning (Teale et al., 2006; Gallavotti, 2013; Saini et al., 2013). Auxin-driven cell morphogenesis relies in the correct localization of auxin carriers, which regulate this hormone's cell-to-cell transport in order to create different concentration gradients, and failure to efficiently transport auxin across cells results in reduced tissue differentiation (Lacek et al., 2017). Therefore, correct auxin transporter localization is of utmost importance for correct auxin distribution.

It has been reported that the actin cytoskeleton has a role in auxin carrier distribution, and its disturbance results in delocalized PIN transporters (Yamamoto and Kiss, 2002; Hou et al., 2003; Lanza et al., 2012). Previous work has revealed that the lack of functional Arp2/3 complex affects auxin transporter localization leading to reduced basipetal and radial transport in mature stems. Also, issues in the generation of proper auxin maxima have been observed in these mutant lines (Sahi et al., 2018).

Our work aims to resolve in higher detail the involvement of the Arp2/3 complex in auxin signaling. For this, we analyzed Arp2/3 complex subunit expression patterns and the effect of auxin on their transcription, demonstrating that two Arp2/3 subunits' expression is sensitive to auxin. Focusing on cotyledon pavement cells as a morphogenetic model, we analyzed the role of Arp2/3 complex in auxin-driven cell expansion through PIN3-mediated auxin transport. Our results indicate increased PIN3 targeting to vacuoles in early phases of pavement cells expansion and changed auxin balance in plants lacking functional Arp2/3 complex. Since we also demonstrate that Arp2/3 mutant pavement cells show defect in vacuolar fusion, we hypothesize that the loss of Arp2/3 results in endomembrane trafficking regulation defects, which lead to defects in precise timing of auxin transporters targeting. Our results indicate that correct morphogenesis relies in the coordinated action of auxin and the Arp2/3 complex.

MATERIALS AND METHODS

Plant Material and Growth

Plants were grown in peat pellets or *in vitro* (vertical agar plates containing half-strength Murashige and Skoog medium supplemented with 1% w/v sucrose) under a photoperiod of 16h light:8h darkness and 23°C and light intensity 110 μmol/m^2/s.

Arabidopsis thaliana genotypes used in this study were Col-0 (wild-type), *arp2* (SALK_077920.56.00), *arpc4* (SALK_013909.27.65), *arpc5* (SALK_123936.41.55), and *yuc1D* (Zhao et al., 2001).

The reporter line *pPIN3::PIN3:YFP* (Žádníková et al., 2010), *DII-VENUS* (Brunoud et al., 2012) and *yuc1D* were crossed to *arpc5*, and γ*TIP-mCherry* (ABRC stock #CD3-975; Nelson et al., 2007) was crossed to *arp2*, *arpc4* and *arpc5*. Then, the F_2 generation was screened for homozygous *arpc5* mutants expressing the reporter or showing the *yuc1D* phenotype. For *pPIN3::PIN3:YFP* and *arpc5* crosses, three independent homozygous lines (L1-L3) were used in this study.

Auxin Treatment

Three-day-old seedlings were transferred to 1 ml of liquid half-strength Murashige and Skoog medium supplemented with 1% w/v sucrose. Plants were supplied with either IAA (5 μM, Sigma #I2886), NAA (5 μM, Sigma #N0640) or DMSO (0.1%) and cultivated for 48 h in the cultivation room with mild shaking.

For histochemical promoter-GUS activity, three-day-old seedlings were submerged in 1 μM NAA-containing liquid medium for 24 h.

Auxin Metabolic Profiling

Auxin and its conjugates were measured in 14 DAG seedlings of Col-0 and *arp2, arpc4* and *arpc5* lines. Approximately 100 mg of fresh plant material were frozen in liquid nitrogen and stored at −80°C until analysis. Samples were analyzed as described in Dobrev and Vankova (2012). Three biological replicates were performed.

Cloning and Plant Transformation

To generate the promoter::GUS reporter lines we amplified arbitrarily 1–2 kbp promoter regions from Col-0 genomic DNA as described in **Table 1**.

The resulting fragments were cloned into pDrive (#231124, Qiagen, Hilden, Germany) and sequenced. Subsequently, the fragments were transferred to the binary vector pRD410 (Datia et al., 1992).

Four to five-week-old Col-0 plants were transformed according to the modified floral dip method described in Narusaka et al. (2010). T2 progeny of independent transformants

TABLE 1 | List of primers used for promoter activity analysis.

Vector name	Positions (relative to start codon)	Product size	Primer sequence
pARP2	−3 to −1347 bp	1344 bp	pARP2-F 5'-AAGCTTTAACTGT GGGAAGGTTTTGAACTAG-3'
			pARP2-R 5'-GGATCCTCTC CGATTTCTATAGAGACTACAGA-3'
pARPC3	−16 to −1173 bp	1157 bp	pARPC3-F 5'-AAGCTTTGTTTTT ACGACATGAAGGGTTTC -3'
			pARPC3-R 5'-GGATCCACAAT GAAGCGATATCAGGAAGGA-3'
pARPC4	2 to −1655 bp	1657 bp	pARPC4-F 5'- AAGCTTTTCGTC CTGTTCCATCATCAAAG-3'
			pARPC4-R 5'-GGATCCATGTCCTAGAAA TGATGTTATTCTACTC-3'
pARPC5	−3 to −1420 bp	1417 bp	pARPC5-F 5'- AAGCTTCAACCACATCT CCAACTTTTCAG-3'
			pARPC5-R 5'- CTGCAGTCGATTCGATC TTTCTCTCCGA-3'

were tested for GUS staining and representative lines with stronger GUS intensity were used in further experiments.

Histochemistry

Whole seedlings were harvested and incubated immediately in ice-cold 90% acetone for approximately 30 min. Then, plants were washed twice in phosphate buffer (280 mM KH_2PO_4, 720 mM K_2HPO_4, pH 7.2). Subsequently, they were incubated in GUS staining buffer (0.1 M phosphate buffer, 0.5 mM $K_3[Fe(CN)_6]$, 0.5 mM $K_4[Fe(CN)_6]$, 2 mM X-Gluc 5-Bromo-4-chloro-3-indoxyl-beta-D-glucoronide) at 37°C until the blue stain was visible (30 min to overnight). Seedlings were transferred to 70% EtOH and subsequently observed using an Olympus Provis AX 70 transmitted light microscope.

Immunostaining

Longitudinal sections of 5-week-old *A. thaliana* stems were hand-sectioned with a help of a razor blade. The obtained material was submerged in EM grade 4% paraformaldehyde in aqueous solution (PFA, Electron Microscopy Sciences #15714) in MTSB (50 mM PIPES, 5 mM EGTA, 5 mM $MgSO_4$; pH = 6.8) and fixed in a vacuum desiccator for one hour (pressure: 500 hPa). Samples were washed 5 times in MTSBT (0.1% Triton X-100 in MTSB) for 15 min. After this, samples were washed 5 times in 0.1% triton X-100 in water for 15 min and subsequently incubated in a solution of 0.05% pectolyase in 0.4 M mannitol in MTSBT at 37°C for 30 min. Samples were washed 5 times in MTSBT for 15 min, and 2 times in 10% DMSO/3% IGEPAL CA-630 in MTSBT for 30 min. Sections were washed 5 times in MTSBT for 5 min and incubated in 2% BSA in MTSBT for 1 h. Samples were transferred to a 2% BSA solution in MTSBT containing goat polyclonal anti-PIN1 aP-20 (1:500, Santa Cruz Biotechnologies #sc-27163) and incubated at 37°C for 4 h. Stems sections were washed 8 times in MTSBT for 15 min and then incubated for 3 h at 37°C in 2% BSA in MTSBT with secondary antibody Alexa Fluor 488 mouse anti-goat (1:1000, Abcam #ab150113). Samples were washed 5 times in MTSBT and 5 times in water for 15 min and transferred to a 0.02% sodium azide in 50% glycerol until observation under confocal microscope. All steps were performed at RT if not stated otherwise. Immunostaining was done in three biological replicates.

qRT-PCR

Total RNA was extracted from 5DAG seedlings using the NucleoSpin® RNA Plant Kit (#740949, MACHEREY-NAGEL GmbH & Co., KG, Düren, Germany). 1 µg of RNA was additionally treated with DNase I (#EN0525, Thermo Fisher Scientific). After this, cDNA was synthetized using RevertAid reverse transcriptase (#K1691, Thermo Fisher Scientific) and Oligo(dT) primers. Quantitative PCR was performed using the Light Cycler 480 instrument (Roche Applied Science, Mannheim, Germany). Reaction mixture contained 5 µl iQ™ SYBR Green Supermix (#1708882, BioRad, Irvine, CA, United States), 0.2 µl of 0.01 mM primers (**Table 2**) and 1 µl of 2.5X diluted cDNA in a final volume of 10 µl. Cycling conditions were as follows: initial denaturation for 3 min at 94°C was followed by 50 cycles of 15 s at 94°C, 10 s at 58°C, and 20 s at 72°C. Samples were measured in triplicates for three biological replicates and RNA samples as well as the premixes alone were used as negative control. Amplification efficiencies were estimated using LinRegPCR software (Ramakers et al., 2003). The relative expression of a target gene was calculated using **Equation 1**.

$$\frac{E_{ref}^{C_P^{ref}}}{E_{target}^{C_P^{target}}} \quad (1)$$

where E_{ref} and E_{target} correspond to the PCR efficiencies of the reference and target genes, respectively, and C_P^{ref} C_P^{target} correspond to the crossing points.

Pavement Cell Analysis

Cotyledons of seedlings grown for 5 days (treated and untreated) were incubated for 20-30 min in an aqueous solution of propidium iodide (PI) of a final concentration of 0.01 mg/ml. Pavement cell shape parameters were measured using Fiji platform (Schindelin et al., 2012). Pavement cell shape analysis was carried out as described in Sahi et al. (2018). The analysis was performed in three biological replicates.

DII-VENUS Quantification

Col-0/*DII-VENUS* and *arpc5*/*DII-VENUS* were measured at 1DAG. Seedlings were incubated in a 0.01 mg/ml PI solution for 10 min and taken for observation under confocal microscope. Images were processed using the Fiji platform (Schindelin et al., 2012). Nuclear DII-VENUS signal was quantified in the slice with higher fluorescence intensity in individual pavement cells, corrected for background signal and normalized to guard cell fluorescence intensity. Values are represented relative to the

TABLE 2 | List of primers used for qRT-PCR analysis of subunit expression.

Primer name	Sequence (5′ → 3′)
ARP2-F	ACCATGTACCCAGGATTACC
ARP2-R	CGATCCGCAATCTGAGTTTC
ARP3-F	AAATTACGTCTCAACCGGTGGA
ARP3-R	CAACTCGCGAAAAACTCAGGAG
ARPC1A-F	TCTCTGTCCTAACAACACTGA
ARPC1A-R	CGATTTTGTTGGACTTTGAGC
ARPC2A-F	TAGAGAAGTGGTGATGGGTG
ARPC2A-R	AGTGACTTTATCCGCCTGAG
ARPC3-F	CTCCTTCCTGATATCGCTTC
ARPC3-R	AAGGTGATTGCCTCGTCTAC
ARPC4-F	TAAGTCTGGTGCAAGTCTCG
ARPC4-R	TTCTGTAAGCACATGGCAGC
ARPC5-F	AATCGAGGAAGATTGAAAGCC
ARPC5-R	CGACATCAAGAGCATTGAGC
EF1α-F	TGAGCACGCTCTTCTTGCTTTCA
EF1α-R	GGTGGTGGCATCCATCTTGTTACA
UBC9-F	GCTCTCACAATTTCCAAGGTGCTGC
UBC9-R	AGGGTCCTTCCTTAAGGACAGTATTTGTG

wild-type control. Samples were measured in three independent biological replicates.

FRAP Analysis

For FRAP experiments, we employed the Zeiss LSM880 confocal microscope with C-Apochromat 40×/1.2 W Corr FCS M27 objective. The experiment was performed in two independent lines in three biological replicates. For bleaching, a region of interest was chosen at the transversal plasma membrane of pavement cells. Bleaching with 80% laser intensity was followed by tracking fluorescence recovery for approximately 159 s capturing an image every 1.1 s. To compensate for the fluorescence bleaching during recovery image acquisition, an additional non-bleached ROI was applied and values on the bleached ROI were corrected for this background. Data analysis, curve fitting and parameter estimation were done using the SigmaPlot software (Systat Software, San Jose, CA, United States). PIN3-YFP was assumed to freely diffuse in the plasma membrane, therefore a simple exponential equation (**Equation 2**) was used to fit the normalized FRAP curve.

$$I(t) = A\ 1 - e^{\tau t} \quad (2)$$

where A corresponds to the mobile fraction or end value of the recovered intensity, t is time and τ is the fitted parameter. The latter one was next used to determine the halftime of the recovery by the following equation (**Equation 3**).

$$T_{1/2} = \frac{\ln 0.5}{-\tau} \quad (3)$$

PIN3-YFP Localization and FM4-64 Co-localization

pPIN3::PIN3:YFP seedlings were used for measurement of PIN3-YFP intensity at the plasma membrane in 1-day-old seedlings. After stratification for 2 days at 4°C, plates were transferred to the cultivation room for 24–48 h. Only those seedlings that had emerged from the seed coat in the stage before cotyledon greening were used for observation and subsequent quantification. The intensity was measured as the mean gray value for the areas representing the plasma membrane and within the cotyledon pavement cells. For colocalization of FM4-64 and PIN3-YFP, Col-0/*pPIN3::PIN3:YFP* and *arpc5/pPIN3::PIN3:YFP* seedlings were grown in 0.5 ml of liquid half-strength Murashige and Skoog medium supplemented with 1% w/v sucrose on a horizontal shaker (slow agitation at 50 rpm) for 24 h. Subsequently, FM4-64 was added to a final concentration of 4 μM in a water solution and seedlings were cultivated overnight on a horizontal shaker (50 rpm). Cotyledons were observed using the Zeiss LSM880. Images were processed using the Fiji platform (Schindelin et al., 2012).

Vacuole Shape Analysis

Seedlings harboring the γ*TIP-mCherry* reporter were grown for 6 days and adaxial cotyledon pavement cells were observed immediately under the Leica TCS SP8 confocal microscope. Alternatively, seedlings grown for 5, 9, or 14 days were incubated overnight in 4 μM FM4-64 water solution and adaxial cotyledon surface was observed under the Leica TCS SP2 confocal microscope.

Image analysis was carried out using the Fiji platform (Schindelin et al., 2012). Mid-plane of pavement cell was used for measurements. A square region of approximately 600 μm^2 was placed framing three-way junctions of three cells. The selected areas were thresholded and binarized, delimiting the plasma membrane and tonoplast. The area occupied by the central vacuole was measured in relation of the total size of the selected region and represented as a percentage (vacuolar occupancy). Three biological replicates were performed.

Confocal Microscopy

Zeiss LSM880 with C-Apochromat 63×/1.2 W Corr FCS M27 objective was used for the observation of *pPIN3::PIN3:YFP* (ex: 488 nm, em: 499–552 nm), FM4-64 (ex: 488 nm, em: 579–686 nm), *DII-VENUS* (ex: 488 nm, em: 499–552 nm), and propidium iodide (488 nm; em: 593–668 nm). For pavement cell shape analysis and vacuole shape analysis, propidium iodide-stained (ex: 488 nm; em: 593–668 nm) and FM4-64 (ex: 514 nm; em: 617–802 nm) stained cotyledons were observed under the laser scanning microscope Leica TCS SP2 using HC PL APO 20.0x/0.70 IMM/CORR UV objective or HCX PL APO 63.0x/1.20 W CORR UV objective, respectively. For vacuole shape analysis in seedlings harboring the γ*TIP-mCherry* reporter, Leica TCS SP8 confocal microscope and HC PL APO CS2 63x/1.20 W objective, ex: 633 nm; em: 794–799 nm, was used.

RESULTS

Arp2/3 Complex Subunits Are Expressed in Developing Tissues, Epidermal Cells and Vascular Tissues

In order to pinpoint specific tissues where the Arp2/3 complex has a relevant role, we analyzed the activity of the promoter of several of its subunits fused to GUS at several developmental stages. GUS histochemical analysis of independent lines for each of the construct revealed comparable expression patterns. Generally, independent subunits showed strong expression around the vasculature tissues in both above ground tissues and roots (**Figure 1**). Although the signal strength was somewhat lower in pARP2::GUS line, the pattern was found to be similar for all tested lines.

Concerning the root, the reporter presence was always detected in root columella and lateral root cap, more prominently for the Arp2/3 complex subunits *ARPC3*, *ARPC4*, and *ARPC5*. Expression was also observed around the vascular tissues in the root elongation zone for all studied subunits (**Figure 1A**). Root cross-section of GUS-stained pARP2::GUS line allowed us to localize the GUS signal to phloem cells of the vascular bundle (**Supplementary Figure 1**). Further, the reporter was detected in root epidermal cells in a discontinuous pattern. The promoter activity in phloem in the vasculature was first detected

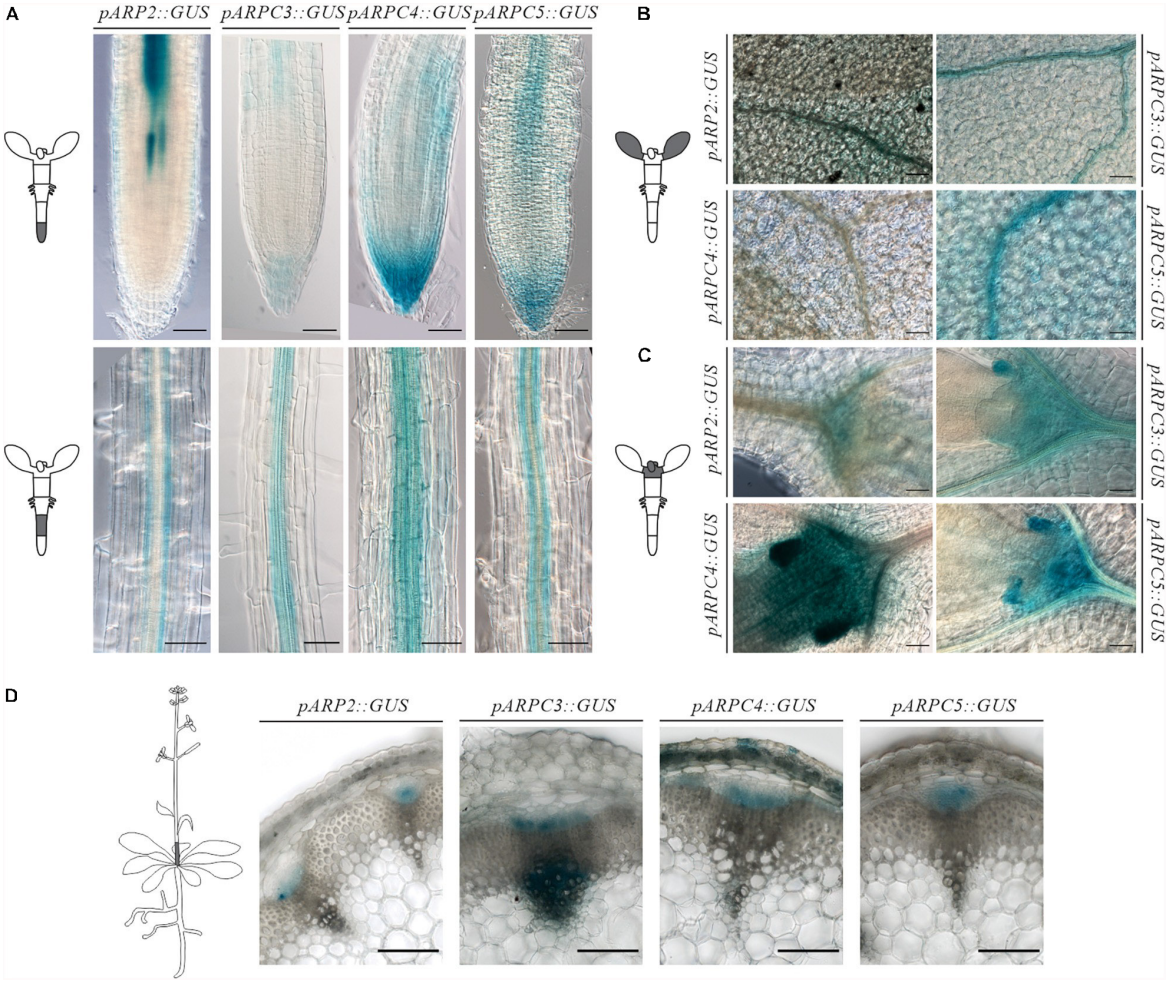

FIGURE 1 | Spatiotemporal expression pattern of individual ARP2/3 complex subunits genes (ARP2, ARPC3, ARPC4 and ARPC5) as revealed by promoter-GUS activity. Analysis of GUS histochemical staining was done in *Arabidopsis thaliana* 7-day-old seedlings roots (A), cotyledons (B), shoot apical meristem (C). Reporter signal was present at the provasculature, columella and quiescent center, pavement cells, mesophyll, stomata and shoot apical meristem (D) GUS production was tested in transverse sections at the base of six-week-old plants showing promoter activity in vascular bundles. Scale bar = 100 μm.

in the root elongation zone (**Figure 1A**) and was detectable in all other parts of seedlings including the hypocotyl and cotyledons (**Figures 1A,B**).

In young cotyledons, all analyzed Arp2/3 subunits were expressed on varying levels (**Figure 1B**). Also here, stronger signal was always observed around the vasculature. However, other cell types such as mesophyll, pavement cells and stomata showed promoter activity as well. This is consistent with previously described phenotypes of Arp2/3 mutants, which include changed morphology of pavement cells.

All studied subunits showed strong expression in the shoot apical meristem and developing leaves. Higher levels of expression were observed in stipules, which have been associated with leaf vascular development (Aloni et al., 2003; Cheng et al., 2007) (**Figure 1C**).

In 6-week-old inflorescences, β-glucoronidase activity was detected in procambium and protophloem tissues as well as in metaxylem for all studied subunits (**Figure 1D**). Interestingly, expression levels were not detected equally in all vascular bundles within the same plant. This may suggest the need of higher Arp2/3 complex activity in certain developmental situations, such as developing/differentiating vascular tissues, and its decline in already differentiated tissues.

These results indicate that Arp2/3 subunits are required especially in developing tissues (root and shoot apical meristem) and in epidermal cells. The GUS reporter further showed characteristic expression in vascular bundles.

Arp2/3 Subunits' Expression Is Stimulated by Auxin

Previously, the Arp2/3 complex has been shown to have a role in auxin distribution (Sahi et al., 2018). To investigate the importance of auxin in regulating individual subunit expression, we characterized their expression after the increase of auxin levels. For this, generated transgenic lines carrying promoter

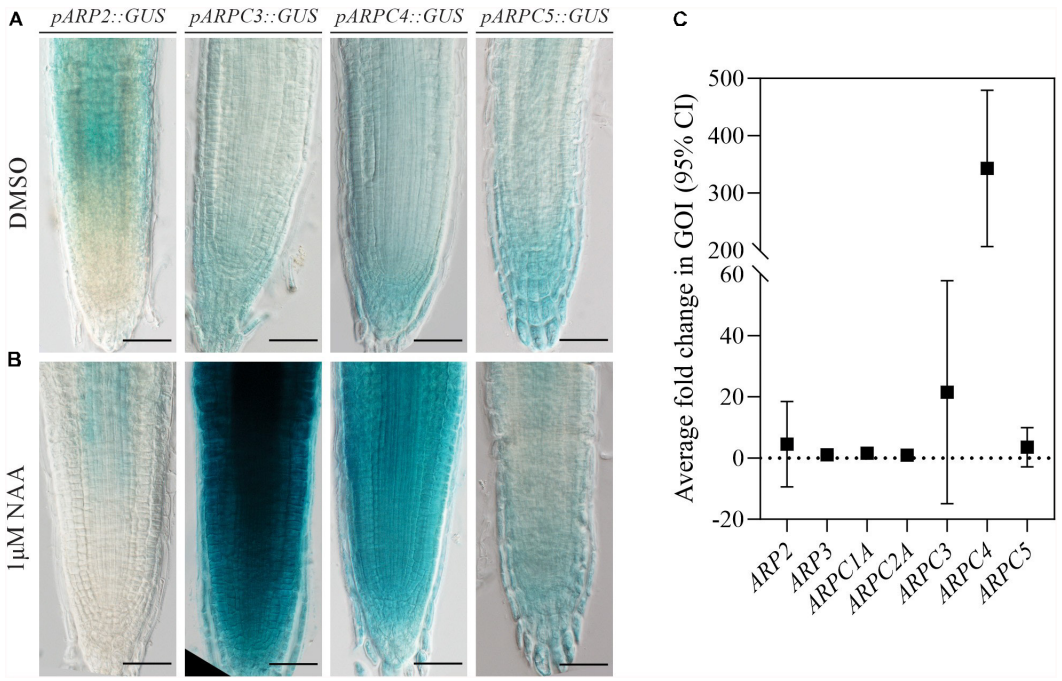

FIGURE 2 | ARP2/3 subunit expression is stimulated by increased auxin levels. Plants expressing the GUS reporter gene under the control of individual ARP2/3 complex subunits' promoters (pARP2, pARPC3, pARPC4 and pARPC5) were stained for GUS activity after 24-h treatment with 0.1 % DMSO (A) or 1 μM NAA (B). (C) Relative transcription levels of individual complex subunits were quantified in five-fay-old *YUC1D* seedlings by qRT-PCR in three biological replicates. Scale bar = 100 μm).

fusions were subjected to NAA treatment. Strikingly, just two of the subunits analyzed (*AtARPC3* and *AtARPC4*) showed increased promoter activity when compared to the control treatment (**Figures 2A,B**).

To test the susceptibility of expression of Arp2/3 subunits to auxin under conditions more physiological than external auxin application, we used the previously described dominant gain-of-function auxin over-production mutant *YUC1D* (Zhao et al., 2001), which shows increased free IAA endogenous level when compared to wild-type plants, to analyze the expression of Arp2/3 subunits. qRT-PCR analysis confirmed the previous result, because only *AtARPC3* and *AtARPC4* exhibited higher RNA levels in *YUC1D* line when compared to wild type (Col-0) (**Figure 2C**).

Taken together, two different methods demonstrated that the transcription of *ARPC3* and *ARPC4* genes coding Arp2/3 complex subunits was enhanced in the presence of higher auxin levels, while other subunits showed no significant change.

Auxin Aggravates Pavement Cell Morphology Defects in Plants Lacking Functional Arp2/3 Complex

Along with distorted shape of leaf trichomes, pavement cell shape change is one of the first described phenotypes of plants with dysfunctional Arp2/3 complex (Deeks and Hussey, 2003). Since all mutant lines lacking either one of the Arp2/3 subunit or Arp2/3-activation complex subunits show this characteristic phenotype, it is considered as a typical phenotype of Arp2/3 mutants (Li et al., 2003; Mathur et al., 2003a,b; Djakovic et al., 2006). Auxin has also been long discussed to play a role in pavement cell interdigitation (Li et al., 2011; Xu et al., 2014; Gao et al., 2015; Belteton et al., 2018). We therefore decided to use pavement cell shape as a morphogenesis model to answer the question of whether auxin and Arp2/3 were connected in the cell shape control.

We crossed the *arpc5* knockout plants with the previously mentioned auxin over-producing line *YUC1D*. Double homozygous lines were selected, and pavement cell size and shape parameters were determined. Both single and double mutant visibly showed larger cells and reduced cell complexity (**Figure 3A**), represented by increased area (**Figure 3B**) and higher circularity values (**Figure 3C**), which is consistent with known phenotypes of Arp2/3 mutant plants and plants with increased auxin level. However, *YUC1D/arpc5* exhibited a more dramatic defect in lobe formation than single mutants, suggesting an interaction between the two pathways (**Figures 3B,C**). This observation was further confirmed in our experiments, where auxin was applied externally to pavement cells. The application of 5 μM IAA or NAA to *arpc5* mutant for 48 h mimicked the phenotype of *YUC1D/arpc5* plants, because the formation of lobes was reduced after treatment with auxins (**Figure 3D**). No effect of auxin treatment was observed in wild-type or *arpc5* plants. Changes in cell area were only due to the lack of functional Arp2/3 complex (**Figures 3E,F**).

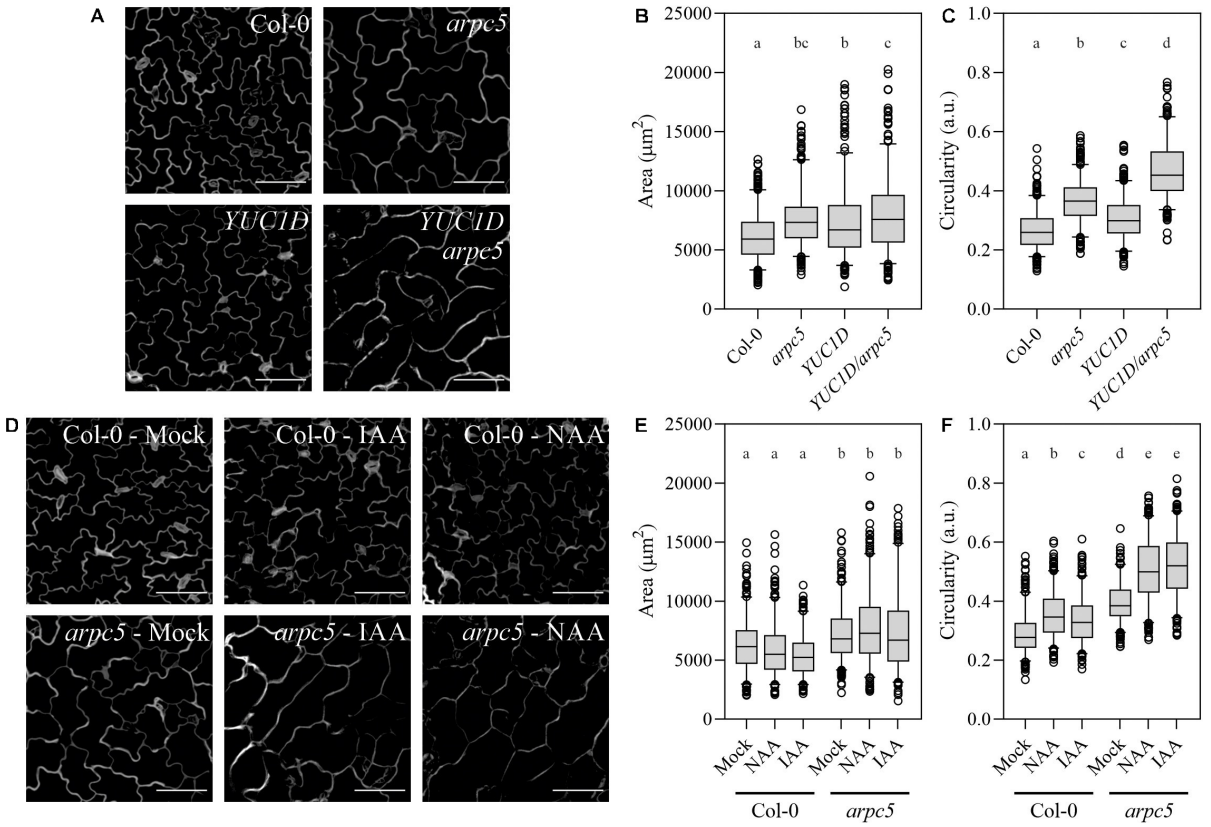

FIGURE 3 | Pavement cells morphology upon increased auxin levels. (A–C) The effect of increased endogenous auxin level in *YUC1D* plants crossed with *arpc5*. Representative pictures (A) and quantitative cell shape analysis (B,C) of five-day-old Col-0, *arpc5*, and *YUC1D*, *YUC1D/arpc5* epidermal lobed cells is shown. (D–F) The shape phenotype observed in *YUC1D* and *YUC1D/arpc5* could be mimicked by 48 h treatment with 5 μM auxin (IAA and NAA) of three-day-old Col-0 and *arpc5* seedlings. Illustrative pictures are shown in (D), quantitative cell shape analysis is depicted in (E) and (F). Scale bar = 100 μm. n = 250–350 cells, three biological replicates (Tukey HSD, $p < 0.001$; $p < 0.05$ for the area comparison between *YUC1D* and *YUC1D/arpc5*).

Our results confirmed cell expansion defect in plants lacking Arp2/3 complex, and an additive effect on cell shape in Arp2/3 mutant with increased auxin level.

Elevated Levels of oxIAA and IAA Marker in Cotyledon Pavement Cells Suggest Altered Auxin Balance in Cells of Arp2/3 Mutants

Since auxin has an effect in pavement cell morphogenesis and Arp2/3 mutants seem to show an enhanced response to increased levels of this hormone, we sought to determine whether auxin levels were affected in Arp2/3 complex mutants. We analyzed endogenous auxin levels in seedlings of wild-type and *arpc5*, *arpc4* and *arp2* mutants. The biochemical analysis of active IAA suggests that mutant plantlets contain IAA levels comparable to those found in wild type. However, a clear increase of oxIAA-GE levels in mutants (considered to be an inactive form of auxin, Pěnčík et al., 2013) was repeatedly and consistently detected in all tested Arp2/3 mutant lines (**Table 3**).

This prompted us to analyze auxin-driven proteasomal degradation of DII-VENUS marker in individual cells of cotyledon epidermal lobed cells. We generated *arpc5* crosses with DII-VENUS and analyzed nuclei fluorescence using confocal microscopy (**Figure 4A**). Interestingly, *arpc5* was the only Arp2/3 mutant line successfully crossed with this marker. When compared to Col-0 carrying DII-VENUS, *arpc5* plants displayed a significant decrease of DII-VENUS signal (**Figure 4B**). This result indirectly suggests that there is either a mild increase in auxin levels or increased auxin response in *arpc5*.

Altogether, the present data show that Arp2/3 mutants could have mildly increased concentration of intracellular auxin in pavement cells, and that general balancing of auxin concentration in tissues results in higher levels of inactivated auxin, suggesting that the Arp2/3 complex is important to maintain the correct auxin balance at the cellular and tissue level.

PIN3 Does Not Show Mobility Defects in the Plasma Membrane

PIN protein dynamics in the plasma membrane has been shown to be important for the proper regulation of auxin homeostasis (Geldner et al., 2001; Abas et al., 2006; Kleine-Vehn et al., 2011), and the cytoskeleton has been shown to be involved in these processes (Geldner et al., 2001; Friml et al., 2002; Rahman et al.,

TABLE 3 | Quantification of endogenous auxin levels in Arabidopsis thaliana seedlings.

	IAA		oxIAA-GE	
	Above ground tissues	Roots	Above ground tissues	Roots
Col-0	68.35 ± 3.79	122.12 ± 23.07	886.02 ± 298.11	1102.03 ± 552.34
arp2	60.48 ± 3.58	162.27 ± 31.57	1517 ± 266.58	3739.72 ± 1747.12
arpc4	50.22 ± 7.57	143.64 ± 18.20	1307.14 ± 133.04	3953.52 ± 2239.16
arpc5	84.69 ± 19.13	130.55 ± 35.01	1892.99 ± 576.35	3450.99 ± 2269.34

Values in pmol/gFW; average of three biological replicates +/– SD.

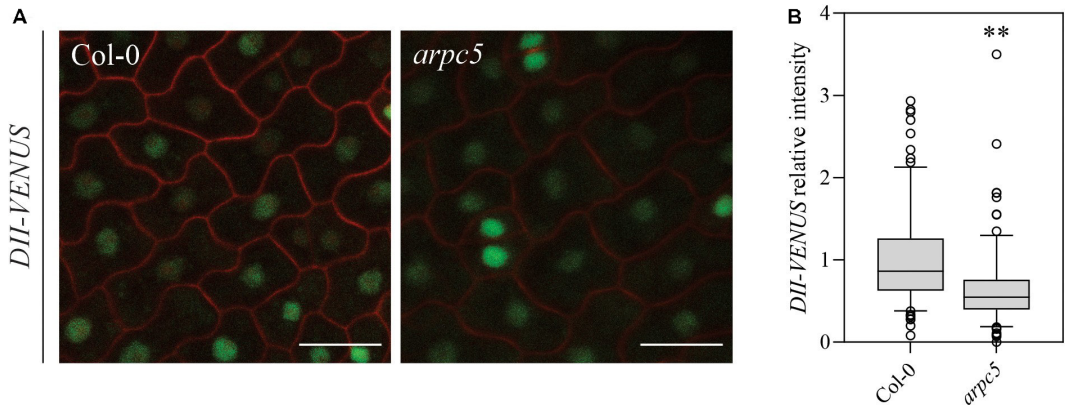

FIGURE 4 | Plants lacking functional ARP2/3 complex show increased active auxin-driven proteasomal degradation of the auxin input sensor DII-VENUS. (A) *In vivo* observation of *DII-VENUS* (green) in one-day-old wild-type and *arpc5* seedlings (scale bar = 20 µm) co-stained with PI (red). (B) Normalized DII-VENUS relative intensity (n = 167 cells; three biological replicates; Student's t-test, $p < 0.0001$).

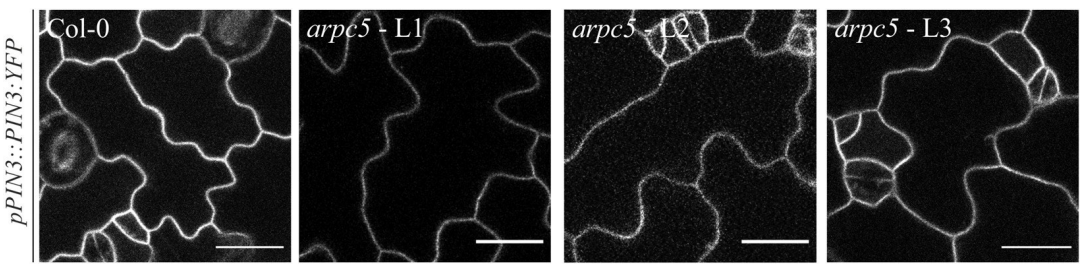

FIGURE 5 | *In vivo* observation of *pPIN3::PIN3:YFP* in three-day-old *arpc5* plants. L1, L2 and L3 correspond to three independent crosses between *pPIN3::PIN3:YFP* and *arpc5* lines used in this study (scale bar = 20 µm).

2007; Kleine-Vehn et al., 2008b; Lanza et al., 2012). PIN3 is one of the predominant PINs expressed in pavement cells (Le et al., 2014). We therefore analyzed PIN3-YFP localization in pavement cells and tested the mobility of PIN3 in the plasma membrane of pavement cells in three-day-old seedlings by FRAP (Fluorescence Recovery After Photobleaching, **Figures 5**, **6**). Our results show that the localization of PIN3-YFP was not changed in *arpc5* mutants (**Figure 5**). Likewise, the mobile fraction and halftime recovery time values (**Figures 6D,E**) in *arpc5* plants were comparable to those observed in wild-type (**Figure 6C**). Although it has been reported to be Brefeldin A (BFA) sensitive (Friml et al., 2002), the analysis of PIN3 cycling between endosomes and plasma membrane in cotyledon pavement cells using this inhibitor treatment was not possible, because PIN3 localization in pavement cells was not sensitive to BFA and no BFA-compartment was observed (data not shown). This indicates that PIN3 localization and lateral membrane dynamics are not changed in 3-d-old cotyledons of plants lacking functional Arp2/3 complex.

Precise Localization of PIN3 and PIN1 Is Inefficient in Mutants Lacking Functional Arp2/3 Complex

It has been previously reported that pavement cell shape determination occurs predominantly within the first two days after germination (Zhang et al., 2011; Armour et al., 2015; Wu et al., 2016). We investigated whether Arp2/3 takes part in PIN3

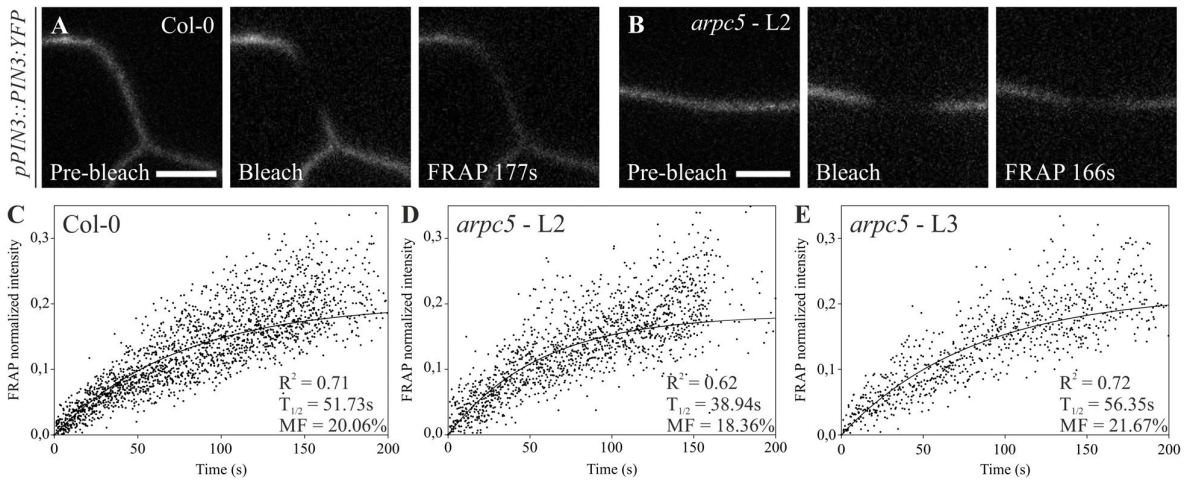

FIGURE 6 | Fluorescence recovery after photobleaching (FRAP) of *pPIN3::PIN3:YFP* auxin carrier in Col-0 (A,C) and *arpc5* lines L2 (B,D) and L3 (E). Photobleaching followed by its recovery was analyzed in transversal PM (plasma membrane) of three-day-old cotyledons expressing PIN3-YFP. Simple exponential fit was applied to normalized FRAP data; individual fluorescence intensities for multiple plants (n = 6–14) are shown (scale bar = 5 μm). The analysis was performed in three biological replicates.

localization at these initial steps of epidermal cell morphogenesis. Indeed, when observing one-day-old plants, a decrease in the *pPIN3::PIN3:YFP* intensity ratio between the plasma membrane and the cell interior was detected (**Figures 7A,B**). Absolute intensity values indicate that the reason for this decrease in the ratio is a result of reduced amounts of PIN3 at the plasma membrane and increased intracellular signal (**Figures 7C,D**).

In our previous work we demonstrated that auxin transport in stems is very limited in plants lacking functional Arp2/3 complex (Sahi et al., 2018). As PIN1 is the main auxin transporter mediating basipetal polar auxin transport through plant tissues (Gälweiler et al., 1998), we assayed if also PIN1 localization is affected in mutants plants' stems. Consistent with our previous observations, analysis of longitudinal stem sections with immunolocalized PIN1 showed localization to basal membranes of elongated parenchyma cells in wild-type plants. Basal localization of PIN1 was disturbed in Arp2/3 mutant lines, where signal was found also on adjacent lateral membranes, demonstrating inefficient polar localization of PIN1 here (**Supplementary Figure 2**).

Taken together, our results demonstrate the contribution of Arp2/3 complex in PIN3 localization to the plasma membrane in very early stages of pavement cells development. Our finding of PIN1 inefficient polar localization also point on a broader need of the Arp2/3 complex in maintaining efficient PIN localization throughout plant growth.

Plants Lacking a Functional Arp2/3 Complex Show Altered Vacuolar System

The staining with FM4-64 confirmed that the compartments with accumulated PIN3-YFP are vacuoles (**Figure 8**). FM4-64 limited staining of plasma membrane of *arpc5* pavement cells, observed in our experiments (**Figure 8B**), may indicate changed plasma membrane properties in *arpc5* line, which became visible under conditions of overnight exposure to water solution with the dye. PIN transporters are known to cycle between the plasma membrane and endosome, and they are eventually degraded in vacuoles (Kleine-Vehn et al., 2008a). Since PIN3 accumulated in vacuolar compartments, we hypothesized that general intracellular trafficking of proteins such as vacuolar targeting may be changed in *arpc5* mutant. We therefore decided to analyze vacuolar compartment in pavement cells of plants lacking functional Arp2/3 complex. A thorough analysis of vacuole occupancy revealed that vacuolar structure is affected in Arp2/3 complex mutants (**Figure 9**), suggesting a more fragmented architecture. Interestingly, the defect in the fusion of vacuolar membrane, manifested as fragmented vacuoles, was detectable also in later stages of cotyledon development (**Supplementary Figure 3**). The phenotype was hardly distinguishable in 1-day-old seedlings, where vacuoles have very complex shape in both WT and mutants due to early steps of central lytic vacuole formation (**Supplementary Figure 4**). The defect in central vacuole formation in pavement cells of mutants may affect the cycling and vacuolar targeting of proteins such as early development-associated PIN3 targeting to the vacuole and plasma membrane.

DISCUSSION

Arp2/3 complex has been shown to be involved in numerous stages of plant development such as pavement cells, stomata and trichomes morphology, or stem thickness and cell wall quality (Le et al., 2003; Li et al., 2003; Mathur et al., 2003a,b; Brembu et al., 2004; Deeks et al., 2004; El-Assal et al., 2004; Djakovic et al., 2006; Dyachok et al., 2008, 2011; Jiang et al., 2012; Sahi et al., 2018). Promoter fusion studies have proven to be useful in hinting the importance of a protein's function in a determined tissue or developmental stage. In our study, we aimed to determine

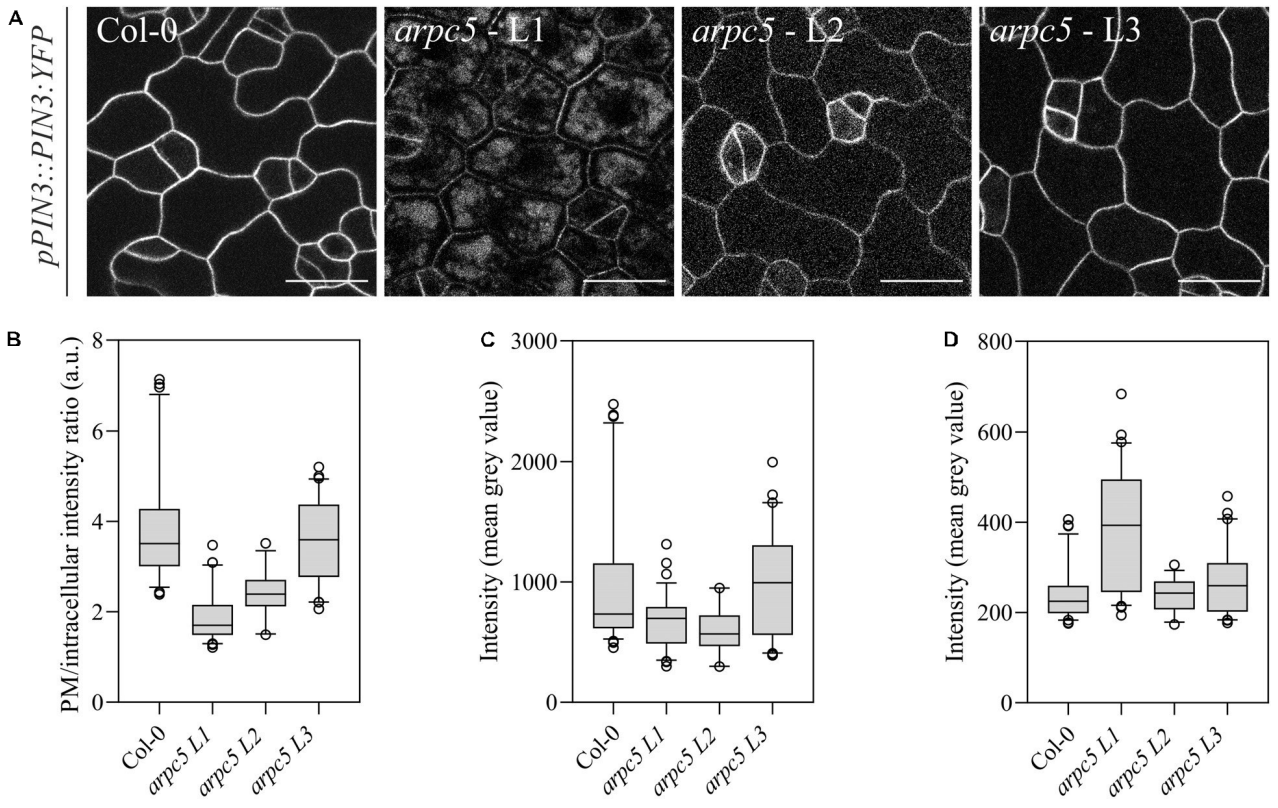

FIGURE 7 | Plants lacking functional ARP2/3 complex show altered PIN3 localization. (A) *In vivo* observation of *pPIN3::PIN3:YFP* in one-day-old plants was altered in three independent crosses between *pPIN3::PIN3:YFP* and *arpc5* lines (L1-3); scale bar = 20 µm. (B) The ratio between PM and intracellular PIN3-YFP intensity is reduced *arpc5* mutants. (C,D) PIN3-YFP intensity was measured as the mean gray value for the areas representing the plasma membrane (C) and within the cell (D). Results show that the differences in ratio are due to increased intracellular signal. $n = 45–70$ cells, three biological replicates (Tukey, HSD $p < 0.001$).

the patterns of expression of Arp2/3 complex subunits in order to reveal the sites where their promoters are most active. Since Arp2/3 functions as a complex, we expected similar expression patterns for all tested subunits. Indeed, we can conclude that the subunits studied are expressed roughly in the same tissues during the growth of *A. thaliana*, although some minor differences can be seen in the root tip. The expression of Arp2/3 subunits was detected in most tissues reported previously to be affected in mutants lacking the active complex, including pavement cells. All subunits are shown to have prominent promoter activity in the provascular region, as it was previously described by Klahre and Chua (Klahre and Chua, 1999). Interestingly, the root cross section allowed us to localize the expression to phloem cells, while xylem precursor cell files were stained in the work of Klahre and Chua (1999). Although no severe phenotypes have been reported in vasculature in young seedlings of Arp2/3 complex mutant lines, we have previously showed that AUX1 expression in procambial and protoxylem cells in stem vascular bundles is reduced in *arpc5* line (Sahi et al., 2018). This suggests that Arp2/3 complex may be needed for vasculature development. Indeed, the cytoskeleton plays a role in its formation, as many of its mutants show vasculature formation defects (Hepler and Fosket, 1971; Falconer and Seagull, 1985; Gardiner et al., 2003; Mao et al., 2006; Oda et al., 2010; Pesquet et al., 2010; Bao et al., 2012; Oda and Fukuda, 2012, 2013; Sasaki et al., 2017; Vukašinovic´ et al., 2017; Sugiyama et al., 2019). As the Arp2/3 complex has been reported to have a role in plant cell wall deposition (Sahi et al., 2018) and autophagy (Wang et al., 2016), we could speculate that the complex participates in the building of specialized cell walls and autophagy needed for differentiation of vascular tissue. More detailed study is needed to confirm or disprove this hypothesis.

Our previous work has shown a series of auxin-related phenotypes which include reduced auxin transporter abundance and auxin transport in mature tissues as well as reduced auxin maxima in early stage cotyledons (Sahi et al., 2018). Also, and in agreement with the expression observed through the analysis of promoter fusions, *DR5:GUS* maxima were observed to be reduced around the vascular tissue (Sahi et al., 2018). Therefore, we aimed to explore closer the role of Arp2/3 complex in auxin signaling. The presented data demonstrate that the expression of Arp2/3 complex subunits can be induced by auxin. We do not know the rationale of the selective increased transcription of only two of the subunits (*ARPC3* and *ARPC4*). Although high concentration of externally applied auxin was used in this study (1 µM), the same pattern of expression (*ARPC3* and *ARPC4*) was detected in *YUC1D* line, which contains increased endogenous level of auxin (Zhao et al., 2001). This suggests that increased expression of these two subunits reflected the response

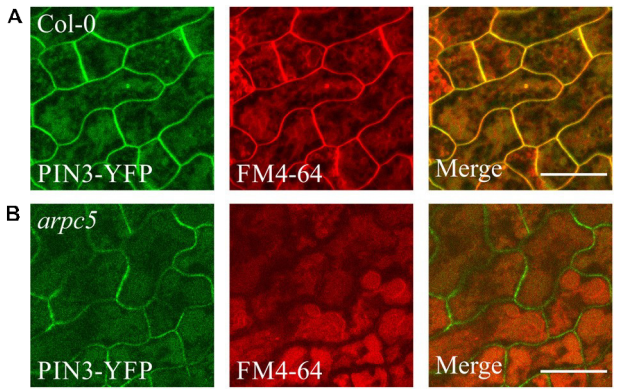

FIGURE 8 | PIN3-YFP localization to the vacuole in 3DAG wild type (A) and *arpc5* (B) seedlings. 2DAG plants expressing *pPIN3::PIN3:YFP* were incubated in darkness overnight in a solution of 4 μM FM4-64 to allow for vacuolar staining (scale bar = 20 μm).

to auxin, not the stress response to externally applied high auxin concentration. The regulation of the Arp2/3 complex may involve also post-transcriptional and post-translational control mechanisms, such as mRNA or protein stability, which were not assayed here. We could hypothesize these two subunits could be important for the regulation (or trigger) of the complex assembly. Plant Arp2/3 complex has been reported to play a role in cell expansion, possibly contributing to cell wall properties and polar growth. Especially pavement cell shape morphogenesis is studied in the context of Arp2/3 complex role, although its function is yet not well understood (Mathur et al., 1999, 2003a,b; Le et al., 2003; Li et al., 2003; Schwab et al., 2003; Deeks et al., 2004; El-Assal et al., 2004; Djakovic et al., 2006; Dyachok et al., 2008; Zhang et al., 2013; Yanagisawa et al., 2015; Sahi et al., 2018). Auxin has long been discussed to play a role in epidermal cell morphogenesis too, and has been proposed to play a role in cell wall permissivity (Xu et al., 2010, 2014; Nagawa et al., 2012; Gao et al., 2015; Belteton et al., 2018). We aimed to test the interplay between Arp2/3 and auxin in pavement cell growth. We distinguish between two processes controlling pavement cell morphogenesis: cell shape formation (cell circularity) and cell expansion (cell size). Our results revealed that an increase in auxin concentration, both constitutive (*YUC1D* line) or temporal (auxin treatment), leads to a decrease in cell shape complexity, which is more severe in the case of plants lacking a functional Arp2/3 complex. The additive effect of auxin in Arp2/3 mutant lines, as well as the fact that plants lacking Arp2/3 are still responsive to auxin, suggests partly independent functions of auxin and Arp2/3 in cell lobes formation. Cell expansion, on the other hand, is the main function of Arp2/3 complex. While *YUC1D/arpc5* line shows mildly deepened phenotype, the cell expansion of mutant line is not altered by externally applied auxin. It is important to note here that the treatment with 5 μM auxin may induce also secondary effects, which could explain the slight difference in cell expansion between *YUC1D/arpc5* and *arpc5* treated with auxin. Nevertheless, this concentration of auxin was needed to mimic *YUC1D* phenotype concerning cell shape. We can conclude that these results pinpoint the involvement of the complex in mediating the cell expansion in response to auxin.

However, our results suggest also a direct functional link between auxin and Arp2/3. The expression of Arp2/3 subunits is positively regulated by auxin, and mutants lacking Arp2/3 complex have reduced basipetal transport of auxin (Sahi et al., 2018). We also show here that Arp2/3 mutants have changed auxin metabolism in respect to increased pool of inactivated auxin, as well as increased auxin concentration in pavement cells. One of the most important factors that regulate auxin levels within and outside the cell is polar auxin transport (Lacek et al., 2017). We tested whether transporter localization was also an issue in pavement cell formation. Our previous findings on cell wall composition prompted us to first analyze whether PIN transporter dynamics were affected at the plasma membrane level, as this factor has been shown to affect plasma membrane motility of integral proteins (Feraru et al., 2011; Nakayama et al., 2012; Braybrook and Peaucelle, 2013; Ganguly et al., 2014).

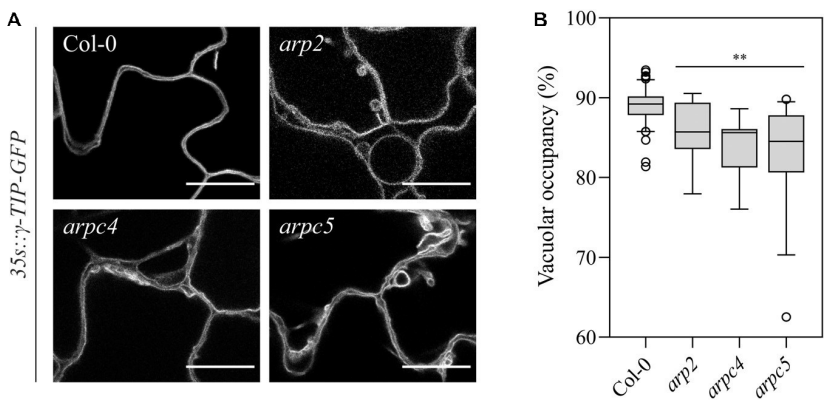

FIGURE 9 | (A) Observation of vacuolar organization in wild-type and *arp2*, *arpc4* and *arpc5* in 6DAG cotyledon expressing the γ*TIP-mCherry* marker (scale bar = 20 μm). (B) Vacuolar occupancy quantifications at three-way cellular junctions. (Analysis performed in three biological replicates; Student's *t*-test; $^{**}p < 0.01$; $^{*}p < 0.05$).

We show that PIN3 lateral mobility in the plasma membrane is not altered in *arpc5* mutants. However, we show that PIN3 localization is affected in *arpc5* plants at a very young stage of development, showing increased amounts in the vacuole and reduced signal at the plasma membrane. The reduction of PIN3 at the plasma membrane could result in changes in auxin homeostasis in mutant plants, which was indirectly suggested by DII-VENUS marker that showed increased auxin-driven proteasomal degradation in *arpc5* pavement cells. Of course, since we failed to generate mDII-VENUS cross with *arpc5* line, we cannot fully exclude the possibility that transcriptional activity in general or the activity of 35S promotor in *arpc5* epidermal cells is lower than in WT. It is also important to stress out that although *arpc5* line shows slightly increased auxin levels or response in pavement cells, it is still responsive to high auxin levels. Rather moderate and perhaps local or temporal increase in endogenous auxin in pavement cells of Arp2/3 mutants was further confirmed by the analysis of general auxin content in *arpc5* seedlings, because no significant increase was detected. Nevertheless, as a signaling molecule, even a small shift in endogenous auxin concentration in *arpc5* line may be physiologically relevant. In this respect, the observation that oxIAA-GE, inactivated form of auxin, is increased in three independent Arp2/3 mutant lines indeed suggests shifted auxin homeostasis. Interestingly, vacuolar localization of PIN3 is only observed at very early stages of pavement cell development. This phenomenon could be explained by several possible scenarios. The first possibility is that Arp2/3 activity is mainly required at early stages of epidermal cell morphogenesis and not later on. This would be consistent with the fact that pavement cell shape determination occurs predominantly within the first two days after germination (Zhang et al., 2011; Armour et al., 2015; Wu et al., 2016). The second hypothesis would be that at later stages, PIN3 is still localized in the vacuole, but remains unobservable due to YFP susceptibility to vacuolar pH (Kremers et al., 2016; Shinoda et al., 2018) and less concentrated amounts of PIN3 within the organelle as a result of its larger size. We could not assay PIN3 cycling between endosomal compartment and the plasma membrane, because PIN3 in pavement cells is not sensitive to BFA, a drug commonly used for this assay. Therefore, the hypothesis that PIN3 cycling between the plasma membrane and cell interior is controlled by Arp2/3 remains to be tested. However, the effect of Arp2/3 complex loss on the localization of PIN transporters may be rather general, as suggested by immunolocalization of PIN1 in stems and inefficient basal localization in parenchyma cells.

Vacuolar homeostasis is relevant in a variety of processes during plant development, ranging from turgor preservation during cell morphogenesis to protein trafficking (Krüger and Schumacher, 2018; Shimada et al., 2018). Our observation that PIN3 protein is inefficiently transported to the plasma membrane and that PIN3-YFP vacuolar concentration is increased in *arpc5* line in early stages of development pointed to the vacuolar function. In fact, vacuolar targeting depending on retromer complex function is a commonly known degradation pathway for PIN proteins (Koltzscher et al., 2003; Abas et al., 2006; Laxmi et al., 2008; Shirakawa et al., 2009; Bachmair et al., 2012; Baster et al., 2013; Belteton et al., 2018; Salanenka et al., 2018). Vacuolar shape is also modulated by auxin (Löfke et al., 2015) and in turn, vacuoles may play an important role in auxin homeostasis (Kramer and Ackelsberg, 2016). Actin cytoskeleton controls remodeling of vacuolar membranes (Zhang et al., 2014) and Arp2/3 complex has been shown to participate in vacuolar morphology control in stomata and trichomes (Mathur et al., 2003a; Saedler et al., 2004; Li et al., 2013).

Vacuolar fusion is a critical process during cell maturation and function (Viotti et al., 2013; Krüger and Schumacher, 2018). Our results point out the involvement of Arp2/3 complex in vacuolar fusion during pavement cell development as well, because two independent mutant lines (*arpc5* and *arpc4*) had fragmented vacuoles in pavement cells. The incorrect function of vacuolar compartment could be responsible for its reduced efficiency in protein recycling, being PIN3 and PIN1 an example of its consequences. Also, the lack of a larger vacuole could lead to reduced cell turgor which, in its turn, can be detrimental for cell adhesion and cell expansion itself. Interestingly, the vacuolar fusion deficiency is detectable throughout the cotyledon development.

In summary, we have shown here that Arp2/3 subunits are expressed throughout the plant tissue including pavement cells, trichomes, hypocotyls and root tips. The transcription of ARPC3 and ARPC4 subunits is positively regulated by auxin, and plants lacking functional Arp2/3 complex have increased auxin concentration in pavement cells. Investigating the relationship between auxin and Arp2/3 in pavement cell shape formation we found out that Arp2/3 complex has a restrictive role in cell expansion, which is partially independent of auxin-induced cell expansion. On the other hand, the additive effect of auxin in mutants in the formation of cell lobes suggests cooperation of Arp2/3 and auxin in the control of pavement cell shape formation. The direct interaction between auxin and Arp2/3 complex in this context may lay in the function of the complex regarding auxin transporters trafficking. Our results imply general intracellular trafficking defects in plants lacking Arp2/3 complex. This is supported by observed inefficient PIN1 polar localization in stems, inefficient PIN3 targeting to the plasma membrane, and vacuolar biogenesis defects. Altered performance of intracellular trafficking may lead to deficient auxin transport and therefore altered hormone homeostasis within single cells, contributing to the impaired cell wall remodeling that we observe in Arp2/3 complex mutants.

DATA AVAILABILITY STATEMENT

All datasets generated for this study are included in the article/**Supplementary Material**.

AUTHOR CONTRIBUTIONS

JG-G, KS, and JP conceived and designed the experiments. JG-G, KS, and IK generated the lines used in this study. JG-G, KS,

ŠK, MS, and JL performed the experiments and analyzed the data obtained. JG-G and KS wrote the manuscript.

FUNDING

This project was supported by Charles University Grant Agency, project no. 962316. Microscopy was performed in the Laboratory of Confocal and Fluorescence Microscopy co-funded by the European Regional Development Fund and the state budget of the Czechia, project nos. CZ.1.05/4.1.00/16.0347 and CZ.2.16/3.1.00/21515, and supported by the Czech-BioImaging large RI project LM2015062.

SUPPLEMENTARY MATERIAL

The Supplementary Material for this article can be found online at: https://www.frontiersin.org/articles/10.3389/fpls.2020.00486/full#supplementary-material

FIGURE 1 | Cross section of a root of pARP2::GUS line. GUS reporter was visualized in 7 DAG plants as described in Materials and methods. Roots were then embedded into 2.5 % agarose. Agarose block was fixed to a holder of vibratome and sectioned to obtain root cross sections of a thickness of 50 µm. Sections were observed using Olympus Provis AX 70 microscope. GUS reporter expressed within the vascular bundle is focused in regions corresponding to phloem cells (Dinneny and Yanofsky 2004). P, phloem; X, xylem. Scale bar = 20 µm.

FIGURE 2 | (A) Immunostaining of PIN1 in longitudinal stem sections five-week-old wild-type plants and plants lacking functional ARP2/3 complex (*arp2*, *arpc4* and *arpc5*) showing disturbed localization of PIN1 at the basal end xylem parenchyma cells. Scale bar = 20 µm. (B) Detail of the squared area in (A) (scale bar = 5 µm, three biological replicates).

FIGURE 3 | (A) Vacuolar organization in wild-type and *arpc5* plants at 5DAG, 9DAG and 14DAG. (B) Vacuolar occupancy quantifications at three-way cellular junctions of cotyledons stained overnight with 4 µM FM4-64 at multiple growth timepoints (5DAG, 9DAG and 14DAG) for Col-0 and *arpc5*. S (Pairwise comparisons with Student's *t*-test; $^{**}p<0.01$; three biological replicates). Scale bar = 50 µm.

FIGURE 4 | Vacuolar organization in wild-type and *arp2*, *arpc4* and *arpc5* in 1DAG cotyledon expressing the lytic vacuole γ*TIP-mCherry* marker. Scale bar = 10 µm.

REFERENCES

Abas, L., Benjamins, R., Malenica, N., Paciorek, T., Wi´sniewska, J., Wirniewska, J., et al. (2006). Intracellular trafficking and proteolysis of the Arabidopsis auxin-efflux facilitator PIN2 are involved in root gravitropism. *Nat. Cell Biol.* 8, 249–256. doi: 10.1038/ncb1369

Aloni, R., Schwalm, K., Langhans, M., and Ullrich, C. I. (2003). Gradual shifts in sites of free-auxin production during leaf-primordium development and their role in vascular differentiation and leaf morphogenesis in *Arabidopsis*. *Planta* 216, 841–853. doi: 10.1007/s00425-002-0937-8

Armour, W. J., Barton, D. A., Law, A. M. K., and Overall, R. L. (2015). Differential growth in periclinal and anticlinal walls during lobe formation in Arabidopsis cotyledon pavement cells. *Plant Cell* 27, 2484–2500. doi: 10.1105/tpc.114.126664

Bachmair, A., Zazimalova, E., Petrasek, J., Luschnig, C., Korbei, B., Leitner, J., et al. (2012). Lysine^{63} -linked ubiquitylation of PIN2 auxin carrier protein governs hormonally controlled adaptation of *Arabidopsis* root growth. *Proc. Natl. Acad. Sci. U.S.A.* 109, 8322–8327. doi: 10.1073/pnas.1200824109

Bao, C., Wang, J., Zhang, R., Zhang, B., Zhang, H., Zhou, Y., et al. (2012). Arabidopsis VILLIN2 and VILLIN3 act redundantly in sclerenchyma development via bundling of actin filaments. *Plant J.* 71, 962–975. doi: 10.1111/j.1365-313X.2012.05044.x

Baster, P., Robert, S., Kleine-Vehn, J., Vanneste, S., Kania, U., Grunewald, W., et al. (2013). SCFTIR1/AFB-auxin signalling regulates PIN vacuolar trafficking and auxin fluxes during root gravitropism. *EMBO J.* 32, 260–274. doi: 10.1038/emboj.2012.310

Belteton, S. A., Sawchuk, M. G., Donohoe, B. S., Scarpella, E., and Szymanski, D. B. (2018). Reassessing the roles of PIN proteins and anticlinal microtubules during pavement cell morphogenesis. *Plant Physiol.* 176, 432–449. doi: 10.1104/pp.17.01554

Braybrook, S. A., and Peaucelle, A. (2013). Mechano-chemical aspects of organ formation in *Arabidopsis thaliana*: the relationship between Auxin and pectin. *PLoS One* 8:e0057813. doi: 10.1371/journal.pone.0057813

Brembu, T., Winge, P., Seem, M., and Bones, A. M. (2004). NAPP and PIRP encode subunits of a putative wave regulatory protein complex involved in plant cell morphogenesis. *Plant Cell* 16, 2335–2349. doi: 10.1105/tpc.104.023739

Brunoud, G., Wells, D. M., Oliva, M., Larrieu, A., Mirabet, V., Burrow, A. H., et al. (2012). A novel sensor to map auxin response and distribution at high spatio-temporal resolution. *Nature* 482, 103–106. doi: 10.1038/nature10791

Cheng, Y., Dai, X., and Zhao, Y. (2007). Auxin synthesized by the YUCCA Flavin Monooxygenases is essential for embryogenesis and leaf formation in *Arabidopsis*. *Plant Cell* 19, 2430–2439. doi: 10.1105/tpc.107.053009

Datia, R. S. S., Hammerlindl, J. K., Panchuk, B., Pelcher, L. E., and Keller, W. (1992). Modified binary plant transformation vectors with the wild-type gene encoding NPTII. *Gene* 122, 383–384. doi: 10.1016/0378-1119(92)90232-E

Deeks, M. J., and Hussey, P. J. (2003). Arp2/3 and 'the shape of things to come'. *Curr. Opin. Plant Biol.* 6, 561–567. doi: 10.1016/j.pbi.2003.09.013

Deeks, M. J., Kaloriti, D., Davies, B., Malhó, R., and Hussey, P. J. (2004). Arabidopsis NAP1 is essential for Arp2/3-dependent trichome morphogenesis. *Curr. Biol.* 14, 1410–1414. doi: 10.1016/j.cub.2004.06.065

Djakovic, S., Dyachok, J., Burke, M., Frank, M. J., and Smith, L. G. (2006). BRICK1/HSPC300 functions with SCAR and the ARP2/3 complex to regulate epidermal cell shape in *Arabidopsis*. *Development* 133, 1091–1100. doi: 10.1242/dev.02280

Dobrev, P. I., and Vankova, R. (2012). Quantification of abscisic Acid, cytokinin, and auxin content in salt-stressed plant tissues. *Methods Mol. Biol.* 913, 251–261. doi: 10.1007/978-1-61779-986-0_17

Dyachok, J., Shao, M. R., Vaughn, K., Bowling, A., Facette, M., Djakovic, S., et al. (2008). Plasma membrane-associated SCAR complex subunits promote cortical F-actin accumulation and normal growth characteristics in *Arabidopsis* roots. *Mol. Plant* 1, 990–1006. doi: 10.1093/mp/ssn059

Dyachok, J., Zhu, L., Liao, F., He, J., Huq, E., and Blancaflor, E. B. (2011). SCAR mediates light-induced root elongation in *Arabidopsis* through photoreceptors and proteasomes. *Plant Cell* 23, 3610–3626. doi: 10.1105/tpc.111.088823

El-Assal, S. E. D., Le, J., Basu, D., Mallery, E. L., and Szymanski, D. B. (2004). Distorted2 encodes an ARPC2 subunit of the putative *Arabidopsis* ARP2/3 complex. *Plant J.* 38, 526–538. doi: 10.1111/j.1365-313X.2004.02065.x

Falconer, M. M., and Seagull, R. W. (1985). Xylogenesis in tissue culture: Taxol effects on microtubule reorientation and lateral association in differentiating cells. *Protoplasma* 128, 157–166. doi: 10.1007/BF01276337

Feraru, E., Feraru, M. I., Kleine-Vehn, J., Martinic˘re, A., Mouille, G., Vanneste, S., et al. (2011). PIN polarity maintenance by the cell wall in Arabidopsis. *Curr. Biol.* 21, 338–343. doi: 10.1016/j.cub.2011.01.036

Friml, J., Wi´sniewska, J., Benková, E., Mendgen, K., and Palme, K. (2002). Lateral relocation of auxin efflux regulator PIN3 mediates tropism in *Arabidopsis*. *Nature* 415, 806–809. doi: 10.1038/415806a

Gallavotti, A. (2013). The role of auxin in shaping shoot architecture. *J. Exp. Bot.* 64, 2593–2608. doi: 10.1093/jxb/ert141

Gälweiler, L., Guan, C., Müller, A., Wisman, E., Mendgen, K., Yephremov, A., et al. (1998). Regulation of polar auxin transport by AtPIN1 in Arabidopsis vascular tissue. *Science* 282, 2226–2230. doi: 10.1126/science.282.5397.2226

Ganguly, A., Park, M., Kesawat, M. S., and Cho, H.-T. (2014). Functional analysis of the hydrophilic loop in intracellular trafficking of Arabidopsis PIN-FORMED proteins. *Plant Cell* 26, 1570–1585. doi: 10.1105/tpc.113.118422

Gao, Y., Zhang, Y., Zhang, D., Dai, X., Estelle, M., and Zhao, Y. (2015). Auxin binding protein 1 (ABP1) is not required for either auxin signaling or Arabidopsis development. *Proc. Natl. Acad. Sci. U.S.A.* 112, 2275–2280. doi: 10.1073/pnas.1500365112

Gardiner, J. C., Taylor, N. G., and Turner, S. R. (2003). Control of cellulose synthase complex localization in developing xylem. *Plant Cell* 15, 1740–1748. doi: 10.1105/tpc.012815

Geldner, N., Friml, J., Stierhof, Y. D., Jürgens, G., and Palme, K. (2001). Auxin transport inhibitors block PIN1 cycling and vesicle trafficking. *Nature* 413, 425–428. doi: 10.1038/35096571

Hepler, P. K., and Fosket, D. E. (1971). The role of microtubules in vessel member differentiation inColeus. *Protoplasma* 72, 213–236. doi: 10.1007/BF01279052

Hou, G., Mohamalawari, D. R., and Blancaflor, E. B. (2003). Enhanced gravitropism of roots with a disrupted cap. *Plant Physiol.* 131, 1360–1373. doi: 10.1104/pp.014423.amyloplasts

Jiang, K., Sorefan, K., Deeks, M. J., Bevan, M. W., Hussey, P. J., and Hetherington, A. M. (2012). The ARP2/3 complex mediates guard cell actin reorganization and stomatal movement in *Arabidopsis*. *Plant Cell* 24, 2031–2040. doi: 10.1105/tpc.112.096263

Klahre, U., and Chua, N. H. (1999). The Arabidopsis ACTIN-RELATED PROTEIN 2 (AtARP2) promoter directs expression in xylem precursor cells and pollen. *Plant Mol. Biol.* 41, 65–73. doi: 10.1023/A:1006247600932

Kleine-Vehn, J., Leitner, J., Zwiewka, M., Sauer, M., Abas, L., Luschnig, C., et al. (2008a). Differential degradation of PIN2 auxin efflux carrier by retromer-dependent vacuolar targeting. *Proc. Natl. Acad. Sci. U.S.A.* 105, 17812–17817. doi: 10.1073/pnas.0808073105

Kleine-Vehn, J., Wabnik, K., Martinicˇre, A., Łangowski, Ł., Willig, K., Naramoto, S., et al. (2011). Recycling, clustering, and endocytosis jointly maintain PIN auxin carrier polarity at the plasma membrane. *Mol. Syst. Biol.* 7:540. doi: 10.1038/msb.2011.72

Kleine-Vehn, J., Wi´sniewska, J., Brewer, P. B., Friml, J., Dhonukshe, P., and Łangowski, Ł. (2008b). Cellular and molecular requirements for polar PIN targeting and transcytosis in plants. *Mol. Plant* 1, 1056–1066. doi: 10.1093/mp/ssn062

Koltzscher, M., Neumann, C., Kö, S., and Gerke, V. (2003). Ca^{2+} -dependent Binding and Activation of Dormant Ezrin by Dimeric S100P. *Mol. Biol. Cell* 14, 2372–2384. doi: 10.1091/mbc.E02

Kramer, E. M., and Ackelsberg, E. M. (2016). Do vacuoles obscure the evidence for auxin homeostasis? *Mol. Plant* 9, 4–6. doi: 10.1016/j.molp.2015.05.002

Kremers, G.-J., Davidson, M. W., Sell, B. R., Baird, M. A., Lavagnino, Z., Ustione, A., et al. (2016). Quantitative assessment of fluorescent proteins. *Nat. Methods* 13, 557–562. doi: 10.1038/nmeth.3891

Krüger, F., and Schumacher, K. (2018). Pumping up the volume - vacuole biogenesis in *Arabidopsis thaliana*. *Semin. Cell Dev. Biol.* 80, 106–112. doi: 10.1016/j.semcdb.2017.07.008

Lacek, J., Retzer, K., Luschnig, C., and Zažímalová, E. (2017). "Polar auxin transport," in *eLS*, (Chichester: John Wiley & Sons, Ltd), 1–11. doi: 10.1002/9780470015902.a0020116.pub2

Lanza, M., Garcia-Ponce, B., Castrillo, G., Catarecha, P., Sauer, M., Rodriguez-Serrano, M., et al. (2012). Role of actin cytoskeleton in brassinosteroid signaling and in its integration with the auxin response in plants. *Dev. Cell* 22, 1275–1285. doi: 10.1016/j.devcel.2012.04.008

Laxmi, A., Pan, J., Morsy, M., and Chen, R. (2008). Light plays an essential role in intracellular distribution of auxin efflux carrier PIN2 in *Arabidopsis thaliana*. *PLoS One* 3:e0001510. doi: 10.1371/journal.pone.0001510

Le, J., El-Assal, S. E.-D., Basu, D., Saad, M. E., and Szymanski, D. B. (2003). Requirements for *Arabidopsis ATARP2* and *ATARP3* during epidermal development. *Curr. Biol.* 13, 1341–1347. doi: 10.1016/S0960-9822(03)00493-7

Le, J., Liu, X.-G., Yang, K.-Z., Chen, X.-L., Zou, J.-J., Wang, H.-Z., et al. (2014). Auxin transport and activity regulate stomatal patterning and development. *Nat. Commun.* 5:3090. doi: 10.1038/ncomms4090

Le, J., Mallery, E. L., Zhang, C., Brankle, S., and Szymanski, D. B. (2006). *Arabidopsis* BRICK1/HSPC300 is an essential WAVE-complex subunit that selectively stabilizes the Arp2/3 activator SCAR2. *Curr. Biol.* 16, 895–901. doi: 10.1016/j.cub.2006.03.061

Li, H., Lin, D., Dhonukshe, P., Nagawa, S., Chen, D., Friml, J., et al. (2011). Phosphorylation switch modulates the interdigitated pattern of PIN1 localization and cell expansion in *Arabidopsis* leaf epidermis. *Cell Res.* 21, 970–978. doi: 10.1038/cr.2011.49

Li, L.-J., Ren, F., Gao, X.-Q., Wei, P.-C., and Wang, X.-C. (2013). The reorganization of actin filaments is required for vacuolar fusion of guard cells during stomatal opening in *Arabidopsis*. *Plant Cell Environ.* 36, 484–497. doi: 10.1111/j.1365-3040.2012.02592.x

Li, S., Blanchoin, L., Yang, Z., and Lord, E. M. (2003). The putative Arabidopsis arp2/3 complex controls leaf cell morphogenesis. *Plant Physiol.* 132, 2034–2044. doi: 10.1104/pp.103.028563.the

Löfke, C., Dünser, K., Scheuring, D., and Kleine-Vehn, J. (2015). Auxin regulates SNARE-dependent vacuolar morphology restricting cell size. *eLife* 4:e05868. doi: 10.7554/eLife.05868

Mao, G., Buschmann, H., Doonan, J. H., and Lloyd, C. W. (2006). The role of MAP65-1 in microtubule bundling during Zinnia tracheary element formation. *J. Cell Sci.* 119, 753–758. doi: 10.1242/jcs.02813

Mathur, J., Mathur, N., Kernebeck, B., and Hülskamp, M. (2003a). Mutations in actin-related proteins 2 and 3 affect cell shape development in Arabidopsis. *Plant Cell* 15, 1632–1645. doi: 10.1105/tpc.011676

Mathur, J., Mathur, N., Kirik, V., Kernebeck, B., Srinivas, B. P., and Hülskamp, M. (2003b). Arabidopsis CROOKED encodes for the smallest subunit of the ARP2/3 complex and controls cell shape by region specific fine F-actin formation. *Development* 130, 3137–3146. doi: 10.1242/dev.00549

Mathur, J., Spielhofer, P., Kost, B., and Chua, N. (1999). The actin cytoskeleton is required to elaborate and maintain spatial patterning during trichome cell morphogenesis in *Arabidopsis thaliana*. *Development* 126, 5559–5568.

Nagawa, S., Xu, T., Lin, D., Dhonukshe, P., Zhang, X., Friml, J., et al. (2012). ROP GTPase-dependent actin microfilaments promote PIN1 polarization by localized inhibition of clathrin-dependent endocytosis. *PLoS Biol.* 10:e1001299. doi: 10.1371/journal.pbio.1001299

Nakayama, N., Smith, R. S., Mandel, T., Robinson, S., Kimura, S., Boudaoud, A., et al. (2012). Mechanical regulation of auxin-mediated growth. *Curr. Biol.* 22, 1468–1476. doi: 10.1016/j.cub.2012.06.050

Narusaka, M., Shiraishi, T., Iwabuchi, M., and Narusaka, Y. (2010). The floral inoculating protocol: a simplified *Arabidopsis thaliana* transformation method modified from floral dipping. *Plant Biotechnol.* 27, 349–351. doi: 10.5511/plantbiotechnology.27.349

Nelson, B. K., Cai, X., and Nebenführ, A. (2007). A multicolored set of *in vivo* organelle markers for co-localization studies in Arabidopsis and other plants. *Plant J.* 51, 1126–1136. doi: 10.1111/j.1365-313X.2007.03212.x

Oda, Y., and Fukuda, H. (2012). Initiation of cell wall pattern by a Rho- and microtubule-driven symmetry breaking. *Science* 337, 1333–1336. doi: 10.1126/science.1222597

Oda, Y., and Fukuda, H. (2013). Rho of Plant GTPase signaling regulates the behavior of *Arabidopsis* kinesin-13A to establish secondary cell wall patterns. *Plant Cell* 25, 4439–4450. doi: 10.1105/tpc.113.117853

Oda, Y., Iida, Y., Kondo, Y., and Fukuda, H. (2010). Wood cell-wall structure requires local 2D-microtubule disassembly by a novel plasma membrane-anchored protein. *Curr. Biol.* 20, 1197–1202. doi: 10.1016/j.cub.2010.05.038

Pénc˘ík, A., Simonovik, B., Petersson, S. V., Henyková, E., Simon, S., Greenham, K., et al. (2013). Regulation of auxin homeostasis and gradients in *Arabidopsis* roots through the formation of the indole-3-acetic acid catabolite 2-oxindole-3-acetic acid. *Plant Cell* 25, 3858–3870. doi: 10.1105/tpc.113.114421

Pesquet, E., Korolev, A. V., Calder, G., and Lloyd, C. W. (2010). The microtubule-associated protein AtMAP70-5 regulates secondary wall patterning in *Arabidopsis* wood cells. *Curr. Biol.* 20, 744–749. doi: 10.1016/j.cub.2010.02.057

Rahman, A., Bannigan, A., Sulaman, W., Pechter, P., Blancaflor, E. B., and Baskin, T. I. (2007). Auxin, actin and growth of the *Arabidopsis thaliana* primary root. *Plant J.* 50, 514–528. doi: 10.1111/j.1365-313X.2007.03068.x

Ramakers, C., Ruijter, J. M., Lekanne Deprez, R. H., and Moorman, A. F. M. (2003). Assumption-free analysis of quantitative real-time polymerase chain reaction (PCR) data. *Neurosci. Lett.* 339, 62–66. doi: 10.1016/S0304-3940(02)01423-4

Saedler, R., Zimmermann, I., Mutondo, M., and Hülskamp, M. (2004). The *Arabidopsis KLUNKER* gene controls cell shape changes and encodes the AtSRA1 homolog. *Plant Mol. Biol.* 56, 775–782. doi: 10.1007/s11103-004-4951-z

Sahi, V. P., Cifrová, P., Garciá-González, J., Kotannal Baby, I., Mouillé, G., Gineau, E., et al. (2018). *Arabidopsis thaliana* plants lacking the ARP2/3 complex show

defects in cell wall assembly and auxin distribution. *Ann. Bot.* 122, 777–789. doi: 10.1093/aob/mcx178

Saini, S., Sharma, I., Kaur, N., and Pati, P. K. (2013). Auxin: a master regulator in plant root development. *Plant Cell Rep.* 32, 741–757. doi: 10.1007/s00299-013-1430-5

Salanenka, Y., Verstraeten, I., Löfke, C., Tabata, K., Naramoto, S., Glanc, M., et al. (2018). Gibberellin DELLA signaling targets the retromer complex to redirect protein trafficking to the plasma membrane. *Proc. Natl. Acad. Sci. U.S.A.* 115, 3716–3721. doi: 10.1073/pnas.1721760115

Sasaki, T., Fukuda, H., and Oda, Y. (2017). CORTICAL MICROTUBULE DISORDERING1 is required for secondary cell wall patterning in xylem vessels. *Plant Cell* 29, 3123–3139. doi: 10.1105/tpc.17.00663

Schindelin, J., Arganda-Carreras, I., Frise, E., Kaynig, V., Longair, M., Pietzsch, T., et al. (2012). Fiji: an open-source platform for biological-image analysis. *Nat. Methods* 9, 676–682. doi: 10.1038/nmeth.2019

Schwab, B., Mathur, J., Saedler, R., Schwarz, H., Frey, B., Scheidegger, C., et al. (2003). Regulation of cell expansion by the DISTORTED genes in *Arabidopsis thaliana*: actin controls the spatial organization of microtubules. *Mol. Genet. Genomics* 269, 350–360. doi: 10.1007/s00438-003-0843-1

Shimada, T., Takagi, J., Ichino, T., Shirakawa, M., and Hara-Nishimura, I. (2018). Plant vacuoles. *Annu. Rev. Plant Biol.* 69, 123–145. doi: 10.1146/annurev-arplant-042817-040508

Shinoda, H., Shannon, M., and Nagai, T. (2018). Fluorescent proteins for investigating biological events in acidic environments. *Int. J. Mol. Sci.* 19:1548. doi: 10.3390/ijms19061548

Shirakawa, M., Ueda, H., Shimada, T., Nishiyama, C., and Hara-Nishimura, I. (2009). Vacuolar SNAREs function in the formation of the leaf vascular network by regulating auxin distribution. *Plant Cell Physiol.* 50, 1319–1328. doi: 10.1093/pcp/pcp076

Sugiyama, Y., Nagashima, Y., Wakazaki, M., Sato, M., Toyooka, K., Fukuda, H., et al. (2019). A Rho-actin signaling pathway shapes cell wall boundaries in Arabidopsis xylem vessels. *Nat. Commun.* 10, 468. doi: 10.1038/s41467-019-08396-7

Teale, W. D., Paponov, I. A., and Palme, K. (2006). Auxin in action: signalling, transport and the control of plant growth and development. *Nat. Rev. Mol. Cell Biol.* 7, 847–859. doi: 10.1038/nrm2020

Viotti, C., Krüger, F., Krebs, M., Neubert, C., Fink, F., Lupanga, U., et al. (2013). The endoplasmic reticulum is the main membrane source for biogenesis of the lytic vacuole in *Arabidopsis*. *Plant Cell* 25, 3434–3449. doi: 10.1105/tpc.113.114827

Vukašinovic´, N., Oda, Y., Pejchar, P., Synek, L., Pec˘enková, T., Rawat, A., et al. (2017). Microtubule-dependent targeting of the exocyst complex is necessary for xylem development in Arabidopsis. *New Phytol.* 213, 1052–1067. doi: 10.1111/nph.14267

Wang, P., Richardson, C., Hawes, C., and Hussey, P. J. (2016). *Arabidopsis* NAP1 regulates the formation of autophagosomes. *Curr. Biol.* 26, 2060–2069. doi: 10.1016/j.cub.2016.06.008

Welch, M. D., DePace, A. H., Verma, S., Iwamatsu, A., and Mitchison, T. J. (1997). The human Arp2/3 complex is composed of evolutionarily conserved subunits and is localized to cellular regions of dynamic actin filament assembly. *J. Cell Biol.* 138, 375–384. doi: 10.1083/jcb.138.2.375

Wu, T.-C., Belteton, S. A., Pack, J., Szymanski, D. B., and Umulis, D. M. (2016). LobeFinder: a convex hull-based method for quantitative boundary analyses of lobed plant cells. *Plant Physiol.* 171, 2331–2342. doi: 10.1104/pp.15.00972

Xu, T., Dai, N., Chen, J., Nagawa, S., Cao, M., Li, H., et al. (2014). Cell surface ABP1-TMK auxin-sensing complex activates ROP GTPase signaling. *Science* 343, 1025–1028. doi: 10.1126/science.1245125

Xu, T., Wen, M., Nagawa, S., Fu, Y., Chen, J.-G., Wu, M.-J., et al. (2010). Cell surface- and rho GTPase-based auxin signaling controls cellular interdigitation in *Arabidopsis*. *Cell* 143, 99–110. doi: 10.1016/j.cell.2010.09.003

Yamamoto, K., and Kiss, J. Z. (2002). Disruption of the actin cytoskeleton results in the promotion of gravitropism in inflorescence stems and hypocotyls of Arabidopsis. *Plant Physiol.* 128, 669–681. doi: 10.1104/pp.010804

Yanagisawa, M., Desyatova, A. S., Belteton, S. A., Mallery, E. L., Turner, J. A., and Szymanski, D. B. (2015). Patterning mechanisms of cytoskeletal and cell wall systems during leaf trichome morphogenesis. *Nat. Plants* 1:15014. doi: 10.1038/nplants.2015.14

Žádníková, P., Petrasek, J., Marhavy, P., Raz, V., Vandenbussche, F., Ding, Z., et al. (2010). Role of PIN-mediated auxin efflux in apical hook development of *Arabidopsis thaliana*. *Development* 137, 607–617. doi: 10.1242/dev.041277

Zhang, C., Halsey, L. E., and Szymanski, D. B. (2011). The development and geometry of shape change in *Arabidopsis thaliana* cotyledon pavement cells. *BMC Plant Biol.* 11:27. doi: 10.1186/1471-2229-11-27

Zhang, C., Hicks, G. R., and Raikhel, N. V. (2014). Plant vacuole morphology and vacuolar trafficking. *Front. Plant Sci.* 5:476. doi: 10.3389/fpls.2014.00476

Zhang, C., Mallery, E. L., and Szymanski, D. B. (2013). ARP2/3 localization in Arabidopsis leaf pavement cells: a diversity of intracellular pools and cytoskeletal interactions. *Front. Plant Sci.* 4:238. doi: 10.3389/fpls.2013.00238

Zhao, Y., Christensen, S. K., Fankhauser, C., Cashman, J. R., Cohen, J. D., Weigel, D., et al. (2001). A role for flavin monooxygenase-like enzymes in auxin biosynthesis. *Science* 291, 306–309. doi: 10.1126/science.291.5502.306

Conflict of Interest: The authors declare that the research was conducted in the absence of any commercial or financial relationships that could be construed as a potential conflict of interest.

3.2.5. An Arabidopsis mutant deficient in phosphatidylinositol-4-phosphate kinases ß1 and ß2 displays altered auxin-related responses in roots

Authors: Anastasiia Starodubtseva, Tetiana Kalachova, Katarzyna Retzer, Adriana Jelínková, Petre Dobrev, Jozef Lacek, Romana Pospíchalová, Jindřiška Angelini, Anne Guivarc'h, Stéphanie Pateyron, Ludivine Soubigou-Taconnat, Lenka Burketová, Eric Ruelland

Summary:

This study was focused on analyzing of mutants of PHOSPHATIDYLINOSITOL-4-PHOSPHATE KINASES ß1 and ß2 (PI4Kß1ß2). These mutants have a dwarf phenotype, which, interestingly with lower ability to adapt to changes of gravity vector, might suggest auxin-signaling-related process. Transcriptomic data are similar to plants that were treated with exogenous auxin. The double mutant lost sensitivity to exogenous application of IAA. qPCR data of the auxin responsive genes show minimal increase after adding of exogenous auxin. Based on detecting increased pool of IAA-glutamate and increased expression of enzymes of GH3 family, we suggest constitutive deactivation of IAA through conjugation. We also detected changes in abundance and localization of PIN2 and lower stability of actin filaments. All those information show that PI4Kß1ß2 are involved in the auxin regulatory mechanisms but further study is required to determine their exact function in the auxin mechanism of action cascade.

My contribution: I contributed by performing experiments and analyzing measurements of hormonal content and occurrence of native auxin metabolites.

scientific reports

Check for updates

OPEN

An Arabidopsis mutant deficient in phosphatidylinositol-4-phosphate kinases ß1 and ß2 displays altered auxin-related responses in roots

Anastasiia Starodubtseva[1,2,3], Tetiana Kalachova[1✉], Katarzyna Retzer[1], Adriana Jelínková[1], Petre Dobrev[1], Jozef Lacek[1], Romana Pospíchalová[1], Jindřiška Angelini[2], Anne Guivarc'h[3], Stéphanie Pateyron[4,5], Ludivine Soubigou-Taconnat[4,5], Lenka Burketová[1] & Eric Ruelland[6]

Phosphatidylinositol 4-kinases (PI4Ks) are the first enzymes that commit phosphatidylinositol into the phosphoinositide pathway. Here, we show that *Arabidopsis thaliana* seedlings deficient in PI4Kβ1 and β2 have several developmental defects including shorter roots and unfinished cytokinesis. The *pi4kß1ß2* double mutant was insensitive to exogenous auxin concerning inhibition of root length and cell elongation; it also responded more slowly to gravistimulation. The *pi4kß1ß2* root transcriptome displayed some similarities to a wild type plant response to auxin. Yet, not all the genes displayed such a constitutive auxin-like response. Besides, most assessed genes did not respond to exogenous auxin. This is consistent with data with the transcriptional reporter DR5-GUS. The content of bioactive auxin in the *pi4kß1ß2* roots was similar to that in wild-type ones. Yet, an enhanced auxin-conjugating activity was detected and the auxin level reporter DII-VENUS did not respond to exogenous auxin in *pi4kß1ß2* mutant. The mutant exhibited altered subcellular trafficking behavior including the trapping of PIN-FORMED 2 protein in rapidly moving vesicles. Bigger and less fragmented vacuoles were observed in *pi4kß1ß2* roots when compared to the wild type. Furthermore, the actin filament web of the *pi4kß1ß2* double mutant was less dense than in wild-type seedling roots, and less prone to rebuilding after treatment with latrunculin B. A mechanistic model is proposed in which an altered PI4K activity leads to actin filament disorganization, changes in vesicle trafficking, and altered auxin homeostasis and response resulting in a pleiotropic root phenotypes.

Plant health and productivity depends on root outgrowth, which allows water and nutrient uptake, and is equally crucial for an efficient photosynthesis rate[1,2]. Root morphogenesis is a complex process, orchestrated by a complex signaling crosstalk at different levels, from single-cell metabolism to hormone transport within plant organs. On-point spatial and temporal organization of cell organelles, polar establishment of cell architecture and directed shoot ward auxin transport are fundamental for correct root cell differentiation. Root hair cell priming and plasticity require fine-tuned, interconnected cellular processes driven by a properly established cytoskeleton that controls the polar delivery of membranes to the root apex in order to enlarge the cell unidirectionally, and by the transport of auxin through the root tip[1,2]. Auxin regulates cell polarity through the activation of ROPs (Rho-like GTPase) that participate in the polar localization of PIN-FORMED (PIN) family proteins. Carriers of the PIN family are plasma membrane-integrated auxin efflux carriers responsible for the direction and intensity

[1]Institute of Experimental Botany of the Czech Academy of Sciences, Rozvojová 263, 165 02, Prague, Czech Republic. [2]University of Chemistry and Technology, Technická 5, 16628 Prague, Czech Republic. [3]Sorbonne Université, UPEC, CNRS, IRD, INRAE, Institute of Ecology and Environmental Sciences of Paris (iEES), 75005 Paris, France. [4]Université de Paris, CNRS, INRAE, Institute of Plant Sciences Paris-Saclay (IPS2), 91405 Orsay, France. [5]Université Paris-Saclay, CNRS, INRAE, Univ Evry, Institute of Plant Sciences Paris-Saclay (IPS2), 91405 Orsay, France. [6]Université de Technologie de Compiègne, Enzyme and Cell Engineering Laboratory, CNRS, 60203 Compiègne, France. ✉email: kalachova@ueb.cas.cz

of auxin flow through the plant body. Their cellular localization and activity are regulated at many levels[3–5], and rely on the lipid composition of the membrane they are in.

Phosphoinositides, minor components of plasma membrane, are phosphorylated derivatives of phosphatidylinositol (PI), such as phosphatidylinositol-4-phosphate (PI4P) and phosphatidylinositol-4,5-bisphosphate (PI4,5P2). Phosphoinositides are important signaling molecules as they are substrates or cofactors of important signaling enzymes. In plants, both PI4P and PI4,5P2 can be substrates to phospholipases C (PLCs) leading to diacylglycerol and the corresponding phosphorylated inositol. PI4,5P2 is a cofactor of some phospholipases D (PLDs), that catalyze the production of phosphatidic acid, a major plant signaling lipid[6]. More generally, phosphoinositides can directly interact with membrane proteins (such as ion channels or G protein-coupled receptors) or cytosolic proteins that they can recruit to membranes[7,8]. Interestingly, specific relative levels of phosphoinositides are a characteristic feature of different membranes: plasma membrane, endoplasmic reticulum and Golgi membranes do not have the same relative composition in phosphoinositides[7–9]. Besides, membrane nanoclusters enriched in certain proteins crucial for signal transduction and transport proteins also have a specific composition in phosphoinositides[8,10]. Formation of membrane domains enriched in PI4P and PI4,5P2 is a crucial component of plasma membrane dynamics. Such phosphoinositide-enriched domains are important for the localization of REMORINs, scaffold proteins governing PM–bound signaling[11], and FLS2, a pattern-recognition receptor that determines the specific perception of the bacterial protein flagellin[12].

Composition in phosphoinositides is modified by the activities of lipid kinases. PI4Ks phosphorylate the 4th hydroxyl position in the inositol head group of PI to generate PI4P. PI4P can be further phosphorylated by phosphatidylinositol-4,5-kinases (PI4,5 K) into PI4,5P2. There are two types of PI4Ks according to their primary sequences and pharmacological sensitivities. Type-II PI4Ks are inhibited by adenosine while type III PI4Ks are inhibited by micromolar concentrations of wortmannin, a steroid produced by the fungi *Penicillium funiculosum*. In the *A. thaliana* genome, twelve putative PI4K isoforms have been identified. Eight belong to type-II (*At*PI4Kγ1-8), and four belong to type-III (*At*PI4Kα1 and α2 and *At*PI4Kβ1 and β2)[13]. Not much is known about type-II PI4Ks and they could actually be protein kinases and not lipid kinases[13,14]. We have previously shown that type-III PI4Ks are upstream of the PLC activity that controls the responses of tobacco BY2 cells to cryptogein, a fungi elicitor[15]. Type-III PI4Ks are also upstream of plant cold response PLC activity[16] but also of the PLC activity that controls gene expression, in basal, non-stimulated conditions[17]. Type-III PI4Ks have been shown also to be activated in response to salicylic acid (SA), and the consequent increase in phosphoinositides is an important part of the specific response of Arabidopsis to this phytohormone[18–20]. *AtPI4Kα2* is a pseudogene and viable homozygous *PI4Kα1* mutants have never been obtained. We have worked previously on a double mutant defective in both *PI4Kβ* genes. In 4-week-old plants, *pi4kβ1β2* exhibited a constitutively high SA level that led to a stunted phenotype[21]. However, SA accumulation did not occur in young *pi4kβ1β2* seedlings[21,22] and therefore, they appeared to be the material of choice to study the roles of PI4Ks and phosphoinositides in root development. Several aspects of the role of PI4Ks in plant cell biology have been discovered using *pi4kß1ß2* double mutant, such as the involvement of PI4K*β*1 in cell plate formation during cytokinesis[23], in the formation of secretory vesicles[24], root hair shaping and polar growth[25]. Here, we show that the *pi4kß1ß2* double mutant exhibits several root phenotypes: impaired primary root growth, lower sensitivity to exogenous indole-3-acetic acid (IAA), impaired elongation and bending in response to gravistimulation, and misshapen root hair growth. These changes appeared to coincide with an altered subcellular distribution and turnover of PIN2, a less stable actin cytoskeleton and generally altered intracellular trafficking dynamics. Moreover, expression of several auxin-associated genes in roots was not responsive to exogenous auxin. However, some transcript levels in non-treated mutant roots were already at the auxin-response levels of wild type (WT) roots, thus displaying an apparent auxin-like response. Remarkably, the measured content of bioactive IAA in double mutant roots did not differ from that of WT, but a considerable increase of glutamate-conjugated form of auxin was monitored. Besides, the auxin level reporter DII-VENUS did not respond to exogenous auxin in *pi4kß1ß2* mutant. Our data, therefore, link altered PI4K activity to the modification of vesicular trafficking and actin filaments organization one the one hand to altered auxin response likely due to alteration in auxin homeostasis one the other hand.

Results

The *pi4kß1ß2* mutant is impaired in root growth. The PI4Kß1ß2 deficiency in *pi4kß1ß2* seedlings led to a decreased primary root length of up to fourfold compared to the WT control (Fig. 1a,b). The shorter primary root of the mutant appeared to be due to shorter meristem and elongation zones (Fig. 1c). The shorter meristem of *pi4kß1ß2* was due to fewer cells (Fig. 1d), some of which showed unfinished cytokinesis. Interestingly, the CycB1::GUS associated signal occupied a smaller percentage area of the meristem in *pi4kß1ß2* roots when compared to the WT (Fig. 1e,f). The elongation zone was almost missing. In the differentiation zone, the *pi4kß1ß2* mutant had smaller cortical cells (Supplementary Fig. S1) and either similar or very small root hair lengths when compared to the WT. This created apparent "bald-like" zones (Fig. 1g,h), while the overall total root hair density in *pi4kß1ß2* plants did not differ to that of the WT (Fig. 1i). An analysis of the epidermal cell lines[26] showed that the regularity of trichoblasts/atrichoblasts formation was not affected in the mutant (Supplementary Fig. S2). This confirmed that the apparent "bald-like zones'' were not due to an absence of hairs but to shorter root hairs.

Responses to IAA and to gravistimulation are impaired in *pi4kß1ß2*. Mutant and WT 5-day-old seedlings were transferred to a cultivation medium containing various phytohormones. Seven days later, the lengths of the primary root, of the meristem and of the cortical cells within the differentiation zone were measured. The presence of IAA led to a decrease in the root length of WT plants; the decrease was more than 60% at 100 nM IAA. The *pi4kß1ß2* mutant was less sensitive to the auxin treatment, the decrease being only 20% at the

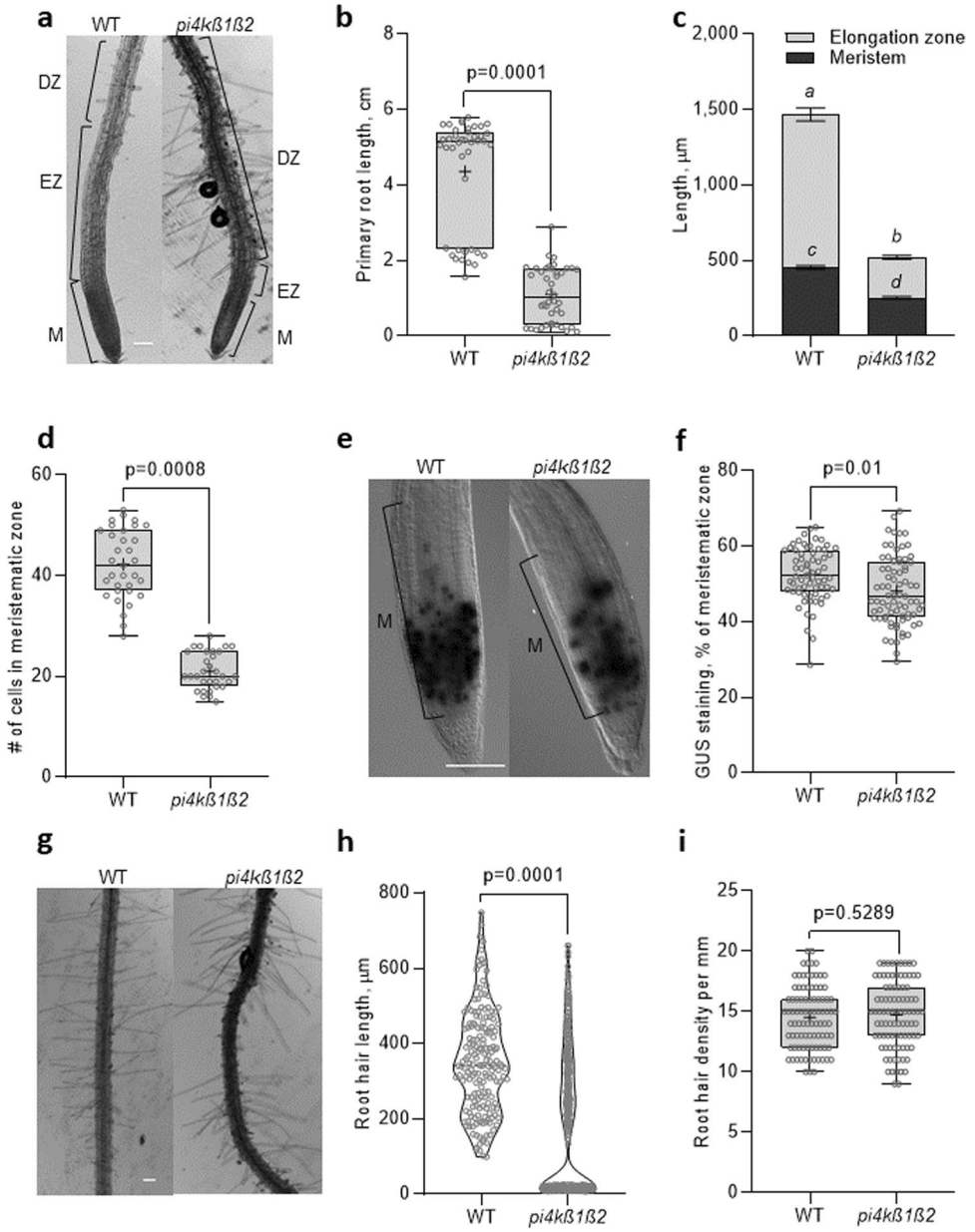

Figure 1. Impaired root growth and morphological characteristics of the *pi4kß1ß2* mutant. (**a**) representative pictures of the apical root parts of 11-day-old seedlings of *Arabidopsis thaliana* Col-0 (WT) and the *pi4kß1ß2* mutant: meristem (M), elongation zone (EZ) and differentiation zone (DZ) are marked, scale bar=100 µm; (**b**) primary root length, n=40; (**c**) length of the meristematic and elongation zones, n=12, error bars represent mean±SEM; different letters indicate statistically significant groups, one-way ANOVA with Tukey-HSD post-hoc test ($p>0.05$); (**d**) number of separated cells in the meristem, n=36; (**e**) representative images of GUS staining in the root meristem of 4-day-old plants expressing CycB1::GUS, scale bar=100 µm; (**f**) relative area of CycB1::GUS expression, % of the meristematic zone; n=72; (**g**) representative images of root hair distribution in the DZ of roots, scale bar=100 µm; (**h**) root hair length, n=180; (**i**) root hair density, n=90. Central line of the boxplots represents the median, plus represents the mean, circles represent individual values from three biological repeats. *p*-value was calculated by Student t-test.

concentrations tested (Fig. 2a, Supplementary Fig. S3). A lower sensitivity to exogenous auxin was also detected at the cellular and/or tissue levels. At 50 nM IAA, the length of WT cortical cells showed a 30% decrease compared to the control, while the mutant was insensitive. At 1 µM IAA, the decrease in length of WT cortical cells was 50%, compared to the control, while the mutant remained insensitive (Supplementary Fig. S4a). Concerning meristem size, 100 nM IAA caused a 20% shortening of its length in WT seedlings but no response was observed for the *pi4kß1ß2* mutant; this difference in IAA sensitivity was still apparent even at 1 µM (Supplementary Fig. S4b). Interestingly, the sensitivity of primary root length to a cytokinin (BAP) or to salicylic acid (SA) did not

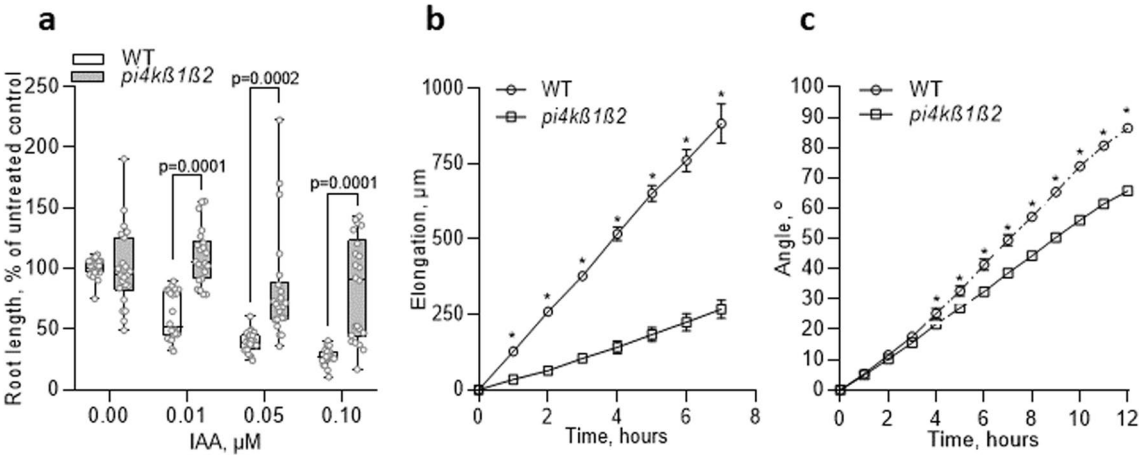

Figure 2. Auxin-related phenotypes of the *pi4kß1ß2* mutant. (**a**) primary root length of 11-day-old seedlings in response to different IAA concentrations, n = 22. Central line of the boxplots represents the median, circles represent individual values; *p*-value is indicated for significantly different groups; *t*-test with correction for multiple comparisons; (**b**) Elongation rate of primary root under gravistimulation, n = 10; (**c**) root tip orientation angle, n = 10; (**b**,**c**) gravitropic assay, 5-day-old seedlings were rotated to 90° on a horizontal microscope, images were taken every hour. Asterisks indicate statistically significant differences between genotypes, $p<0.05$, paired *t*-test with correction for unequal variances. Experiments were repeated three times; data from a representative repeat are shown.

differ between *pi4kß1ß2* and WT seedlings (Supplementary Fig. S4c,d), thus indicating a specific response to auxins.

We then focused on another auxin-related process, the response to gravistimulation. Interestingly, both root elongation (i.e. the distance that the root tip grew since the 0′ time-point) and root orientation (i.e. the angle between the root tip at current and 0′ time-point) were affected in the double mutant in due course of 12 h experiment (Fig. 2b,c Supplementary Fig. S5, Supplementary movie SM1 for WT, Supplementary movie SM2 for *pi4kß1ß2*).

The transcriptome of *pi4kß1ß2* roots shows partial similarities to IAA-treated WT roots. In order to better detail the *pi4kß1ß2* root phenotypes, an RNAseq transcriptomic analysis of roots was performed (Supplementary table S2). It was found that 2517 and 3418 genes were either up- or down-regulated, respectively, in *pi4kß1ß2* roots compared to WT roots. To be more stringent, we then only considered the genes passing a threshold of log2-fold change of 1.5. On these genes we performed a Gene Ontology classification (Supplementary Fig. S6). Among the genes induced in *pi4kß1ß2* roots compared to WT, we found enrichment in genes encoding extracellular, plasma membrane, or cell wall localized proteins, and underrepresentation of genes encoding cytoskeleton or mitochondria-associated proteins. Interestingly, among the repressed genes, the cell wall-associated proteins were also enriched, while cytoskeleton-localized proteins were overrepresented. As for biological processes, we found enrichment in the categories of "response to stress", "signal transduction"and "development" for both groups of genes. Results of the RNAseq analysis were confirmed by qPCR on a selection of genes (Supplementary Fig. S7). Among the genes most induced in *pi4kß1ß2* roots, we found several that were involved in response to hypoxia, oxidative stress and induced systemic resistance (Supplementary Fig. S8). A focus on genes involved in auxin transport or metabolism is displayed (Supplementary table S4). *GH3.12* (AT5G13320) and *GH3.3* (AT2G23170) are markedly up-regulated in *pi4kß1ß2* roots compared to WT ones.

Next, the list of the 200 most up-regulated and 200 most down-regulated genes in *pi4kß1ß2* mutant roots versus WT roots was used as a signature to interrogate public transcriptomic data using the Genevestigator similarity search program[25]. This was performed against curated root experiments dealing with root samples and classified as "Hormone", "Temperature" or "Stress". Out of the 10 most similar experiments, 7 concerned treatments with auxin (Fig. 3a). Within this set of curated root experiments (Fig. 3a), we then only selected the experiments dealing with response to auxins. According to the responses in these experiments of the 200 most repressed genes in our *pi4kß1ß2* versus WT root comparison, the experiments and the genes were clustered (Fig. 3b). This allowed the identification of clusters of genes, down-regulated in *pi4kß1ß2* mutant roots compared to WT ones and down-regulated in some experiments dealing with the response to auxin (Fig. 3b, clusters A,B,C; list of genes of these clusters in supplementary table 3). We did the same with the 200 most up-regulated genes in the *pi4kß1ß2* double mutant compared to WT roots and thus identified genes upregulated both in *pi4kß1ß2* mutant roots versus WT and up-regulated in curated experiments dealing with response to auxin in roots (Fig. 3c, cluster E). These clusters represent genes for which the effect of the *pi4kß1ß2* double mutation in the root compared to WT is similar to a treatment with auxin. Yet other clusters exist, consisting of genes that are down-regulated in *pi4kß1ß2* roots, but were shown to be upregulated by auxins in public transcriptomics data (Fig. 3b, cluster D; supplementary table S3), or genes that are up-regulated in *pi4kß1ß2* roots, but were

shown to be upregulated by auxins in public transcriptomics data (Fig. 3c, cluster F; supplementary table S3). The transcript levels of selected auxin responsive genes representing different clusters were monitored by qPCR in mutant and WT plants, treated or not with 10 nM IAA for 24 h (Fig. 3d). The transcript level of *AT1G64590, CSLB5, SAUR9, NPF2.4* and *BRU6* in the untreated roots of *pi4kß1ß2* mutant was similar to that in WT roots treated with auxins. On the other hand, the transcription of *CSLB5, FLA13* and *BRU6* did not change in response to auxin in the *pi4kß1ß2* mutant, showing another evidence of affected auxin response.

Assessing auxin sensitivity of *pi4kß1ß2* roots. We next checked auxin transcriptional response by a reporter system, introducing by crossing the auxin sensitive synthetic promoter DR5[27] fused to a GUS reporter gene into *pi4kß1ß2* background. Surprisingly, the basal level of DR5 promoter activity was lower in root and leaf meristem of the *pi4kß1ß2* plants (Fig. 4a,b). After exposure to 10 nM IAA, an important increase of DR5-GUS signal was detected in WT meristems, but not in the *pi4kß1ß2* mutant (Fig. 4a,b), confirming that the sensitivity to IAA is impaired in the mutant line.

The DII-VENUS[28] construct was introduced into the *pi4kß1ß2* mutant by floral-dip agrobacterium transformation. DII-VENUS is a fast maturing form of a yellow fluorescent protein fused in-frame to the Aux/IAA-interaction domain (termed domain II;) and it is rapidly degraded in response to auxin[28]. It is used as a reporter of auxin level. As the DII-VENUS reporter was introduced by agrobacterium transformation, the potential positional effect of the insert cannot be excluded, so the basal fluorescent signal cannot be compared between the lines but signals can be compared within one line. After exposure to 10 nM IAA, a significant decrease of DII-VENUS fluorescence signal was detected in WT plants, but not in the *pi4kß1ß2* mutant (Fig. 4c,d). To check whether the mutant insensitivity to IAA might be a consequence of an elevated IAA level in control conditions, we extracted hormones from the total root system and measured the content of IAA metabolites and conjugates. No difference in the measured free IAA content was detected between genotypes, while IAA-Glu, CamX, I3A and IAN concentrations were higher in the *pi4kß1ß2* mutant than in the wild type (Fig. 4e).

Localization of auxin efflux transporter PIN2 is altered in the *pi4kß1ß2* mutant. As auxin signaling is relying on the correct auxin transport between and within the cells, we investigated the localization and dynamics of auxin transporter PIN2. We analyzed plants expressing PIN2::PIN2-GFP by immunostaining (Fig. 5a–e) and confocal microscopy of PIN2-GFP in both WT and *pi4kß1ß2* backgrounds (Fig. 5f–k). Overall, PIN2-GFP was distributed on the plasma membrane in the same cell types and with a similar polar distribution in mutant roots compared to WT roots. However, in the *pi4kß1ß2* mutant, several "black holes" in the signal were detected along the plasma membrane (Fig. 5b–e, Supplementary Fig. S9). When counterstained with FM 4–64, a dye that labels the plasma membrane, it was seen that the unstained parts in the *pi4kß1ß2* roots corresponded to tunnels between adjacent cells (Fig. 5c–e). Confocal microscopy color-coded projections of pictures were taken over time to track PIN2-GFP intracellular movement in the meristematic zone. The chaotic distribution of vesicles in *pi4kß1ß2* compared to the vesicles aligned in WT showed not only differences in the amount of GFP-marked intracellular vesicles, but also that their movement was less rectilinear and very fast in *pi4kß1ß2* (compare Fig. 5f–h, where vesicles are indicated by white arrows, and the corresponding Supplementary movies SM3 for WT and SM4 for *pi4kß1ß2*). Differences in vacuolar morphology were also observed in *pi4kß1ß2* (Fig. 5i,j; Supplementary Fig. S10), with bigger and less fragmented vacuoles than the WT. When focused on growing root hair cells, altered movement of fluorescent marked vesicles in mature root hair cells and elongating root hairs in *pi4kß1ß2 PIN2::PIN2-GFP* was observed (Supplementary movies SM5 for WT and SM6 for *pi4kß1ß2*). Bright field imaging also revealed differences in the flow of cytoplasmic streaming. Circulation of the cytoplasmic stream occurred close to the plasma membrane and in a straight path in the WT, whereas in the mutant stream the stream flowed in less coordinated lanes. We then studied the response to a dark shift of whole seedlings, a treatment known to enhance PIN2-GFP delivery to the lytic vacuole[26]. A 1 h dark shift caused the translocation of PIN2-GFP to lytic vacuoles in WT roots but not in the double mutant (Fig. 5k,l). All these results point to altered intracellular trafficking dynamics in the roots of *pi4kß1ß2* seedlings.

Actin stability and remodeling are affected in the *pi4kß1ß2* mutant. Five-day-old *pi4kß1ß2* seedlings expressing 35S::LifeAct-GFP were sprayed with 10 µM latB, a drug that inhibits actin polymerization. Treated seedlings were then observed under a confocal microscope (Fig. 6a). Without a latB treatment, the fluorescence signal occupancy was lower in *pi4kß1ß2* compared to WT seedlings. After a 90 min exposure to latB, the fluorescence signal occupancy in *pi4kß1ß2* decreased 40%, while no change was detected in WT plants (Fig. 6b). After a 150 min of exposure to latB, the signal occupancy in WT showed a 35% decrease compared to the control, while the occupancy decreased to 54% for the *pi4kß1ß2* mutant compared to control conditions. Interestingly, while WT roots showed a gradual decrease in actin filament bundling (Fig. 6c) in due course of latB treatment, no significant changes were observed in the *pi4kß1ß2* double mutant.

Discussion

Here, we show that PI4Kß1ß2 deficiency led to up to a fourfold decrease of primary root length compared to WT seedlings. A dwarf phenotype, both in the roots and aerial parts, has already been reported for the *pi4kß1ß2* mutant[21]. Notably, the small rosette size of 4-week-old *pi4kß1ß2* mutant plants has been linked to an increased constitutive SA level[21]. Indeed, a *pi4kß1ß2sid2* triple mutant did not accumulate SA and it did not display the stunted rosette phenotype. However, *pi4kß1ß2sid2* seedlings still exhibited shorter roots than WT plants, thus showing that this root phenotype was a SA-independent process[21,22]. Furthermore, SA accumulation did not occur in young *pi4kß1ß2* seedlings[22], thereby confirming that the root length phenotype was not due to high SA levels. Similar SA levels in *pi4kß1ß2* and WT roots were found in this work (Supplementary Fig. S11), thus

Figure 3. Transcriptomic analysis of *pi4kß1ß2* roots. (**a**) Similarity between the *pi4kß1ß2* roots transcriptome (compared to WT) and the stress-, hormone- or temperature- responsive transcriptomes. The 200 genes most up-regulated in *pi4kß1ß2* roots compared to the WT and the 200 genes most down-regulated in *pi4kß1ß2* roots compared to the WT were used as a signature to search for transcriptome experiments with the highest similarity. The similarity search was performed against the 56 root experiments classified as "stress", "temperature" or "hormone" by Genevestigator (Hruz et al., 2008). Experiments were sorted according to Euclidean distance. Expression of the signature genes in the 10 most similar experiments are shown in color-scale; (**b,c**) Hierarchical clustering of curated root experiments dealing with the response to auxins. The 9 curated root experiments dealing with auxins in Genevestigator were retrieved. According to the expression in these experiments of the 200 most down-regulated (**b**) genes in our *pi4kß1ß2 vs. WT* root comparison, the genes and experiments were clustered with the Biclustering tool in Genvestigator. The same was done using the 200 most up-regulated (**c**) genes in our *pi4kß1ß2 vs. WT* root comparison. Similarities between expression profiles were determined using Pearson correlation. For each experiment, the duration of hormone treatment is indicated. Separated gene clusters with highest levels of induction/repression are labeled and genes are specified on the right panel; (**d**) Response of selected genes to auxin. Five-day-old seedlings were transferred to a medium containing 10 nM IAA, and roots for RNA extraction were harvested after 24 h. The data are presented in means ± SE, n = 9, with a Tukey honestly significant difference (HSD) multiple mean comparison post hoc test. Different letters indicate a significant difference (one-way ANOVA, Tukey HSD, p-value < 0.05).

confirming that the observed root phenotype was not related to altered SA levels and therefore it was an SA-independent process.

So what causes the short root phenotype of *pi4kß1ß2* seedlings? To answer this question, a detailed analysis of root morphology was undertaken (Fig. 1). The shorter primary roots of the double mutant appeared to be due to a reduced meristematic zone due to a lower number of cells. The CycB1::GUS associated signal occupied a significantly smaller (about 10%) area of the meristematic zone in *pi4kß1ß2* seedling roots when compared to the WT. This might explain in part why there were fewer cells in the meristematic zone of the mutant. An absent or a very short transition zone might also result from elevated auxin levels or an enhanced response to auxin. Indeed, the transition zone in a root begins where auxin levels attain a minimum[28]. The shorter primary root length in the *pi4kß1ß2* double mutant was also associated with smaller cortical cells measured in the differentiation zone. A reduced meristematic zone in the *pi4kß1ß2* mutant has been documented previously[29], but we have supplemented these data by measuring meristem cell number and cell length in the differentiation zone. Concerning root hair length, we observed a bimodal distribution in the *pi4kß1ß2* plants, with very short hairs that gave the impression of bald zones. Interestingly, the regularity of trichoblasts/atrichoblasts formation was not affected in the mutant.

Due to the observed root phenotypes, an obvious next step was to assess the sensitivity of the double mutant to different hormones known to alter root growth. Root sensitivity to BAP or SA did not differ between *pi4kß1ß2* and WT seedlings. On the contrary, a loss of sensitivity in the double mutant to exogenous IAA was observed with respect to inhibition of primary root length, inhibition of cortical cell elongation, and elongation of the meristematic zone (Fig. 2, Supplementary Fig. S4a,b). This was in agreement with the experiments of Löfke et al., 2015, showing that altered vesicular trafficking due to inhibited PI4Kß1ß2 activity resulted in lower sensitivity to auxin NAA, altered vacuolar morphology and cell elongation[30]. Interestingly, *pi4kß1ß2* double mutant was less efficient in response to gravistimulation, another auxin-related process. Notably, not only the root elongation, but also the root tip orientation towards gravity vector were impaired in the mutant, suggesting gravity sensing defects. To detail the cellular processes that were interfering with the response to stimulation in mutant roots, we performed full transcriptomic analysis. We found that differences in gene expression between *pi4kß1ß2* and WT roots were in part similar to those observed between auxin treated and non-treated WT roots. Yet, not all genes followed this trend and thus this similarity is only apparent. Besides, we tested by qPCR the response to auxin on a selection of genes, previously described as auxin responsive. The addition of exogenous IAA had no or only a small effect on the expression of those genes in *pi4kß1ß2* compared to the WT. Similarly, DR5-GUS was not induced in the *pi4kß1ß2* mutant after exposure to exogenous IAA. Besides, we also monitored a lower activity of the transcriptional reporter DR5-GUS in non-treated *pi4kß1ß2* mutant meristems (in root tip or cotyledon tip) compared to wild type ones. Therefore, there seems to be a lower sensitivity to auxin, either exogenous or endogenous, as far as gene expression is concerned.

Why is the double mutant less sensitive to exogenous IAA? A possibility could be that the mutant is no longer responsive because of a constitutive high auxin level. As mentioned above, some of the observed root traits of the double mutant (such as a very short transition zone) already resemble an auxin response even in non-treated conditions. Yet, the DR5-GUS in control conditions does not plead for higher IAA content in the mutant. Besides, the level of free bioactive IAA was comparable between mutant and WT roots. The use of the DII-VENUS, a reporter directly related to the bioactive signal itself[31], gives another block of valuable information. DII corresponds to the auxin binding domain of AUX/IAA ; when IAA binds to this domain, AUX/IAA proteins are released from ARF factors and they can interact with SCF^{TIR1} that ubiquitinylates them for degradation by the proteasome. Because the reporter was introduced by transformation in the *pi4kß1ß2* mutant, we cannot directly compare data obtained in wild type to mutant background, but we can compare data within one line. In the mutant background, the DII-VENUS fluorescence was not significantly reduced by addition of exogenous IAA, as it was in WT seedlings. This is coherent with a non- or low- sensitivity to auxin we already documented based on gene expression data. The point is therefore to understand why DII-VENUS fluorescence is not reduced by addition of exogenous IAA. An explanation might be related to auxin homeostasis. In the *pi4kß1ß2* mutant, we detected elevated levels of several inactive auxin metabolites including the glutamate-conjugate form. IAA-Glu is an early

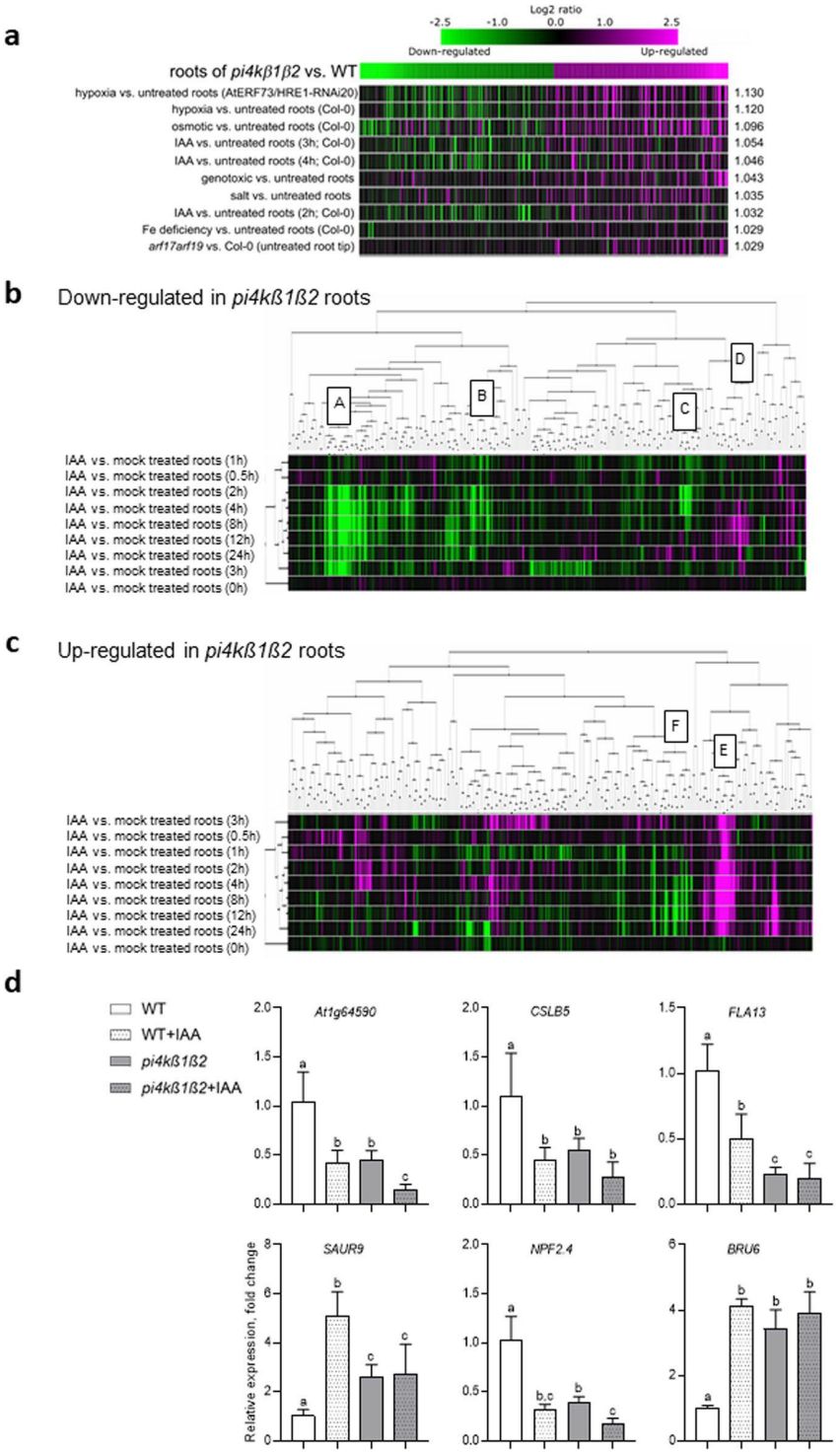
a
Log2 ratio
-2.5 -1.0 0.0 1.0 2.5
Down-regulated
Up-regulated
roots of pi4kβ1β2 vs. WT
hypoxia vs. untreated roots (AtERF73/HRE1-RNAi20) 1.130
hypoxia vs. untreated roots (Col-0) 1.120
osmotic vs. untreated roots (Col-0) 1.096
IAA vs. untreated roots (3h; Col-0) 1.054
IAA vs. untreated roots (4h; Col-0) 1.046
genotoxic vs. untreated roots 1.043
salt vs. untreated roots 1.035
IAA vs. untreated roots (2h; Col-0) 1.032
Fe deficiency vs. untreated roots (Col-0) 1.029
arf17arf19 vs. Col-0 (untreated root tip) 1.029
b
Down-regulated in pi4kß1ß2 roots
A
B
C
D
IAA vs. mock treated roots (1h)
IAA vs. mock treated roots (0.5h)
IAA vs. mock treated roots (2h)
IAA vs. mock treated roots (4h)
IAA vs. mock treated roots (8h)
IAA vs. mock treated roots (12h)
IAA vs. mock treated roots (24h)
IAA vs. mock treated roots (3h)
IAA vs. mock treated roots (0h)
c
Up-regulated in pi4kß1ß2 roots
E
F
IAA vs. mock treated roots (3h)
IAA vs. mock treated roots (0.5h)
IAA vs. mock treated roots (1h)
IAA vs. mock treated roots (2h)
IAA vs. mock treated roots (4h)
IAA vs. mock treated roots (8h)
IAA vs. mock treated roots (12h)
IAA vs. mock treated roots (24h)
IAA vs. mock treated roots (0h)
d
WT
WT+IAA
pi4kß1ß2
pi4kß1ß2+IAA
At1g64590
CSLB5
FLA13
SAUR9
NPF2.4
BRU6
Relative expression, fold change

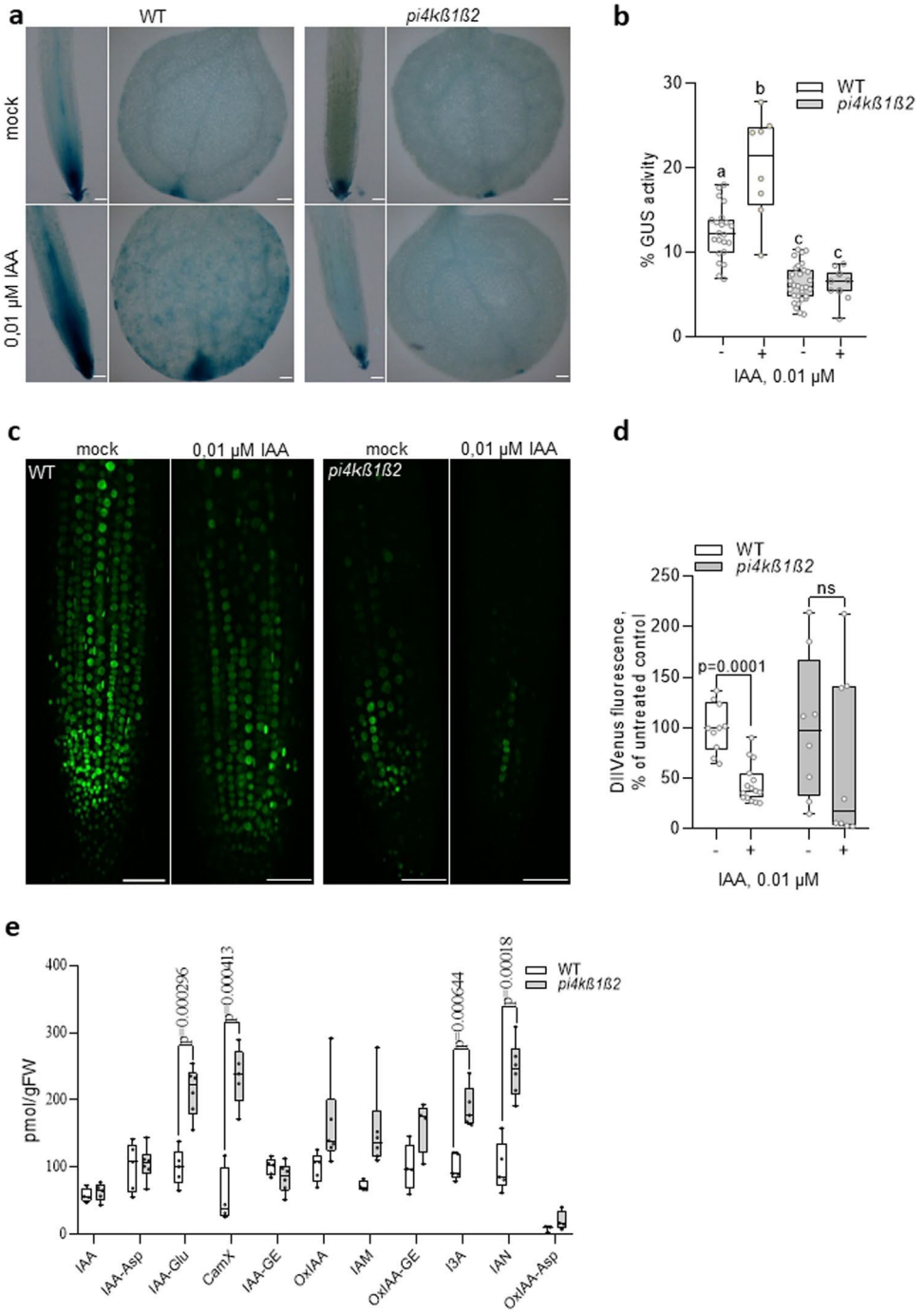

Figure 4. Auxin sensitivity of the *pi4kß1ß2* mutant. (**a**) representative images of DR5-GUS activity in 5-day-old root and cotyledons in the presence or not of 0.01 µM IAA for 12 h, scale bar=100 µm; (**b**) DR5-GUS quantification, % of GUS-stained area in root meristem, n=10; (**c**) representative images of DII-VENUS fluorescence in root tip of 7-day-old seedlings in the presence or not of 0.01 µM IAA for 1 h, maximum intensity Z-projections of 10 nm stacks, scale bar=50 µm; (**d**) DII-VENUS fluorescence quantification, % of meristematic zone; n=10; (**e**) quantitation of IAA metabolites and conjugates in 7-day-old roots, n=6; Central line of the boxplots represents the median, circles represent individual values; *p*-value is indicated for significantly different groups, ns – non significant; unpaired *t*-test (**d**,**e**); The data are presented in means ± SD, n=10, with a Tukey honestly significant difference (HSD) multiple mean comparison post hoc test. Different letters indicate a significant difference (one-way ANOVA, Tukey HSD, $P<0.05$) (**b**); Experiments were repeated three times; data from a representative repeat are shown. IAA = indole-3-acetic acid, IAA-Asp = IAA-aspartate, IAA-Glu = IAA-glutamate, CamX = camalexin, IAA-GE = IAA-glucose ester, OxIAA = oxo-IAA, IAM = Indole-3-acetamide (IAA precursor), OxIAA-GE = oxo-IAA-glucose ester, I3A = indole-3-aldehyde, IAN = Indole-3-acetonitrile (IAA precursor), OxIAA-Asp = oxo-IAA-aspartate.

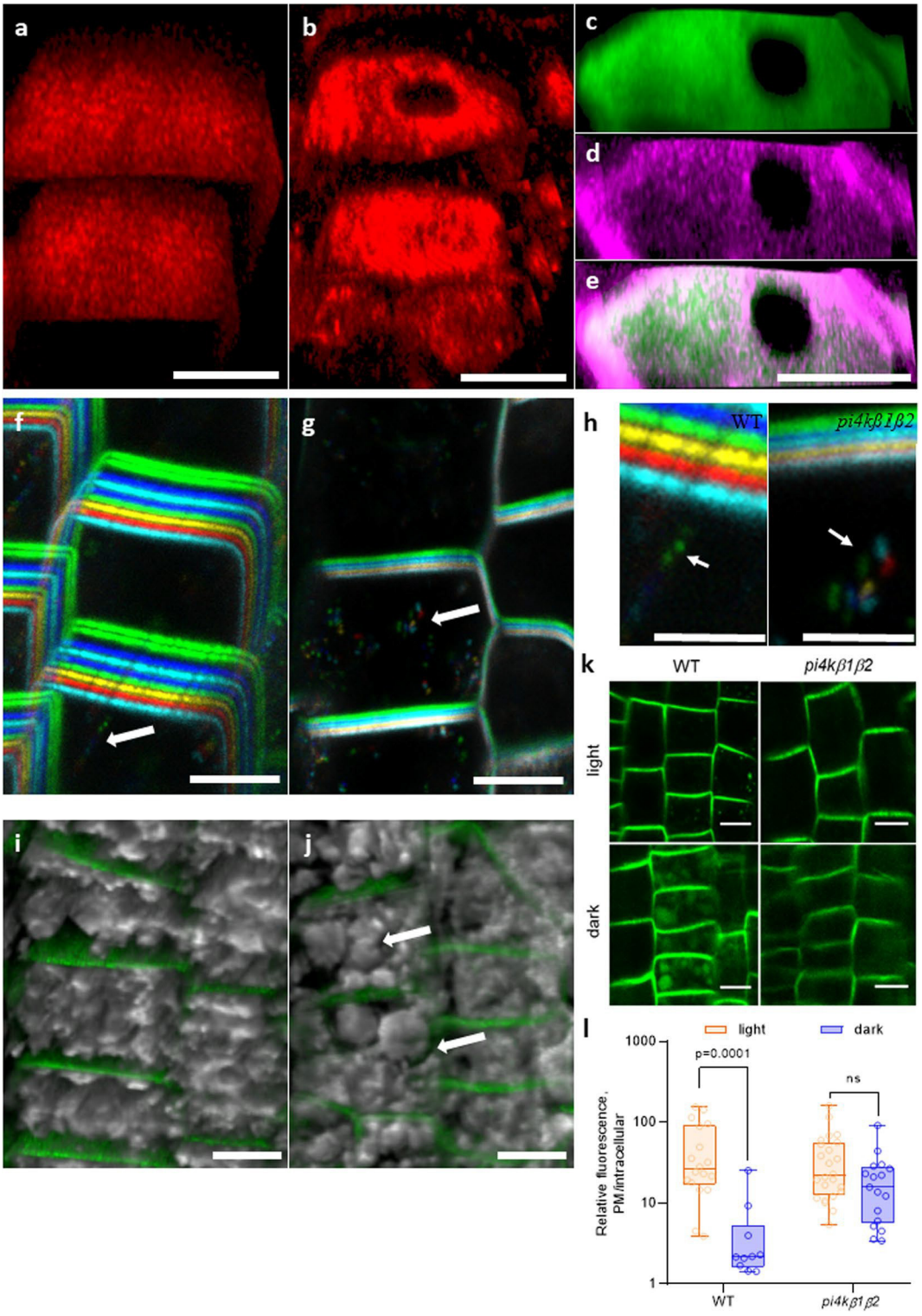

Figure 5. Visualization of PIN2-GFP subcellular distribution by confocal microscopy. (**a**) distribution of PIN2 along the PM in WT roots, immunostaining; (**b**) distribution of PIN2-GFP along the plasma membrane in *pi4kβ1β2* roots, immunostaining; (**c,d,e**) show PIN2-GFP signal overlapping with FM4-64 dye, (**c**, FM4-64; **d**, PIN2-GFP; **e**, merged signals); (**f,g**) color-coded projection of PIN2-GFP distribution and intracellular movement over time in (**f**) WT and (**g**) *pi4kβ1β2* backgrounds; arrows point to vesicles moving in time; (**h**), zoomed part of f and g, scale bars 5 µm, arrows point to vesicles moving in time; (**i,j**) merged 3D reconstruction of pictures taken along the z-axis of the bright field and fluorescent channel of PIN2 distribution along the plasma membrane and vacuole morphology in (**i**) WT and (**j**) *pi4kβ1β2* backgrounds; arrows point to enlarged vacuoles in *pi4kβ1β2*; (**k**) visualization of PIN2-GFP movement towards the lytic vacuole upon a dark shift of whole seedlings. After 1 h, the GFP signal was visible in the WT background, but not in *pi4kβ1β2*; (**l**) quantification of the GFP signal intensity in the lytic vacuole, each circle represents the plasma membrane/intracellular ratio for a single cell; *p*-value is indicated for significantly different groups, ns—non significant; unpaired *t*-test with correction for multiple comparisons; n=25; scale bars 10 µm.

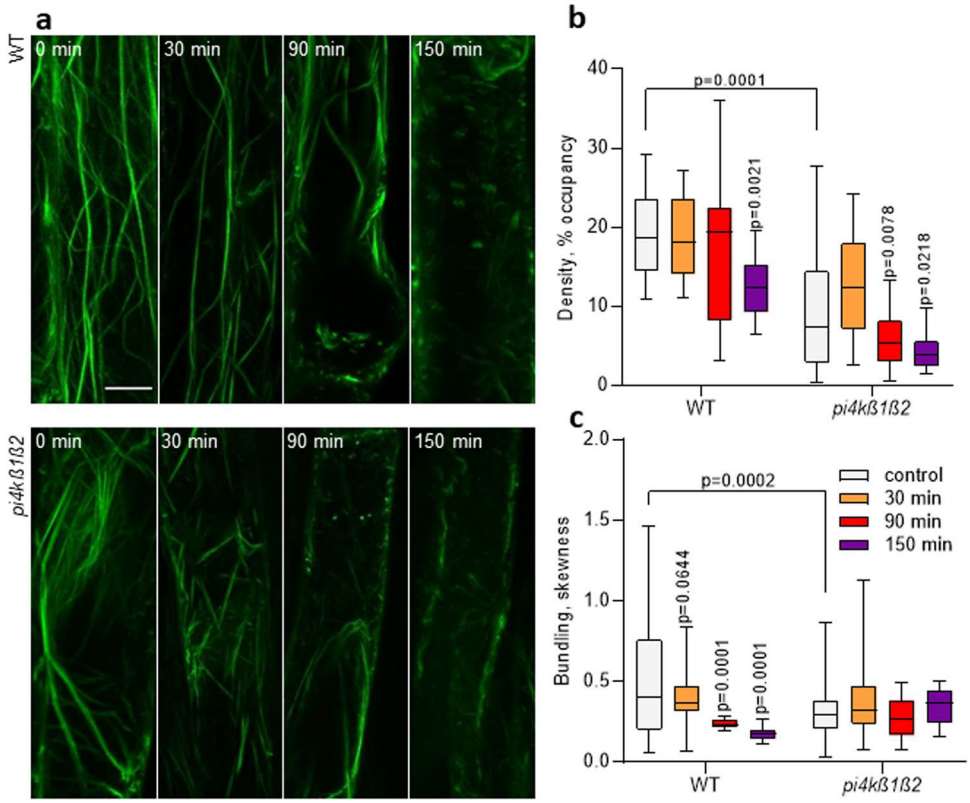

Figure 6. Actin reorganization in the *pi4kß1ß2* mutant in response to latrunculin B. Five-day-old seedlings expressing 35S::LifeAct-GFP were sprayed with 10 µM latB. (**a**) representative maximum intensity projections of root epidermis of WT and *pi4kß1ß2* plants; confocal microscopy, scale bar=10 µm; (**b**) quantitative analysis of the density (expressed as percentage of occupancy) of actin filament arrays in epidermal cells; (**c**) quantitative analysis of the extent of filament bundling (expressed as skewness) in epidermal cells. Central line of the boxplots represents the median, plus represents the mean; circles represent individual values; *p*-value is indicated for significantly different time points within each genotype and for the comparison of genotypes immediately after treatment; one-way ANOVA with Tukey HSD *post-hoc* test; n=10.

metabolite and storage form of IAA and is synthesized upon incubation of plants with high concentrations of IAA, and is considered precursors for auxin degradation[32]. High level of IAA-Glu might result from a constitutive conjugation activity in the double mutant. Transcripts of different GH3 enzymes involved in aminoacid conjugation are indeed markedly up-regulated in the *pi4kß1ß2* roots. The affected balance between precursors or conjugates or IAA might then explain partial auxin-like response in roots. Conversely, this affected balance also probably reflects the affected sensitivity to active auxin. It is likely that in *pi4kß1ß2* mutant, exogenous IAA is conjugated, resulting in the IAA level not changing, as seen by DII-Venus monitoring.

The *pi4kß1ß2* mutant also showed an altered subcellular trafficking behaviour of PIN2, including trapping of the PIN2-GFP fusion protein in rapidly moving vesicles and a reduced transport towards the lytic vacuole upon a dark shift of *pi4kß1ß2* seedlings. Differences in *pi4kß1ß2* vacuolar morphology were also observed, with bigger and less fragmented vacuoles compared to the WT. This phenotype corresponds to that observed when WT Arabidopsis were treated with wortmannin, an inhibitor of PI4K activity[33]. In *pi4kß1ß2* roots, PIN2 localization by immunostaining and staining with FM64 evidenced "black holes" or stubs corresponding to tunnels between adjacent cells, also referred to as "cell wall stubs". This can be linked with unfinished cytokinesis[23,34]. Caillaud et al. (2008)[35] demonstrated that map65-3/ple mutants displayed cell wall stubs and multiple nuclei in the root meristem, both features of cytokinesis-defective mutants. Interestingly, MAP65-3 is a downstream target for inhibition by MAP kinase MPK4, and also a physical interaction between PI4Kβ1 and MPK4 has been reported[23]. Lin et al., (2019)[23] proposed that PI4Kβ1 and MPK4 influence localization and activity of MAP65-3, acting synergistically to control phragmoplast dynamics. The altered cytoskeleton organization in our mutant could explain some of the trafficking issues, as the movement of membrane vesicles depends on the cytoskeleton[36]. For example, it was shown that PIN1 cycling is actin-dependent[37]. Proper assembly of the cytoskeleton in concert with the molecular motors, myosins, is essential for active internal transport, and therefore proper distribution of cargos, like PIN2[1,38]. Rho proteins mediate signals for cytoskeletal reorganization and cell polarity and they are also implicated in the regulation of endo- and exocytosis, and correct localization of PIN1[39]. Moreover, a direct interaction between both PI4Kβ1 and PI4Kβ2 and another GTPase protein involved in membrane trafficking, RabA4B, has been reported[40]. Membrane recruitment of ROP-GTPase ROP6 (and possibly also other ROPs) is

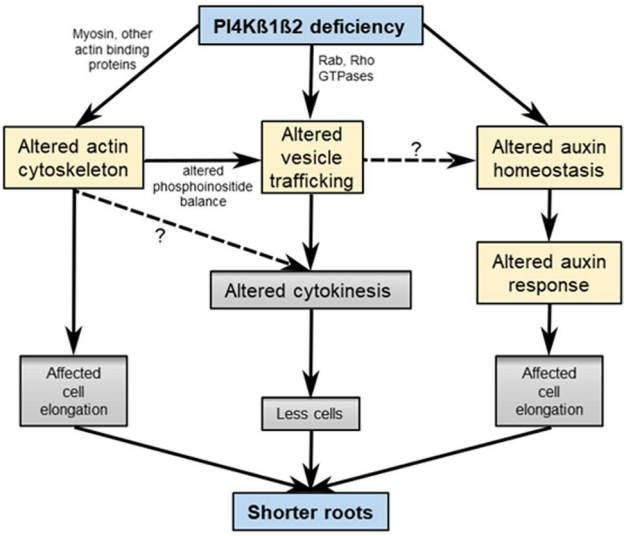

Figure 7. Working model for the impact of *pi4kß1ß2* mutations on root length. The *pi4kß1ß2* mutations lead to an altered actin cytoskeleton, an altered vesicle trafficking and an altered sensitivity to auxin including at the gene expression level. Altered trafficking can be linked to PI4K interacting with small G proteins like Rab or Rho proteins; it could also be a consequence of the weakened cytoskeleton. It is hypothesized that both altered cytoskeleton and trafficking prevent a correct cytokinesis. Finally, we propose that the short root phenotype results from multiple causes: altered actin cytoskeleton, altered cytokinesis, altered trafficking, and altered auxin responses.

also dependent on anionic phospholipids[41,42]. We therefore suggest that an altered regulation of Rho proteins by phosphoinositides could help explain, in part, the observed problems of *pi4kß1ß2* roots.

Can the alteration in trafficking and cytoskeleton explain the insensitivity to auxin? Proper spatial and temporal distribution of auxin in the root tip ensures differentiation of cell files and therefore conditions normal root hair outgrowth. This relies on an auxin efflux carrier modulating auxin circulation within root tip[1]. Therefore, altered trafficking can have consequences on root response to endogenous auxin. Concerning exogenously added auxin, the temporal distribution might not be the key factor and as mentioned above, auxin homeostasis probably explain the phenotypes.

Similar root phenotypes have been observed already in mutants affected in other steps of phosphoinositide turn-over. The *pip5k1pi5k2* mutant lacking two isoforms of PI4,5 K also showed shorter roots, a reduced meristematic zone and a lower sensitivity to exogenous auxins[43]. The *pip5k2* mutant has less lateral root formation and impaired gravitropism[43,44]. On the contrary, our *pi4kß1ß2* mutant has more lateral roots[45]. We can thus speculate that some of the observed phenotypes of *pi4kß1ß2* seedlings are in part due to altered production of PI4,5P2. As mentioned earlier, *pi4kß1ß2* roots did not respond to a gravitropic stimulus, which is dependent on fine-tuned spatial and temporal modulation of PIN2 distribution as well as auxin gradient regulation[46–49]. On the other hand, root bending requires a functional cytoskeleton network[49]. Proper actin cytoskeleton assembly is also required to trigger and maintain root hair integrity[50,51], which is compromised in the *pi4kß1ß2* mutant. Furthermore, phosphoinositides can regulate actin dynamics by direct interaction with actin-binding proteins (ABPs)[52,53], or affect actin polymerization, dynamics, and association with membranes indirectly through regulation of the activity and localization of Rho GTPases[54] or via recruiting scaffolding proteins to the PM[52,55]. Indeed an altered actin cytoskeleton was observed in our mutant and phosphoinositides are well known to regulate actin organization[56]. A *pi4p5k10/11* double mutant also displayed an increased sensitivity to latB, whereas PI4P5K10 overexpression resulted in aggregation of the apical actin fringe in tobacco pollen tubes[43].

Nevertheless, the intermediate signaling links connecting PI4Kbeta 1/2 deficiency and the resulting misregulation of PI4P on endomembranes with altered ectopic auxin signaling activities remain to be clarified. For instance, root gravitropic growth requires establishing of PIN2 polarity, that also involves MEMBRANE ASSOCIATED KINASE REGULATOR 4, MAKR4, acting downstream of auxin receptors TRANSMEMBRANE KINASE1 (TMK1). At the same time, PIN2 and MAKR4 plasma membrane localisation is dependent on anionic phospholipids turnover[57]. On the other hand, root bending requires cell wall modification that is under control of AHA H^+-ATPases in cooperation with TMKs[58]. Interestingly, a mutant *cngc2*, deficient in plasma membrane-localized CYCLIC NUCLEOTIDE-GATED ION CHANNEL 2 exhibits a phenotype, partially similar to *pi4kß1ß2*. This concerns stunted root and rosette growth, SA accumulation in the leaves, lower gravitropic bending and impaired sensitivity to exogenous auxin, but, unlike *pi4kß1ß2*, *cngc2* mutant accumulates higher endogenous IAA[59].

Based on our observations, a working model is proposed that assembles multiple causes leading to the short root phenotype of the *pi4kß1ß2* mutant that arises from several root developmental defects, including reduced cell number and length (Fig. 7). Many correlate with altered dynamics of intracellular delivery processes. Plasma

membrane establishment remains incomplete, cell architecture is misshaped, and PIN2 turnover is altered in the root elongation zone. This can be associated with a lower stability of the actin filaments network. Based on DII-VENUS degradation and gene expression, there appears to be a lack of response to auxin, endogenous or exogenous, in the *pi4kß1ß2* mutant. A link between altered trafficking/cytoskeleton integrity and this lack of gene expression response will require further investigations.

Materials and methods

Plant material. Experiments were performed using *A. thaliana* Col-0 as the WT control and the following mutant lines: *pi4kβ1β2* (SALK_040479/SALK_09069[30]), CycB1::GUS[60], DR5::GUS[27], PIN2::PIN2-GFP[43], PIN2::PIN2-GFP in a *pi4kβ1β2* background[23], DII-VENUS[28], DII-VENUS in *pi4kβ1β2* (this study), 35S::LifeAct-GFP, 35S::LifeAct-GFP in a *pi4kβ1β2* background[61]. The DII-VENUS construct was introduced into *pi4kβ1β2* by floral dip transformation; three independent lines were selected and the T4 generation was studied. CycB1::GUS[60] and DR5::GUS[27] constructs were introduced into the *pi4kβ1β2* background by crossing, and homozygous F3 seeds were used. Genotyping primers are listed in Supplementary Table 1. This study complies with relevant institutional, national, and international guidelines and legislation for using plant material. Analytical grade chemicals used in this study were purchased from Sigma Aldrich (St. Louis, Missouri, USA).

Plant cultivation. Seeds were surface sterilized with 1.6% sodium hypochlorite (30% of SAVO®, Unilever) solution containing 0.02% (v/v) TWEEN20 (Sigma Aldrich, St. Louis, Missouri, USA). Seeds were stratified for 2 days at 4 °C in the dark. Seeds were germinated for 3 days in Petri dishes containing half-strength Murashige–Skoog basal salt medium (Duchefa, Haarlem, Netherlands), pH 5.7, supplemented with 1% (w/v) sucrose and 0.8% (w/v) plant agar (Duchefa, Haarlem, Netherlands) at 22 °C under a 16 h light/8 h dark regime in a vertical position.

For the primary root length analysis, 4 days after germination, seedlings were transferred to square Petri plates containing the same medium supplemented or not with hormones (IAA at 0.05, 0.1 or 1 μM final concentration; BAP, at 0.1, 0.5, 1 or 5 μM; SA at 2, 10 or 20 μM). Stock solutions at 200 mM were prepared in distilled water and few drops of 1 N NaOH. After 7 days of cultivation in vertical position Petri dishes were scanned for the primary root length measurement (Epson Perfection V700 Photo, Suwa, Japan, at 600 dpi resolution). For the measurement of the lengths of meristem, elongation zone and cortical cells, roots were observed under an ApoTome Zeiss microscope with a 5 × objective at bright field settings. Images were analyzed with FiJi software[62]. At least 12 seedlings were analyzed for each variant. For the measurement of root hair length and density, 5-day-old seedlings were photographed under a stereo microscope (SteREO Discovery V8, Carl Zeiss GmbH, Jena, Germany) equipped with an AxioCam HRc camera. Images were imported into FiJi software and root hair length was measured manually using a segmented line tool. At least 60 root hairs from 10 seedlings were analyzed for each variant. For PIN2 localization and dynamics analysis, DII-Venus assay or actin structure evaluation, 7-days old seedlings were used. For actin structure evaluation, seedlings expressing 35S::LifeAct-GFP were sprayed with 10 μM latB (latrunculin B) for different time incubations (30 min, 90 min and 150 min) and were used for confocal microscopy. For DII-VENUS assay, seedlings were transferred to the media supplemented 0.01 μM IAA for 1 h and subjected to microscopy. The fluorescence intensity of nuclei was extracted using FiJi software.

Gravitropic test. Gravitropic response test was performed as previously described[46]. Five-day-old seedlings were transferred onto fresh Petri Dishes containing half-strength Murashige–Skoog basal salt medium (Duchefa, Haarlem, Netherlands), pH 5.7, supplemented with 1% (w/v) sucrose and 0.8% (w/v) plant agar (Duchefa, Haarlem, Netherlands) and aligned in a horizontal orientation. Plants were scanned at indicated time points using a Horizontal LSM880 with Airyscan module for 12 h and images were used to determine root reorientation. The root turning angle and length were calculated for each time point. Ten roots were imaged for each genotype.

GUS staining. GUS staining was performed as previously described[63]. Briefly, 4- or 8-day-old seedlings were incubated in 2 mM X-Gluc, 50 mM NaH_2PO_4, pH 7, 0.5% (v/v) Triton-X, 0.5 mM K-ferricyanide, for 16 h at 37 °C. Chlorophyll was removed by repeated washing with 80% (v/v) ethanol. Imaging was performed using an ApoTome Zeiss microscope with a 5× objective at bright field settings.

Confocal microscopy. A Zeiss LSM 880 inverted confocal laser scanning microscope (Carl Zeiss AG, Germany) was used with a 40 × C-Apochromat objective (NA = 1.2 W). Fluorescence signals were processed with Zen Blue software (Zeiss), where PIN2 distribution was evaluated as a ratio of mean fluorescence intensity at the apical PM to mean intracellular fluorescence intensity of individual cells. Fluorescence associated with actin filaments (LifeAct-GFP) or DII-VENUS was acquired by excitation at 488 nm and emission at 490–540 nm for GFP. Images were acquired in z-stacks (step size 0.43 μm, 40–50 sections per stack). Actin filaments density and DII-VENUS signal intensity was calculated by FiJi software as the percent occupancy of GFP signal in each Maximum intensity projection. For each variant, fluorescent intensity of at least 5 roots was analyzed with 1–5 ROI (region of interest) per 1 root (ROI corresponds to one entire cell for actin; ROI corresponds to meristematic zone for DII-VENUS). For analyzing the skewness, all z-stack images were skeletonized and projected using a plugin moment calculator.

For tracking PIN2-GFP distribution in WT and *pi4kß1ß2* over time (supplementary movies SM3 and SM4), ten frames were continuously obtained by confocal microscopy to track the movement of PIN2:GFP in root epidermis cells in the transition zone and compiled to a movie. PIN2-GFP subcellular distribution and cell properties were monitored on a Zeiss LSM880 microscope (AxioObserver, objective C-Apochromat 40x/1.2 W

Korr FCS M27, Filter 493–598, Laser 488 nM, using zoom factor 6. Original picture size is 35,42 µm × 35,42 µm, scale bar is 10 µm.

For root hair video showing cytoplasmic streaming (supplementary movies SM5 and SM6), maximum intensity projections of a Z-stack of a root hair were taken over time. Fluorescent channel and bright field are presented together. Fluorescent channel: visualization of cytoplasmic streaming in root hair cell outgrowing a root hair, based on differential movement of fluorescent intracellular structures in the line PIN2::PIN2-GFP compared to the mutant expressing PIN2-GFP. The movie was reconstructed from confocal pictures captured in 20 frames (time-lapse) and in 18 (WT background)/19 slices (mutant background) through the root hair along the z-axis. Original picture size is 106.27 µm × 106.27 µm, pictures were captures with EC Plan-Neofluar 20x/0.50 (WD = 2.0 mm) objective, using zoom factor 4. Scale bar is 10 µm. Brightfield channel: visualization of cytoplasmic streaming in a movie reconstructed from confocal pictures captured in 20 frames (time-lapse) and in 18 (WT background)/19 slices (mutant background) along the root hair in the z-axis. Original picture size is 106.27 µm × 106.27 µm, pictures were captures with EC Plan-Neofluar 20x/0.50 (WD = 2.0 mm) objective, using zoom factor 4. Scale bar is 10 µm.

FM 4–64 staining of the plasma membrane. Five-day-old *A. thaliana* seedlings expressing PIN2::PIN2-GFP[47] were incubated with 2 µM FM 4–64 (Molecular Probes, catalogue number T13320) in half-strength Murashige and Skoog (Sigma Aldrich, St. Louis, Missouri, USA) liquid medium in multi-well plates for 5 min and then rinsed 3 times in liquid medium[64]. The seedlings were observed using a confocal scanning microscope Zeiss LSM 880 with Airyscan module.

PIN2 immunolocalization. Whole mount immunolocalization of 5–day–old seedlings was performed as described previously[65] with minor changes. The protocol was adapted to the InSituPro VS liquid-handling robot (Intavis AG, Germany). Prior to immunolocalization, seedlings were fixed 1 h with 4% paraformaldehyde dissolved in MTSB (50 mM PIPES, 5 mM EGTA, 5 mM $MgSO_4{\cdot}7H_2O$ pH 7, adjusted with KOH), at room temperature, with no vacuum. In the robot, the procedure started with several washes with MTSB-T (MTSB + 0.01% TritonX-100) then cell walls were digested with 0.05% Pectolyase Y-23 in MTSB-T and membranes were permeated with DMSO/Igepal in MTSB-T. Samples were blocked with BSA (blocking solution: 2% BSA in MTSB-T) and incubated first with anti-PIN2 rabbit antibody (kindly provided by Prof. C. Luschnig, dilution 1:500) and then a secondary anti-rabbit Alexa Fluor 546 antibody (Thermo Fisher Scientific, dilution 1:1000). Both antibodies were diluted in BSA. Between the described steps, washes with MTSB-T were provided and at the end MTSB-T was exchanged for deionized water. Seedlings were then transferred from the robot to 50% glycerol in deionized water and the fluorescence signal was measured using a confocal scanning microscope Zeiss LSM 880 with Airyscan module.

RNA extraction and RNA-seq. For each of the 3 biological repetitions, RNA samples were obtained by pooling RNAs from more than 70 plants. Seven-days-old seedlings roots (100–200 mg fresh weight) were frozen in liquid N_2. Roots were homogenized in tubes with 1 g of 1.3 mm silica beads using a FastPrep-24 instrument (MP Biomedicals, USA). Total RNA was isolated using a Spectrum Plant Total RNA kit (Sigma-Aldrich, USA) and treated with a DNA-free kit (Ambion, USA). The quantity of extracted RNA was measured using NanoDrop. Sequencing was carried out using an Illumina NexSeq500 (IPS2 POPS platform). RNA-seq libraries were made using the TruSeq Stranded mRNA kit (Illumina®, California, USA). The RNA-seq samples were Single End (SE) sequenced, stranded with a sizing of 260 bp and a read length of 75 bases, lane repartition and barcoding gave approximately 45 million SE reads per sample.

Gene transcription measurement was conducted as described previously[61]. In general, 1 µg of RNA was converted into cDNA with M-MLV RNase H–Point Mutant reverse transcriptase (Promega Corp., USA) and an anchored oligo dT21 primer (Metabion, Germany). Gene expression was quantified by qRT-PCR using a LightCycler 480 SYBR Green I Master kit and LightCycler 480 (Roche, Switzerland). The PCR conditions were 95 °C for 10 min followed by 45 cycles of 95 °C for 10 s, 55 °C for 20 s, and 72 °C for 20 s. Melting curve analysis was then conducted. CT values of target genes were normalized to the housekeeping gene TIP41. A list of the analyzed genes and primers is available in Supplementary table 1.

RNA-seq bioinformatic treatments and analyses. To facilitate comparisons, each sample followed the same steps from trimming to counts. RNA-Seq preprocessing included trimming library adapters and performing quality controls. The raw data (fastq) were trimmed using the Trimmomatic[66] tool for a Phred Quality Score Qscore > 20, read length > 30 bases, and ribosome sequences were removed with the sortMeRNA tool[67]. The genomic mapper STAR (version 2.7. 3a[68]) was used to align reads against the *A. thaliana* genome (from TAIRv10), with options–outSAMprimaryFlag AllBestScore–outFilterMultimapScoreRange 0 to keep the bests results. Transcript abundance of each gene was calculated with STAR and counts only single reads for which reads map unambiguously one gene, thus removing multi-hits. According to these rules, around 97% of SE reads were associated with a gene, 1–2% of SE reads were unmapped and 1.22–1.66% of SE reads with multi-hits were removed. Differential analyses followed the procedure previously described[69]. Briefly, genes with less than 1 read after a counts-per-million (CPM) normalization in at least one half of the samples were discarded. Library size was normalized using the trimmed mean of M-value (TMM) method and count distribution was modeled with a negative binomial generalized linear model. Dispersion was estimated by the edgeR method[70] in the statistical software 'R'[71] (Version 3.2.5 R Development Core Team (2005). Expression differences compared 2 samples using likelihood ratio tests and *p*-values were adjusted with the Benjamini–Hochberg procedure to control False Discovery Rate (FDR). A gene was declared differentially expressed if the adjusted *p*-value < 0.05.

Genes were classified using the Classification SuperViewer Tool developed by[72] as described previously[20]. The classification source was set to Gene Ontology categories as defined by[73]. The frequency of each category was normalized to the whole Arabidopsis set. The mean and standard deviation for 100 boot-straps of our input set were calculated to provide some idea as to over- or under-representation reliability. Similarity analysis were performed using tools developed by Genevestigator[29]. The "Hierarchical clustering" tool works on the expression matrix defined by a microarray experiment selection and a gene selection. The "Biclustering" tool identifies groups of genes that are expressed above or under a set threshold ratio in a subset of conditions rather than in all conditions.

Hormone measurements. Whole roots (50–100 mg) were harvested from 7-day-old vertical grown seedlings. At least 6 samples were analyzed for WT and *pi4kβ1β2*. Hormone analysis was performed with a LC/MS system consisting of UHPLC 1290 Infinity II (Agilent, Santa Clara, CA, USA) coupled to 6495 Triple Quadrupole Mass Spectrometer (Agilent, Santa Clara, CA, USA), operating in MRM mode, with quantification by the isotope dilution method. Detailed methodology was described previously[74].

Data deposition. Experimental steps, from growth conditions to bioinformatic analyses, have been deposited in the CATdb database[75] as ProjectID NGS2020_14_pi4kb1b2 and further submitted to the international repository GEO[76] as ProjetID=GSE179635.

Statistical analysis. At least three biological repetitions were carried out for all experiments, and at least 10 seedlings were analyzed for each treatment. Student's *t*-test with correction for multiple comparisons and one-way ANOVA with Tukey's HSD post-hoc test were applied; the exact number of values and statistical procedures are stated in the figure legends.

Received: 17 November 2021; Accepted: 4 April 2022
Published online: 28 April 2022

References

1. Retzer, K. & Weckwerth, W. The TOR–auxin connection upstream of root hair growth. *Plants* **10**, 150 (2021).
2. Waldie, T. & Leyser, O. Cytokinin targets auxin transport to promote shoot branching. *Plant Physiol.* **177**, 803–818 (2018).
3. Luschnig, C. & Vert, G. The dynamics of plant plasma membrane proteins: PINs and beyond. *Development (Cambridge, England)* **141**, 2924–2938 (2014).
4. Habets, M. & Offringa, R. PIN-driven polar auxin transport in plant developmental plasticity: A key target for environmental and endogenous signals. *The New Phytol.* **203**, 1 (2014).
5. Semeradova, H., Montesinos, J. C. & Benkova, E. All roads lead to Auxin: Post-translational regulation of Auxin transport by multiple hormonal pathways. *Plant Commun.* **1**, 100048 (2020).
6. Pokotylo, I., Kravets, V., Martinec, J. & Ruelland, E. The phosphatidic acid paradox: Too many actions for one molecule class? Lessons from plants. *Prog. Lipid Res.* **71**, 43–53 (2018).
7. Noack, L. C. & Jaillais, Y. Functions of anionic lipids in plants. *Annu. Rev. Plant. Biol.* **71**, 71–102 (2020).
8. Jaillais, Y. & Ott, T. The nanoscale organization of the plasma membrane and its importance in signaling: A proteolipid perspective1. *Plant Physiol.* **182**, 1682–1696 (2020).
9. Gronnier, J. *et al.* Structural basis for plant plasma membrane protein dynamics and organization into functional nanodomains. *eLife* **6**, e26404 (2017).
10. Galvan-Ampudia, C. S. *et al.* Temporal integration of auxin information for the regulation of patterning. *eLife* **9**, e55832 (2020).
11. Ke, M. *et al.* Salicylic acid regulates PIN2 auxin transporter hyperclustering and root gravitropic growth via Remorin-dependent lipid nanodomain organisation in Arabidopsis thaliana. *New Phytol.* **229**, 963–978 (2021).
12. McKenna, J. F. *et al.* The cell wall regulates dynamics and size of plasma-membrane nanodomains in Arabidopsis. *PNAS* **116**, 12857–12862 (2019).
13. Akhter, S. *et al.* Role of Arabidopsis AtPI4Kγ3, a type II phosphoinositide 4-kinase, in abiotic stress responses and floral transition. *Plant Biotechnol. J.* **14**, 215–230 (2016).
14. Galvão, R. M., Kota, U., Soderblom, E. J., Goshe, M. B. & Boss, W. F. Characterization of a new family of protein kinases from Arabidopsis containing phosphoinositide 3/4-kinase and ubiquitin-like domains. *Biochem. J.* **409**, 117–127 (2008).
15. Cacas, J.-L. *et al.* Revisiting plant plasma membrane lipids in tobacco: A focus on sphingolipids. *Plant Physiol* **170**, 367–384 (2016).
16. Delage, E., Ruelland, E., Guillas, I., Zachowski, A. & Puyaubert, J. Arabidopsis type-III phosphatidylinositol 4-kinases β1 and β2 are upstream of the phospholipase C pathway triggered by cold exposure. *Plant Cell Physiol.* **53**, 565–576 (2012).
17. Djafi, N. *et al.* The Arabidopsis DREB2 genetic pathway is constitutively repressed by basal phosphoinositide-dependent phospholipase C coupled to diacylglycerol kinase. *Front. Plant Sci.* **4**, 307 (2013).
18. Krinke, O., Novotná, Z., Valentová, O. & Martinec, J. Inositol trisphosphate receptor in higher plants: Is it real?. *J. Exp. Bot.* **58**, 361–376 (2007).
19. Ruelland, E. *et al.* Salicylic acid modulates levels of phosphoinositide dependent-phospholipase C substrates and products to remodel the Arabidopsis suspension cell transcriptome. *Front. Plant Sci.* **5**, 608 (2014).
20. Kalachova, T. *et al.* The inhibition of basal phosphoinositide-dependent phospholipase C activity in Arabidopsis suspension cells by abscisic or salicylic acid acts as a signalling hub accounting for an important overlap in transcriptome remodelling induced by these hormones. *Environ. Exp. Bot.* **123**, 37–49 (2016).
21. Šašek, V. *et al.* Constitutive salicylic acid accumulation in pi4kIIIβ1β2 Arabidopsis plants stunts rosette but not root growth. *New Phytol.* **203**, 805–816 (2014).
22. Pluhařová, K. *et al.* "Salicylic Acid Mutant Collection" as a Tool to Explore the Role of Salicylic Acid in Regulation of Plant Growth under a Changing Environment. *Int. J. Mol. Sci.* **20**, 1 (2019).
23. Lin, F. *et al.* A dual role for cell plate-associated PI4Kβ in endocytosis and phragmoplast dynamics during plant somatic cytokinesis. *The EMBO Journal* **38**, e100303 (2019).
24. Kang, B.-H., Nielsen, E., Preuss, M. L., Mastronarde, D. & Staehelin, L. A. Electron tomography of RabA4b- and PI-4Kβ1-labeled trans Golgi network compartments in Arabidopsis. *Traffic* **12**, 313–329 (2011).

25. Preuss, M. L. *et al.* A role for the RabA4b effector protein PI-4Kbeta1 in polarized expansion of root hair cells in Arabidopsis thaliana. *J. Cell Biol.* **172**, 991–998 (2006).
26. Singh, S. K., Fischer, U., Singh, M., Grebe, M. & Marchant, A. Insight into the early steps of root hair formation revealed by the procuste1 cellulose synthase mutant of Arabidopsis thaliana. *BMC Plant Biol.* **8**, 57 (2008).
27. Ulmasov, T., Liu, Z. B., Hagen, G. & Guilfoyle, T. J. Composite structure of auxin response elements. *Plant Cell* **7**, 1611–1623 (1995).
28. Brunoud, G. *et al.* A novel sensor to map auxin response and distribution at high spatio-temporal resolution. *Nature* **482**, 103–106 (2012).
29. Hruz, T. *et al.* Genevestigator V3: A Reference Expression Database for the Meta-Analysis of Transcriptomes. *Adv. Bioinf.* **2008**, e420747 (2008).
30. Preuss, M. L., Serna, J., Falbel, T. G., Bednarek, S. Y. & Nielsen, E. The arabidopsis rab GTPase RabA4b localizes to the tips of growing root hair cells. *Plant Cell* **16**, 1589–1603 (2004).
31. Sassi, M. *et al.* COP1 mediates the coordination of root and shoot growth by light through modulation of PIN1- and PIN2-dependent auxin transport in Arabidopsis. *Development* **139**, 3402–3412 (2012).
32. Staswick, P. E. The tryptophan conjugates of jasmonic and indole-3-acetic acids are endogenous Auxin inhibitors. *Plant Physiol.* **150**, 1310–1321 (2009).
33. Löfke, C., Dünser, K., Scheuring, D. & Kleine-Vehn, J. Auxin regulates SNARE-dependent vacuolar morphology restricting cell size. *eLife* **4**, e05868 (2015).
34. Kang, B.-H., Busse, J. S. & Bednarek, S. Y. Members of the arabidopsis dynamin-like gene family, ADL1, are essential for plant cytokinesis and polarized cell growth[W]. *Plant Cell* **15**, 899–913 (2003).
35. Caillaud, M.-C. *et al.* MAP65-3 microtubule-associated protein is essential for nematode-induced giant cell ontogenesis in arabidopsis. *Plant Cell* **20**, 423–437 (2008).
36. Glanc, M., Fendrych, M. & Friml, J. PIN2 polarity establishment in arabidopsis in the absence of an intact cytoskeleton. *Biomolecules* **9**, 222 (2019).
37. Geldner, N., Friml, J., Stierhof, Y.-D., Jürgens, G. & Palme, K. Auxin transport inhibitors block PIN1 cycling and vesicle trafficking. *Nature* **413**, 425–428 (2001).
38. Goldstein, R. E. & van de Meent, J.-W. A physical perspective on cytoplasmic streaming. *Interface Focus* **5**, 20150030 (2015).
39. Nagawa, S. *et al.* ROP GTPase-dependent actin microfilaments promote PIN1 polarization by localized inhibition of clathrin-dependent endocytosis. *PLOS Biol.* **10**, e1001299 (2012).
40. Antignani, V. *et al.* Recruitment of PLANT U-BOX13 and the PI4Kβ1/β2 phosphatidylinositol-4 kinases by the small GTPase RabA4B plays important roles during salicylic acid-mediated plant defense signaling in arabidopsis. *Plant Cell* **27**, 243–261 (2015).
41. Smokvarska, M., Jaillais, Y. & Martinière, A. Function of membrane domains in rho-of-plant signaling. *Plant Physiol.* **185**, 663–681 (2021).
42. Smokvarska, M. *et al.* A plasma membrane nanodomain ensures signal specificity during osmotic signaling in plants. *Curr. Biol.* **30**, 4654-4664.e4 (2020).
43. Ischebeck, T. *et al.* Phosphatidylinositol 4,5-bisphosphate influences PIN polarization by controlling clathrin-mediated membrane trafficking in Arabidopsis. *Plant Cell* **25**, 4894–4911 (2013).
44. Mei, Y., Jia, W.-J., Chu, Y.-J. & Xue, H.-W. Arabidopsis phosphatidylinositol monophosphate 5-kinase 2 is involved in root gravitropism through regulation of polar auxin transport by affecting the cycling of PIN proteins. *Cell Res.* **22**, 581–597 (2012).
45. Reyes-Hernández, B. J. *et al.* Root stem cell niche maintenance and apical meristem activity critically depend on threonine synthase1. *J. Exp. Bot.* **70**, 3835–3849 (2019).
46. Retzer, K. *et al.* Brassinosteroid signaling delimits root gravitropism via sorting of the Arabidopsis PIN2 auxin transporter. *Nat. Commun.* **10**, 5516 (2019).
47. Abas, L. *et al.* Intracellular trafficking and proteolysis of the Arabidopsis auxin-efflux facilitator PIN2 are involved in root gravitropism. *Nat Cell Biol* **8**, 249–256 (2006).
48. Luschnig, C., Gaxiola, R. A., Grisafi, P. & Fink, G. R. EIR1, a root-specific protein involved in auxin transport, is required for gravitropism in Arabidopsis thaliana. *Genes Dev.* **12**, 2175–2187 (1998).
49. Kleine-Vehn, J. *et al.* Differential degradation of PIN2 auxin efflux carrier by retromer-dependent vacuolar targeting. *PNAS* **105**, 17812–17817 (2008).
50. Ketelaar, T. The actin cytoskeleton in root hairs: all is fine at the tip. *Curr Opin Plant Biol* **16**, 749–756 (2013).
51. Grierson, C., Nielsen, E., Ketelaarc, T. & Schiefelbein, J. Root Hairs. *Arabidopsis Book* **12**, e0172 (2014).
52. Wu, C.-Y. *et al.* The role of phosphoinositide-regulated actin reorganization in chemotaxis and cell migration. *Br. J. Pharmacol.* **171**, 5541–5554 (2014).
53. Sun, T., Li, S. & Ren, H. Profilin as a regulator of the membrane-actin cytoskeleton interface in plant cells. *Front. Plant Sci.* **4**, 512 (2013).
54. Molendijk, A. *et al.* Arabidopsis thaliana Rop GTPases are localized to tips of root hairs and control polar growth. *EMBO J.* **20**, 2779–2788 (2001).
55. Pleskot, R., Pejchar, P., Staiger, C. & Potocký, M. When fat is not bad: the regulation of actin dynamics by phospholipid signaling molecules. *Front. Plant Sci.* **5**, 5 (2014).
56. Janmey, P. A., Bucki, R. & Radhakrishnan, R. Regulation of actin assembly by PI(4,5)P2 and other inositol phospholipids: An update on possible mechanisms. *Biochem. Biophys. Res. Commun.* **506**, 307–314 (2018).
57. Marquès-Bueno, M. M. *et al.* Auxin-regulated reversible inhibition of TMK1 signaling by MAKR2 modulates the dynamics of root gravitropism. *Curr. Biol.* **31**, 228-237.e10 (2021).
58. Lin, W. *et al.* TMK-based cell-surface auxin signalling activates cell-wall acidification. *Nature* **599**, 278–282 (2021).
59. Chakraborty, S. *et al.* Cyclic nucleotide-gated ion channel 2 modulates Auxin homeostasis and signaling. *Plant Physiol* **187**, 1690–1703 (2021).
60. Colón-Carmona, A., You, R., Haimovitch-Gal, T. & Doerner, P. Spatio-temporal analysis of mitotic activity with a labile cyclin–GUS fusion protein. *Plant J.* **20**, 503–508 (1999).
61. Kalachova, T. *et al.* Interplay between phosphoinositides and actin cytoskeleton in the regulation of immunity related responses in Arabidopsis thaliana seedlings. *Environ. Experim. Bot.* **167**, 103867 (2019).
62. Schindelin, J. *et al.* Fiji: an open-source platform for biological-image analysis. *Nat. Methods* **9**, 676–682 (2012).
63. Figueroa-Balderas, R. E., García-Ponce, B. & Rocha-Sosa, M. Hormonal and stress induction of the gene encoding common bean acetyl-coenzyme A carboxylase. *Plant Physiol.* **142**, 609–619 (2006).
64. Marhava, P. *et al.* Plasma membrane domain patterning and self-reinforcing polarity in Arabidopsis. *Dev. Cell* **52**, 223-235.e5 (2020).
65. Sauer, M. *et al.* Canalization of auxin flow by Aux/IAA-ARF-dependent feedback regulation of PIN polarity. *Genes Dev* **20**, 2902–2911 (2006).
66. Bolger, A. M., Lohse, M. & Usadel, B. Trimmomatic: a flexible trimmer for Illumina sequence data. *Bioinformatics* **30**, 2114–2120 (2014).
67. Kopylova, E., Noé, L. & Touzet, H. SortMeRNA: fast and accurate filtering of ribosomal RNAs in metatranscriptomic data. *Bioinformatics* **28**, 3211–3217 (2012).
68. Dobin, A. *et al.* STAR: ultrafast universal RNA-seq aligner. *Bioinformatics* **29**, 15–21 (2013).

69. Rigaill, G. *et al.* Synthetic data sets for the identification of key ingredients for RNA-seq differential analysis. *Brief Bioinform.* **19**, 65–76 (2018).
70. McCarthy, D. J., Chen, Y. & Smyth, G. K. Differential expression analysis of multifactor RNA-Seq experiments with respect to biological variation. *Nucl. Acids Res.* **40**, 4288–4297 (2012).
71. R Core Team. R: A Language and Environment for Statistical Computing. (2018).
72. Zhu, T. A browser-based functional classification SuperViewer for Arabidopsis genomics. (2003).
73. Ashburner, M. *et al.* Gene Ontology: tool for the unification of biology. *Nat. Genet.* **25**, 25–29 (2000).
74. Prerostova, S. *et al.* Light quality and intensity modulate cold acclimation in Arabidopsis. *Int. J. Mol. Sci.* **22**, 2736 (2021).
75. Gagnot, S. *et al.* CATdb: A public access to Arabidopsis transcriptome data from the URGV-CATMA platform. *Nucl. Acids Res.* **36**, D986-990 (2008).
76. Edgar, R., Domrachev, M. & Lash, A. E. Gene Expression Omnibus: NCBI gene expression and hybridization array data repository. *Nucl. Acids Res.* **30**, 207–210 (2002).

Acknowledgements

This work was supported by the European Regional Development Fund, Project "Centre for Experimental Plant Biology" [Grant No. CZ.02.1.01/0.0/0.0/16_019/0000738] and Czech Science Foundation (Grant No. 19-13375Y). IEB Imaging Facility is supported by a project of the Ministry of Education, Youth and Sports "National Infrastructure for Biological and Medical Imaging (Czech-BioImaging – LM2018129)". The POPS platform benefits from the support of the LabEx Saclay Plant Sciences-SPS (ANR-10-LABX-0040-SPS). AS benefited from the French government grant for PhD studies in co-tutelle.

Author contributions

A.S., T.K. and E.R. designed the study. A.S., T.K., K.R., A.J., P.D., J.L., R.P., J.A., A.G., S.P., L.S.-T. performed the experiments. A.S.., T.K., L.B. and E.R. analyzed data. A.S., T.K., and E.R. wrote the manuscript. All authors read and approved the final manuscript.

Competing interests

The authors declare no competing interests.

Additional information

Supplementary Information The online version contains supplementary material available at https://doi.org/10.1038/s41598-022-10458-8.

Correspondence and requests for materials should be addressed to T.K.

Reprints and permissions information is available at www.nature.com/reprints.

Publisher's note Springer Nature remains neutral with regard to jurisdictional claims in published maps and institutional affiliations.

4. Discussion

Roots need to expand through the soil to ensure water and nutrient uptake, but to avoid harmful growth conditions. Therefore, efficient modulation of directional root growth decides about plant fitness. Root evolved to simultaneously respond to manifold signals, which allow the plant to survive outdoors. Experiments in laboratories that investigate molecular and biochemical processes, which underpin root development and growth regulation, are often performed in rather stressful setups for the root. Several approaches were recently published that aim to reduce unnecessary stress triggered during the experiments, and my studies and reviews contributed to a better understanding how complex responses are to different cultivation conditions. Root growth responses, including the modulation of directional root growth, were shown to be differently regulated when the root is exposed to a combination of exogenous stimuli compared to stress-reduced cultivation setups. Several studies pointed especially towards the impact of direct root illumination on the outcome of evaluation of phenotypes and biochemical assays, from subcellular to organ levels. Moreover, direct root illumination changes roots' responses, which are simultaneously triggered by multiple exogenous signals, including gravitropic or mechanical stimuli. In fact, the substantial impact of light on root development is not surprising, as light is not a natural environmental cue for below-ground organs, such as roots. The more it is surprising that for many years, root were cultivated under light, thus producing results describing non-native conditions.

A central key regulator of root growth adaptation is auxin, a phytohormone that is actively distributed through the root tip to differently modulate cell responses to steer the direction of root growth. Previous studies showed that depending on exogenous stimuli, local auxin homeostasis can vary significantly. It includes auxin transport and metabolism (i.e. auxin biosynthesis, (de)conjugation and degradation). Changes in local auxin homeostasis then result in differential root growth pattern depending on environmental conditions. Furthermore, intrinsic events affect the modulation of directional growth, too. Intrinsic cues that were described in my articles, include changes in crosstalk between signaling molecules, and/or loss of function of proteins involved in control of auxin homeostasis.

4.1 Post-translational regulation of the auxin efflux transporter PIN-FORMED2

The plasma-membrane located auxin efflux transporter PIN-FORMED 2 (PIN2) is a well-studied key player of directional auxin transport, especially in *Arabidopsis thaliana.* Its specific localization and function in the root tip allow to study molecular events of its regulation and the resulting mechanical and biochemical cellular responses. Manifold post-translational regulatory events were previously described, but we were the first to point out the specific role of two evolutionary conserved cysteines in the protein

sequence of PIN2 for proper protein and root function. Substitution of the cysteines to alanines resulted in changed protein distribution along the plasma membrane and finally altered root growth pattern.

The results published in Retzer et al., 2017, combined with results published by other research teams, point out that beside the abundance modulation, especially the fine-tuning of spatio-temporal distribution of PIN2 appears to underpin efficient modulation of directional root growth, which is displayed in root growth patterns (*36*). Therefore, as a continuation of our studies, we decided to further dissect the regulatory events at post-translational level of PIN2. In Retzer et al., 2019, my colleagues demonstrated that ubiquitylation of PIN2 results in enhanced endocytosis and decreased PIN2 abundance at the plasma membrane (*45*). Currently, we investigate newly generated lines to find interactors that orchestrate the events at the PM. We obtained mutated lines of a constitutively ubiquitylated PIN2 through ethyl methane sulfonate mutagenesis, and already selected two promising lines that have restored PIN2 signal at the PM. I will study these two lines further to contribute to dissect the molecular mechanism behind ubiquitylation-triggered endocytosis of PIN2 and the resulting impact on directional root growth.

4.2 Directional root growth adaptation in context of external stimuli and auxin transport

Plasticity of plant growth is essential in securing plant survival, and I described different levels of exogenous and intrinsic signaling events that steer directional root growth in Lacek et al., 2021 (*50*). I summarize the impact of exogenous stimuli in Figure 1. Roots of higher plants evolved to adjust their shape and function depending on the continuously changing environmental conditions, and because soil is a heterogenous mixture, unilateral stimuli and changes in soil strength demand continuous adaptation of growth direction. The auxin influx carrier AUX1 is a crucial modulator of root system architecture and steers directional growth. A recent study in rice showed that AUX1 is important to modulate root circumnutation, a root movement that in loose soil can help to reduce the energy needed to explore the soil (*178*). At the same time, we published an article that described that loss-of-function mutant *aux1-7* displays difficulties to penetrate growth medium, and reduced ability of root twisting. We conducted the studies in the D-root setup (i.e. roots cultivated in darkness), compared the impact of medium composition further, and could thereby underpin the crucial role of AUX1 for efficient maneuver of the root through the growth medium.

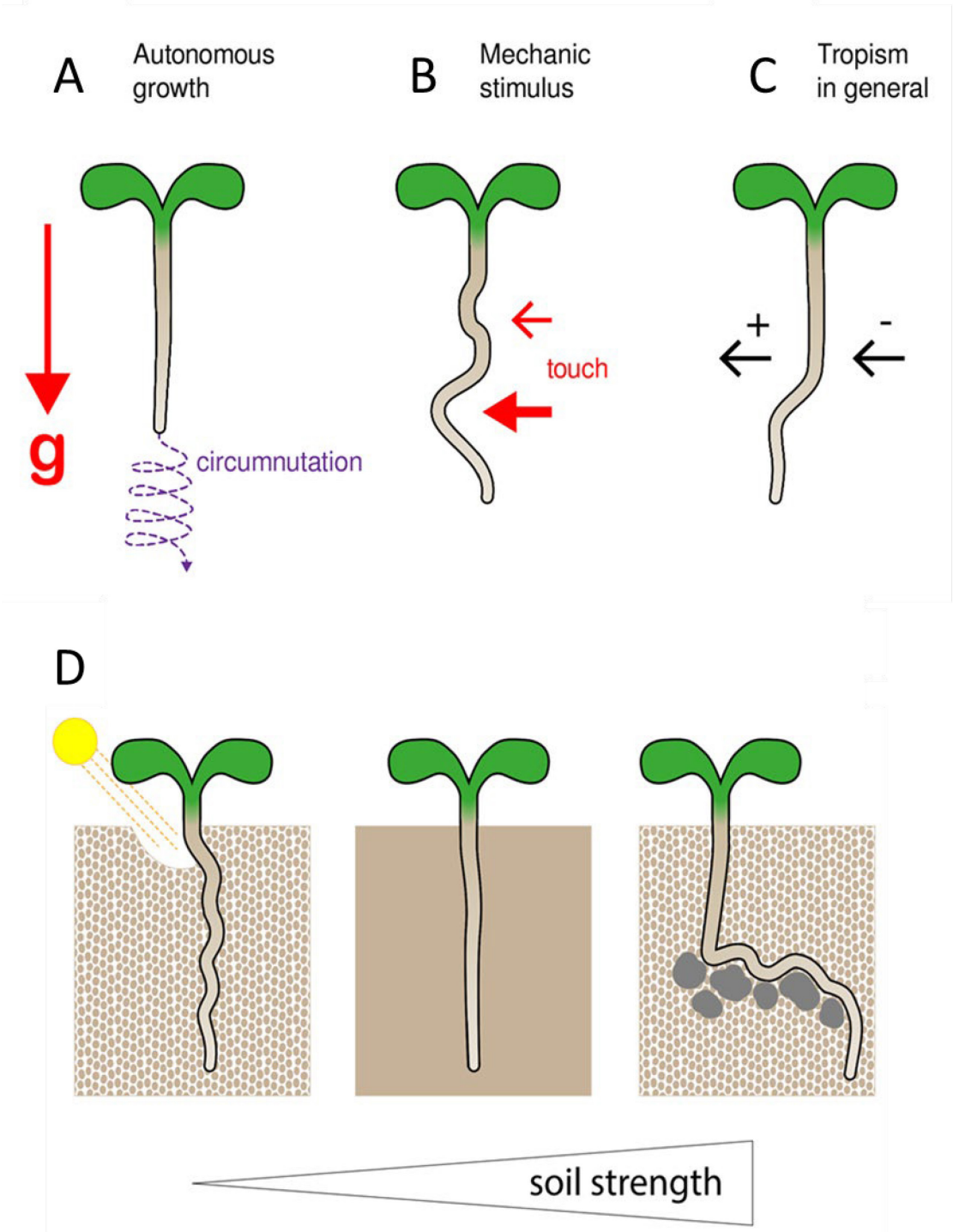

Figure 2: Intrinsic and exogenous signals together orchestrate root growth movements. A, Autonomous growth is largely orchestrated by energy and resource availability according to genetic predisposition to mediate root growth along the gravity vector (g), and defines the degree of root circumnutation. B, Besides the consistent force of g, roots are exposed to diverse mechanical/touch stimuli continuously, which results in deviation of root growth from vertical. C, because soil is a heterogeneous mixture, not only regarding its consistency but also nutrients, water, and

toxins occur randomly, the root grows towards (positive tropism) or away from the stimuli (negative tropism). D, Root growth adaptation upon gravity and touch (mechanical) stimulus is difficult to dissect, as both responses are tightly integrated to direct root growth through the soil. Soil consistency is highly heterogeneous and can change rapidly. Roots can adjust their growth rate and pattern depending on if they encounter loose or compact soil or even obstacles that cannot be penetrated anymore (figure adapted from Retzer and Weckwerth, review in preparation).

Plant roots are constantly adapting to their environment which consists of multiple external stimuli at once. This requires response of several regulation mechanisms at the same time, which is causing difficulties in deciphering each mechanism responding to specific stimuli. Conventional experimental methods of growing *Arabidopsis thaliana* include transparent petri dishes, which allow direct root illumination, and roots are growing on the surface of the growth substrate, which is often enriched with sucrose. All these things are perceived by root as external stimuli and can cause or mask phenotypes, which are key in deciphering root growth and adaptation mechanisms.

Roots evolved to penetrate the soil and grow shaded from direct illumination. Several research teams showed that root illumination causes stress to the organ and is affecting several signaling cascades, which are essential to proper execution of regulation mechanisms of root growth and adaptation (summarized recently in Lacek et al., 2021 (*50*)). Therefore, in recent years we established alternative methods to cultivate seedlings for root experiments, in a way that roots are grown in darkness, and under conditions that are much closer to the native ones, and we hope to be able to uncover mechanisms that control root growth *in vivo*.

5. Conclusions

Exogenous and intrinsic stimuli together define plant shape and function. During my studies of directional root growth regulations, I implemented innovative cultivation methods to delimit the amount of undesirable exogenous stimuli that would affect root growth, and therefore alter or mask the outcome. Furthermore, I focused on deciphering the impact of cultivation conditions, especially direct root illumination, in context of shootward auxin transport, by evaluating the ability of loss-of-function mutants of PIN2 and AUX1 to steer directional root growth. Additionally, I contributed to a better understanding of how PIN2 protein function defines its function in underpinning root growth pattern formation. Finally, I contributed to uncover auxin metabolic processes involved in fine tuning of root growth.

6. Outlook

The hierarchy of processes regulating directional root growth is studied for decades. Several key players were identified but the mechanisms behind are still not fully understood. More studies are needed to untangle gravity response mechanisms from responses of other exogenous triggers; especially mechanical stress responses require further research. Another important information required to better understand mechanisms that regulate root growth, is to identify the impact of growth limiting factors, such as energy and resource status of the studied growth environment, and the ability of plants to adapt to these factors. Thus, our future experimental work will be focused on further understanding the mechanisms involved in the gravity response, and differentiating them from other responses to exogenous factors, to better understand plant growth and adaptation processes.

7. References

1. F. Kögl, A. J. Haagen-Smit, Über die chemie des wuchsstoffs. *K. Akad. van Wet. Amsterdam Proc. Sect. Sci.* **34**, 1411–1416 (1931).

2. E. A. Schneider, C. W. Kazakoff, F. Wightman, Gas chromatography-mass spectrometry evidence for several endogenous auxins in pea seedling organs. *Planta*. **165**, 232–241 (1985).

3. S. Marumo, H. Hattori, H. Abe, K. Munakata, Isolation of 4-Chloroindolyl-3-acetic Acid from Immature Seeds of Pisum sativum. *Nature*. **219**, 959–960 (1968).

4. F. Wightman, D. L. Lighty, Identification of phenylacetic acid as a natural auxin in the shoots of higher plants. *Physiol. Plant.* **55**, 17–24 (1982).

5. J. Petrasek, J. Friml, Auxin transport routes in plant development. *Development*. **136**, 2675–2688 (2009).

6. S. Vanneste, J. Friml, Auxin: A Trigger for Change in Plant Development. *Cell*. **136**, 1005–1016 (2009).

7. K. Retzer, H. Butt, B. Korbei, C. Luschnig, The far side of auxin signaling: Fundamental cellular activities and their contribution to a defined growth response in plants. *Protoplasma* (2014), , doi:10.1007/s00709-013-0572-1.

8. K. Retzer, B. Korbei, C. Luschnig, "Auxin and tropisms" in *Auxin and Its Role in Plant Development* (2014).

9. M. Adamowski, J. Friml, PIN-Dependent Auxin Transport: Action, Regulation, and Evolution. *Plant Cell Online*. **27**, 20–32 (2015).

10. M. Gallei, C. Luschnig, J. Friml, Auxin signalling in growth: Schrödinger's cat out of the bag. *Curr. Opin. Plant Biol.* (2020), , doi:10.1016/j.pbi.2019.10.003.

11. H. Semeradova, J. C. Montesinos, E. Benkova, All Roads Lead to Auxin: Post-translational Regulation of Auxin Transport by Multiple Hormonal Pathways. *Plant Commun.* (2020), , doi:10.1016/j.xplc.2020.100048.

12. J. Friml, Fourteen Stations of Auxin. *Cold Spring Harb. Perspect. Biol.* (2021),

doi:10.1101/cshperspect.a039859.

13. M. M. Geisler, A Retro-Perspective on Auxin Transport. *Front. Plant Sci.* **12** (2021), p. 756968.

14. U. Z. Hammes, A. S. Murphy, C. Schwechheimer, Auxin Transporters-A Biochemical View. *Cold Spring Harb. Perspect. Biol.* (2021), doi:10.1101/cshperspect.a039875.

15. K. Retzer, W. Weckwerth, The tor–auxin connection upstream of root hair growth. *Plants* (2021), doi:10.3390/plants10010150.

16. O. Leyser, Auxin signaling. *Plant Physiol.* (2018), , doi:10.1104/pp.17.00765.

17. K. Müller, P. I. Dobrev, A. Pěnčík, P. Hošek, Z. Vondráková, R. Filepová, K. Malínská, F. Brunoni, L. Helusová, T. Moravec, K. Retzer, K. Harant, O. Novák, K. Hoyerová, J. Petrášek, DIOXYGENASE FOR AUXIN OXIDATION 1 catalyzes the oxidation of IAA amino acid conjugates. *Plant Physiol.* **187**, 103–115 (2021).

18. C. Luschnig, G. Vert, The dynamics of plant plasma membrane proteins: PINs and beyond. *Dev.* (2014), , doi:10.1242/dev.103424.

19. P. Grones, J. Friml, Auxin transporters and binding proteins at a glance. *J. Cell Sci.* (2015), doi:10.1242/jcs.159418.

20. C. Delker, A. Raschke, M. Quint, Auxin dynamics: The dazzling complexity of a small molecule's message. *Planta*. **227**, 929–941 (2008).

21. K. Mockaitis, M. Estelle, Auxin receptors and plant development: a new signaling paradigm. *Annu. Rev. Cell Dev. Biol.* **24**, 55–80 (2008).

22. A. Ivakov, S. Persson, Plant cell shape: Modulators and measurements. *Front. Plant Sci.* (2013), , doi:10.3389/fpls.2013.00439.

23. R. D.-W. Lee, H.-T. Cho, Auxin, the organizer of the hormonal/environmental signals for root hair growth. *Front. Plant Sci.* **4**, 448 (2013).

24. M. Schepetilnikov, L. A. Ryabova, Auxin signaling in regulation of plant translation reinitiation. *Front. Plant Sci.* (2017), , doi:10.3389/fpls.2017.01014.

25. M. E. J. Habets, R. Offringa, PIN-driven polar auxin transport in plant developmental plasticity: A key target for environmental and endogenous signals. *New Phytol.* **203** (2014), pp. 362–377.

26. G. Parry, A. Delbarre, A. Marchant, R. Swarup, R. Napier, C. Perrot-Rechenmann, M. J. Bennett,

Novel auxin transport inhibitors phenocopy the auxin influx carrier mutation aux1. *Plant J.* **25**, 399–406 (2001).

27. R. Swarup, E. M. Kramer, P. Perry, K. Knox, H. M. O. Leyser, J. Haseloff, G. T. S. Beemster, R. Bhalerao, M. J. Bennett, Root gravitropism requires lateral root cap and epidermal cells for transport and response to a mobile auxin signal. *Nat. Cell Biol.* (2005), doi:10.1038/ncb1316.

28. D. J. Carrier, N. T. A. Bakar, R. Swarup, R. Callaghan, R. M. Napier, M. J. Bennett, I. D. Kerr, The binding of auxin to the arabidopsis auxin influx transporter AUX1. *Plant Physiol.* (2008), doi:10.1104/pp.108.122044.

29. J. Petrášek, J. Mravec, R. Bouchard, J. J. Blakeslee, M. Abas, D. Seifertová, J. Wiśniewska, Z. Tadele, M. Kubeš, M. Čovanová, P. Dhonukshe, P. Skůpa, E. Benková, L. Perry, P. Křeček, O. R. Lee, G. R. Fink, M. Geisler, A. S. Murphy, C. Luschnig, E. Zažímalová, J. Friml, PIN proteins perform a rate-limiting function in cellular auxin efflux. *Science (80-.).* (2006), doi:10.1126/science.1123542.

30. B. Titapiwatanakun, J. J. Blakeslee, A. Bandyopadhyay, H. Yang, J. Mravec, M. Sauer, Y. Cheng, J. Adamec, A. Nagashima, M. Geisler, T. Sakai, J. Friml, W. A. Peer, A. S. Murphy, ABCB19/PGP19 stabilises PIN1 in membrane microdomains in Arabidopsis. *Plant J.* **57**, 27–44 (2009).

31. C. Ambrose, J. F. Allard, E. N. Cytrynbaum, G. O. Wasteneys, A CLASP-modulated cell edge barrier mechanism drives cell-wide cortical microtubule organization in Arabidopsis. *Nat. Commun.* (2011), doi:10.1038/ncomms1444.

32. J. Kleine-Vehn, K. Wabnik, A. Martinière, Ł. Łangowski, K. Willig, S. Naramoto, J. Leitner, H. Tanaka, S. Jakobs, S. Robert, C. Luschnig, W. Govaerts, S. W Hell, J. Runions, J. Friml, Recycling, clustering, and endocytosis jointly maintain PIN auxin carrier polarity at the plasma membrane. *Mol. Syst. Biol.* (2011), , doi:10.1038/msb.2011.72.

33. C. Löfke, C. Luschnig, J. Kleine-Vehn, Posttranslational modification and trafficking of PIN auxin efflux carriers. *Mech. Dev.* **130**, 82–94 (2013).

34. C. Zhang, N. V. Raikhel, G. R. Hicks, CLASPing Microtubules and Auxin Transport. *Dev. Cell* (2013), , doi:10.1016/j.devcel.2013.03.008.

35. C. Luschnig, G. Vert, The dynamics of plant plasma membrane proteins: PINs and beyond. *Development*. **141**, 2924–2938 (2014).

36. K. Retzer, J. Lacek, R. Skokan, C. I. Del Genio, S. Vosolsobě, M. Laňková, K. Malínská, N. Konstantinova, E. Zažímalová, R. M. Napier, J. Petrášek, C. Luschnig, Evolutionary conserved cysteines function as cis-acting regulators of arabidopsis PIN-FORMED 2 distribution. *Int. J. Mol. Sci.* **18** (2017), doi:10.3390/ijms18112274.

37. I. C. R. Barbosa, U. Z. Hammes, C. Schwechheimer, Activation and Polarity Control of PIN-FORMED Auxin Transporters by Phosphorylation. *Trends Plant Sci.* (2018), , doi:10.1016/j.tplants.2018.03.009.

38. G. Singh, K. Retzer, S. Vosolsobě, R. Napier, Advances in understanding the mechanism of action of the auxin permease aux1. *Int. J. Mol. Sci.* (2018), , doi:10.3390/ijms19113391.

39. R. Swarup, R. Bhosale, Developmental Roles of AUX1/LAX Auxin Influx Carriers in Plants. *Front. Plant Sci.* (2019), , doi:10.3389/fpls.2019.01306.

40. L. S. Halat, K. Gyte, G. O. Wasteneys, Microtubule-associated protein CLASP is translationally regulated in light-dependent root apical meristem growth. *Plant Physiol.* (2020), doi:10.1104/pp.20.00474.

41. K. Ötvös, M. Marconi, A. Vega, J. O'Brien, A. Johnson, R. Abualia, L. Antonielli, J. C. Montesinos, Y. Zhang, S. Tan, C. Cuesta, C. Artner, E. Bouguyon, A. Gojon, J. Friml, R. A. Gutiérrez, K. Wabnik, E. Benková, Modulation of plant root growth by nitrogen source-defined regulation of polar auxin transport. *EMBO J.* (2021), doi:10.15252/embj.2020106862.

42. I. Kashkan, M. Hrtyan, K. Retzer, J. Humpolíčková, A. Jayasree, R. Filepová, Z. Vondráková, S. Simon, D. Rombaut, T. B. Jacobs, M. J. Frilander, J. Hejátko, J. Friml, J. Petrášek, K. Růžička, Mutually opposing activity of PIN7 splicing isoforms is required for auxin-mediated tropic responses in Arabidopsis thaliana. *New Phytol.* **233**, 329–343 (2022).

43. J. Leitner, J. Petrášek, K. Tomanov, K. Retzer, M. Pařezová, B. Korbei, A. Bachmair, E. Zažímalová, C. Luschnig, Lysine63-linked ubiquitylation of PIN2 auxin carrier protein governs hormonally controlled adaptation of Arabidopsis root growth. *Proc. Natl. Acad. Sci. U. S. A.* (2012), doi:10.1073/pnas.1200824109.

44. J. Leitner, K. Retzer, N. Malenica, R. Bartkeviciute, D. Lucyshyn, G. Jäger, B. Korbei, A. Byström, C. Luschnig, Meta-regulation of Arabidopsis Auxin Responses Depends on tRNA Maturation. *Cell Rep.* **11**, 516–526 (2015).

45. K. Retzer, M. Akhmanova, N. Konstantinova, K. Malínská, J. Leitner, J. Petrášek, C. Luschnig,

Brassinosteroid signaling delimits root gravitropism via sorting of the Arabidopsis PIN2 auxin transporter. *Nat. Commun.* (2019), doi:10.1038/s41467-019-13543-1.

46. B. Korbei, J. Moulinier-Anzola, L. De-Araujo, D. Lucyshyn, K. Retzer, M. A. Khan, C. Luschnig, Arabidopsis TOL proteins act as gatekeepers for vacuolar sorting of PIN2 plasma membrane protein. *Curr. Biol.* **23**, 2500–2505 (2013).

47. K. Retzer, J. Lacek, R. Skokan, C. I. Del Genio, S. Vosolsobě, M. Laňková, K. Malínská, N. Konstantinova, E. Zažímalová, R. M. Napier, J. Petrášek, C. Luschnig, Evolutionary conserved cysteines function as cis-acting regulators of arabidopsis PIN-FORMED 2 distribution. *Int. J. Mol. Sci.* (2017), doi:10.3390/ijms18112274.

48. Y. Zhao, X. Q. Wang, The hot issue: TOR signalling network in plants. *Funct. Plant Biol.* (2020), , doi:10.1071/FP20071.

49. X. Yuan, P. Xu, Y. Yu, Y. Xiong, Glucose-TOR signaling regulates PIN2 stability to orchestrate auxin gradient and cell expansion in Arabidopsis root. *Proc. Natl. Acad. Sci. U. S. A.* (2020), doi:10.1073/pnas.2015400117.

50. J. Lacek, J. García-González, W. Weckwerth, K. Retzer, Lessons Learned from the Studies of Roots Shaded from Direct Root Illumination. *Int. J. Mol. Sci.* **22** (2021), doi:10.3390/ijms222312784.

51. S. Kaiser, D. Scheuring, To Lead or to Follow: Contribution of the Plant Vacuole to Cell Growth. *Front. Plant Sci.* (2020), , doi:10.3389/fpls.2020.00553.

52. J. Kleine-Vehn, Ł. Łangowski, J. Wiśniewska, P. Dhonukshe, P. B. Brewer, J. Friml, Cellular and molecular requirements for polar PIN targeting and transcytosis in plants. *Mol. Plant*. **1**, 1056–1066 (2008).

53. X. Chen, S. Wu, Z. Liu, J. Friml, Environmental and Endogenous Control of Cortical Microtubule Orientation. *Trends Cell Biol.* (2016), , doi:10.1016/j.tcb.2016.02.003.

54. D. Scheuring, C. Löfke, F. Krüger, M. Kittelmann, A. Eisa, L. Hughes, R. S. Smith, C. Hawes, K. Schumacher, J. Kleine-Vehn, Actin-dependent vacuolar occupancy of the cell determines auxin-induced growth repression. *Proc. Natl. Acad. Sci. U. S. A.* **113**, 452–7 (2016).

55. M. Lanza, B. Garcia-Ponce, G. Castrillo, P. Catarecha, M. Sauer, M. Rodriguez-Serrano, A. Páez-García, E. Sánchez-Bermejo, M. Tc, Y. Leo del Puerto, L. M. Sandalio, J. Paz-Ares, A. Leyva, Role of Actin Cytoskeleton in Brassinosteroid Signaling and in Its Integration with the Auxin

Response in Plants. *Dev. Cell* (2012), doi:10.1016/j.devcel.2012.04.008.

56. F. Brandizzi, G. O. Wasteneys, Cytoskeleton-dependent endomembrane organization in plant cells: An emerging role for microtubules. *Plant J.* (2013), doi:10.1111/tpj.12227.

57. J. Kleine-Vehn, Z. Ding, A. R. Jones, M. Tasaka, M. T. Morita, J. Friml, Gravity-induced PIN transcytosis for polarization of auxin fluxes in gravity-sensing root cells. *Proc. Natl. Acad. Sci. U. S. A.* **107**, 22344–22349 (2010).

58. M. Schwihla, B. Korbei, The Beginning of the End: Initial Steps in the Degradation of Plasma Membrane Proteins. *Front. Plant Sci.* (2020), , doi:10.3389/fpls.2020.00680.

59. M. Sauer, J. Kleine-Vehn, PIN-FORMED and PIN-LIKES auxin transport facilitators. *Dev.* (2019), doi:10.1242/dev.168088.

60. J. Mravec, P. Skůpa, A. Bailly, K. Hoyerová, P. Krecek, A. Bielach, J. Petrásek, J. Zhang, V. Gaykova, Y.-D. Stierhof, P. I. Dobrev, K. Schwarzerová, J. Rolčík, D. Seifertová, C. Luschnig, E. Benková, E. Zazímalová, M. Geisler, J. Friml, Subcellular homeostasis of phytohormone auxin is mediated by the ER-localized PIN5 transporter. *Nature*. **459**, 1136–1140 (2009).

61. M. Geisler, B. Wang, J. Zhu, Auxin transport during root gravitropism: Transporters and techniques. *Plant Biol.* (2014), , doi:10.1111/plb.12030.

62. M. Geisler, B. Aryal, M. Di Donato, P. Hao, A critical view on ABC transporters and their interacting partners in auxin transport. *Plant Cell Physiol.* (2017), doi:10.1093/pcp/pcx104.

63. E. Zazímalová, A. S. Murphy, H. Yang, K. Hoyerová, P. Hosek, Auxin transporters--why so many? *Cold Spring Harb. Perspect. Biol.* **2** (2010), , doi:10.1101/cshperspect.a001552.

64. G. Krouk, B. Lacombe, A. Bielach, F. Perrine-Walker, K. Malinska, E. Mounier, K. Hoyerova, P. Tillard, S. Leon, K. Ljung, E. Zazimalova, E. Benkova, P. Nacry, A. Gojon, Nitrate-regulated auxin transport by NRT1.1 defines a mechanism for nutrient sensing in plants. *Dev. Cell* (2010), doi:10.1016/j.devcel.2010.05.008.

65. I. Sairanen, O. Novák, A. Pěnčík, Y. Ikeda, B. Jones, G. Sandberg, K. Ljung, Soluble carbohydrates regulate auxin biosynthesis via PIF proteins in arabidopsis. *Plant Cell* (2013), doi:10.1105/tpc.112.104794.

66. K. Ljung, Auxin metabolism and homeostasis during plant development. *Dev.* (2013), doi:10.1242/dev.086363.

67. M. Ruiz Rosquete, E. Barbez, J. Kleine-Vehn, Cellular auxin homeostasis: Gatekeeping is housekeeping. *Mol. Plant* (2012), doi:10.1093/mp/ssr109.

68. M. Sauer, S. Robert, J. Kleine-Vehn, Auxin: Simply complicated. *J. Exp. Bot.* (2013), , doi:10.1093/jxb/ert139.

69. H. Han, M. Adamowski, L. Qi, S. S. Alotaibi, J. Friml, PIN-mediated polar auxin transport regulations in plant tropic responses. *New Phytol.* **232**, 510–522 (2021).

70. L. Li, I. Verstraeten, M. Roosjen, K. Takahashi, L. Rodriguez, J. Merrin, J. Chen, L. Shabala, W. Smet, H. Ren, S. Vanneste, S. Shabala, B. De Rybel, D. Weijers, T. Kinoshita, W. M. Gray, J. Friml, Cell surface and intracellular auxin signalling for H(+) fluxes in root growth. *Nature*. **599**, 273–277 (2021).

71. M. M. Marquès-Bueno, L. Armengot, L. C. Noack, J. Bareille, L. Rodriguez, M. P. Platre, V. Bayle, M. Liu, D. Opdenacker, S. Vanneste, B. K. Möller, Z. L. Nimchuk, T. Beeckman, A. I. Caño-Delgado, J. Friml, Y. Jaillais, Auxin-Regulated Reversible Inhibition of TMK1 Signaling by MAKR2 Modulates the Dynamics of Root Gravitropism. *Curr. Biol.* (2021), doi:10.1016/j.cub.2020.10.011.

72. Y. Hu, M. Omary, Y. Hu, O. Doron, L. Hoermayer, Q. Chen, O. Megides, O. Chekli, Z. Ding, J. Friml, Y. Zhao, I. Tsarfaty, E. Shani, Cell kinetics of auxin transport and activity in Arabidopsis root growth and skewing. *Nat. Commun.* **12**, 1657 (2021).

73. B. Péret, K. Swarup, A. Ferguson, M. Seth, Y. Yang, S. Dhondt, N. James, I. Casimiro, P. Perry, A. Syed, H. Yang, J. Reemmer, E. Venison, C. Howells, M. A. Perez-Amador, J. Yun, J. Alonso, G. T. S. Beemster, L. Laplaze, A. Murphy, M. J. Bennett, E. Nielsen, R. Swarup, *Plant Cell*, in press, doi:10.1105/tpc.112.097766.

74. R. Swarup, B. Péret, AUX/LAX family of auxin influx carriers-an overview. *Front. Plant Sci.* **3**, 225 (2012).

75. A. Marchant, R. Bhalerao, I. Casimiro, J. Eklöf, P. J. Casero, M. Bennett, G. Sandberg, AUX1 promotes lateral root formation by facilitating indole-3-acetic acid distribution between sink and source tissues in the Arabidopsis seedling. *Plant Cell*. **14**, 589–97 (2002).

76. K. Swarup, E. Benkova, R. Swarup, I. Casimiro, B. Peret, Y. Yang, G. Parry, E. Nielsen, I. De Smet, S. Vanneste, M. P. Levesque, D. Carrier, N. James, V. Calvo, K. Ljung, E. Kramer, R. Roberts, N. Graham, S. Marillonnet, K. Patel, J. D. Jones, C. G. Taylor, D. P. Schachtman, S. May,

G. Sandberg, P. Benfey, J. Friml, I. Kerr, T. Beeckman, L. Laplaze, M. J. Bennett, The auxin influx carrier LAX3 promotes lateral root emergence. *Nat Cell Biol*. **10**, 946–954 (2008).

77. Y. Yang, U. Z. Hammes, C. G. Taylor, D. P. Schachtman, E. Nielsen, High-Affinity Auxin Transport by the AUX1 Influx Carrier Protein. *Curr. Biol.* **16**, 1123–1127 (2006).

78. K. Hoyerová, L. Perry, P. Hand, M. Lanková, T. Kocábek, S. May, J. Kottová, J. Paces, R. Napier, E. Zazímalová, Functional characterization of PaLAX1, a putative auxin permease, in heterologous plant systems. *Plant Physiol.* **146**, 1128–1141 (2008).

79. K. Hoyerova, P. Hosek, M. Quareshy, J. Li, P. Klima, M. Kubes, A. A. Yemm, P. Neve, A. Tripathi, M. J. Bennett, R. M. Napier, Auxin molecular field maps define AUX1 selectivity: many auxin herbicides are not substrates. *New Phytol.* **217**, 1625–1639 (2018).

80. K. Swarup, E. Benková, R. Swarup, I. Casimiro, B. Péret, Y. Yang, G. Parry, E. Nielsen, I. De Smet, S. Vanneste, M. P. Levesque, D. Carrier, N. James, V. Calvo, K. Ljung, E. Kramer, R. Roberts, N. Graham, S. Marillonnet, K. Patel, J. D. G. Jones, C. G. Taylor, D. P. Schachtman, S. May, G. Sandberg, P. Benfey, J. Friml, I. Kerr, T. Beeckman, L. Laplaze, M. J. Bennett, The auxin influx carrier LAX3 promotes lateral root emergence. *Nat. Cell Biol.* **10**, 946–954 (2008).

81. R. Swarup, J. Friml, A. Marchant, K. Ljung, G. Sandberg, K. Palme, M. Bennett, Localization of the auxin permease AUX1 suggests two functionally distinct hormone transport pathways operate in the Arabidopsis root apex. *Genes Dev.* **15**, 2648–2653 (2001).

82. J. García-González, J. Lacek, W. Weckwerth, K. Retzer, Throttling Growth Speed: Evaluation of aux1-7 Root Growth Profile by Combining D-Root system and Root Penetration Assay. *Plants*. **11** (2022), doi:10.3390/plants11050650.

83. H. L. Rutschow, T. I. Baskin, E. M. Kramer, The carrier AUXIN RESISTANT (AUX1) dominates auxin flux into Arabidopsis protoplasts. *New Phytol.* **204**, 536–544 (2014).

84. S.-I. Inoue, K. Takahashi, H. Okumura-Noda, T. Kinoshita, Auxin Influx Carrier AUX1 Confers Acid Resistance for Arabidopsis Root Elongation Through the Regulation of Plasma Membrane H+-ATPase. *Plant Cell Physiol.* **57**, 2194–2201 (2016).

85. M. Fendrych, M. Akhmanova, J. Merrin, M. Glanc, S. Hagihara, K. Takahashi, N. Uchida, K. U. Torii, J. Friml, Rapid and reversible root growth inhibition by TIR1 auxin signalling. *Nat. Plants* (2018), doi:10.1038/s41477-018-0190-1.

86. K. Retzer, G. Singh, R. M. Napier, It starts with TIRs. *Nat. plants*. **4**, 410–411 (2018).

87. R. S. Arieti, C. J. Staiger, Auxin-induced actin cytoskeleton rearrangements require AUX1. *New Phytol.* **226**, 441–459 (2020).

88. R. Swarup, M. J. Bennett, *Root Gravitropism* (American Cancer Society, 2009).

89. C. Spitzer, F. C. Reyes, R. Buono, M. K. Sliwinski, T. J. Haas, M. S. Otegui, The ESCRT-related CHMP1A and B proteins mediate multivesicular body sorting of auxin carriers in Arabidopsis and are required for plant development. *Plant Cell*. **21**, 749–766 (2009).

90. Y. Boutté, K. Jonsson, H. E. McFarlane, E. Johnson, D. Gendre, R. Swarup, J. Friml, L. Samuels, S. Robert, R. P. Bhalerao, ECHIDNA-mediated post-Golgi trafficking of auxin carriers for differential cell elongation. *Proc. Natl. Acad. Sci. U. S. A.* **110**, 16259–16264 (2013).

91. T. Nodzynski, M. I. Feraru, S. Hirsch, R. De Rycke, C. Niculaes, W. Boerjan, J. Van Leene, G. De Jaeger, S. Vanneste, J. Friml, Retromer subunits VPS35A and VPS29 mediate prevacuolar compartment (PVC) function in Arabidopsis. *Mol. Plant*. **6**, 1849–1862 (2013).

92. P. Sun, Q. Y. Tian, J. Chen, W. H. Zhang, Aluminium-induced inhibition of root elongation in Arabidopsis is mediated by ethylene and auxin. *J. Exp. Bot.* **61**, 347–356 (2010).

93. J. Petrásek, J. Mravec, R. Bouchard, J. J. Blakeslee, M. Abas, D. Seifertová, J. Wisniewska, Z. Tadele, M. Kubes, M. Covanová, P. Dhonukshe, P. Skupa, E. Benková, L. Perry, P. Krecek, O. R. Lee, G. R. Fink, M. Geisler, A. S. Murphy, C. Luschnig, E. Zazímalová, J. Friml, J. Petrasek, PIN Proteins Perform a Rate-Limiting Function in Cellular Auxin Efflux. *Science (80-.).* **312**, 914–918 (2006).

94. J. Wisniewska, J. Xu, D. Seifertová, P. B. Brewer, K. Ruzicka, I. Blilou, D. Rouquié, E. Benková, B. Scheres, J. Friml, Polar PIN localization directs auxin flow in plants. *Science*. **312**, 883 (2006).

95. E. Zazímalová, A. S. Murphy, H. Yang, K. Hoyerova, P. Hosek, Auxin Transporters — Why So Many ? *Cold Spring Harb. Perspect. Biol.* **2**, a001552 (2010).

96. E. Benková, M. Michniewicz, M. Sauer, T. Teichmann, D. Seifertová, G. Jürgens, J. Friml, Local, Efflux-Dependent Auxin Gradients as a Common Module for Plant Organ Formation. *Cell*. **115**, 591–602 (2003).

97. J. Friml, A. Vieten, M. Sauer, D. Weijers, H. Schwarz, T. Hamann, R. Offringa, G. Jürgens, Efflux-dependent auxin gradients establish the apical-basal axis of Arabidopsis. *Nature*. **426**, 147–153 (2003).

98. A. Vieten, S. Vanneste, J. Wiśniewska, E. Benková, R. Benjamins, T. Beeckman, C. Luschnig, J. Friml, Functional redundancy of PIN proteins is accompanied by auxin-dependent cross-regulation of PIN expression. *Development* (2005), doi:10.1242/dev.02027.

99. H. Tanaka, P. Dhonukshe, P. B. Brewer, J. Friml, Spatiotemporal asymmetric auxin distribution: A means to coordinate plant development. *Cell. Mol. Life Sci.* **63**, 2738–2754 (2006).

100. J. Wisniewska, J. Xu, D. Seifartová, P. B. Brewer, K. Růžička, L. Blilou, D. Rouquié, E. Benková, B. Scheres, J. Friml, Polar PIN localization directs auxin flow in plants. *Science (80-.).* (2006), doi:10.1126/science.1121356.

101. K. Okada, J. Ueda, M. K. Komaki, C. J. Bell, Y. Shimura, Requirement of the Auxin Polar Transport System in Early Stages of Arabidopsis Floral Bud Formation. *Plant Cell*. **3**, 677–684 (1991).

102. L. Gälweiler, C. Guan, A. Müller, E. Wisman, K. Mendgen, A. Yephremov, K. Palme, Regulation of polar auxin transport by AtPIN1 in Arabidopsis vascular tissue. *Science (80-.).* (1998), doi:10.1126/science.282.5397.2226.

103. J. Friml, J. Wišniewska, E. Benková, K. Mendgen, K. Palme, Lateral relocation of auxin efflux regulator PIN3 mediates tropism in Arabidopsis. *Nature* (2002), doi:10.1038/415806a.

104. A. Marchant, J. Kargul, S. T. May, P. Muller, A. Delbarre, C. Perrot-Rechenmann, M. J. Bennett, AUX1 regulates root gravitropism in Arabidopsis by facilitating auxin uptake within root apical tissues. *EMBO J.* **18**, 2066–2073 (1999).

105. C. Luschnig, R. A. Gaxiola, P. Grisafi, G. R. Fink, EIR1, a root-specific protein involved in auxin transport, is required for gravitropism in Arabidopsis thaliana. *Genes Dev.* **12**, 2175–2187 (1998).

106. L. Abas, R. Benjamins, N. Malenica, T. Paciorek, J. Wiśniewska, J. C. Moulinier-Anzola, T. Sieberer, J. Friml, C. Luschnig, Intracellular trafficking and proteolysis of the Arabidopsis auxin-efflux facilitator PIN2 are involved in root gravitropism. *Nat. Cell Biol.* **8**, 249–256 (2006).

107. N. Konstantinova, B. Korbei, C. Luschnig, Auxin and Root Gravitropism: Addressing Basic Cellular Processes by Exploiting a Defined Growth Response. *Int. J. Mol. Sci.* **22** (2021), doi:10.3390/ijms22052749.

108. J. Lacek, K. Retzer, Ch. Luschnig, E. Zazimalova, "Polar Auxin Transport" in *eLS* (2017).

109. J. Friml, Fourteen Stations of Auxin. *Cold Spring Harb. Perspect. Biol.* **14** (2022),

doi:10.1101/cshperspect.a039859.

110. A. Laxmi, J. Pan, M. Morsy, R. Chen, Light plays an essential role in intracellular distribution of auxin efflux carrier PIN2 in Arabidopsis thaliana. *PLoS One* (2008), doi:10.1371/journal.pone.0001510.

111. M. Singh, A. Gupta, A. Laxmi, Striking the Right Chord: Signaling Enigma during Root Gravitropism. *Front. Plant Sci.* **8**, 1304 (2017).

112. M. Sassi, Y. Lu, Y. Zhang, J. Wang, P. Dhonukshe, I. Blilou, M. Dai, J. Li, X. Gong, Y. Jaillais, X. Yu, J. Traas, I. Ruberti, H. Wang, B. Scheres, T. Vernoux, J. Xu, COP1 mediates the coordination of root and shoot growth by light through modulation of PIN1- and PIN2-dependent auxin transport in Arabidopsis. *Dev.* (2012), doi:10.1242/dev.078212.

113. J. P. Vandenbrink, J. Z. Kiss, Plant responses to gravity. *Semin. Cell Dev. Biol.* **92**, 122–125 (2019).

114. G. Aronne, L. W. F. Muthert, L. G. Izzo, L. E. Romano, M. Iovane, F. Capozzi, A. Manzano, M. Ciska, R. Herranz, F. J. Medina, J. Z. Kiss, J. J. W. A. van Loon, A novel device to study altered gravity and light interactions in seedling tropisms. *Life Sci. Sp. Res.* **32**, 8–16 (2022).

115. Y. Wan, J. Jasik, L. Wang, H. Hao, D. Volkmann, D. Menzel, S. Mancuso, F. Baluška, J. Lin, The signal transducer NPH3 integrates the phototropin1 photosensor with PIN2-based polar auxin transport in Arabidopsis root phototropism. *Plant Cell*. **24**, 551–565 (2012).

116. F. Sun, W. Zhang, H. Hu, B. Li, Y. Wang, Y. Zhao, K. Li, M. Liu, X. Li, Salt modulates gravity signaling pathway to regulate growth direction of primary roots in arabidopsis. *Plant Physiol.* (2008), doi:10.1104/pp.107.109413.

117. M. Zourelidou, B. Absmanner, B. Weller, I. C. R. Barbosa, B. C. Willige, A. Fastner, V. Streit, S. A. Port, J. Colcombet, S. de la F. van Bentem, H. Hirt, B. Kuster, W. X. Schulze, U. Z. Hammes, C. Schwechheimer, Auxin efflux by PIN-FORMED proteins is activated by two different protein kinases, D6 PROTEIN KINASE and PINOID. *Elife*. **2014** (2014), doi:10.7554/eLife.02860.

118. M. Zwiewka, V. Bilanovičová, Y. W. Seifu, T. Nodzyński, The Nuts and Bolts of PIN Auxin Efflux Carriers. *Front. Plant Sci.* **10**, 985 (2019).

119. H. Shin, H. S. Shin, Z. Guo, E. B. Blancaflor, P. H. Masson, R. Chen, Complex regulation of Arabidopsis AGR1/PIN2-mediated root gravitropic response and basipetal auxin transport by cantharidin-sensitive protein phosphatases. *Plant J.* **42**, 188–200 (2005).

120. J. Leitner, K. Retzer, B. Korbei, C. Luschnig, Dynamics in PIN2 auxin carrier ubiquitylation in gravity-responding Arabidopsis roots. *Plant Signal. Behav.* **7**, 1271–1273 (2012).

121. J. Silva-Navas, M. A. Moreno-Risueno, C. Manzano, B. Téllez-Robledo, S. Navarro-Neila, V. Carrasco, S. Pollmann, F. J. Gallego, J. C. Del Pozo, Flavonols mediate root phototropism and growth through regulation of proliferation-to-differentiation transition. *Plant Cell* (2016), doi:10.1105/tpc.15.00857.

122. J. Silva-Navas, M. A. Moreno-Risueno, C. Manzano, M. Pallero-Baena, S. Navarro-Neila, B. Téllez-Robledo, J. M. Garcia-Mina, R. Baigorri, F. J. Gallego, J. C. Del Pozo, D-Root: A system for cultivating plants with the roots in darkness or under different light conditions. *Plant J.* (2015), doi:10.1111/tpj.12998.

123. J. Cabrera, C. M. Conesa, J. C. Del Pozo, May the dark be with roots: a perspective on how root illumination may bias in vitro research on plant-environment interactions. *New Phytol.* **233**, 1988–1997 (2022).

124. K. Yokawa, T. Koshiba, F. Baluška, Light-dependent control of redox balance and auxin biosynthesis in plants. *Plant Signal. Behav.* (2014), doi:10.4161/psb.29522.

125. G. B. Monshausen, T. N. Bibikova, M. A. Messerli, C. Shi, S. Gilroy, Oscillations in extracellular pH and reactive oxygen species modulate tip growth of Arabidopsis root hairs. *Proc. Natl. Acad. Sci. U. S. A.* (2007), doi:10.1073/pnas.0708586104.

126. A. Eljebbawi, Y. D. C. R. Guerrero, C. Dunand, J. M. Estevez, Highlighting reactive oxygen species as multitaskers in root development. *iScience*. **24**, 101978 (2021).

127. S. Mangano, S. P. Denita-Juarez, H.-S. Choi, E. Marzol, Y. Hwang, P. Ranocha, S. M. Velasquez, C. Borassi, M. L. Barberini, A. A. Aptekmann, J. P. Muschietti, A. D. Nadra, C. Dunand, H.-T. Cho, J. M. Estevez, Molecular link between auxin and ROS-mediated polar growth. *Proc. Natl. Acad. Sci. U. S. A.* **114**, 5289–5294 (2017).

128. E. J. Drdová, L. Synek, T. Pečenková, M. Hála, I. Kulich, J. E. Fowler, A. S. Murphy, V. Žárský, The exocyst complex contributes to PIN auxin efflux carrier recycling and polar auxin transport in Arabidopsis. *Plant J.* (2013), doi:10.1111/tpj.12074.

129. J. Li, Brassinosteroid signaling: From receptor kinases to transcription factors. *Curr. Opin. Plant Biol.* (2005), , doi:10.1016/j.pbi.2005.07.009.

130. J. Kleine-Vehn, J. Leitner, M. Zwiewka, M. Sauer, L. Abas, C. Luschnig, J. Friml, Differential

degradation of PIN2 auxin efflux carrier by retromer-dependent vacuolar targeting. *Proc. Natl. Acad. Sci. U. S. A.* (2008), doi:10.1073/pnas.0808073105.

131. V. Žárský, Exocyst functions in plants: secretion and autophagy. *FEBS Lett.* **596**, 2324–2334 (2022).

132. K. Yokawa, R. Fasano, T. Kagenishi, F. Baluška, Light as stress factor to plant roots – Case of root halotropism. *Front. Plant Sci.* (2014), doi:10.3389/fpls.2014.00718.

133. E. B. Blancaflor, G.-C. Hou, D. R. Mohamalawari, The promotive effect of latrunculin B on maize root gravitropism is concentration dependent. *Adv. Sp. Res. Off. J. Comm. Sp. Res.* . **31**, 2215–2220 (2003).

134. M. Geisler, B. Wang, J. Zhu, Auxin transport during root gravitropism: Transporters and techniques. *Plant Biol.* **16** (2014), pp. 50–57.

135. L. de Bang, A. Paez-Garcia, A. E. Cannon, S. Chin, J. Kolape, F. Liao, J. A. Sparks, Q. Jiang, E. B. Blancaflor, Brassinosteroids Inhibit Autotropic Root Straightening by Modifying Filamentous-Actin Organization and Dynamics. *Front. Plant Sci.* **11**, 5 (2020).

136. H. Rakusová, M. Fendrych, J. Friml, Intracellular trafficking and PIN-mediated cell polarity during tropic responses in plants. *Curr. Opin. Plant Biol.* **23** (2015), pp. 116–123.

137. B. Moulia, M. Fournier, The power and control of gravitropic movements in plants: a biomechanical and systems biology view. *J. Exp. Bot.* **60**, 461–486 (2009).

138. L. Armengot, M. M. Marquès-Bueno, Y. Jaillais, Regulation of polar auxin transport by protein and lipid kinases. *J. Exp. Bot.* **67** (2016), pp. 4015–4037.

139. C. Brunetti, A. Fini, F. Sebastiani, A. Gori, M. Tattini, Modulation of Phytohormone Signaling: A Primary Function of Flavonoids in Plant-Environment Interactions. *Front. Plant Sci.* **9**, 1042 (2018).

140. J. García-González, J. Lacek, K. Retzer, Dissecting Hierarchies between Light, Sugar and Auxin Action Underpinning Root and Root Hair Growth. *Plants* . **10** (2021), , doi:10.3390/plants10010111.

141. J. García-González, J. Lacek, W. Weckwerth, K. Retzer, Exogenous carbon source supplementation counteracts root and hypocotyl growth limitations under increased cotyledon shading, with glucose and sucrose differentially modulating growth curves. *Plant Signal. Behav.*,

1969818 (2021).

142. E. Kolb, V. Legué, M.-B. Bogeat-Triboulot, Physical root-soil interactions. *Phys. Biol.* **14**, 65004 (2017).

143. R. Pierik, C. Testerink, The art of being flexible: How to escape from shade, Salt, And drought1. *Plant Physiol.* (2014), doi:10.1104/pp.114.239160.

144. B. S. Mishra, M. Singh, P. Aggrawal, A. Laxmi, Glucose and auxin signaling interaction in controlling arabidopsis thaliana seedlings root growth and development. *PLoS One* (2009), doi:10.1371/journal.pone.0004502.

145. P. Sun, Q.-Y. Tian, J. Chen, W.-H. Zhang, Aluminium-induced inhibition of root elongation in Arabidopsis is mediated by ethylene and auxin. *J. Exp. Bot.* **61**, 347–356 (2010).

146. R. Roy, D. C. Bassham, Root growth movements: waving and skewing. *Plant Sci.* **221**–**222**, 42–47 (2014).

147. K. Van Gelderen, C. Kang, R. Pierik, Light signaling, root development, and plasticity. *Plant Physiol.* (2018), , doi:10.1104/pp.17.01079.

148. K. van Gelderen, C. Kang, P. Li, R. Pierik, Regulation of Lateral Root Development by Shoot-Sensed Far-Red Light via HY5 Is Nitrate-Dependent and Involves the NRT2.1 Nitrate Transporter. *Front. Plant Sci.* **12**, 660870 (2021).

149. L. W. F. Muthert, L. G. Izzo, M. van Zanten, G. Aronne, Root Tropisms: Investigations on Earth and in Space to Unravel Plant Growth Direction. *Front. Plant Sci.* **10** (2020), doi:10.3389/fpls.2019.01807.

150. C. Grierson, E. Nielsen, T. Ketelaarc, J. Schiefelbein, Root hairs. *Arab. B.* **12**, e0172–e0172 (2014).

151. M. Braun, G. O. Wasteneys, "Actin in Characean Rhizoids and Protonemata" in *Actin: A Dynamic Framework for Multiple Plant Cell Functions* (2000).

152. A. Barrada, M. H. Montané, C. Robaglia, B. Menand, Spatial regulation of root growth: Placing the plant TOR pathway in a developmental perspective. *Int. J. Mol. Sci.* (2015), , doi:10.3390/ijms160819671.

153. M. Ramon, T. V. T. Dang, T. Broeckx, S. Hulsmans, N. Crepin, J. Sheen, F. Rolland, Default activation and nuclear translocation of the plant cellular energy sensor SnRK1 regulate metabolic

stress responses and development. *Plant Cell* (2019), doi:10.1105/tpc.18.00500.

154. Y. Miotto, C. T. Da Costa, R. Offringa, J. Kleine-Vehn, F. D. Maraschin, Effects of light intensity on root development in a D-Root growth system. *Front. Plant Sci.* (2021), doi:Effects of light intensity on root development in a D-Root growth system.

155. B. S. Mishra, M. Sharma, A. Laxmi, Role of sugar and auxin crosstalk in plant growth and development. *Physiol. Plant.* (2021), doi:10.1111/ppl.13546.

156. M. Sharma, M. Sharma, M. Jamsheer K, A. Laxmi, Jasmonic Acid coordinates with Light, Glucose and Auxin signalling in Regulating Branching Angle of Arabidopsis Lateral Roots. *Plant. Cell Environ.* (2022), doi:10.1111/pce.14290.

157. C. Nunes, L. F. Primavesi, M. K. Patel, E. Martinez-Barajas, S. J. Powers, R. Sagar, P. S. Fevereiro, B. G. Davis, M. J. Paul, Inhibition of SnRK1 by metabolites: Tissue-dependent effects and cooperative inhibition by glucose 1-phosphate in combination with trehalose 6-phosphate. *Plant Physiol. Biochem.* (2013), doi:10.1016/j.plaphy.2012.11.011.

158. L. A. Ryabova, C. Robaglia, C. Meyer, Target of Rapamycin kinase: Central regulatory hub for plant growth and metabolism. *J. Exp. Bot.* (2019), , doi:10.1093/jxb/erz108.

159. L. Huang, L.-J. Yu, X. Zhang, B. Fan, F.-Z. Wang, Y.-S. Dai, H. Qi, Y. Zhou, L.-J. Xie, S. Xiao, Autophagy regulates glucose-mediated root meristem activity by modulating ROS production in Arabidopsis. *Autophagy*. **15**, 407–422 (2019).

160. F. Fichtner, I. M. Dissanayake, B. Lacombe, F. Barbier, Sugar and Nitrate Sensing: A Multi-Billion-Year Story. *Trends Plant Sci.* (2020), , doi:10.1016/j.tplants.2020.11.006.

161. T. I. Baskin, E. L. Remillong, J. E. Wilson, The impact of mannose and other carbon sources on the elongation and diameter of the primary root of <emph type="2">Arabidopsis thaliana</emph>. *Funct. Plant Biol.* **28**, 481–488 (2001).

162. J. Raya-González, J. S. López-Bucio, J. C. Prado-Rodríguez, L. F. Ruiz-Herrera, Á. A. Guevara-García, J. López-Bucio, The MEDIATOR genes MED12 and MED13 control Arabidopsis root system configuration influencing sugar and auxin responses. *Plant Mol. Biol.* **95**, 141–156 (2017).

163. L. Wang, Y.-L. Ruan, Regulation of cell division and expansion by sugar and auxin signaling. *Front. Plant Sci.* **4**, 163 (2013).

164. J. Verbančič, J. E. Lunn, M. Stitt, S. Persson, Carbon Supply and the Regulation of Cell Wall

Synthesis. *Mol. Plant*. **11**, 75–94 (2018).

165. T. Najrana, J. Sanchez-Esteban, Mechanotransduction as an Adaptation to Gravity. *Front. Pediatr.* **4**, 140 (2016).

166. C. Darwin, F. Darwin, *The power of movement in plants* (London :John Murray,1880., 1880).

167. Y. Zhang, G. Xiao, X. Wang, X. Zhang, J. Friml, Evolution of fast root gravitropism in seed plants. *Nat. Commun.* **10**, 3480 (2019).

168. S. Chin, E. B. Blancaflor, Plant Gravitropism: From Mechanistic Insights into Plant Function on Earth to Plants Colonizing Other Worlds. *Methods Mol. Biol.* **2368**, 1–41 (2022).

169. E. M. Sato, H. Hijazi, M. J. Bennett, K. Vissenberg, R. Swarup, New insights into root gravitropic signalling. *J. Exp. Bot.* **66**, 2155–2165 (2015).

170. E. B. Blancaflor, J. M. Fasano, S. Gilroy, Laser ablation of root cap cells: implications for models of graviperception. *Adv. Sp. Res. Off. J. Comm. Sp. Res.* . **24**, 731–738 (1999).

171. A. Grabov, M. K. Ashley, S. Rigas, P. Hatzopoulos, L. Dolan, F. Vicente-Agullo, Morphometric analysis of root shape. *New Phytol.* **165**, 641–651 (2005).

172. L. Muller, M. J. Bennett, A. French, D. M. Wells, R. Swarup, Root Gravitropism: Quantification, Challenges, and Solutions. *Methods Mol. Biol.* **1761**, 103–112 (2018).

173. N. B. C. Serre, M. Fendrych, ACORBA: Automated workflow to measure Arabidopsis thaliana root tip angle dynamic. *bioRxiv* (2021), doi:10.1101/2021.07.15.452462.

174. K. Retzer, Continuous tracking of gravistimulated roots in a chambered coverslip by confocal microscopy allows first glimpse on mechanoadaptation of cell files during curvature initiation. *bioRxiv* (2021), doi:10.1101/2021.09.05.459030.

175. Y. Wan, K. Yokawa, F. Baluška, Arabidopsis Roots and Light: Complex Interactions. *Mol. Plant* (2019), , doi:10.1016/j.molp.2019.10.001.

176. J. García-González, Š. Kebrlová, M. Semerák, J. Lacek, I. Kotannal Baby, J. Petrášek, K. Schwarzerová, Arp2/3 Complex Is Required for Auxin-Driven Cell Expansion Through Regulation of Auxin Transporter Homeostasis . *Front. Plant Sci.* . **11** (2020), p. 486.

177. A. Starodubtseva, T. Kalachova, K. Retzer, A. Jelínková, P. Dobrev, J. Lacek, R. Pospíchalová, J. Angelini, A. Guivarc'h, S. Pateyron, L. Soubigou-Taconnat, L. Burketová, E. Ruelland, An Arabidopsis mutant deficient in phosphatidylinositol-4-phosphate kinases ß1 and ß2 displays

altered auxin-related responses in roots. *Sci. Rep.* **12**, 6947 (2022).

178. I. Taylor, K. Lehner, E. McCaskey, N. Nirmal, Y. Ozkan-Aydin, M. Murray-Cooper, R. Jain, E. W. Hawkes, P. C. Ronald, D. I. Goldman, P. N. Benfey, Mechanism and function of root circumnutation. *Proc. Natl. Acad. Sci. U. S. A.* **118** (2021), doi:10.1073/pnas.2018940118.